Adhesion measurement techniques: A comparative study using latex beads and bacterial spores.

Fenton, Adam

Adhesion Measurement Techniques: A Comparative Study Using Latex Beads and Bacterial Spores

by

ADAM FENTON B.Sc. (Hons)

September 2001

Thesis submitted in fulfilment of the requirements of the University of Wales in candidature for the degree of Doctor of Philosophy.

Department of Biochemical Engineering,
University of Wales Swansea,
Singleton Park,
Swansea.
SA2 8PP.

Tel. No: (01792) 295195
Fax. No: (01792) 295701

Head of Department: Professor Paul Preece.

DECLARATION

Declaration

This work has not been accepted in substance for any degree and is not being concurrently submitted in candidature for any degree.

Signed ..... (Candidate)
Date ..... 27 SEPT 2001 .....

Statement 1

This thesis is the result of the author's original work, except where acknowledgment to other authors is expressly made. A bibliography is appended.

Signed ..... (Candidate)
Date ..... 27 SEPT 2001 .....

Statement 2

I hereby give consent for my thesis, if accepted, to be available for photocopying, for inter-library loan, and for the title and summary to be available for outside organisations.

Signed .... (Candidate)
Date ..... 27 SEPT 2001 .....

TABLE OF CONTENTS

ACKNOWLEDGEMENTS

Firstly I would like to acknowledge my supervisor, Dr. R.W. Lovitt, for his guidance and invaluable assistance throughout the period of this research.

I would like to acknowledge the funding that the Biotechnology and Biological Sciences Research Council have provided me with throughout this study.

I extend my thanks to Professor Paul Preece, Head of the Chemical and Biological Process Engineering Department at the University of Wales Swansea, for providing access to the necessary facilities and the resources to conduct this research.

I would also like to express my appreciation to the members of the technical and academic staff of the department, especially Dr. Greg Coss, Dr. Haitham Yousef, Dr. Paul Williams, Mr. Phil Huxtable, Mr. Adrian Jenkins, Mr. Glyn Phillips, Mr. Gary Tuckett, and Dr. Peter Williams.

I would like to extend my special thanks to Dr Chris Wright, and Dr. Tony Knights, who have not only given me help, but also encouragement, and support over the last four years. I would also like to thank my friends and skippers, Steve, Darren, Sej, Pete, Karl, Shane, and Deng.

Last but not least, I would like to extend my gratitude to my parents, John and Alison for their patience and financial support allowing me to live in the luxury to which I am accustomed, I am deeply grateful. Finally, I would like to thank my brother, Giles, who provided support and motivation throughout this project.

SUMMARY

Adhesion Measurement Techniques: A Comparative Study Using Latex Beads and Bacterial Spores

Cellular adhesion has many implications in process engineering, medicine, and within the environment. The adhesion process consists of several steps, and it is unclear as to the contribution that the properties of the cells and collector surfaces have on adhesion. The deposition of cells is the initial phase in biofilm formation, and control of this process would be beneficial in all areas of science and technology.

The aim of the project was to develop and apply three methods of quantitatively studying particle adhesion, developed from previous related work. The Packed Column, the Spinning Disc and the Radial Flow Chamber (RFC) were chosen due to their practicality and ability to assess the effect of hydrodynamic shear on particle adhesion. The effects of variable parameters were investigated, allowing characterisation of each system.

The methods were developed and used in conjunction with glass and stainless steel to assess the effect of pH on the adhesion of aminated and carboxylated latex beads, and the spores of *Bacillus mycoides* and *Bacillus subtilis*. Measurements of surface charge and hydrophobicity of the collector surface and colloidal particles were performed, and compared with the results generated using the three assessment techniques. Particle zeta potential and hydrophobicity ranged from +10 mV to –40 mV and 0 to 95%, respectively. The collector hydrophobicity of glass and stainless steel, measured by contact angles, ranged from 21 to 76°. Surface preparation techniques provided consistent surface roughness. Particle hydrophobicity was independent of surface charge.

The findings showed that adhesion agreed qualitatively using the three methods of assessment, but not quantitatively. These findings agreed with previous work using similar methods to assess cellular adhesion. Steel promoted adhesion more than glass. *B.mycoides* provided greatest adhesion followed by aminated beads, carboxylated beads, and finally *B.subtilis*, with the highest levels of adhesion occurred at low pH (ranging from 0 – 7000 mm^{-2}). Adhesion varied greatly (up to 70%), attributed to the heterogeneity of the particle, collector surface, and flow within each system.
DLVO theory could not be used to predict adhesion, although did aid the explanation of observations when applied to the experimental data. Hydrophobicity contributed to adhesion more than the surface charge, attributed to the longer range that the force operated over. Spores could not be treated as simple colloidal particles, attributed to the complexity of the cell wall structure.

The three systems used within this work provided complementary results that allowed an understanding of adhesion. Each system showed differing flow characteristics and this was reflected in the experimental data.
The Packed Column provided a comprehensive understanding of the combined contributions of hydrophobicity and surface charge, with particle recovery ranging from 0 to 95%. The results obtained using the Spinning Disc and the RFC were dependent on applied shear force (0 – 2 Nm^{-2}), and showed comparable results in the case of stainless steel, ranging from 200 to 7000 mm^{-2}. This relationship was not linear, and consequently no definitive value for the shear force required to inhibit adhesion could be generated, which would require further analysis. Values obtained using the RFC reflected the hydrophobicity of the collector surface, whereas the Spinning Disc showed more contribution from the particle properties, attributed to the very different flow patterns generated from the two systems.

With further work, these methods can be employed successfully to systematically and quantitatively investigate the fundamentals of particle and cellular adhesion.

NOMENCLATURE

A	Absorbance at 660nm
$\mathbf{A_{sphere}}$	Surface Area of Particle (m^2)
$\mathbf{A_{collector}}$	Surface Area of Collector (m^2)
c	Concentration (g/ℓ)
D	Dielectric constant
δ_0	Boundary Layer Thickness (m)
e	Column Voidage
h	Height between plates in the Radial Flow Chamber (m)
l	Cuvette path length (cm)
μ	Fluid Viscosity (kg/ms)
ν	Kinematic Viscosity (m^2/s)
OD	Optical Density
RFC	Radial Flow Chamber
θ	Contact Angle of a Liquid with a Surface (°)
Q	Flow Rate within the Radial Flow Chamber (ℓ/min)
ρ	Fluid Density (kg/m^3)
r	Radial Distance (m)
R	Particle Radius (m)
$\mathbf{R_a}$	Average Surface Roughness (nm)
$\mathbf{R_q}$	Root Mean Square Surface Roughness (nm)
$\mathbf{R_t}$	Maximum Profile Height of Surface (nm)
Re	Reynold's Number
t	Experimental Duration Time (minutes)
τ	Applied Shear Stress (N/m^2)
$\mathbf{u_E}$	Electrophoretic Mobility ($m^2/secV$)
V	Volume (m^3)
ω	Angular Velocity (radians/s)
y	Perpendicular Distance of a Particle from a Surface (m)
ζ	Zeta Potential (mV)

CHAPTER ONE

Introduction to Microbial Adhesion: Relevance and Previous Methods of Study

1.1 Introduction

The measurement of microbial adhesion has been a problem throughout many areas of science and technology, including bioprocesses, food technology, and medicine and related subjects.

The study of microbial adhesion has tended to provide qualitative explanations of the process of adhesion, rather than quantitative measurements of the physical and chemical processes involved. There are many problems encountered when addressing microbial adhesion, such as the definition of adhesion, and consideration of the different physical and chemical processes occurring within the interaction of colloid and collector.

The aim of the work in this project was to consider previous methods of assessing microbial adhesion, and subsequently to identify and develop three different and contrasting methods that provided reliable measurement of adhesion.

1.2 Relevance of Adhesion Studies

1.2.1 What Is Adhesive Force?

To define the forces associated with adhesion, the process of attachment must firstly be fully understood. The process of cellular adhesion is a three-stage process that depends on many factors, shown in Figure 1.1. The properties of the cell and the collector surface, and solution chemistry will determine these factors that govern adhesion.

The first phase of adhesion is the approach of a cell to the collector surface (A), and is controlled by physicochemical forces, such as hydrodynamic shear and dispersion of the particle. The initial interaction between particle and collector is reversible (B) and the cell can interact directly with the collector via structures on the cell surface, if present. Subsequently, the second stage of adhesion (C) occurs where molecular recognition occurs, and binding between the cell and the collector surface is irreversible. This stage may or may not be promoted by the presence of structures such as fimbriae and pili on the surface of the cell (Bunt *et al*, 1995).

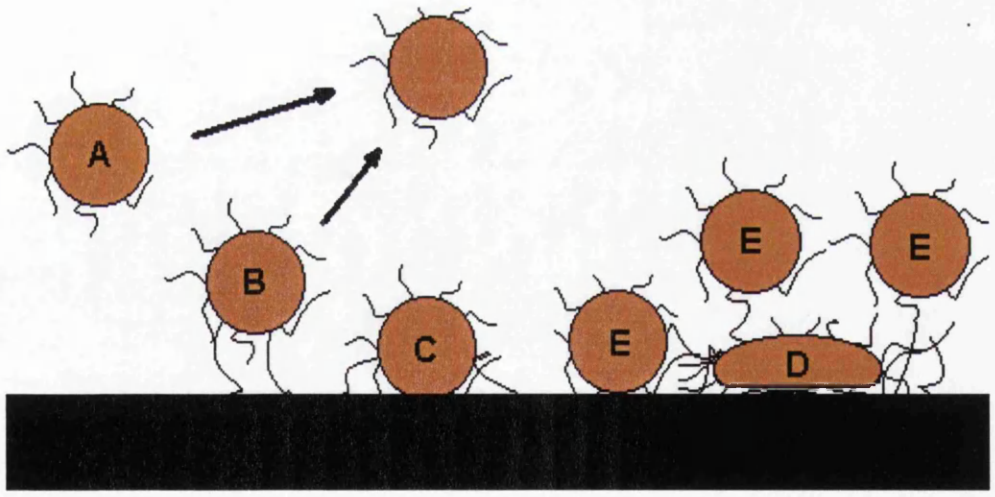

Figure 1.1: The approach of a cell to a collector surface. Cell A approaches the surface under physicochemical forces, and reversibly binds, as is represented by cell B. Once the cell has bound C, the interaction is irreversible, and the cell D secretes an extracellular matrix promoting the adhesion of other bacteria from solution E.

Once the cell is irreversibly attached, the cell can grow and reproduce (in the case of spores, germination occurs first). As colonies develop (D), extra-cellular compounds are secreted by the cells, increasing the protection of the cell from both physical and chemical effects from the local environment (An and Friedman, 1997).
The forces involved in attachment of cells differ greatly to the force required to detach a cell from a collector surface, as shown by Bowen and Epstein (1979). This is also reflected in the approach of a yeast cell to a mica surface measured using an Atomic Force Microscope, where the force required to detach a cell from the surface was significantly larger than the attractive force of the cell when approaching the surface (Bowen *et al*, 1998a).
The most important phase in the adhesion of bacteria is therefore the initial reversible phase. This must be fully understood to either inhibit or promote the irreversible phase of attachment, and subsequent biofilm formation. If the initial, reversible stage of adhesion can be controlled, then the subsequent processes of irreversible adhesion and biofilm formation can also be controlled, which would be beneficial in all areas of science and technology as detailed below in Section 1.2.2.

1.2.2 Why Study Adhesion?

The adhesion of microbial particles to differing surfaces is of relevance in several areas of science and technology. Both the inhibition and promotion of cellular adhesion have relevance and applications in Bioprocess Technology, Medicine, Dentistry, Ophthalmics, and the Environment.

1.2.2.1 The Importance of Microbial Adhesion Studies in Medicine, Dentistry, and Ophthalmics

The use of polymers and metals within medicine, dentistry, and ophthalmics has increased significantly in recent years, as new polymers and alloys are developed (Yung *et al*, 1996). Examples of these implants are vascular devices, urinary tract catheters, intrauterine devices, contact lenses, dental materials and endotracheal

tubes (Neu *et al*, 1994). These materials, whether they are permanent or temporary, must not increase the likelihood of bacterial infection, promote the formation of conditioning films, or provoke subsequent immune reaction from the host (Costerton and Stewart, 2000). Bacterial adhesion to biomaterial surfaces is accepted as the first and most critical step in device-centred infection (Shive *et al*, 1999), and the removal of adherent bacteria is imperative before they become established on the surface.

The major role of bacteria in the colonisation of implanted devices was exemplified by Neu *et al* (1994), where 79 bacterial and 39 yeast strains were isolated from biofilms formed on silicone rubber voice prostheses, which possessed varying degrees of hydrophobicity.

The use of foreign surfaces within a patient provides two problems for the host's immune system. Firstly, and of lesser importance, a foreign object can provoke an immune response, and subsequent rejection from the host as a result of opsinisation, and plasma protein deposition on the implant by the complement cascade. This in turn, results in cells of the host's immune system attracted to the site, and immunological rejection (Yung *et al*, 1996). The minimisation of protein deposition onto these surfaces would therefore minimise rejection by the host's immune system.

The second, and larger, problem is that foreign surfaces provide an ideal environment for bacterial colonisation, and also impede the bactericidal activities of leukocytic phagocytosis and antibiotics (Shive *et al*, 1999). Deposition of bacteria on a foreign surface will generate an immune response due to the presence of antigens, and subsequent rejection or infection of the implant will result.

When implants are used, such as replacement hips or heart valves, it is common practice to subdue the host's immune system, lowering the chance of rejection of the implant by the host. As a result of this, the chance of bacterial infection of the implant is increased, as the immune system is subdued. The unusual resistance of bacteria in the hospital environment to antibiotic treatments also contributes to the prevalence of infection (Wang *et al*, 1993b).

The development of polymers that minimise the deposition of both infectious cells and proteins, whether they are microbial or of the immune system, is therefore of great importance. To achieve this, methods of assessing the adhesion of cells must

therefore be developed to allow practical assessments that simulate hemodynamic shear, and are not time consuming.

Much work has been performed on the adhesion of bacteria responsible for commonly observed infections. An important example of this context is *Staphylococcus epidermidis*, which has been studied extensively under hemodynamic shear conditions (Shive *et al*, 1999; Wang *et al*, 1995, 1993a, 1993b; Vacheethasanee *et al*, 1998; Oga *et al*, 1993).

Escherichia coli is another bacterium that has received much publicity in the national press recently and is also a subject of adhesion studies with biomedical reference. *E.coli* is of great relevance in the pathogenesis of infections of mucosal membranes (Old, 1985), especially in the case of urinary tract infections, where the adhesion of the bacterium is dependent on the morphology of the cell, hydrophobicity, and the presence of fimbriae on the surface (Romano Carratelli *et al*, 1987).

The formation of dental plaque, and subsequent tooth decay and gum disease, can be expensive to treat, as well as painful, as many will verify from personal experience (Costerton and Lewandowski, 1997). The role of oral bacteria in this problem is a subject of study of Schilling and Doyle (1995), and Bos *et al* (1994) amongst others.

The recent development of extended wear contact lenses has caused concern with respect to lens related eye disease. Contact lenses will provide bacteria with a surface that will enable biofilm formation, and subsequent infection, and therefore subject to study (Schultz *et al*, 1995; Dart and Badenoch, 1986).

Methods of assessment of materials prior to their use is important to avoid potential problems with the use of new innovative materials used for biomedical implants. Biomaterials should be able to be biocompatible with the host, resist infection, and be physically strong enough to withstand deterioration during exposure to the host environment.

1.2.2.2 The Importance of Microbial Adhesion Studies in Bioprocesses

As stated above, the adhesion of bacteria is seen as detrimental to many manufacturing processes, and therefore needs to be avoided and controlled. To enable optimisation of the biocatalyst in immobilised cell bioreactors, the opposite is true, where cell adhesion and subsequent biofilm formation is essential (Lele *et al*, 1996, Casey *et al*, 2000).

The importance of colloidal and bacterial filtration is of great importance and is a subject of study using the Atomic Force Microscope (Bowen *et al,* 1999, 1998a, and 1998b). The assessment of particle adhesion to a material will determine the effectiveness of a filter made of that material. However, due to the size and the amphipathic character of cells, fouling of membranes is caused by the adhesion of cells, and consequently, characterisation of the adhesion process between specific cells and membrane surfaces is of great importance (Bowen *et al*, 1999).

Filtration of wine, for example removes the bacteria and yeast present from fermentation and maturation, producing an uncontaminated product (Ubeda and Briones, 1999), reducing the likelihood of spoilage or food-borne illnesses.

Food-borne illnesses are one of the most widespread health problems throughout the world, and have escalated in recent years. Health is not the only aspect with food contamination, as the cost of remedying these illnesses is estimated at up to £1 billion pounds per annum, with a loss of 8 million working days (Pritchard and Walker, 1998). Food processing and packaging has been identified as a factor in this, and therefore must be controlled by using aseptic packaging techniques, as well as reliable statistical analyses (Moruzzi *et al*, 2000).

The adherence of bacteria in food processing and its consequences is subject of an extensive review by Pontefract (1991) who recognises the importance of fast reliable methods to detect the presence of contaminant bacteria, so that cleaning and sanitising can be performed during processing rather than after a food-processing run.

Bacterial contamination is of great importance within the dairy industry, where milk is exposed to many potential pathogenic and non-pathogenic bacteria. A healthy cow will produce milk free from micro-organisms, but the farm environment makes the exclusion of bacteria whilst milking impossible. Milk can therefore contain

psychrotrophs, lactic acid bacteria, spore-forming gram-positive rods, coryneform bacteria, micrococci, and coliforms (Rukure and Bester, 2001). The formation of biofilms consisting of *Bacillus* and subsequent detachment of both spores and cells from the biofilms not only poses a hygiene problem, but also causes energy loses and blockages in equipment used in the processing of milk (Parkar *et al*, 2001). The importance of sterilisation of milk is emphasized by Crielly *et al* (1994), who state that *B.licheniformis* is the most common species in ex-farm milk, whilst *B.cereus* is less rare, but found in bulk tank milk, suggesting that the *B.cereus* spores have resistance to pasteurisation. A global approach to spore contamination of equipment is a necessity when treating the dairy processes, but has not yet been attempted (Faille *et al*, 2001).

The production of cheeses is a more biochemically dynamic process than the production of other dairy related products, and implementation of systems ensuring the quality of food standards with respect to cheese have enabled a remarkable improvement in product safety and quality in recent years (Arvanitoyannis and Mavropoulos, 2000), although contamination is still a problem in dairy products.

Fermentation processes are susceptible to contamination, as detailed with cheese production, but the contamination of fermentation processes is not limited to cheese production. The fermentation of beer, cider, and wine are also susceptible to contamination, from fungi on the corks, yeasts and acetic and lactic acid bacteria that are involved in the winemaking environment, and can contaminate up to 50% of unfiltered wines (Ubeda and Briones, 1999). Filtered wines, conversely, have minimal bacterial contaminants, and little yeast contamination. The adhesion of the cells to the process equipment must be inhibited, and the adhesion to the filtration membranes must be promoted, to minimise spoilage.

1.2.2.3 Environmental Aspects of Microbial Adhesion

The effect of the variation of soil heterogeneity on bacterial adhesion has been investigated Huysman and Verstraete (1993), Camesano *et al* (1999), Hermansson (1999), and Grolimund *et al* (1998). These papers study bacterial transport

throughout soils, as well as colloidal particle release (Khilar and Fogler, 1984), which bear great relevance throughout the environment.

Colloidal particles in natural porous media are usually immobile during normal electrolyte and flow conditions. However, when these conditions change, the particles can be released into the aqueous phase and can be transported through the porous media, enhancing the subsurface transport of contaminants sorbed onto the colloids' surface (Roy and Dzombak, 1996b), such as viruses and bacteria (Liu *et al*, 1995).

The transportation of contaminants is not the only problem associated with soils, as the release of colloids plays an important role in the deposition of clays in sediments, and in formation plugging due to artificial recharge or secondary oil recovery (Grolimund *et al*, 1998).

The treatment of wastewater is important when considering biofilm or fixed film reactors and is probably the largest single application of natural biofilm reactors. These methods allow the retention of biomass within a flow-through reactor independent of the liquid phase residency time. Such methods include fixed or packed bed reactors, fluidised beds, and completely mixed reactors (Bryers, 1984).

1.3 Colloidal Interactions

To take a fundamental approach to interactions occurring in the adhesion of particles to a collector surface, the essential processes occurring within adhesion must be considered. These essential processes take place at the sub-micron to molecular level, which is essentially the domain of colloidal interactions.

Colloidal particles range in size from approximately 0.01 to 5μm, and are therefore larger than most inorganic molecules and remain suspended in solution indefinitely. They are large molecules, such as proteins, or groups of molecules, and have many properties, depending on their large specific surface. A colloidal system is not a true solution, but it is not a suspension either, because it does not settle as a suspension will over time. Colloids can be charged and thus interact with long-range forces in a dispersion, as described later in this Section.

Examples of colloids are silver halide and gold sols, clays, polymer latex and silica particles. They play an important role in a numerous products, including polishing slurries, paints, emulsions, and foods.

Biological cells can therefore be considered in some respect as a colloid due to their size, although care must be taken where to differentiate between non-biological and biological particles. Latex beads (2μm) are used within this project, and remain suspended in a colloidal dispersion. The *Bacillus* spores used within this project range between 1 to 2μm (Husmark and Rönner, 1992).

There are three ways of interpreting and predicting the interaction of a biological cell and a collector surface. These are the thermodynamic approach, Derjaguin-Landay-Verwey-Overbeek (DLVO) theory, and an extended DLVO theory (ex-DLVO), and are explained below.

1.3.1 Thermodynamic Approach

The thermodynamic theory of cell adhesion incorporates the Dupré Equation, as shown in Equation 1.1, and considers the three interaction energies between the bacterium, collector, and liquid, (Luckham and Hartley, 1994; Hermansson, 1999).

$$\Delta G^{Adh} = \gamma_{bc} - \gamma_{bl} - \gamma_{lc} \qquad 1.1$$

ΔG^{Adh} represents Gibbs energy of bacterial adhesion, and can be described in terms of the energy between bacteria and collector (γ_{bc}), bacteria and liquid (γ_{bl}), and liquid and collector (γ_{lc}). The adhesion of the bacteria to the collector will occur when (ΔG^{Adh}) is positive. This approach assumes that the process is reversible, which in the case of bacteria, is not often the case. Put simply, if the Gibbs energy of the bacteria adhered to the collector is greater than the sum of the energy of the bacteria in solution and the liquid interacting with the collector, then the bacteria will be deposited onto the collector surface.

The thermodynamic approach has been observed to be applicable in some cases, and not in others (Hermansson, 1999), and for this reason not considered when analysing results within this project.

1.3.2 Derjaguin-Landay-Verwey-Overbeek (DLVO) Theory

The DLVO theory relates the stability of the colloidal dispersion to the energy potential between particle and collector, which is the sum of repulsive and attractive forces between particle and surface, shown in Figure 1.2, and is detailed in an extensive reviews by Hermansson (1999), Luckham and Hartley (1994), and to a lesser extent by Rijnaarts *et al* (1999) with respect to bacterial deposition.

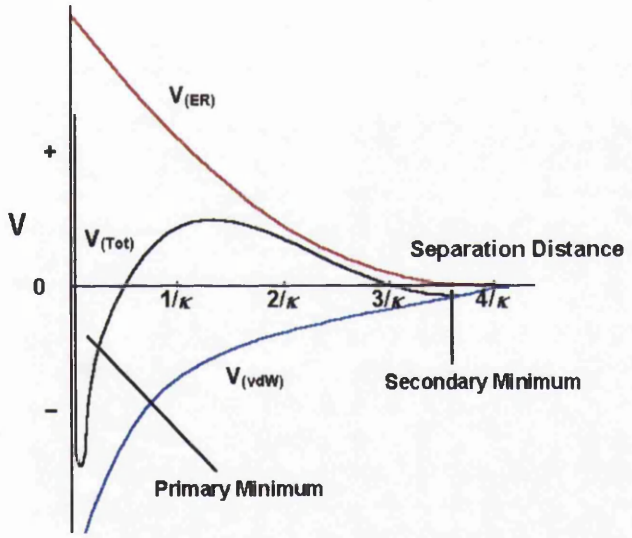

Figure 1.2: The total potential energy of interaction (V_{Tot}), where (V_{ER}) is the potential energy of repulsion due to the electrostatic contribution, and (V_{vdW}) is the total attractive forces due to van der Waals forces.

When two surfaces approach in an electrolyte solution (i.e. as separation distance decreases), their first interaction will be attractive and will be a secondary energy minimum, of low energy level, as shown in Figure 1.2. As the surfaces come closer, a repulsive electrostatic force of high energy will come into action. The electrostatic force is affected by ionic strength of the environment. If the two surfaces have sufficient energy to pass the repulsive barrier, they will fall into a primary attractive minimum a few angstroms apart, and adhesive bonds can form (Weiss, 1968). If separation is reduced, short-range forces dominate the DLVO forces. These short-range forces include the formation of covalent bonds, dipole, and solvation forces, and are considered in Section 1.3.4.

The net interaction, V_{Tot}, can be described using Equation 1.2.

$$V_{Tot} = V_{vdW} + V_{ER} \qquad 1.2$$

where V_{ER} and V_{vdW} represent the electrostatic repulsion and van der Waals' interaction respectively, which are considered separately below in Sections 1.3.2.1 and 1.3.2.2.

1.3.2.1 Electrostatic Repulsion

Electrostatic repulsion is generated by over-lapping of electrical double layers, due to the increased presence of ions in the vicinity of the colloidal particle, and therefore greater osmotic potential. This interaction is therefore affected by the presence of surrounding ions, which are present around the surface of the colloid, and form electrical double layers, as shown in Figure 1.3.

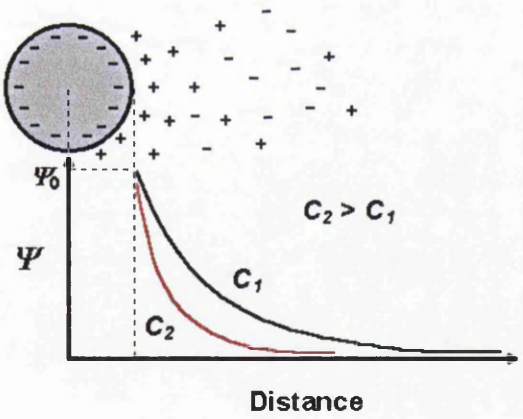

Figure 1.3: The electrostatic potential (Ψ) near an electrically charged colloidal particle. Curve C_2 represents a higher electrolyte concentration than C_1.

The size of the electrical double layer is affected by the ionic strength of the surrounding solution, as the effect of the osmotic potential of the ions in the vicinity of the charged colloid is masked. The thickness of the electrical double layer is inversely proportional to the Debye length (κ). The contribution of electrostatic repulsion (V_{ER}) to DLVO forces can therefore be related to the surface potential (Ψ) and Debye length (κ), where:

$$V_{ER} \propto \Psi^2 e^{-\kappa d} \qquad 1.3$$

Therefore, at high ionic strength, the double layer thickness decreases, and the net interaction of will be governed increasingly by van der Waals contributions (i.e. more attractive). Conversely, at low ionic strengths the electrostatic potential (i.e. repulsion) is comparable or greater than van der Waals forces (Huang *et al*, 1997). The variation of the magnitude of the repulsive electrostatic contribution therefore affects the total interaction as defined in Equation 1.2. van der Waals forces are unaffected by ionic strength, and consequently differing graphs representing the interaction energy of the approach of the colloid to a surface are obtained, as shown in Figure 1.4. Curve A represents a low electrolyte concentration where the electrostatic repulsion is large, Curve B represents a moderate electrolyte concentration where the electrostatic repulsion is approximately the same as the attractive van der Waals forces, and curve C represents a high electrolyte concentration, where the electrical double layer is negated, and therefore the predominant force is the contribution of the van der Waals forces.

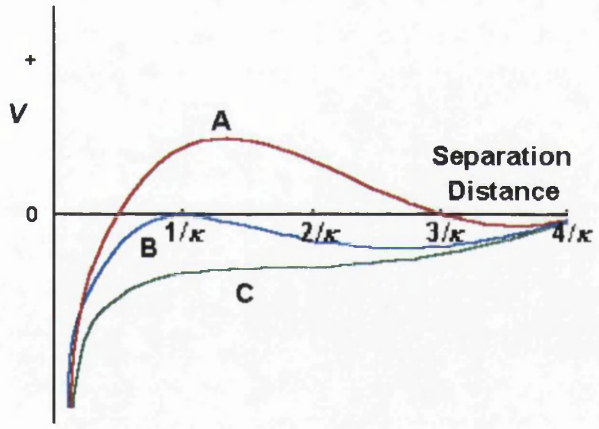

Figure 1.4: The total interaction energies of a low electrolyte concentration (A), a moderate electrolyte concentration (B), and a high electrolyte concentration (C).

Evaluating the surface charge of the colloid and consideration of the electrolyte concentration can be used to assess the contribution of the electrostatic repulsion. Surface charge can be evaluated by the measurement of zeta potentials (Harkes *et al*, 1991).

1.3.2.2 van der Waals (vdW) Forces

As stated, the approach of a cell to a surface is governed initially by the electrostatic repulsion, and then by attractive vdW forces as the separation distance is reduced. For two identical particles, vdW is always attractive and dominates at very close distance, and also at long distance, as shown in Figure 1.2. The electrostatic force is generally repulsive and dominates at intermediate distance (Butkus and Grasso, 1998).

The vdW forces are a result of electromagnetic coupling of surfaces and differ between particles, and result in preferential deposition of different particle types. The forces are not however affected by electrolyte concentration.

The vdW interaction (V_{vdW}) can be defined as:

$$V_{vdW} = -AR / 6d \qquad 1.4$$

where A is the Hamaker constant, d is the separation distance between cell and collector, and R is the radius of the cell.

1.3.2.3 Summary of DLVO Theory

The total interaction energy of a colloidal particle approaching a surface can be interpreted as the sum of attractive van der Waals forces and the Electrostatic repulsion, as shown in Equation 1.2. The total interaction energy between a colloid and a surface is affected by the electrolyte concentration, and the surface type, which consequently affect the electrical double layer (and therefore electrostatic repulsion) and electromagnetic coupling (and therefore van der Waals forces) respectively.

The DLVO theory assumes that the subject particles are hard non-deformable surfaces, which possess well-defined homogenous surfaces. The assumption

discards hydration and steric interactions, as biochemical interactions are not considered, and water is assumed to be a continuous fluid.

As a result of these assumptions, the DLVO theory essentially relates to the sum of electrostatic repulsion and van der Waals forces, and discards the effect of interactions derived, for example from the interaction of the spores' surface molecules.

The latex beads and the *Bacillus* spores used in this project are negatively charged. When considering this, the electrostatic interaction is repulsive experienced between the collectors and the colloidal particles used within this project. However, the spore does not behave as a simple colloid, due to the process of deformation and the presence of extracellular structures that are not considered in the DLVO theory.

1.3.3. Surface Hydrophobicity

The DLVO theory does not consider hydrophobicity, and is one reason why there are so many exceptions to the theory (Hermansson, 1999). When considering the attachment of a variety of bacteria to negatively charged latex, van Loosdrecht *et al*, (1987), showed that hydrophobicity was the dominating influence on adhesion. The measurement of hydrophobicity has been performed in several ways, but only contact angle measurement (CAM) gives a quantitative measurement of surface wettability. Details of the various methods of measuring hydrophobicity are given below in Section 1.6.4.2.

Hydrophobic interactions originate from the hydrogen bonding of water molecules, and therefore the high internal cohesiveness of water (van Oss, 1995). No relationship between hydrophobicity and charge was found, when considering the adhesion of different bacteria (Vacheethasanee *et al*, 1998). Vacheethasanee also concluded that collector hydrophobicity contributed more to cellular attachment than the hydrophobicity of the cell itself.

Bacterial hydrophobicity was the main factor of adhesion to sandy soil, whereas it was of minor importance to adhesion to loam (Huysman and Verstraete, 1993).

Sorongon *et al* (1991), however, concluded that hydrophobicity could only be used as a method of prediction of attachment of closely related strains.

Hydrophobicity contributes to the attachment of a colloid especially to hydrophobic surfaces, but its influence relative to other interactions is indeterminable, as the hydrophobicity is a relative unknown. The hydrophobic force can be taken into consideration when applying an extended DLVO theory.

1.3.4 Extended DLVO Theory (ex-DLVO)

The DLVO theory can be extended to consider other forces between a colloid and a surface, such as hydration pressure, hydrogen bonding forces, hydrophobic effects, solvation forces, disjoining pressure, structural forces, and Lewis acid-base forces (Isrealachvili and Wennerstrom, 1996), which may play a significant role in adhesion and detachment. The ability to predict adhesion however is affected by the presence of non-DLVO forces, which are poorly understood. The forces affecting the interaction are thought to arise from the solvent-boundary layer at the interface (Elimelech *et al*, 1995). The total interaction energy (ΔG^{adh}) can be considered as the sum of electrostatic double layer (ΔG^{dl}), vdW forces (ΔG^{vdW}), and Lewis acid-base interaction energies (ΔG^{AB}), shown in Equation 1.5.

$$\Delta G^{adh} = + \Delta G^{dl} + \Delta G^{AB} + \Delta G^{vdW} \qquad \textbf{1.5}$$

ΔG^{AB} describes attractive hydrophobic interactions and repulsive effect that can be up to 100 fold stronger than the vdW interaction (van Oss, 1995). Work performed by Meinders *et al* (1995), showed that the ex-DLVO theory was better at predicting attachment than the classical DLVO theory, but did not agree quantitatively with experimental data. The ex-DLVO theory is simply adapted to systems that cannot explain the experimental data compared with the theoretical predictions using the standard DLVO theory.

1.3.5 Summary of the Colloidal Interaction

Cellular attachment to a collector surface is not an exact science, but there seems to be cases which support the treatment of cells in a colloidal manner, and therefore DLVO and thermodynamic theories maybe relevant in different phases in adhesion and under differing environmental conditions (Hermansson *et al*, 1999; Rijnaarts *et al*, 1999).

1.4 The Contribution of Cell Surface Morphology to Adhesion

The theories above do not take into account the diversity of most biological cells. The dimensions and negative charge of cells and spores are similar to those of colloidal particles (Gatenholm *et al*, 1988). This subsequently results in spores being considered as colloidal particles, and as a consequence, forces that occur between colloidal particles and collector surfaces. As stated above, there are other interactions that are not considered, as attachment of bacteria surfaces may be controlled by an interplay between extended DLVO and polymer interactions the balance of which depends on many factors (Jucker *et al* 1998). The following characteristics are properties that are exclusive to bacterial cells that contribute to their adhesion.

1.4.1 Bacterial Cell Structure

This Section describes bacterial cell structure. The structure of *Bacillus* spores is described in Section 1.7.2. The interaction of a cell with a surface contains many different interactions. The complexity of this interaction is due to the diversity of molecules contained within the cell membrane.

The bacterial cell is surrounded by the cell membrane, a fluid bi-layer of phospholipids interspersed with proteins of varying penetration, as described by the Singer-Nicolson Fluid Mosaic model (Singer and Nicolson, 1972).

The main constituents of the membrane are phospholipids, which are dipolar due to the presence of a phosphate/charged residue group, and two fatty acid hydrophobic chains.

The most important aspect of the Singer-Nicolson model is the fact that the membrane is fluid. Both phospholipids and proteins can move laterally within the membrane. Bacteria also have a peptidoglycan layer surrounding the membrane, and in the case of gram-negative bacteria, a further bi-layer outside this consisting of lipoprotein, shown in Figure 1.5.

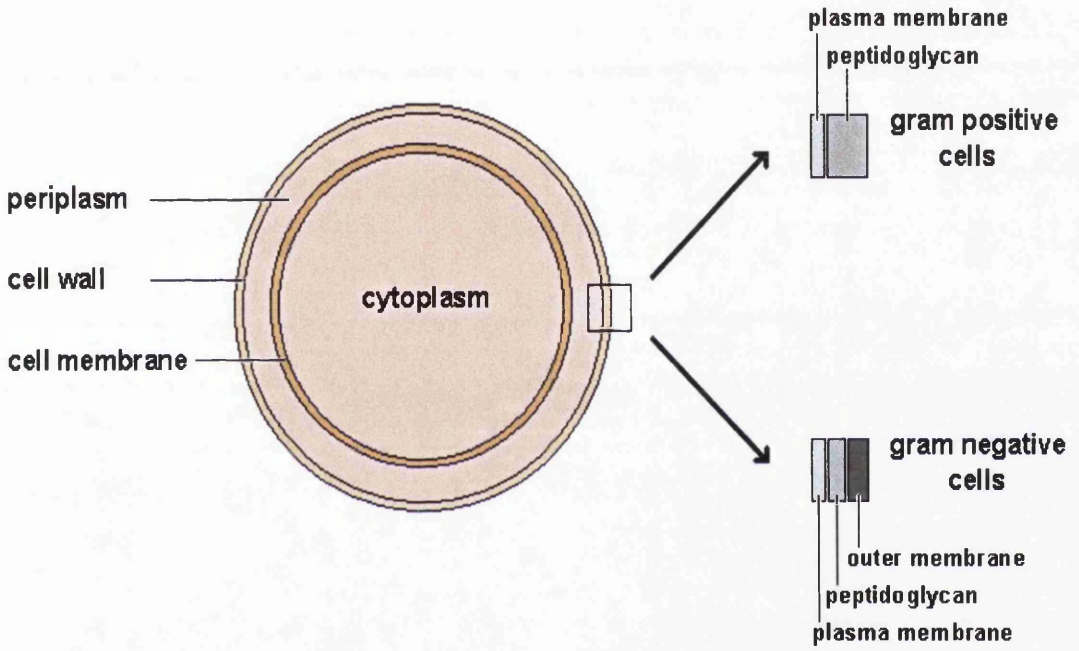

Figure 1.5: The schematic cell structure of gram-positive and gram-negative cells.

The peptidoglycan layer of gram-positive cells can be up to 80nm thick, and primarily consist of N-acetylmuramic acid and N-acetylglucosamine, providing a three-dimensional structure with high mechanical strength, with strands running parallel and perpendicular to the plasma membrane. The peptidoglycan layer of gram-negative cells is a 3-dimensional complex polymer, with a further membrane outside consisting of a phospholipids bi-layer, interspersed with proteins and lipopolysaccharides.

Although the membrane gives the cell an overall negative charge, long-range interactions of the surface are dominated by the effects of the cell wall (Luckham and Hartley, 1994). The presence of negative lipopolysaccharides, which constitute

the outermost cell surface of gram-negative bacteria contribute to the electrostatic repulsion of the cells from a negative collector surface (Jucker *et al*, 1998).

The result of the structural differences between gram-positive and gram-negative bacteria, and variations within the species-specific composition of the cell walls and membranes is the large variation in the adhesive contribution of the morphology of the surface, as exemplified by Husmark and Rönner (1992), when studying the spores of the *Bacillus* species. The structure of the cell therefore has several consequences on adhesion. Firstly, the cell cannot be treated as a simple colloidal particle with respect to the interaction described in the DLVO theory, as detailed in Section 1.3.2. Secondly, the cell wall varies in composition, and the resulting interaction will therefore be a result of the interaction of many molecules with the collector surface. This will result in variation of the interaction, as detailed below in Section 1.5.2. Finally, when considering the DLVO theory, molecular structures on the cell surface are not considered (Hermansson, 1999). However, these structures are the first components of the cell to interact with the collector surface as depicted in Figure 1.1, and are subjected to DLVO forces independent of the cell wall, and can possess differing characteristics to the main bulk of the cell (Harkes *et al*, 1991).

1.4.2 The Contribution of Specific Adhesion Molecules

Specialised macromolecules on the cell have specialised functions with respect to adhesion. Flagella, cilia, fimbriae and pili have functions in propulsion and reproduction, but also contribute largely in surface recognition and subsequent attachment (Luckham and Hartley, 1994). These molecules can extend over larger distances than the interactive forces that are considered in the DLVO theory.

Bunt *et al* (1995) claim that the second irreversible stage of adhesion was due to the presence of fimbriae on the cell surface of *E.coli*, the effect of which can be determined by studying the adhesion of latex particles, which do not possess surface structures, due to the non-biological nature of the beads (Meinders *et al*, 1995).

The complexity of the cell surface, and its constituent structures, therefore contribute to the diversity in adhesion between species, as well as within a species.

This diversity also contributes to local charge and hydrophobicity heterogeneity on individual cells (Walz, 1998). The study and characterisation of these molecules is therefore required if a fundamental and systematic approach to cellular adhesion is to be taken, as will be discussed in Section 9.4.

1.4.3 The Contribution of Non Specific Molecular Adhesion

Steric interactions occur when one or both of the interacting surfaces have surface molecules, whether they are components of a cell, or a conditioning layer on the collector surface. In the case of cells, the species-specific surface layers contain molecules that contribute to cellular attachment. These molecules are not designed specifically to aid adhesion or recognition, but fulfil other cellular functions. The molecules can be polysaccharides, proteins, glycoproteins, or proteoglycans. There is a high degree of heterogeneity within these molecules, as the base units of each polymer may possess either positive or negative charge, and vary greatly in hydrophobicity (Walz, 1998).

Using these materials at low ionic concentration, DLVO forces were observed dominantly repulsive, and at higher concentrations, steric interactions were dominant. The transition is determined by the extent to which macromolecules extend into the medium. Steric interactions either promote adhesion by bridging, or inhibit adhesion by steric repulsion (Rijnaarts *et al*, 1999).

The molecular structure of the cell wall interspersed with proteins is much more complicated than the hard, non-deformable sphere considered in the DLVO theory, and therefore must be considered carefully when applying the DLVO theory to the adhesion of cells.

1.4.4 Surface Conditioning and Biofilm Formation

The work performed in this project considers the adhesion of latex beads and *Bacillus* spores to naked collector surfaces. However, in natural environments, the first substances associated with the surface are not bacteria, but trace organics.

Almost immediately after the clean surface comes into contact with water, an organic layer deposits on the water/solid interface (Mittelman 1995). These organic molecules form a conditioning layer that neutralizes excessive surface charge and surface free energy that may prevent the initial adhesive interaction (Figure 1.1). In addition, the adsorbed organic molecules often serve as a nutrient source for bacteria, and are therefore beneficial to subsequent biofilm formation, the third and final stage in the process (Costerton *et al*, 1999).

The formation of biofilms combines both cells and extra-cellular macromolecules, allowing the protection of bacteria from threats posed by the environment (An and Friedman, 1997; Costerton and Lappin-Scott, 1995). Although latex beads cannot form biofilms, due to their non-biological properties, they do require increased shear stress to remove when in large aggregates (Yamamoto *et al*, 1994).

The biofilm is predominantly occupied by the loosely organized glycocalyx matrix than by bacterial cells. The high water content of the glycocalyx renders any surface covered in a biofilm gelatinous and slippery. As well as trapping nutrient molecules, the glycocalyx net also snares other types of microbial cells through physical restraint and electrostatic interaction. Attached bacteria produce extracellular protein that increase the adhesive strength of the cell, and promote the adhesion of other cells (Boulange-Petermann, 1996; Rijnaarts *et al*, 1996b). These secondary colonizers metabolise wastes from the primary colonizers as well as produce their own waste, which other cells then use in turn. These other bacteria and fungi become associated with the surface following colonization by the pioneering species over a matter of days, and *in vivo* can contain complexes of many differing species (Becker, 1998).

This is exemplified by dental plaque formation, where initial colonies are of gram positive bacteria are followed by gram negative bacteria to form a biofilm of up to 80μm thick, showing co-adhesion Bos *et al* (1994). Even in the case of *S.epidermidis* adhesion to biomedical polymers, the presence of host platelets increases adhesion (Wang *et al*, 1993a). The same bacteria were shown to produce connective strands, and that the resulting background matrix enclosed bacterial colonies (Oga *et al*, 1993).

Therefore, once a biofilm is formed it is very difficult to remove either physically or chemically, and the inhibition of the initial adhesion is necessary to inhibit the subsequent formation of biofilms.

1.5 Importance of Colloid and Collector Surface Heterogeneity

When considering the interaction of molecularly smooth surfaces, practical results and theoretical predictions are in general agreement. However, when these experiments are performed with more natural particles, there are significant differences in adhesion compared to those predicted. This has been explained by heterogeneity of the interacting surfaces, and can result from variation of roughness, hydrophobicity, and surface charge (Walz, 1998), and this is acknowledged by Stollenwerk *et al* (1998), who show that differing *Staphylococcus* strains adherence to biomedical polymers is "patchy". Surface heterogeneity is the common reason for the deviation from expected values when assessing attachment of biological colloids using various methods.

There are several ways in which surface heterogeneity can affect the interaction between colloid and collector, as there are different contributions to the interaction, as detailed above in Section 1.3. These are reviewed extensively by Walz (1998), and examples are given below.

1.5.1 Heterogeneity of Collector Surface Characteristics

The DLVO theory considers the interaction between non-deformable smooth surfaces, as discussed in Section 1.3.2. It is assumed that the particle surface is smooth, relative to the collector surface roughness. Surface roughness is a qualitative measurement, and is relative to the size of the interacting particle. In the case of the work performed in this project, the collector surfaces are assumed to be smooth, as the average surface roughness was 0.5% of the assumed size of the

interacting particles, as discussed in Section 4.3. The factors to be considered when assessing surface roughness are reviewed by Verran and Boyd (2001).

The measurement of surface roughness on the nanometer scale can be performed using the atomic force microscope (AFM). The 3-dimensional analysis of surfaces has acknowledged that the profile of rough surfaces has a fractal appearance, i.e. the same probability distribution of the magnified and original surfaces. Considering this, the roughness must therefore be measured at the most relevant scale compared with the particle (Verran and Boyd, 2001). Features on the nanometer scale, for example, affects the adhesion of conditioning molecules, as discussed in Section 1.4.4.

Variation in surface roughness can affect the attachment of colloids in three ways. The first is that surface roughness can totally disrupt the ordering of solvent molecules (Nakae *et al*, 1998), even on a scale of molecular dimensions, and therefore disrupt forces between collector and colloid dependent on this (Walz, 1998).

The second is that surface roughness provides variation in contact area between collector and colloid, subsequently increasing the number of contact points between the two surfaces as shown in Figure 1.6.

Finally, the surface roughness can provide the adhered cell with differing exposures to shear force, and is one of the contributing factors as to why bacteria form biofilms, as detailed in Section 1.4.4, and as shown in Figure 1.7.

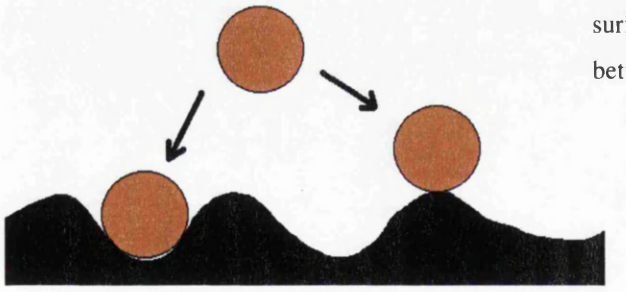

Figure 1.6: Colloid interaction with a rough surface, highlighting the variability of contact area between colloid and collector.

Predictions of adhesion do show good agreement with theory, if the surface is molecularly smooth, for example, mica. However, when considering more natural surfaces such as glass and stainless steel, substantial discrepancies in adhesion are

observed (Walz, 1998), which was confirmed by Wang *et al* (1995), when considering the effect of both surface tension and roughness on the adhesion of *S.epidermidis* to biomedical polymers.

Titanium of varying surface roughness was used to observe the *in vivo* colonisation of oral bacteria, and two important observations were made. Firstly, more plaque formation occurred with rougher surfaces. Secondly, colonisation occurred over badly polished areas (Rimondi *et al*, 1997), showing that surface roughness and surface preparation must be consistent when considering cellular adhesion.

The contribution of surface roughness to attachment is not only a physical effect. When considering forces between the particle and collector, surface roughness has no effect on the vdW interaction, when the roughness is much smaller than the surface separation distance. The opposite is true with the electrostatic contribution, where the effect of roughness remains significant over large separation distances (Walz, 1998).

The effect of roughness contributes mostly to the adhesion of bacteria to soils and packed beds, which is of great importance when considering the Packed Column method used within this project (Huysman and Verstraete, 1993).

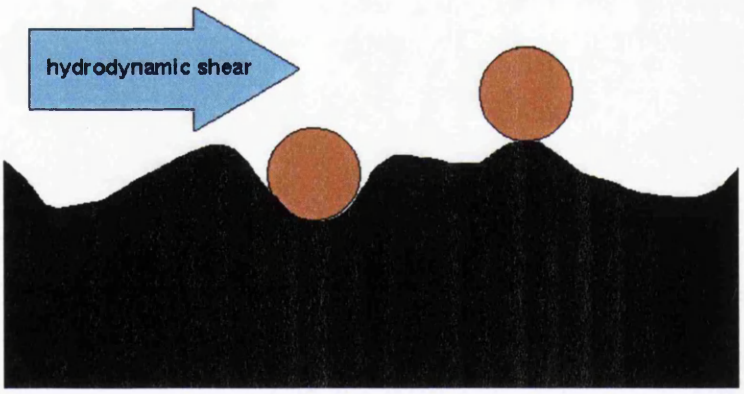

Figure 1.7: The effect of surface roughness on the exposure of adhered cells to hydrodynamic force. The particle on the right will be exposed to the full hydrodynamic shear force, whereas the particle on the left will not.

The roughness of the collector is not the only contributing factor to the variation in adhesion levels. Local areas of charge and hydrophobicity also affect the interaction, and details are given below in Section 1.5.3, as these affect both the collector and the colloid. The composition of differing alloys is also important. For example, stainless steel is comparable to glass for cleanability, as well as disinfection capability but consideration must be given to is composition, which can vary, and result in differing adhesion characteristics (Boulange-Petermann, 1996).

1.5.2 Heterogeneity of Colloids

There is substantially more scope for variation in adhesion when considering the properties of cells that are susceptible to heterogeneity due to their structural complexity. Living cells and spores show much more complexity than the hard, non-deformable spheres that are taken into consideration in adhesion theories, as described in Section 1.3.

Variation in charge and hydrophobicity can affect the cell as a whole, as well as within individual surface molecules. For example, individual flagella and pili may have differing local zeta potentials throughout the molecule (Harkes *et al*, 1991).

The location of these surface structures can also vary over the cell surface, as a result of the fluid membrane. Different methods of assessing hydrophobic characteristics showed that localised hydrophobicity existed in an otherwise hydrophilic cell (Sorongon *et al*, 1991).

There is also variation within a population of cells as to the composition of the cell wall and membrane. Heterogeneity in receptor number may cause an overall heterogeneity, which can affect both colloid and collector surfaces (Goldstein and DiMilla, 1997). The hydrophobicity of *Bacillus* spores varies greatly throughout species, due to structural variations (Husmark and Rönner, 1992; Wiencek *et al*, 1990). Spores are also subject to variation due to the age of the spore (Hermansson, 1999), a property which is also seen with bacterial populations (Sonak and Bhosle, 1995). Consequently, the preparation of the colloids must be consistent to minimise the heterogeneity within a population of cells.

1.5.3 Factors Affecting Both Collector and Colloid

Human error also contributes to the effect of variation in surface heterogeneity. Measurements with materials not carefully selected or treated consistently provide poor agreement (Walz, 1998), highlighted by Rimondi *et al* (1997), who observed that badly polished surfaces resulted in an increase in biofilm formation. The influence of electrochemical heterogeneity of both surfaces is important. The measurement of zeta potential allows the overall characteristics of a population of

colloids to be analysed but, as stated, there is heterogeneity at all levels throughout the population. The deposition of colloids on an oppositely charged collector is not affected by heterogeneity in surface charge, highlighted by the deposition of negative silica on a positive polymer, which showed good agreement with theoretical values. This was not true for the interaction between negative particles and negative surface, and was blamed on the theory not taking into consideration the surface heterogeneity (Bowen and Epstein, 1979). Hull and Kitchener (1969), used polystyrene spheres on smooth plastic films, and demonstrated that in favourable conditions (i.e. oppositely charged), there was good agreement with predicted values. In unfavourable conditions, adherence was magnitudes higher than predicted, initially blamed on surface topography, but then attributed to non-uniform surface charge density. The same observation was made when studying the deposition of latex beads onto glass (Elimelech and O'Melia, 1990). Heterogeneity, therefore, does not only affect biological cells, but also non-biological particles, as well as the collector surface.

1.5.4 Summary

The effect of heterogeneity of both collector and colloid cannot be underestimated (Roy and Dzombak, 1996b). Surface charge, hydrophobicity, and topography all contribute at various levels throughout the interaction, making prediction of the interaction very complex, as shown in Figure 1.8. This is summarised by Litton and Olson (1993), who state that the discrepancy between theoretical and practical deposition rates is not known, and that dynamic interaction factors, surface roughness, heterogeneous surface potentials for both particles and collectors all contribute in varying amounts.

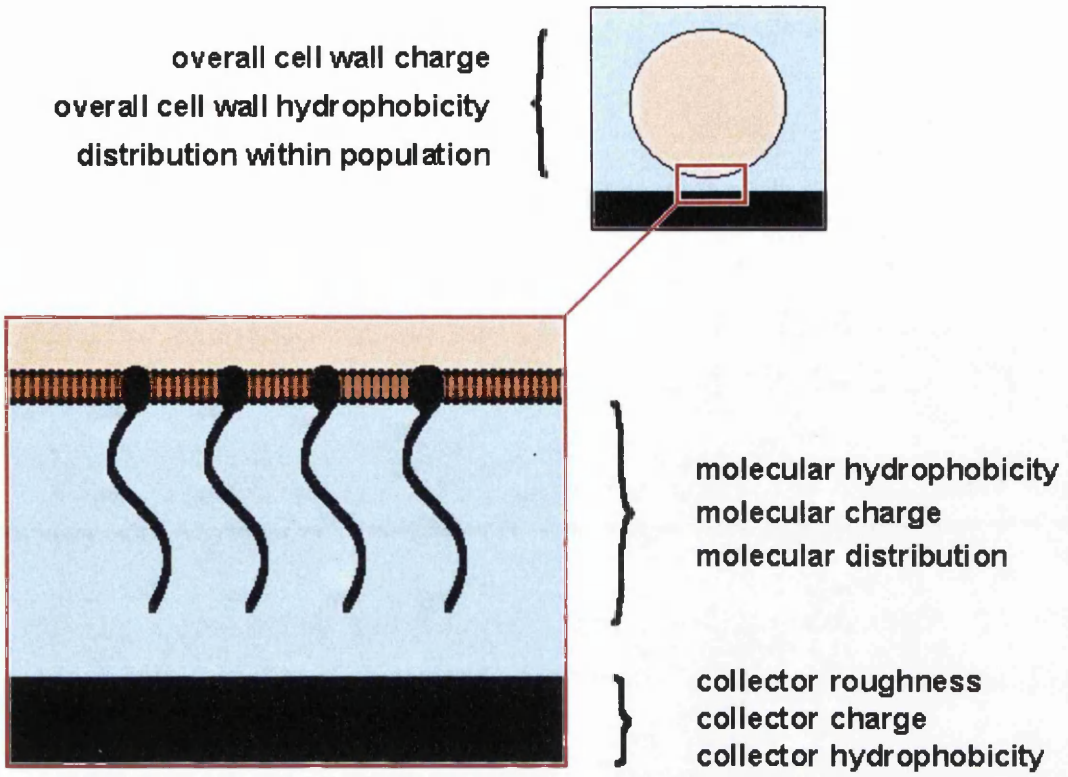

Figure 1.8: The different levels heterogeneity can affect the adhesion of a population of cells/particles to a collector surface. This shows the potential variation within a population, and variation on the cell/particle surface, and molecules thereon, as well as the collector surface.

1.6 Methods of Assessment of Microbial Adhesion

There have been many studies conducted on the adhesion of microbes to surfaces. There have been few, however that provide results that conform to adhesion theories without exception, for the reasons that have been detailed above. There have been none that accurately determine the force of adhesion, which can be attributed to the complexity of the many forces that influence the adhesion of a cell to a surface.

Previous methods of assessment and/or prediction of adhesion can be divided into two categories. The first category involves the application of hydrodynamic shear stress, theoretically allowing a measurement of shear stress that either removes cells, or inhibits adhesion. Depending on the method incorporated to study adhesion, shear stress can be calculated with relative accuracy allowing the dependence of cellular attachment on shear stress to be considered. The second

category are those methods that do not apply any shear force to the adhered particle but qualitatively assess the effect of solution chemistry, and colloid and collector properties.

A brief review on previous methods and techniques used to assess bacterial adhesion is given by An and Friedman (1997).

Two of the three methods used in this project are shear dependent, namely, the Spinning Disc and the Radial Flow Chamber. A third method, the Packed Column, does not use applied shear force to inhibit adhesion (Bergendahl and Grasso, 1999).

1.6.1 The Use of the Packed Column to Assess Microbial Adhesion

The use of the Packed Column provides a method of studying processes that occur in soils, as well as packed bed reactors and filters, and therefore has relevance throughout the environment as well as bioprocess engineering.

1.6.1.1 Theory and Relevance of the Packed Column in Microbial Attachment

As stated, the Packed Column method allows the study of adhesion to granular collector surfaces, and subsequently cannot gauge the effect of surface roughness, as this cannot be measured or kept constant. The colloid surface is assumed to be smooth, as any variation in surface roughness of the colloid will be insignificant compared to the collector (Vaidyanathan and Tien, 1988).

The kinetics of the deposition and detachment of colloids within a packed bed is governed by two factors. The first is the solution chemistry, which determines the forces between collector and colloid. The second is the hydrodynamic properties of a packed bed, and therefore the rate at which the colloids are transported to the collector surface (van de Ven, 1998). The flow geometry within the column is poorly defined compared to those of the Radial Flow Chamber and the Spinning

Disc (van de Ven, 1998) and all particles are assumed that have an equal chance of interaction with the surface.

As stated in Section 1.1, microbial adhesion consists of three phases. The Packed Column allows the assessment of the first two phases of adhesion in a two-site model of both reversible and irreversible binding, as demonstrated by Yan (1996), who estimated the rate constants of deposition and detachment by analysing the resulting breakthrough curves from the column.

When considering the interaction between a particle and collector within the packed column, the particle can: i) adhere, ii) rebound, iii) slide along or iv) roll along. The likelihood of rebounding is very low, due to the low particle inertia, flexibility, and deformability (Vaidyanathan and Tien, 1988), consistent with the findings of Yan (1996), where reversible binding refers to sliding or rolling along the surface.

When performing experiments with the Packed Column, similarly charged collectors and colloids must be used. If oppositely charged particles are used, particle deposition is essentially irreversible (Liu *et al*, 1995), and saturation of the column will occur, resulting in minimal recovery, (Ruckenstein and Prieve, 1976). The materials used within this project are all negatively charged except in the case of *B.mycoides* spores at pH 3.5, as shown in Chapter 3, although this has no effect on the spores' deposition compared with that observed at higher pH.

1.6.1.2 Previous Studies of Attachment Performed with the Packed Column

The Packed Column technique has been employed with many different subjects of study, and is not just limited to colloidal adhesion. The study of the behaviour of polypeptides and isolated proteins on an ion exchange column showed that the average bond energy of globular proteins were comparable to the bond energies of positively charged amino acid residues such as arginine and lysine. This observation suggested that, although negative residues are present, the interaction of the positive residues of a protein with the negative collector surface governed adhesion (Gerstner *et al*, 1994).

Jucker *et al* (1998) also investigated the adhesion of molecules to a Packed Column, when assessing the contribution of lipopolysaccharides (LPS) to the adhesion of five gram-negative bacteria to glass. The LPS form micelles in water, and can be treated as colloidal material, although the molecules can extend 50nm into water. This allowed the comparison of the isolated LPS with the adhesive characteristics of the respective cells, which demonstrated that the LPS contribute significantly to the adhesive characteristics of the cell.

The attachment and detachment of non-biological colloids has been studied extensively to determine the effects of solution upon the adhesion and release of the colloid, and assess predictions made by the DLVO theory. Detachment of hematite from glass, for example, was studied by Kallay *et al* (1986), who demonstrated that the release of hematite particles was not as predicted, which was attributed to redeposition. A further example of the use of packed beds in conjunction with non-biological colloids is the testing of two newly developed models of hydrosol deposition within packed columns (Vaidyanathan and Tien, 1988). The models produced results that more closely agreed with experimental data than previous models, but were still substantially different, although the authors claimed qualitative agreement. More relevant work has been performed on carboxylated latex beads in conjunction with quartz sand and silica, which demonstrates the importance of consistent collector surface preparation (Litton and Olson, 1993). Liu *et al* (1995), also investigated the interaction of aminated latex beads to glass. The positive amine groups did not significantly affect the charge of the latex beads, with zeta potential measurements or adhesion assay observations. Roy and Dzombak (1996a) determined that both ionic strength and ion selectivity affect latex bead release from glass, and this must be taken into consideration when considering natural systems. Further work showed that reduction in ionic strength increased particle release, as the double layer became larger, therefore increasing the electrostatic repulsion between the two surfaces (Roy and Dzombak, 1996b). The same observation was also made by Yan (1996) when the adhesion of sulphated latex beads was studied in conjunction with glass.

The deposition of bacteria within packed columns has been performed demonstrating the effects of hydrophobicity and charge using different soils, teflon, and Glass (Rijnaarts *et al*, 1996a and 1996b; Huysman and Verstraete, 1993).

These examples show that a variety of parameters have been investigated when using the Packed Column as a method of analysing colloidal attachment, whether the system is a biological or non-biological system. Most of these investigations compare their observations to surface charge and hydrophobicity, and generally show good qualitative agreement, although levels of adhesion cannot be predicted in most cases.

1.6.2 The Use of the Spinning Disc to Assess Microbial Adhesion

The use of the Spinning Disc provides a method of applying shear force to a flat surface. The rheology of the Spinning Disc has been well characterised, and shear can be calculated at any radial point on the disc, knowing the angular velocity.

1.6.2.1 Theory and Relevance of the Spinning Disc in Microbial Attachment

The theoretical aspects of the use of the Spinning Disc when measuring adhesion are given in Chapter 6. The Spinning Disc allows a shear gradient to be generated across the collector surface. When rotating in colloidal suspension, liquid is drawn up axially and gains rotational velocity and consequently, the liquid exits radially. As the radial distance increases, the applied shear force across the surface increases linearly. The theory of the Disc's behaviour is described extensively by Benton (1966), Levich (1962), and Daily and Nece (1960).

The benefits of employing the Spinning Disc to study microbial attachment are clear. Firstly, the method provides a linear shear gradient across the surface, allowing the effect of shear force to be examined. Secondly, the flow across the disc has been well studied and characterised, allowing calculation of the applied shear stress at any point on the Disc's surface. Thirdly, the simplicity of the Disc provides a surface of study that can be prepared with relative ease compared with surfaces used in conjunction with the Packed Column. The flat nature of the Spinning Disc

allows both polishing, and subsequent determination of the collector surface topography. This removes the effect of surface roughness that can provide tangential forces that of the same magnitude of DLVO forces (Hermansson, 1999). For the same reason, any surface can be studied, whether it is glass, metal or polymer, and these surfaces can be subjected to surface treatments, affecting their adhesive characteristics (Wang *et al*, 1995, 1993a and b).

Finally, the shear generated within the system can be compared to the forces that cells would be exposed to in hemo- or hydrodynamic conditions (Garcia *et al*, 1997). This makes the use of the Spinning Disc relevant throughout the areas of research detailed in Section 1.2.2.

1.6.2.2 Previous Studies of Colloidal Attachment Performed with the Spinning Disc Technique

The first application of the Spinning Disc technique to study cell adhesion was performed by Leonard Weiss (1961), when he considered the attachment of rat fibroblasts to treated and untreated glass. Interpretation of the resulting data proved to be problematic, but the experiments showed that the applied adhesion force varied depending on the method used to apply the forces. The first comprehensive study of the Spinning Disc used to assess colloidal adhesion to a surface was the deposition of carbon particles to glass, three polymers, and regenerated cellulose (Marshall and Kitchener, 1966), and the work suggested that deposition would only occur with unstable colloidal suspensions. The paper also set a trend when reporting that although adhesion qualitatively agreed with DLVO theory, values of adhesion were higher than predicted, when considering similarly charged colloid/collector combinations. The reason given for these discrepancies was the variation in particle and surface roughness, discussed in Section 1.5.

Clint *et al* (1973) investigated the deposition of polystyrene beads onto polystyrene surfaces, which showed that the DLVO theory could be used accurately when taking into consideration the fact that co-aggregation of particles occurred in solution. Although the paper states that the system is sensitive to variation in disc potential, the interaction of polystyrene surfaces does agree with theoretical

predictions. More recent work on the adhesion of *Staphylococcus epidermidis* has been carried out by Wang *et al* (1993a and 1993b), assessing the effect on adhesion of the characteristics of biomedical polymers, and surface treatment using biomolecules. The papers showed that adhesion did indeed decrease as shear stress increased, and also demonstrated that the system can be successfully used in conjunction with various polymers and surface treatments. Further work by the same author confirmed the successful use of the Spinning Disc, whilst also demonstrating that the thermodynamic approach could not be applied to hydrodynamic techniques of assessing microbial adhesion, and also suggested that the effect of the topography of the collector surface is more pronounced under hydrodynamic flow (Wang *et al*, 1995).

Work on *S.epidermidis* showed that more hydrophobic strains adhered with more force than less hydrophobic strains. However, as shear stress increases, this difference diminishes. The technique allowed the author to conclude that hydrophobicity does not alter the mechanism, but does increase kinetics of the interaction (Vacheethasanee *et al*, 1998).

The examples above show the potential of the Spinning Disc technique, and confirm that the method can be used as a reliable system of assessing cellular attachment under controlled, applied hydrodynamic force. Although no work has been performed on the attachment of *Bacillus* spores using the Spinning Disc, essentially the same theory and observations should apply as with biological cells. The Disc shows large variation in values of attachment, but with sufficient data, shows definite trends when considering the effect of shear on attachment.

1.6.3 The Use of the Radial Flow Chamber (RFC) to Assess Microbial Adhesion

As with the Spinning Disc, the Radial Flow Chamber applies a shear gradient across a flat surface that can be calculated due to previous characterisation of the system. This allows the study of hemo- and hydrodynamic conditions, and there are few limitations when considering the potential subjects of study, with respect to collector surface, colloidal particle, and solution.

1.6.3.1 Theory and Relevance of the Radial Flow Chamber in Microbial Attachment

A detailed explanation of the theory involved using the Radial Flow Chamber is given in Chapter 7. Briefly, the sample particle suspension enters the Radial Flow Chamber (RFC) through a central inlet, and flows over the collector surface (in this case glass and stainless steel), and the suspension exits through three equally spaced outlets. This provides a shear gradient that is inversely proportional to radial distance (Dickinson and Cooper, 1995; Groves and Riley, 1987; Moller, 1963).

The design and use of the RFC was initiated by the Biochemical Engineering Department in Swansea University in post-graduate degree studies (McKay, 1980). These studies allowed development of the system and subsequent study of biofilm formation. The work contained within this PhD project is on the initial stages of bacterial attachment, rather than on biofilm formation. This has two major consequences on the experimental protocol. Firstly, the duration of the assays was substantially shorter, and secondly the method of assessing attachment was far more complicated. The presence of a biofilm could be assessed by eye, and did not require counting of cells within the biofilm. Attachment of colloidal particles, however involves the counting of individual cells over surface by microscope. The development of the system to accommodate these changes is detailed in Section 7.2.

Compared with the Spinning Disc, there are several benefits, when assessing microbial attachment. Firstly, the system allows the inspection of glass and stainless steel during the same experiment, as the glass not only provides a collector surface, but also a window to inspect the second surface. Secondly, the RFC provides a static collector surface for inspection, allowing inspection whilst the experiment is in progress. Although kinetics and mechanisms of attachment are not investigated in this project, the system does provide the ability to inspect these functions of adhesion in conjunction with image analysis packages.

1.6.3.2 Previous Studies of Colloidal Attachment Performed with Flow Chambers

As with the Spinning Disc, there are a variety of studies on colloidal attachment using flow chambers. Below are examples of the use of flow chambers in the assessment of colloidal attachment to surfaces. An extensive review by Busscher and van der Mei (1995a) highlights the considerations that are made when incorporating flow chambers in microbial adhesion.

The strength of adhesion of marine biofilms to six polymers and glass was assessed with respect to the duration that the biofilm was allowed to form (between 3 hours and 8 days), and showed an increase in adhesive strength as time increased (Becker, 1998). The results showed the variation in adhesion in different cell types, and consequently the role that exopolymeric compounds play in adhesion. The dependence of adhesive strength on shear stress was not investigated, as adhesion was only reported at 16 Nm^{-2}, and therefore not using the full potential of the RFC as a technique of assessing adhesion.

Radial Flow Chambers are not the only chambers that can be employed when considering adhesion, although other chambers do not provide an applied shear gradient. For example, the parallel plate chamber employed by the University of Groningen in the Netherlands, did not assess the effect of a shear gradient upon adhesion (Bos *et al*, 1994). This apparatus was used in conjunction with an image analysis that avoids the need to count manually, and therefore avoids scope for human error (Meinders *et al*, 1992). This system was later used to provide information on biofilm formation of oral bacteria (Bos *et al*, 1994; Busscher *et al*, 1995b) and a variety of medically important bacteria (Meinders *et al*, 1995), allowing the study of co-adhesion, the effect of conditioning film, and the relevance of the DLVO approach when considering adhesion respectively. These three papers highlight the potential of flow chambers for assessing bacterial adhesion, even without introducing a shear gradient to the system.

As with the group from the Netherlands, the effect of flow was not investigated when considering the effect of kininogen on the attachment of *Staphylococcus aureus* (Nagel *et al*, 1996), and neutrophils (Yung *et al*, 1996). In both cases, cellular adhesion was decreased in the presence of kininogen, although more

importantly, a great amount of variation was observed in both cases (approximately 20 to 30% in some cases).

The RFC has also been employed to assess the attachment of non-biological colloids. Work performed using silica particles as the colloid once again determined that the experimental adhesion of oppositely charged surfaces showed good agreement with theories predicting adhesion, but was not the case when considering similarly charged surfaces, attributed to surface heterogeneity (Bowen and Epstein, 1979). The paper more importantly shows that radioactive labelling can be employed to assess the kinetics of both attachment and detachment, demonstrating the potential that the RFC has in determining colloidal adhesion.

The effect of surface heterogeneity on adhesion was also observed when assessing the detachment of murine fibroblasts from treated glass (Goldstein and DiMilla, 1997). Adhesion showed a dependence on shear stress, but more importantly, the paper considered models for fluid mechanics, adhesion strength probability distributions, and detachment kinetics. Neither type of model considered the physiological processes involved in the adhesion of cells, and the paper states the requirement for further research into the sources of adhesive heterogeneity.

These examples show the ability of the RFC to assess both colloidal and cellular adhesion. The method combines a well-characterised system with the ability to inspect the collector surface whilst the adhesion assay is in progress. As with the Spinning Disc, no work has been performed on the adhesion of *Bacillus* spores using this system. Providing that sufficient data are gathered to overcome the variable attachment levels generated by surface heterogeneity the system, the apparatus should enable the calculation of shear force required to inhibit the attachment of both latex beads and *Bacillus* spores.

1.6.4 Other Methods of Assessing Microbial Adhesion

The Sections above provide an insight into the theory and previous use of the methods employed within this project. These methods have been chosen for four reasons. Firstly, the chosen methods of assessment have relevance to medicine, bioprocesses, and the environment, as detailed in Section 1.2. Secondly, each

system is well characterised, allowing an understanding of the processes occurring in each system. Thirdly, each method allows a variety of relevant surfaces to be used, with respect to both the collector and colloid. Finally, the three methods are all techniques that are easily performed. Although care must be taken in surface and colloid preparation, the experimental protocol itself is relatively simple.

The following examples are methods that have been previously employed to predict and assess adhesion. These methods are not used within this project, as they do not fulfil one or more of the above criteria.

1.6.4.1 *The Use of the Atomic Force Microscope (AFM) to study Colloidal Adhesion to Surfaces*

The AFM (Binnig *et al*, 1986) is a relatively new scientific tool, and has many potential functions as reviewed by Gould *et al* (1990) and Hansma and Hoh (1994). The use of the AFM allows the interaction between an individual particle and a collector surface to be analysed. The subject of study is fixed to the tip of the AFM cantilever to provide a colloid probe, and is lowered towards the collector surface in solution. This method allows the generation of force distance curves (Bowen *et al*, 1998a), which differ significantly when considering approach and retraction. This represents the difference in attachment and detachment.

Initially the AFM was used in the study of protein/protein interactions using well-characterised interactions such as avidin and biotin derivatives (Florin *et al*, 1994; Lee *et al*, 1994), and adhesion proteoglycans (Dammer *et al*, 1995).

More recently, the Biochemical Engineering Group at Swansea University have performed adhesion experiments investigating the adhesion of yeast cells to mica (Bowen *et al*, 1998a) and polystyrene spheres to ultrafiltration membranes (Bowen *et al*, 1998b), and BSA coated silica colloids to silica (Bowen *et al*, 1998c). All three cases proved that the AFM could be successfully used when assessing the adhesion of an individual colloid to a chosen surface.

There are several drawbacks, however when using the AFM as a tool to measure cellular adhesion. The first is that the method does not take into consideration the

variation in adhesive characteristics throughout a population of cells, and also the heterogeneity in the collector surface studied.

Secondly, preparation of the cell probe is laborious. The process of adhering the cell to the tip of the cantilever is fraught with problems, and is limited to larger cells (personal correspondence with Dr. Chris Wright, 2001).

Thirdly, the AFM measures force perpendicular to the collector surface, as shown in Figure 1.9, whereas the use of the packed column, the Spinning Disc and the Radial Flow Chamber, expose the particle of study to forces that are present in natural environments. The AFM allows the resolution of the perpendicular force, and therefore removes the complexity of the combination of forces observed in the previously mentioned methods. This is emphasised in a direct comparison between the Spinning Disc and AFM techniques where the adhesive force calculated by the Spinning Disc was 10^3 times less than that measured using the AFM (Bowen *et al*, 2000). However, the force of attachment and detachment varies due to stretching of the cell once attached (Bowen *et al*, 1998a).

The AFM, therefore, has its advantages and disadvantages compared with the methods employed in this project, and the technique has been shown to be a useful tool in assessing cellular adhesion.

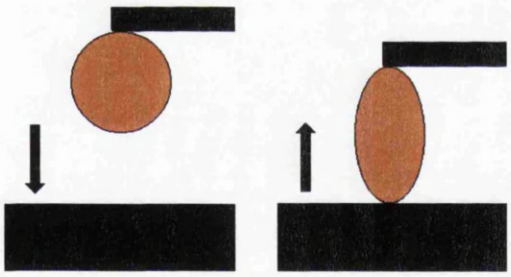

Figure 1.9: The measurement of the force of approach and detachment of a colloid to a collector surface using the AFM.

More recently, the AFM has been developed to assess force in a lateral direction, rather than a perpendicular direction as described in Figure 1.9. Lateral Force Microscopy (LFM) is a scanning probe microscopy (SPM) technique that identifies and maps relative differences in surface frictional characteristics.

During scanning in contact mode, the cantilever bends not only normally to the surface, but torsional (lateral) deformation also occurs. LFM measures the torsional deformation of the cantilever during scanning in contact mode. The torsional deformation depends on frictional (lateral) force acting on the tip (Colchero *et al*,

1992). The torsion, or twisting, of the cantilever supporting the probe will increase or decrease depending on the frictional characteristics of the surface (greater torsion results from increased friction). Since the laser detector has four quadrants, it can simultaneously measure and record topographic data and lateral force data.
This technology can therefore be applied to a cell probe, which will interact differently to surfaces of differing roughness and chemical composition.

1.6.4.2 Other Methods of Assessing Microbial Adhesion and their Weaknesses

There have been several methods of assessing microbial adhesion that do not consider parameters that have been shown to be of great importance upon adhesion, such as the effect of shear force. These methods are fraught with potential areas of error, and are described below.
The simplest of adhesion assays was performed by Sonak and Bhosle (1995), where aluminium was suspended for varying durations in cellular suspension, rinsed manually and finally stained. The method provided results that appeared accurate for such a haphazard method with a standard deviation ranging between 2% and 16%, especially as surface roughness was not monitored. The use of manual rinsing techniques poses three problems. Firstly, the amount of shear applied at each rinse will differ between rinses. Secondly, there will be a shielding effect between particles deposited on the surface. Finally, the choice of rinsing method must be kept constant. The force exerted on a cell is approximately 10^{-7}N when dipping, whereas the force when rinsing is approximately 10^{-10}N as represented in Figure 1.10 (Busscher and van der Mei, 1995a).

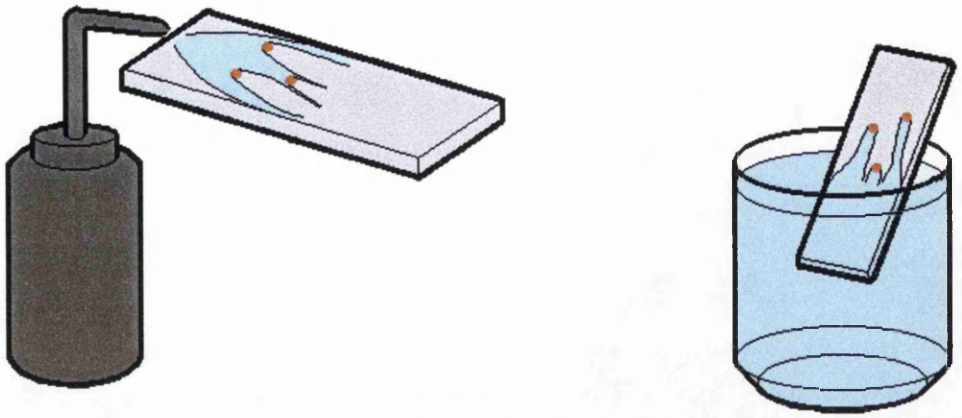

Figure 1.10: The difference between rinsing techniques. Rinsing (left) exerts an average force of 10^{-10}N per cell, whereas dipping exerts 10^{-7}N per cell (Busscher and van der Mei, 1995a).

Work performed by St John (1994) identified the need to minimise the shear force exerted on adhered lymphoid cells by the surface tension of water when rinsing. Bacterial samples were introduced to a 96-well microtitre plate coated with proteins to allow adsorption. The plate was then submerged in PBS, and then gently inverted and allowed to float, with gentle agitation from a flea. Non-adherent cells were subsequently dislodged using minimal force, and enumeration of the adhered bacteria was performed.

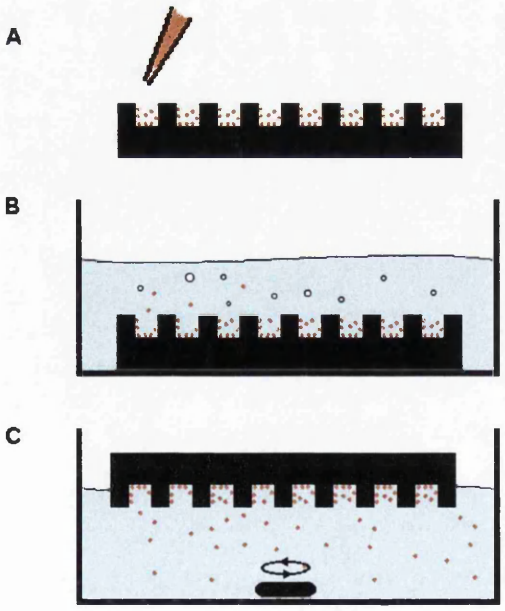

Figure 1.11: The minimal shear force adhesion assay designed and used by St. John (1994). A 96-well microtitre plate coated with proteins was subjected to bacterial samples (A). The plate was submerged to remove air from the system (B), and finally inverted, allowing a minimal amount of shear to be applied by a magnetic stirrer.

This method provided three times the amount of attached cells compared to a method that aspirated the cells, and does indeed show that this is a method worth considering. The presence of the flea still provided a minimal, but immeasurable shear force, and perhaps the reason for the standard deviation in error being approximately 6-20%.

An alternative method of removing non-adherent cells by minimising shear was developed using buoyancy (Goodwin and Pauli, 1995), as depicted in Figure 1.12.

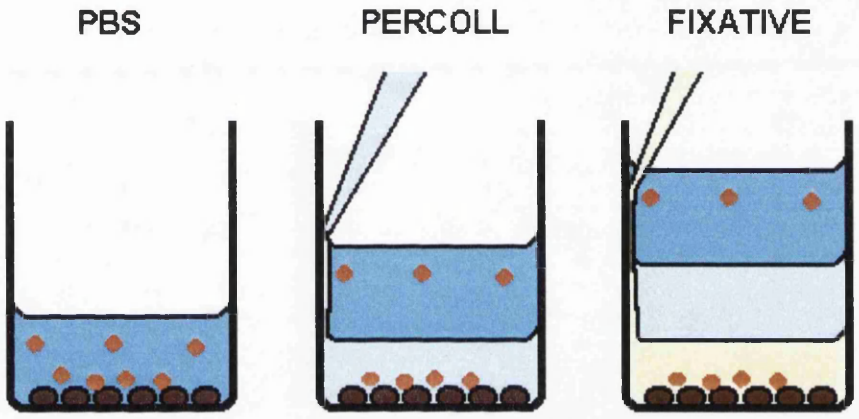

Figure 1.12: The use of buoyancy to remove non-adherent cells. Percoll, (1.10g/mℓ), and Fixative (1.13g/mℓ) were used to remove non-adherent cells and fix them from PBS (1.01g/mℓ), as detailed by Goodwin and Pauli (1995).

Human endothelial cells were seeded in microtitre plates and a suspension of leukocytes were added, and allowed to bind. Percoll was then added gradually, removing non-adherent cells using buoyancy. Those leukocytes bound were then fixed with glutaraldehyde. The system applied a weak, but consistent shear force, providing consistent results (Goodwin and Pauli, 1995).

The two methods detailed above are a qualitative assessment of whether or not cells adhere to their respective surfaces. The cells are subjected to minimal external shear force, and therefore cannot be used to determine the force of adhesion.

The use of applied shear force is not limited to just the Spinning Disc technique and Flow Chambers. The modified Robbins device allowed the assessment of adhesion of *S.epidermidis* to stainless steel, titanium, hydroxyapatite, and hydroxyapatite coated titanium (Oga *et al*, 1993). The Robbins device was also used in comparison to a modified vortex device for studying the adhesion of ocular bacteria to contact

lenses (Schultz *et al*, 1995). Both of these methods employ shear that is reproducible, but not determinable. If the shear force cannot be calculated then the effect of this shear can only be taken into consideration qualitatively.

The vortex device provides a 'whirlpool-type force' to detach adhered bacteria, whereas the Robbins device relies on a 'free flow fluid environment', supplied by a peristaltic pump. Both methods however do give results (with 10% standard deviation), which are in agreement with other work performed with similar subjects of study, using different methods.

The four methods detailed above are examples of techniques used to study microbial adhesion qualitatively. They are simple techniques that are effective as standard laboratory techniques. Their ability to assess adhesion is limited to comparisons with other surfaces and other colloids studied within the same system.

The contribution of hydrophobicity and surface charge to adhesion is stated in Section 1.3, and as a result is often used as a means of prediction of adhesive force. The majority of papers mentioned in this literature survey use surface charge and hydrophobicity as a means of comparison when analysing adhesion results. The measurement of hydrophobicity and surface charge is also performed in this project, and detailed in Chapter 3.

Briefly, as stated in Section 1.3.3, hydrophobicity can be seen as the dominating force between a cell and a collector surface, and consequently the controlling factor when considering bacterial adhesion. There are various methods of assessing cell surface hydrophobicity (CSH). These methods, reviewed by Bunt *et al* (1993 and 1995), are namely hydrophobic interaction chromatography (HIC), the salt aggregation test (SAT), contact angle measurement (CAM) and the bacterial adhesion to hydrocarbon (BATH) test.

All these methods essentially determine the bacteria's preference to be deposited in a hydrophobic rather than aqueous environment. The methods do generally show good agreement with each other (Jones *et al*, 1996; Bunt *et al*, 1995).

If considering hydrophobicity as a determinant of cellular adhesion, the surface charge of the particle must also be considered, as there is no relationship between hydrophobicity and charge (Vacheethasanee *et al*, 1998). This property can be measured in one of two ways, namely zeta potentials (derived by electrophoretic mobility), and electrostatic interaction chromatography (ESIC). As is observed with

the hydrophobicity assays, good agreement is observed between the two methods (Jones *et al*, 1996).

The choice of method used to assess adhesion is therefore important, and must be considered carefully. Table 1.1 shows the advantages and disadvantages of several methods used to study microbial adhesion.

	Advantages	**Disadvantages**
Packed Column	Simple experimental protocol	Indeterminable shear force Requires specific apparatus
Spinning Disc	Applied shear force gradient Relatively simple protocol	Requires specific apparatus and surface preparation
Flow Chambers	Applied shear force gradient Relatively simple protocol Assessment whilst the experiment is in progress	Requires specific apparatus and surface preparation
Atomic Force Microscopy	Direct and accurate quantification of perpendicular force between colloid and collector surface on a cellular scale, as well as torsional forces, resolved by lateral force microscopy	LFM relatively new technology Laborious preparation and experimental protocol Variation in surface properties requires multiple repetitions of the experiment Requires specific apparatus
Rinsing and Staining	Very simple experimental protocol, and enumeration Requires only standard lab. equipment	Prone to variation in results, due to variation in forces exerted by rinsing Subject to variation in results
Minimal Shear Force Adhesion Assay	Simple experimental protocol and enumeration Requires only standard lab. equipment	Indeterminable shear applied to lightly adhered cells Subject to variation in results
Buoyancy Assays	Allows assessment of lightly adhered cells Easy experimental protocol Requires only standard lab. equipment	Does not allow the effect of shear force to be determined Subject to variation in results

Table 1.1: The advantages and disadvantages of laboratory techniques used to assess microbial adhesion, as detailed in Section 1.6.

1.7 The Relevance of Materials Studied

Having reviewed the methods used within this project, the relevance of the materials to be studied must also be addressed. Glass and stainless steel were investigated, in conjunction with aminated and carboxylated latex beads, as well as the spores of *Bacillus mycoides* and *Bacillus subtilis*.

1.7.1 The Use and Relevance of Latex Beads

The use of latex beads in the study of microbial adhesion provides a control when a comparison is made with the *Bacillus* spores. The latex beads can be compared in size with *Bacillus* spores, which have been reported to be between 1 and 2μm (Husmark and Rönner, 1992). Their overall negative charge also provides similar properties to the spores as seen in Chapter 3. The beads used within this project are modified with amine or carboxyl groups. These two groups are the most abundant on the surface of a biological cell, due to their presence in proteins and protein conjugates derived from amino acid residues. The latex beads provide a colloid that is relatively simple in structure compared to the spores used within this work. Latex beads have also been the subject of many investigations, and have proved a good subject of study Elimelech and O'Melia, 1990; Clint *et al*, 1973; Hull and Kitchener, 1969). The use of latex beads allows an interpretation of the role of cell surface structures in the process of adhesion (Meinders *et al*, 1995).

1.7.2. The Use and Relevance of Bacillus Spores

In Section 1.2.2, microbial adhesion has consequences in many areas of science and engineering, and the choice of subject bacteria is wide. The decision to study two types of *Bacillus* spores was made for three reasons.

Firstly, *Bacillus* spores have been proven to be involved in the contamination of foods and can be the cause of food poisoning especially in the case of *Bacillus cereus* (Andersson *et al*, 1995; Faille *et al*, 2001). Although *B.cereus* is not studied

in this work, the spores of *B.mycoides* possess similar properties and are non-pathogenic, and therefore a safer subject to work with (Husmark and Rönner, 1992). The choice of *B.subtilis* spores provided completely opposite properties to that of *B.mycoides* spores and subsequently differing adhesion levels, shown in Table 1.2.

Species	Appendages	Exosporium	Relative Hydrophobicity	Adhesion to Hydrophobic Glass (mm^{-2})	Adhesion to Hydrophilic Glass (mm^{-2})
B.mycoides	Yes	Yes	42%	1603 +/- 444	333 +/- 125
B.subtilis	No	No	11%	317 +/- 349	95 +/- 59
B.cereus	Yes	Yes	45%	2190 +/- 952	111+/- 84

Table 1.2: The relative properties of *Bacillus* spores and their subsequent adhesion levels to both hydrophobic and hydrophilic glass, adapted from work performed by Husmark and Rönner (1992).

Figure 1.13 shows the structure of a generalized *Bacillus* endospore, details of which differ from species to species (Helgason *et al*, 1998; Kramer and Gilbert, 1989). Upon exposure of a vegetative cell to harsh environmental conditions, sporulation occurs. One spore is produced per vegetative cell. The central core (protoplast, or germ cell) carries the constituents of the future vegetative cell, accompanied by the genetic material, low enzyme content, and dipicolinic acid, which is essential to the heat resistance of the spore.

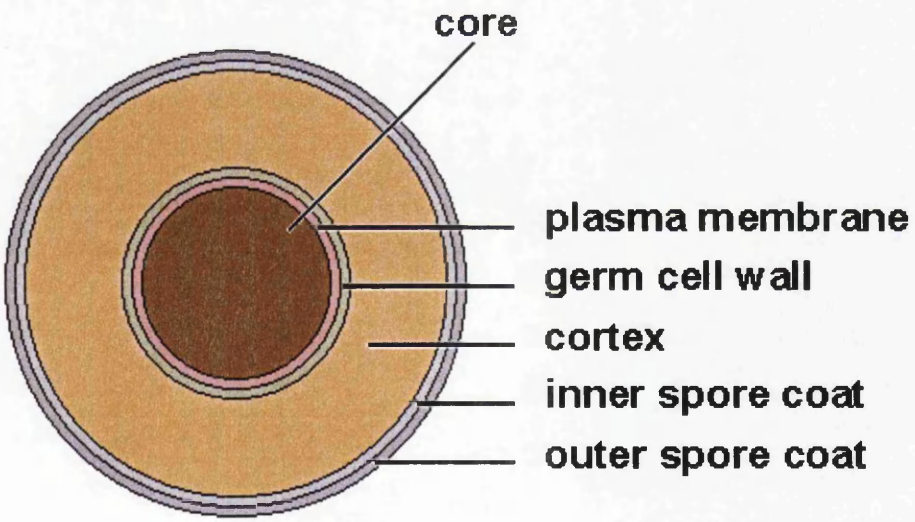

Figure 1.13: The generalised structure of *Bacillus* spores. This can be surrounded by an exosporium and associated filamentous or pilus-like structures. The composition and size of the cell wall, and spore coats vary between species.

Surrounding the core is a cortex consisting largely of peptidoglycan (murein), which is also important in the heat and radiation resistance of the spore. The inner coat becomes the cell wall of the new vegetative cell when the spore germinates. The spore coats, which constitute up to 50 percent of the volume of the spore, protect it from chemicals, enzymes, and other physico-chemical agents.

The spore coat of *B.subtilis* is much more complicated than the simple coat of *B.mycoides* (Aronson and Fitz-James, 1976; Aronson and Pandey, 1978), with a much greater variety of molecular components than the *B.mycoides* spore (Driks, 1999). The outer spore coat is occasionally covered with exosporium, as seen in the case of *B.mycoides* but not present with *B.subtilis*.

The exosporium of *B.mycoides* is a multi-layered shell that surrounds the entire spore, including the coat, but is not connected to the spore or the coat. In contrast, in *B.subtilis* this structure is tightly associated with the outer coat, and generally considered to be part of the outer coat (Husmark and Rönner, 1992). It should be noted that in addition to an exosporium, filamentous or pilus-like structures are present on the spores of a variety of *Bacillus* species, including *B.mycoides*, but have not been observed in *B.subtilis* (Hachisuka 1984).

Cleaning methods incorporated within the dairy industry have less success with spores compared to vegetative cells (Parkar *et al*, 2001), as spores are exceptionally resistant to heat and physico-chemical treatments (Rukure and Bester, 2001; Brown, 2000; Gould, 1971). When considering *Bacillus* spores, inhibition of adhesion is a more desired quality than maintenance of a sterile environment.

Secondly, the growth, sporulation, preparation, and storage of spores are simple processes (Gould, 1971). Spores are formed as the cells starve, and remain dormant until they germinate. Once spores are formed, they can be suspended in water, and stored by freezing without germination. Thirdly, spores are dormant, and therefore remove problems encountered when studying vegetative cells. Growth phase, hydration, starvation and metabolic processes affect both cell adhesion and the assessment of adhesion by altering cell size and distribution of cell surface structures (Verran *et al*, 1994; Weyn et al, 1998).

1.7.3 The Use and Relevance of Glass and Stainless Steel

Glass and stainless steel are chosen for three reasons. Firstly, the surfaces are cheap and readily accessible, and therefore the reason for use in industry. The surfaces are also easily reproducibly prepared, and can be applied to the three methods used in this project. Secondly, they possess different hydrophobic qualities as determined in Section 4.1, allowing the effect of surface hydrophobicity to be compared. Thirdly, they are well-characterised surfaces that provide model systems when used in conjunction with the Packed Column, Spinning Disc and RFC. The surfaces used in this project are naked, and only treated by polishing. Natural collector surfaces however are not naked, as is discussed in Section 1.4.4.

Other surfaces such as biomedical polymers (Wang *et al*, 1995, 1993a and 1993b), Hydroxylapatite (Schilling and Doyle, 1995; Oga *et al*, 1993), and Titanium (Rimondi *et al*, 1997; Oga *et al*, 1993), are all relevant to microbial adhesion when considering medicine and dentistry, but are not used within this project, due to their expensive or lack of availability. These surfaces, however, can all be applied as collector surfaces using the methods incorporated within this project.

1.8 Summary of Microbial Adhesion and its Measurement

The problem of assessing microbial adhesion can be summarised by the fact that the methods previously employed to assess adhesion answer 'yes' or 'no' to the question 'how much?' i.e. only qualitative answers have been reliable, while the quantitative analysis is poor.

The underlying problem throughout investigations of microbial adhesion is that there is a balance of forces between a colloid and a surface that are functions of the properties of the colloid, surface, and the solution, which are not completely understood. Several theories have been used to predict adhesion and have given good agreement with experimental results in some cases, but not all. This is attributed to the fact that theories consider both collector surface and adhering

colloid to be perfectly smooth, and homologous with respect to charge and hydrophobicity. This is not true in most real cases.

There are many parameters that affect colloidal and microbial adhesion to surfaces, such as temperature, solution pH and ionic strength, the hydrophobicity and surface charge of the collector and the particle, the assessment method, and surface and colloid preparation techniques. These effects are compounded by the heterogeneity of collector surface charge, topography, and hydrophobicity as detailed in Section 1.5.

The same observations apply to the cell, where heterogeneity is due to the complexity of biological surfaces. With respect to both charge and hydrophobicity, there is heterogeneity within the individual molecules on a cell's surface, and the distribution of the molecules upon that cell's surface is uneven. There is also variation within a population of cells, resulting in cells of the same strain possessing different adhesive characteristics.

When considering all of these variables, and additionally human and mechanical error, it is of no surprise that there are no reliable models predicting microbial adhesion, and that researchers have found it hard to explain observations obtained from previous adhesion assays.

1.8.1 Aims and Objectives

Having identified the problems within the science of the assessment of microbial adhesion, this project was initially designed to develop three methods that would enable the successful assessment and interpretation of microbial adhesion. This can be divided into five main areas.

1. The development of the Packed Column, the Spinning Disc Technique, and the Radial Flow Chamber, from previously used methods of assessing related phenomena, to enable the assessment of microbial adhesion.

2. The investigation of the difference in adhesive characteristics of two collector surfaces, namely glass and stainless steel, in conjunction with aminated and

carboxylated latex beads and the spores of *Bacillus mycoides*, and *Bacillus subtilis*.

3. The investigation of the effect that pH has on the surface properties of both the respective colloids and collectors used within the project, and to relate this to the materials' adhesive characteristics.

4. The investigation of the effect and influence of applied shear force on particulate adhesion.

5. The analysis of resultant data, to allow comparison of the methods of assessing adhesion. This analysis also considers the characteristics of the particles and the surfaces, and explains the observations made when comparing the three methods of assessment.

These five areas allow a greater understanding of the strength and weaknesses of the methods used to assess adhesion, both practically and theoretically, and therefore allow the study of adhesion processes occurring in real systems in a more precise way.

CHAPTER TWO

Materials and Methods

2.1 Introduction

The following Chapter details the standard materials and methods used in the characterisation of the particles and the collector surfaces used in Chapters 3 and 4 respectively. Details are also given regarding the general materials and methods used in the Packed Column, Spinning Disc and Radial Flow Chamber methods to assess adhesion. Any specific materials or methods used in the work performed to assess adhesion using the Packed Column, the Spinning Disc and the Radial Flow Chamber are covered in their respective Chapters.

Details are also given of the preliminary work that was performed initially to assess the viability of the project, which was beneficial to the investigative techniques used within the project, rather than an exercise in data collection.

2.2 Materials and Instruments

2.2.1 Latex Beads and Spores

The aminated and carboxylated latex beads used in all experiments were supplied by Sigma-Aldrich and catalogue numbers are shown in Table A.1.
The spores of *Bacillus mycoides* and *Bacillus subtilis* were used in experiments performed using the Packed Column, Spinning Disc, and Radial Flow Chamber, and the strain codes of *B.mycoides* and *B.subtilis* are given in Table A.2.

2.2.2 Collector Surfaces

Annealed soda glass and stainless steel alloy 316L were used in all cases, except where stated. The collector surfaces were characterised by measuring contact angles and surface topography to determine the hydrophobicity and the surface roughness respectively, as detailed in Chapter 4.

2.2.3 Solutions

Solutions in all cases were 25mM NaH_2PO_4 (Fisher) in distilled water, unless otherwise stated. Adjustment of the solution pH was made using HCl (1M) or NaOH (1M). The buffered solution allowed the maintenance of a constant pH, irrespective of any potential variations in the solution chemistry influenced by the presence of latex beads, cells, or spores.

2.2.4 Chemicals

The chemicals used within this project were obtained from Sigma-Aldrich or Fisher, and were reagent grade or better, unless otherwise stated.

2.2.5 Spectrophotometer

The optical density of all colloid types was measured at a wavelength of 660nm. The dual path spectrophotometer used to assess optical density was supplied by Pye Unicam (Model SP6-400). Distilled water was used as the reference sample in all cases. Optical density was measured in plastic 4mℓ cuvettes, with a path-length of 1cm, except in the case of the Packed Column, where details are given in Section 5.2.2. Particulate absorption has a linear relationship to the concentration of the sample, as stated by the Beer-Lambert law in Equation 2.1, and was investigated in Section 2.4.3. However, this law is not obeyed as the sample concentration is increased to high levels.

$$A = \varepsilon c \ell \qquad 2.1$$

where A is absorbance at any given wavelength, ε is a molar extinction coefficient c is the concentration of the sample, and ℓ is the path length of the light.

2.2.6 Centrifuge

The 'Hi-Spin 19' Centrifuge used to wash and harvest the latex beads, cells, and spores was supplied by MSE (9000 rpm, 12 minutes), which supplied a G-Force of approximately 13,000G. The containers used in conjunction with the centrifuge were made of polypropylene.

2.3 Preparation Methods of Particles and Surfaces

This Section details the preparation of the latex beads, and the *Bacillus* spores used in the experiments performed within this project.

2.3.1 The Preparation of Latex Beads

The aminated and carboxylated latex beads were suspended in 25mM NaH_2PO_4 solution and subjected to sonication in a water bath (5 minutes) to minimise any aggregation prior to use. The solution pH was adjusted as required using HCl (1M) or NaOH (1M) and the beads were allowed to stand for 30.

Both the aminated and carboxylated latex beads were recovered after their use in experiments and recycled. The recycling process consisted of suspending the recovered solution in distilled water (500mℓ), and subsequent sonification (10 minutes). At this point the beads were spun down in the centrifuge as detailed in Section 2.2.6, and the supernatant was discarded. This process was repeated four times, and the washed beads were kept refrigerated. It was noted that some beads remained attached to the polypropylene centrifuge containers used in conjunction with the centrifuge.

2.3.2 Growth and Preparation of B.mycoides and B.subtilis Spores

This Section details the growth and preparation of the spores of *B.mycoides* and *B.subtilis*.

2.3.2.1 Growth of B.mycoides and B.subtilis Spores

The cells of either *B.mycoides* or *B.subtilis* were inoculated in a 250mℓ flask containing a standard medium (100mℓ) as detailed in Tables A.3a and A.3b, and shaken (200rpm) at 25°C. The cells were allowed to sporulate for a period of two weeks, at which point the ratio of cells to spores was negligible. Sporulation occurred as nutrients within the growth medium were depleted, and typically gave a count of approximately 10^9 spores/mℓ. This process was repeated in 20 flasks, for both *B.mycoides* and *B.subtilis*.

The production of the spores of *B.mycoides* and *B.subtilis* was initially attempted in a 10ℓ fermenter. Cells were inoculated in a 24-hour culture (200mℓ), and shaken (200rpm) at 25°C. The medium used is listed in Table A.3. This was then transferred into a 1-litre flask, containing medium (500mℓ), and stirred for 24 hours. The resulting culture was then transferred into a 10ℓ fermenter, and allowed to grow, and ultimately sporulate. After one week, samples were taken from the fermenter at 24-hour intervals and the ratio of the spores to cells in the solution was assessed.

The fermenter during this prolonged spore maturation period was susceptible to infection, and growth of spores using this method was attempted several times, and the same problems were encountered. The method was therefore discarded as a method of producing the spores. Spores were therefore produced using the previous, successful method.

2.3.2.2 Preparation of B.mycoides and B.subtilis Spores

Having allowed the vegetative cells of *B.mycoides* and *B.subtilis* to grow, and subsequently sporulate, the resulting spores were harvested by centrifugation as detailed in Section 2.2.6. The harvested spores were washed three times in distilled water, and finally, the concentrated spores were then frozen in 1.5 mℓ aliquots and stored until required.

The spores were suspended in buffer, and adjusted to the required OD_{660nm} and pH. The spores of *B.mycoides* and *B.subtilis* were not subjected to sonication to avoid alteration of the spore surface characteristics and possible spore disruption. Due to limited time and resources, the effect of freezing the spores was not investigated.

2.3.3 Preparation of Collector Surfaces

The collector surfaces used in all experiments were prepared using the same protocol, except where stated. Both glass and stainless steel were polished using abrasives of decreasing size, finally using 1μm diamond paste (Buehler). The

surfaces were washed with detergent, and then soaked in ethanol for 10 minutes, and then rinsed thoroughly in distilled water three times, and dried at 80°C.
An investigation into the surface topography was performed to assess the effectiveness of this method of sample preparation, as detailed in Section 4.3.

2.4 Preliminary Investigation into Adhesion

The following Section details introductory work, and two experiments that allowed the subsequent study of adhesion.

2.4.1 Introductory Work

Preliminary experiments were performed at the outset of this project to assess the viability of the proposed work that was to be undertaken. The preliminary work allowed the determination of the problems that might be encountered using the optical inspection methods to assess adhesion. These experiments were performed before the ultimate decision was made to use the spores of *B.mycoides* and *B.subtilis*, and as a result of this, *S.cerevisiae* and *E.coli* were used due to their availability. The experiments used a simple method of suspending glass cover slips shown in Figure 2.1 in cellular suspensions of *E.coli* or *S.cerevisiae*. Details of these experiments are given in Appendix A, as well as the corresponding results.

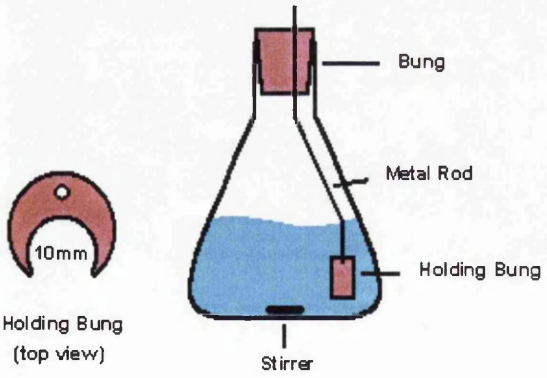

Figure 2.1: The apparatus used for the preliminary experiments, consisting of a conical flask, on a magnetic stirrer, with a bung suspended below the level of the microbial suspension. The holding bung had a hole (10mm) cut vertically, to allow the circular cover slips to be held in the solution.

The experiments provided an appreciation of the future problems that were to be encountered, and highlighted the difficulty in assessing cellular adhesion. The experiments also showed that studying adhesion is a complicated process, and a well-defined system is required to study adhesion. The Packed Column, Spinning Disc, and Radial Flow Chamber were the chosen methods in this project, all of which provide well defined flow conditions.

2.4.2 Counting and Statistics Used in Subsequent Experiments

As part of the analyses incorporated with the Spinning Disc technique and the Radial Flow Chamber in Chapters 6 and 7 respectively, visual inspection was performed on the collector surface to assess the numbers of attached latex beads or *Bacillus* spores. Sufficient numbers were required to make experiments statistically applicable and the subsequent conclusions reliable (Cassell, 1965).

Firmly attached particles were counted, as were aggregated monolayers. In the case of large, multiple-layered aggregates, an alternative area was used for assessment, where aggregation was not present. Aggregation was generally observed with spores, rather than latex beads. An ideal picture for counting is shown in Figure 2.2, where no aggregation has occurred.

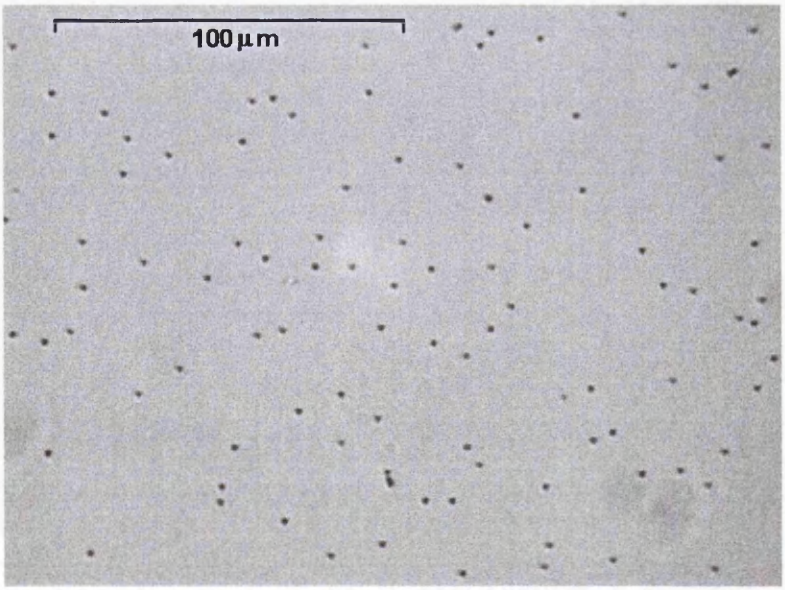

Figure 2.2: An image captured using VideoSnap™. The image shows *B.subtilis* spores adhered to a stainless steel surface. The picture demonstrates an ideal experimental situation, where no aggregation of spores has occurred.

2.4.3 Count Relative to Optical Density

In subsequent experiments to assess adhesion, the suspension concentration of latex beads and *Bacillus* spores was kept constant with respect to count/mℓ, hence eliminating the effect of particle concentration with respect to adhesion. Counting particle numbers to assess adhesion was very laborious, and $OD_{(660nm)}$ was therefore measured. OD has a linear relationship with concentration, as stated in Section 2.2.5, although the molar extinction co-efficient varies with different particles, as defined in Equation 2.1. The assessment of the relationship between particle concentration and $OD_{(660nm)}$ was therefore necessary, and is detailed in this Section.

Materials:

Counting was performed in a chamber of fixed volume. The chamber consisted of a grid of squares of 1/400mm^2 2.5 x 10^{-3}mm^2). The height of the chamber was 0.1mm, when a cover slip was applied. The volume for each square was equivalent to 2.5 x 10^{-7} cm^3. The number of particles per mℓ could therefore be calculated, and related to optical density according to Equation 2.1.

Protocol:

Suspensions of aminated and carboxylated latex beads, and the spores of *B.mycoides* and *B.subtilis* were prepared in NaH_2PO_4 (25mM), at varying concentrations. Each particle suspension was counted at least 96 times, which allowed statistical reliability (Cassell, 1965), and the optical density of these solutions at 660nm (OD_{660nm}) was recorded, allowing the relationship between OD_{660nm} and count/mℓ x 10^7 to be determined.

Results:

The aminated and carboxylated latex beads provided almost identical values and therefore the results for the latex beads were combined. As can be observed in Figure 2.3, there was a substantial amount of error when taking into consideration

the standard deviations of the three curves. However, due to the large numbers that were counted, the relationship between optical density and actual count can be represented in Equations 2.2, 2.3, and 2.4, for latex beads, and the spores of *B.mycoides* and *B.subtilis* respectively.

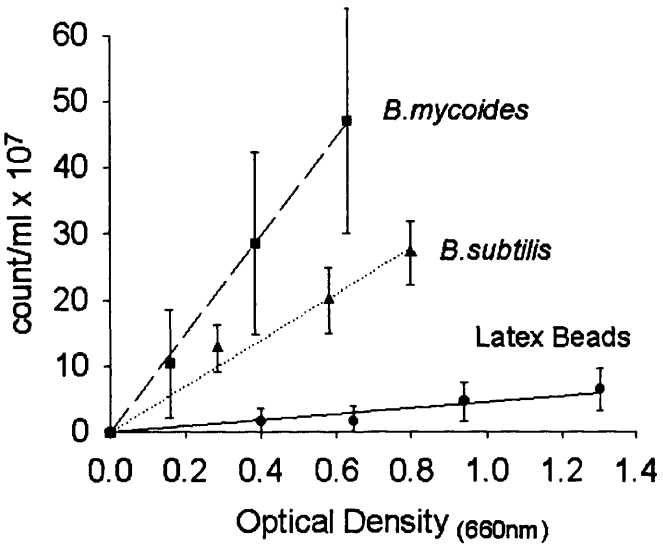

Figure 2.3: The relationship between measured OD_{660nm}, and actual particle count (count/mℓ x 10^7). Each point was counted at least 96 times, using suspension volumes of 2.5 x 10^{-7}ml.

For latex beads: $y = 4.5x$ **2.2**

where $R^2 = 0.92$

For *B.mycoides*: $y = 74.6x$ **2.3**

where $R^2 = 1.00$

For *B.subtilis*: $y = 34.8x$ **2.4**

where $R^2 = 0.98$

where y represents count/mℓ x 10^7, and x is $OD_{(660nm)}$.

The values themselves do not reveal any surface characteristics, except the ability of the particles to refract light. The concentration (count/mℓ) could now be assessed by simply measuring $OD_{(660nm)}$, rather than performing the laborious task of counting each individual sample.

2.5 Summary

The preliminary experiments allowed the appreciation of the requirements of assessing adhesion, and any potential problems that might be encountered when conducting adhesion experiments.

The determination of concentration with respect to optical density allowed the determination of particle concentration to be a relatively simple process. The following Chapters detail the assessment of the characteristics of aminated and carboxylated latex beads, and the spores of *B.mycoides* and *B.subtilis*, in Chapter 3, the characterisation of glass and stainless steel in Chapter 4, and the adhesion of the particles to these surfaces using the Packed Column, Spinning Disc, and Radial Flow Chamber in Chapters 5, 6, and 7, respectively.

CHAPTER THREE

The Measurement of Particle Surface Charge and Hydrophobicity

3.1 Introduction

When investigating the adhesion of a particle to a collector surface, characteristics of both the particle and the collector surface must be considered. Adhesion is governed by the charge and hydrophobicity of the particle and surface, as well as surface roughness (Walz, 1998). In this Chapter, particle zeta potential and hydrophobicity are investigated to allow the prediction and explanation of the adhesion of latex beads and *Bacillus* spores to glass and stainless steel using the three techniques detailed in Chapters 5, 6, and 7.

3.2 The Determination of Electrophoretic Mobility and Zeta Potential

The measurement of electrophoretic mobility (u_E) and the resulting calculation of zeta potential (ζ) allow the contribution of particle charge to be assessed, when considering particle adhesion to a surface. Cell surface charge is not the sole determinant of attachment, but has been shown to contribute to the process of adhesion (Hermansson, 1999).

3.2.1 Theory

Surface charge was assessed by first observing the electrophoretic mobility of a population of particles, and subsequently converting the value for electrophoretic mobility into a value for zeta potential, as detailed below in Section 3.2.1.2. Zeta potential is subject to change with pH, as the presence of protons alters surface charge.

3.2.1.1 Electrophoretic Mobility

The DLVO contribution to the initial adhesion process of two similarly charged surfaces consists of van der Waals forces and electrostatic repulsion between the two surfaces. The electrostatic repulsion is partially governed by the surface charge of the colloid and collector. The determination of the respective particles' electrophoretic mobility was therefore required to enable the calculation of the zeta potential, a direct assessment of surface charge (Harkes *et al*, 1991).
Micro-electrophoresis is the measurement of the movement of colloidal particles in response to an applied electric field. This measurement allows determination of the particles' charge sign, and electrophoretic mobility (u_E), which can be related to surface charge and zeta potential by Equation 3.2, the Smoluchowski Equation (Smoluchowski, 1918).

The measurement of the electrophoretic mobility characterises the overall surface charge of a population of colloids. The technique does not take into account heterogeneity within the population, or variation upon the surface of an individual particle. An important note is that the study within this project does not consider individual particles, but particulate populations.

3.2.1.2 Calculation of Zeta Potential

Smoluchowski (1918), considered the effect of an electric field on the movement of a liquid adjacent to a flat charged surface. The velocity of the liquid varies from zero (plane of shear) to a maximum value, some distance from the wall, where the velocity remains constant. A force balance on an elemental volume of the liquid results in the electro-osmotic mobility, defined in Equation 3.1.

$$u_E = -(\mathbf{D}\,\zeta)/\mu \qquad \mathbf{3.1}$$

where u_E is electro-osmotic mobility (m^2/secV); **D** is the dielectric constant (dimensionless); ζ is the zeta potential mV and μ represents the viscosity of water (kg/ms).

This theory can also be applied to large particles moving within relatively thin double layers in a stationary liquid, taking into consideration that the particle is moving in the opposite direction, and therefore the sign reversed as shown in Equation 3.2. Therefore, once electrophoretic mobility is determined, the Smoluchowski Equation is used to calculate zeta potential.

$$u_E = (\mathbf{D}\,\zeta)/\mu \qquad \mathbf{3.2}$$

u_E now represents the electrophoretic mobility.

3.2.2 The Experimental Determination of Zeta Potential

This Section details the apparatus, solution preparation, and experimental procedure used in the measurement of the zeta potential of aminated and carboxylated latex beads, and the spores of *B.mycoides* and *B.subtilis*.

3.2.2.1 Instruments

Electrophoretic mobility measurements were performed using a heterodyne laser Doppler electrophoresis system. The Malvern ZetaMaster (Malvern Instruments, UK) consisted of an internal 2mW Helium Neon laser, from which the light was split into two beams that were focused within a rectangular shaped cell. One of the beams was passed through the sample, which partially scattered the light. The other beam was aligned directly at the receiver and used as the reference beam. Both beams were collected via an optic assembly and an optical fibre, by a photon-counting photomultiplier. The resultant signal was transferred to a digital correlator that measured both the intensity (counts/second) and the auto-correlation function of the scattered light. The spectrum of electrophoretic particle motion was then analysed by a computer to provide results in terms of zeta potential (mV).

3.2.2.2 Preparation of Solutions

Colloidal particles were suspended in 25mM NaH_2PO_4 to a concentration of approximately 0.1g/ℓ in distilled water (40mℓ), and adjusted to the required pH using 1M HCl or NaOH respectively. The concentration of the sample solution was not determined, as the suspension concentration was of no consequence in this experiment. In the case of latex beads, the suspension was then sonicated in an ultrasound water-bath for 1 minute prior to each experiment. The spores were not treated in this way, in order to avoid alteration of the spore surface characteristics, and possible cell disruption.

3.2.2.3 Experimental Procedure

The sample solution (approximately 40mℓ) was injected into the Malvern Zetamaster, manually. A total of 20 readings were taken per sample, and these measurements were repeated three times for each particle/pH combination.
This protocol allowed direct comparison of not only the effect of pH, but also variation in zeta potential with particle type.
Additionally, carboxylated latex beads of varying sizes (0.5, 1, and 2μm) were also investigated, in order to assess the effect of size on zeta potential with respect to pH.

3.2.3 The Effect of pH on Zeta Potential: Results

The following results represent the zeta potentials of aminated and carboxylated latex beads, and the spores of *B.mycoides* and *B.subtilis* with respect to pH. Direct graphical comparison of zeta potential with respect to particle type is also represented in Section 3.2.4.
The values obtained for the aminated latex beads showed that the overall charge of latex was negative, as shown in Table 3.1. The pKa of latex was approximately 4, which corresponded to change in zeta potentials as pH was increased from 3.5 to 5.5 as shown in Figure 3.1.
The charge of latex was shown to dominate the charge of the amine or carboxyl groups present on the respective beads' surface. The pKa of the amine group was approximately 8, and a change in zeta potential was expected between 7.5, and 9.5, as NH_3^+ was deprotonated to NH_2. If the amine group had the dominant effect, then a positive value for zeta potential would be expected, and a noticeable change between pH 7.5, and 9.5 would be observed. Experimentation showed that this did not occur.
The values obtained for the carboxylated latex beads showed that the beads have an overall negative charge. As observed with the aminated beads, there was a noticeable change between pH 3.5, and pH 5.5, corresponding to the pKa of Latex, and the carboxylate group as shown in Table 3.1. There was little change in zeta

potential as pH was increased past 5.5, as the latex remained negatively charged, and the surface charge was altered in insignificant amounts as represented in Figure 3.1.

The results obtained for *B.mycoides* spores showed relatively low values, and varied between positive and negative values, depending on pH, as shown in Table 3.1. The spore surface charge was altered significantly between pH 3.5 and 5.5, and did not change noticeably after this point, as shown in Figure 3.1. This result corresponds with the pKa of carboxylic acid groups present in abundance in the surface molecules of the spore.

pH	Aminated Beads (mV)	Carboxylated Beads (mV)	*B.mycoides* Spores (mV)	*B.subtilis* Spores (mV)
3.5	-6.48 +/- 1.17	-7.80 +/- 1.61	+7.53 +/- 2.17	-33.73 +/- 1.27
5.5	-37.81 +/- 1.86	-45.58 +/- 1.22	-10.73 +/- 0.96	-43.76 +/- 0.96
7.5	-34.13 +/- 2.67	-45.74 +/- 1.85	-12.98 +/- 1.51	-41.68 +/- 2.16
9.5	-32.19 +/- 1.66	-44.50 +/- 1.68	-13.19 +/- 1.82	-41.17 +/- 2.10

Table 3.1: The zeta potentials of aminated and carboxylated latex beads (2μm) and the spores of *B.mycoides* and *B.subtilis* at varying pH. Electrophoretic mobility was initially determined, and the Smoluchowski Equation was used to convert to zeta potential. All experiments were conducted in 25mM NaH_2PO_4 and adjusted to the required pH using HCl (1M) or NaOH (1M), and at 25 +/- 1°C. Twenty readings were taken per sample, using three different samples.

The surface of the *B.subtilis* spore was negatively charged, as shown in Table 3.1. There was a noticeable difference between pH 3.5 and pH 5.5, as was observed with the spores of *B.mycoides*. The change in zeta potential, however, was approximately 10mV between pH 3.5, and 5.5, which was small relative to that observed with latex beads as recorded in Figure 3.1. This small change in zeta potential between pH 3.5 and 5.5 is considered to be due to the complexity of the surface charge molecules of the spore.

3.2.4 The Effect of pH on Zeta Potential: Summary

When considering the effect of pH on zeta potential, the same trend was observed with all four particles. Between pH 5.5 and 9.5, there was little change in zeta potential, but when the pH was decreased to 3.5, the value became less negative, as is shown in Figure 3.1.

The two types of latex beads both showed the dominant characteristics of latex, rather than their surface charge groups as was confirmed by personal correspondence with Dr. Teodora Doneva, University of Wales Swansea (2001). The carboxylated beads were more negatively charged than the aminated beads between pH 5.5 and pH 9.5, by approximately 10mV, attributed to the contribution that the amine and carboxyl groups had on zeta potential.

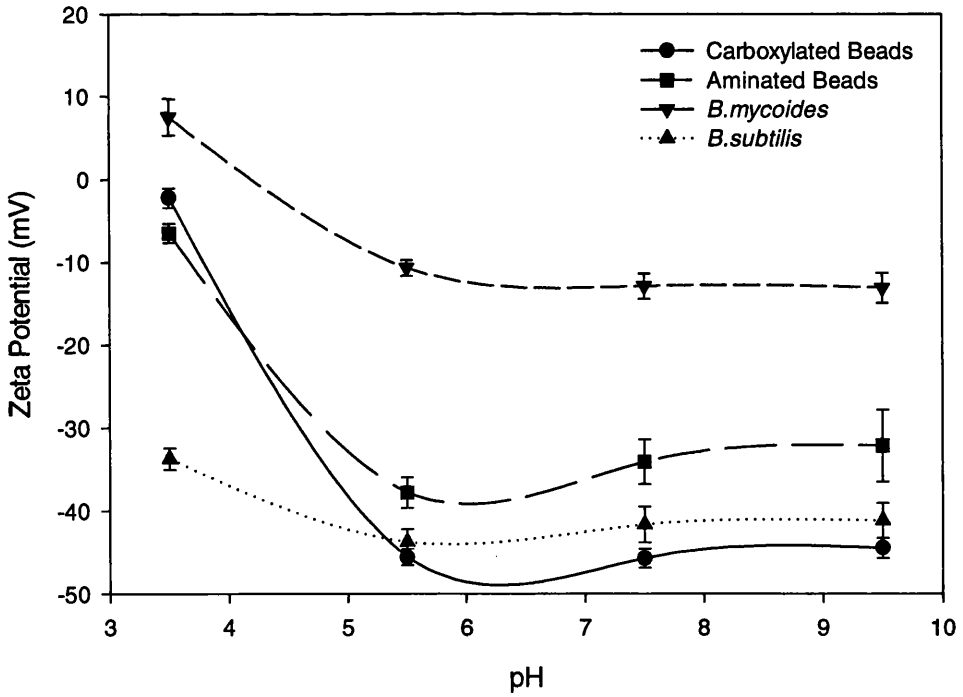

Figure 3.1: The zeta potentials of aminated and carboxylated latex beads (2μm), and the spores of *B.mycoides* and *B.subtilis* relative to pH. Measurements were made in 25mM NaH_2PO_4, and the pH was adjusted using HCl, or NaOH (1M). Experiments were carried out at 25 +/- 1°C. Values were initially obtained for electrophoretic mobility, and then converted into zeta potentials using the Smoluchowski Equation.

The spores of *B.mycoides* showed low values for zeta potential relative to the three other colloidal particles. These low values demonstrate the lack of charged groups on the outer surface of the spore, due to the presence of a predominantly hydrophobic exosporium (Husmark and Rönner, 1992). This type of exosporium is not present on the spores of *B.subtilis*, and the zeta potential measurements reflected this condition.

Zeta potential values recorded for the spores of *B.subtilis* between pH 5.5 and 9.5 were in the same range as those obtained for the latex beads. The difference in values between pH 3.5 and 5.5 was smaller than that observed with latex beads, and was consistent with the variety and heterogeneity of the surface molecules of the spores, compared with the well-defined surfaces of the latex beads.

3.2.5 The Effect of Latex Bead Size on Zeta Potential: Results

The effect of size on zeta potential was investigated using carboxylated latex beads (0.5μm, 1μm, and 2μm). The experiment was performed before the decision was made to use 2μm beads in all subsequent experiments.

The zeta potential values obtained for carboxylated latex beads of 0.5μm were similar to the values observed with 1μm and 2μm beads, as seen in Figure 3.2.

pH	0.5μm (mV)	1μm (mV)	2μm (mV)
3.5	-7.27 +/- 0.86	-9.18 +/- 0.62	-7.80 +/- 1.61
4.5	-25.82 +/- 1.28	-21.16 +/- 0.94	
5.5	-40.08 +/- 0.07	-37.46 +/- 1.29	-45.58 +/- 1.22
6.5	-52.21 +/- 0.20	-39.22 +/- 1.49	
7.5	-46.71 +/- 1.01	-39.89 +/- 2.24	-45.74 +/- 1.85
9.5	-44.52 +/- 0.96	-44.41 +/- 1.32	-44.50 +/- 1.68

Table 3.2: The zeta potentials of carboxylated latex beads (0.5μm, 1μm, and 2μm) at varying pH. Electrophoretic mobility was initially determined, and the Smoluchowski Equation was used to convert to zeta potential. All experiments were conducted in 25mM NaH_2PO_4 and adjusted to the required pH using HCl (1M) or NaOH (1M), and at 25 +/- 1°C. Forty readings were taken in total, using 2 different samples.

At pH 3.5, the value was near zero, and became more negative as pH was increased, Table 3.2. There were noticeable changes in zeta potential between pH 3.5 to 5.5, at which point the values became asymptotic, and this observation coincides with the pKa values of both latex and the carboxyl group, at approximately pH 4.5.

3.2.6 The Effect of Size on Zeta Potential: Summary

The effect of size on zeta potential was negligible, and is illustrated in Figure 3.2. Zeta potential assesses surface charge, which is not necessarily affected by size. The reason for undertaking the experiment was to determine whether the surface charge density of the beads differed as size changed. These experiments showed that this did not occur.

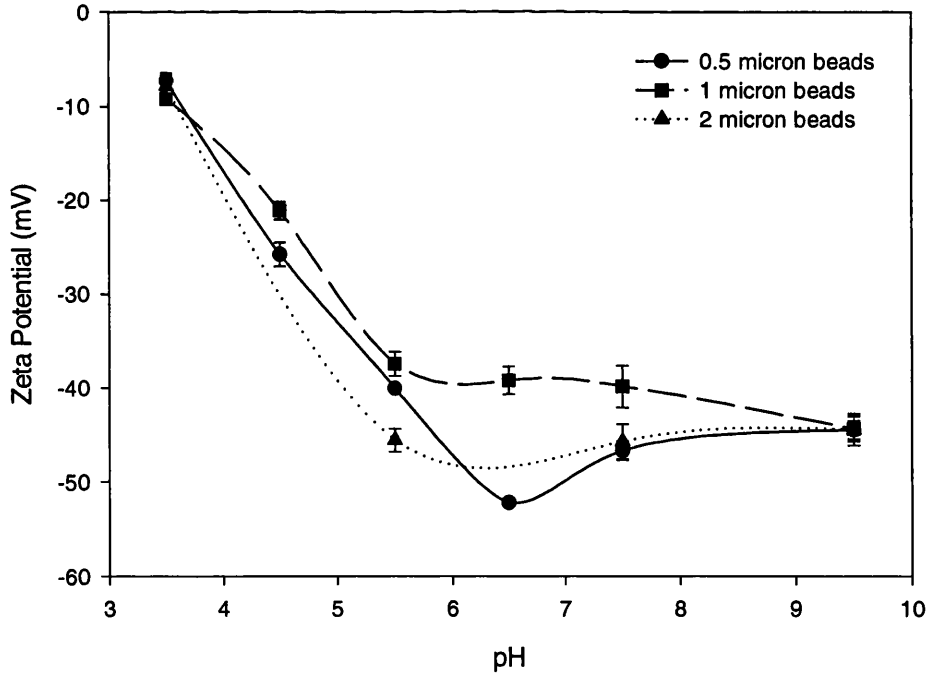

Figure 3.2: The zeta potentials of carboxylated latex beads of various sizes relative to pH. Measurements were made in 25mM NaH_2PO_4, and the pH was adjusted using HCl, or NaOH (1M). Experiments were carried out at 25 +/- 1°C. Values were initially obtained for electrophoretic mobility, and then converted into zeta potentials using the Smoluchowski Equation.

3.3 The Determination of Particle Hydrophobicity

When considering microbial attachment, both hydrophobicity and surface charge are of importance. Section 3.2 determined the cell surface charge, and to complement this, the cell surface hydrophobicity must also be determined.

3.3.1 Theory

The DLVO theory has been applied to initial adherence, stating that two oppositely charged bodies when approaching each other undergo both repulsive and attractive forces, as detailed in Section 1.3.2.

However, at long distances of separation, attractive forces, which include hydrophobic interactions, are predominant. As the surfaces become closer, DLVO forces contribute more to the interaction. However, the hydrophobic interaction between particle and collector surface has been stated as the only interaction worth investigating in colloidal attachment (Van Loosdrecht *et al*, 1987).

The hydrophobic characteristics of the colloids had to be assessed in order to complete the adhesion interaction process with respect to the particle, having already determined the zeta potential.

The determination of hydrophobicity simply assesses the preference of the colloidal particle to be deposited in a hydrocarbon phase, or to remain in an aqueous suspension.

3.3.2 The Experimental Determination of Particle Hydrophobicity

This Section details the solutions, materials, and methods used to perform BATH tests as detailed by Rosenburg *et al* (1980). The values of the relative hydrophobicity of aminated and carboxylated beads and the spores of *B.mycoides* and *B.subtilis* were measured at pH 3.5, 5.5, 7.5, and 9.5.

3.3.2.1 Preparation of Solutions

Colloidal particles were suspended in 25mM NaH_2PO_4 solution, and adjusted to the required pH using 1M HCl or NaOH respectively. In the case of latex beads, the suspension was then sonicated in a water bath for five minutes prior to each experiment. The spores were not treated in this way, in order to avoid alteration of the spore surface characteristics.

3.3.2.2 Experimental Procedure

The optical density of the chosen particulate suspension was determined at 660nm. The particulate suspension (3mℓ) was added to hexadecane (1mℓ) in a test tube. The test tube was agitated by a vortex unit for twenty seconds, and held for 30 minutes to allow for phase separation. The hexadecane phase was then aspirated using a Pasteur pipette and discarded. The aqueous phase was then aspirated carefully, and $OD_{(660nm)}$ recorded. This procedure was repeated five times at each pH. Experiments were conducted at 22 +/- 1C°. The optical density of the resulting aqueous phase was then determined and expressed as relative hydrophobicity, using Equation 3.3.

$$\textbf{Relative Hydrophobicity (\%)} = 100\left[1 - (OD_{aq} / OD_{total})\right] \qquad \textbf{3.3}$$

where $OD_{(total)}$ and $OD_{(aq)}$ are the $OD_{(660nm)}$ values of the start sample and resultant aqueous phase respectively.

3.3.3 The Effect of pH on Relative Hydrophobicity: Results

Table 3.3 shows the results of hydrophobicity experiments performed on aminated and carboxylated latex beads, and the spores of *B.mycoides* and *B.subtilis*.

pH	Aminated Beads (%)	Carboxylated Beads (%)	*B.mycoides* Spores (%)	*B.subtilis* Spores (%)
3.5	78.9 +/- 7.4	78.7 +/- 1.3	51.8 +/- 5.2	55.1 +/- 3.5
5.5	83.7 +/- 1.7	76.5 +/- 5.9	53.8 +/- 5.9	2.6 +/- 7.6
7.5	80.8 +/- 4.7	71.9 +/- 5.5	50.9 +/- 3.9	0.0 +/- 4.0
9.5	86.5 +/- 2.6	90.0 +/- 1.7	53.9 +/- 4.2	2.9 +/- 5.2

Table 3.3: The relative hydrophobicity of aminated and carboxylated latex beads and the spores of *B.mycoides* and *B.subtilis*. The experiment was conducted using hexadecane (1mℓ) and latex beads buffer suspension (25mM NaH_2PO_4,) and the pH was adjusted using HCl, or NaOH (1M). The mixture was vortexed for 20s. and allowed to separate for 30mins. The experiment was carried out at 22 +/- 1°C

The hydrophobicity of both aminated and carboxylated latex beads had very high relative values, which were not affected significantly by pH, Table 3.3. This was expected, as hydrophobicity is governed by the overall colloidal particles' characteristics. There was little change with pH, as surface charge has limited effect on the hydrophobicity when considering latex beads.

The hydrophobicity of *B.mycoides* spores was recorded at approximately 50%, and is shown in Table 3.3. This value of hydrophobicity did not vary when altering the pH. This low variation suggests that the surface of the spore did not have sufficiently charged groups to affect the hydrophobicity of the spore, which is in agreement with the morphology of the spore (Husmark and Rönner, 1992). These results confirmed that the exosporium of the spore consisted of predominantly non-polar molecules, which are not affected by protonation.

The hydrophobicity of *B.subtilis* spores showed a large increase when pH was decreased to pH 3.5, Table 3.3. The spore of *B.subtilis* is regarded as a hydrophilic spore, and showed this characteristic over the pH range between pH 5.5 and 9.5. The lack of a complex exosporium exposed the charged groups of surface molecules that were susceptible to protonation. These charged residues were negative at pH 5.5 and above, but protonation rendered the residues neutral, allowing the non-polar characteristics of the cell wall to be expressed.

3.3.4 The Effect of pH on Relative Hydrophobicity: Summary

The aminated and carboxylated latex beads have similar values of hydrophobicity, as the latex component of the bead was being assessed, rather than the surface charge groups. The aminated and carboxylated latex beads showed high values of hydrophobicity relative to the two spores as shown in Figure 3.3. The hydrophobicity of the aminated and carboxylated latex beads and the spores of *B.mycoides* were not affected by variation in pH. The lack of variation was as expected, as hydrophobicity is not a result of surface characteristics, but of overall properties of the colloid. *B.subtilis* was affected by pH, as the charged groups that determined the hydrophilicity of the spore at pH 5.5 and above were protonated at pH 3.5, rendering them neutral. The protonation allowed the hydrophobic content of the cell surface to be expressed.

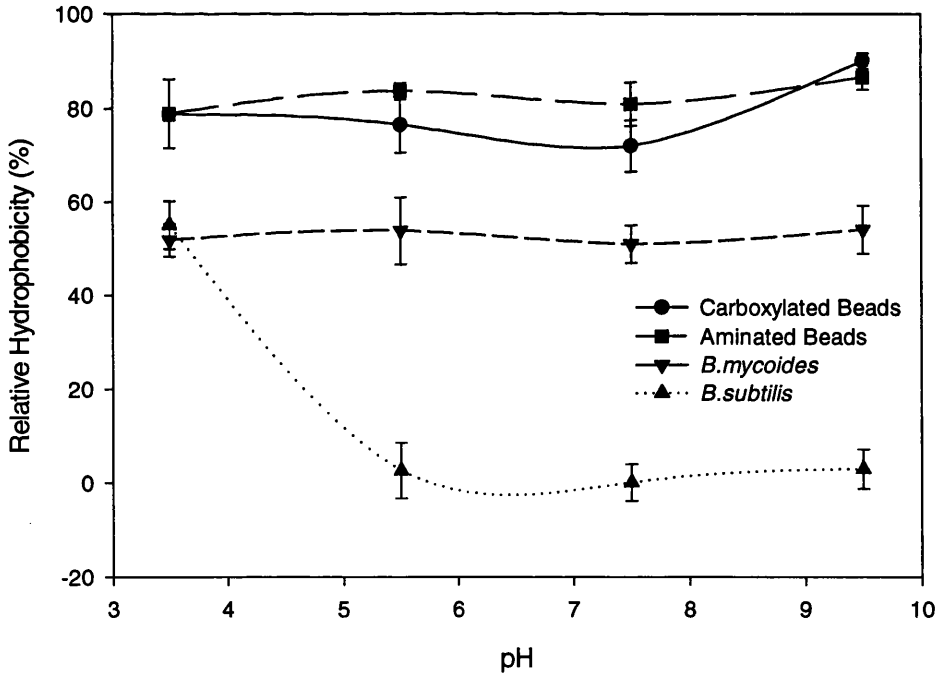

Figure 3.3: The relative hydrophobicity of aminated and carboxylated latex beads (2μm), *B.mycoides*, and *B.subtilis* spores relative to pH. The experiment was conducted using hexadecane (1mℓ) and latex beads buffer suspension (25mM NaH_2PO_4) and the pH was adjusted using HCl, or NaOH (1M). The mixture was vortexed for 20s and allowed to separate for 30mins. The experiment was carried out at 22 +/- 1°C.

3.4 Discussion of the Effect of pH on Surface Charge and Relative Hydrophobicity

The calculation of zeta potential and hydrophobicity by electrophoretic mobility and BATH tests respectively, showed that there was no relation between cell surface charge and hydrophobicity.

The effect of pH was noticeable when considering surface charge. As the pH was decreased to 3.5, the surface charge became less negative in all cases, but with differing degrees. This outcome was attributed to protonation of the latex of the beads, and the negatively charged residues on the surfaces of spores of both *B.mycoides* and *B.subtilis*. The difference in surface charge between the two spores was attributed to the presence of a hydrophobic exosporium that lacked charged-groups in the case of *B.mycoides*, which was not present on the spore of *B.subtilis* (Husmark and Rönner, 1992).

The pH did not, however, alter the hydrophobicity of the particles, except in the case of the spores of *B.subtilis*. The charge on the latex beads' surface did not possess sufficient magnitude to overcome the non-polar properties of the beads. In the case of *B.mycoides* spores, pH did not affect the non-polar exosporium, and therefore constant hydrophobicity was maintained over the range of pH investigated. There was, however, an increase in hydrophobicity of the spores of *B.subtilis* at pH 3.5. The lack of the non-polar exosporium, possessed by *B.mycoides* spores, exposed polar molecules on the surface of *B.subtilis* spores to the effect of pH. At pH 5.5 and above, the polar groups were negatively charged, masking the effect of any non-polar regions on the spores' surface. As pH 3.5 was approached, the polar groups became protonated, and consequently neutrally charged. The masking effect of the charge was removed, allowing the non-polar groups to interact with the hydrocarbon phase in the BATH tests.

The work reported in this Section has allowed inferences made when assessing particle attachment to be explained in terms of surface charge and hydrophobicity. The properties of the collector surface must also be considered when explaining particle attachment, and are experimentally determined in Chapter 4.

CHAPTER FOUR

The Characterisation of Glass and Stainless Steel Collector Surfaces

4.1 Introduction

As stated in Chapter 3, investigation of particle adhesion requires both the particle and the collector surface characteristics to be taken into consideration. This Chapter assesses the hydrophobicity and topography of both glass and stainless steel collector surfaces. Surface charge was not assessed, as facilities were not available for this.

The determination of collector surface hydrophobicity in conjunction with the particle hydrophobicity allows the hydrophobic interaction to be qualitatively assessed. The surface topography was determined to ensure that the surface roughness was the same for both glass and stainless steel, and therefore had no effect on adhesion levels, when comparing results obtained for glass with stainless steel.

4.2 Contact Angle Measurement of Glass and Stainless Steel

The measurement of the contact angle of a liquid interacting with a surface is the most reliable method of assessing the hydrophobicity of the surface (Rijnaarts *et al*, 1999; Hermansson, 1999). This Section describes the measurement of the contact angles of buffered water with glass and stainless steel in relation to pH. Contact angle measurements can be made on a lawn of bacteria, but are not performed within this project, as good agreement has been observed between contact angle measurement and BATH tests (Jones *et al*, 1996; Bunt *et al*, 1995) performed in Chapter 3.

4.2.1 Theory

Performing contact angle measurements was the most practical method of assessing the relevant surface energies, and the relationship between the particle suspension and collector surface. The contact angle (θ) is the angle as defined in Figure 4.1.

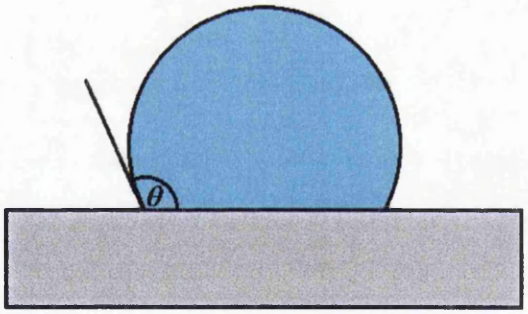

Figure 4.1: Contact angle (θ) relative to the surface and an applied liquid.

There is a direct relationship between contact angle and surface energy in that, as surface energy increases, contact angle decreases, and is described by Equation 4.1.

$$\gamma_L \cos\theta + \gamma_{CL} = \gamma_C - \pi_\theta \qquad \textbf{4.1}$$

where γ_L, γ_C, and γ_{CL}, are the free surface energies (J) of the liquid, collector, and the interface between the two respectively, and π_θ is the equilibrium pressure of absorbed vapour of liquid on solid (N/m^2).

4.2.2 Contact Angle Determination

The following Section details the apparatus used in the measurement of the contact angles of glass and steel, the surface and solution preparation, and the experimental procedure used to perform contact angle measurements.

4.2.2.1 Instruments

The contact angles of buffered water with glass and stainless steel were measured using the FIBRO 1100 DAT Mk II (FIBRO System AB, Sweden). The apparatus is a compact contact angle test instrument, with built in CCD-camera (Charge Coupled Device), supported by a PC equipped with an image analysis package. The instrument can determine the wettability, the adsorption, and the absorption of a fluid applied to a surface via a syringe. The instrument consists of a monochrome CCD camera, with the capture time of 1msec, a precision fluid pump, delivering a drop size of 0.1 to 20μℓ, and an automatic sample feed with variable step length.
The results of the measured contact angle as a function of time can be used to determine the wetting of the surface, as well as the sorption. Depending on the free surface energy, a drop applied to a surface will wet the surface differently. The fluid may also penetrate and disappear into the surface. Should sorption occur, the volume of the applied drop decreases. In the case of absorption, the base diameter remains constant, and the contact angle decreases with time. In the case of adsorption, the base diameter increases, and the contact angle decreases.

4.2.2.2 Surface Preparation

Glass and stainless steel surfaces were cut to provide flat rectangular samples with dimensions of 100mm x 15mm x 2mm. Both glass and stainless steel surfaces were prepared as detailed in Section 2.3.3. Great care was taken to avoid handling the test surface.

4.2.2.3 Solutions

Experiments were performed with 25mM NaH_2PO_4 solution adjusted to pH 3.5, 5.5, 7.5, and 9.5, using HCl (1M) and NaOH (1M).

4.2.2.4 Experimental Procedure

The sample drop of buffered distilled water (4μℓ) was deposited on the collector surface, and 50 images were taken from 60msec (initial contact angle) to 12 seconds, allowing the determination by supporting software of any change in the contact angle of the sample with respect to the collector surface. The results were presented at 0.1, 1, and 10 seconds. The contact angle experiments were carried out at 22 +/-1°C.

The arrangement of the settings of the machine was important to produce the optimum conditions for the measurement of the contact angle of the solution with the surface, therefore avoiding any potential errors. The droplet size and the stroke pulse can both cause unnecessary errors if set incorrectly. The stroke pulse describes the force applied to detach the liquid droplet from the outlet of the syringe. The droplet size should be such that the droplet requires minimal force to remove it from the tip of the syringe. The outlet must be positioned so that there was no splash effect. The stroke pulse should be sufficient to remove the droplet, and no more. In short, the droplet should be in contact with both the collector surface and the syringe outlet at the time of release.

The contact angle of the sample solution at a given pH was measured on both glass and stainless steel. Examples of captured images for both glass and stainless steel are given below in Figure 4.2.

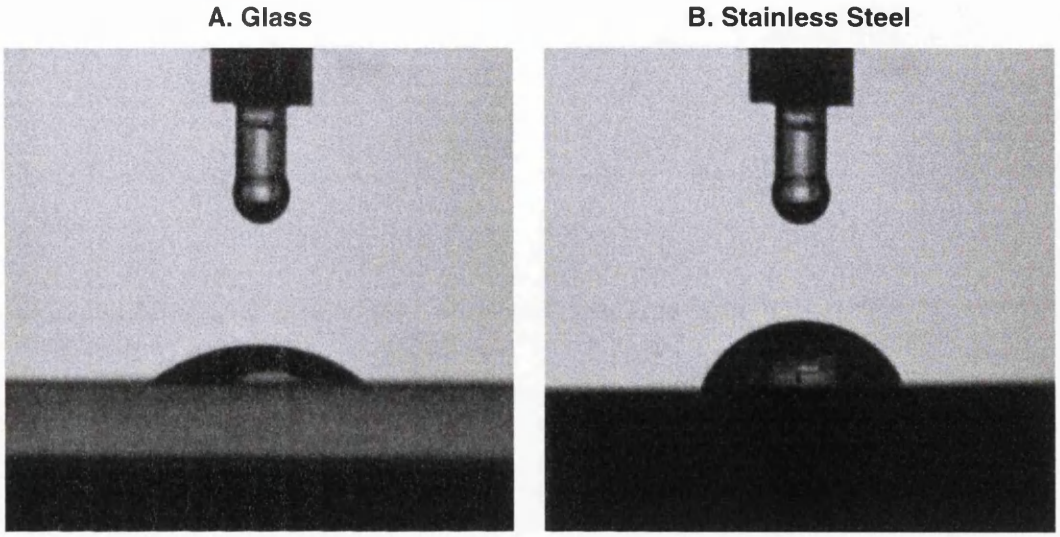

Figure 4.2: Captured images of 25mM NaH_2PO_4 in distilled water on a) glass, and b) stainless steel at pH 3.5, one second after application. The volume of liquid applied to the surface was 4µℓ. The images allowed the determination of the contact angles, 33.4 +/- 5.6°, and 73.8+/- 4.6°, respectively.

4.2.3 The Effect of pH on Contact Angle: Results

This Section presents the results of the contact angle of buffer solution on both glass and stainless steel as a function of pH and time, as detailed by Section 4.2.2. Results are presented at 0.1, 1, and 10 seconds from release of the respective solution onto the sample surface.

4.2.3.1 The Effect of pH on Contact Angle (t = 0.1s)

As expected, the contact angle of glass at 0.1 seconds was noticeable lower than that observed with stainless steel, as shown in Table 4.1.The second observation was that the contact angle was dependent on pH, as illustrated in Figure 4.3.

The contact angle decreased as pH increased for both glass and stainless steel, and can be explained by the decrease in $[H^+]$ ions present within the applied solution. There was a large difference between the values recorded for glass and stainless steel, ranging between 35° and 50°, depending on pH.

	Glass	Stainless Steel
pH 3.5	41.5+/-8.8°	76.1+/-4.0°
pH 5.5	27.7+/-3.0°	75.9+/-0.1°
pH 7.5	28.2+/-6.0°	66.6+/-6.8°
pH 9.5	21.0+/-5.7°	62.4+/-3.3°

Table 4.1: The Contact Angles for Glass and Stainless Steel with respect to pH, at t = 0.1 second. 25mM NaH_2PO_4 was adjusted to the required pH using either HCl or NaOH (1M). Experiments were conducted at 22 +/- 1°C.

The relationship between contact angle and pH was not linear, however, and is depicted in Figure 4.3. These values are taken into consideration when assessing the adhesion of aminated and carboxylated beads, and the spores of *B.mycoides* and *B.subtilis* to glass and stainless steel, at the corresponding pH.

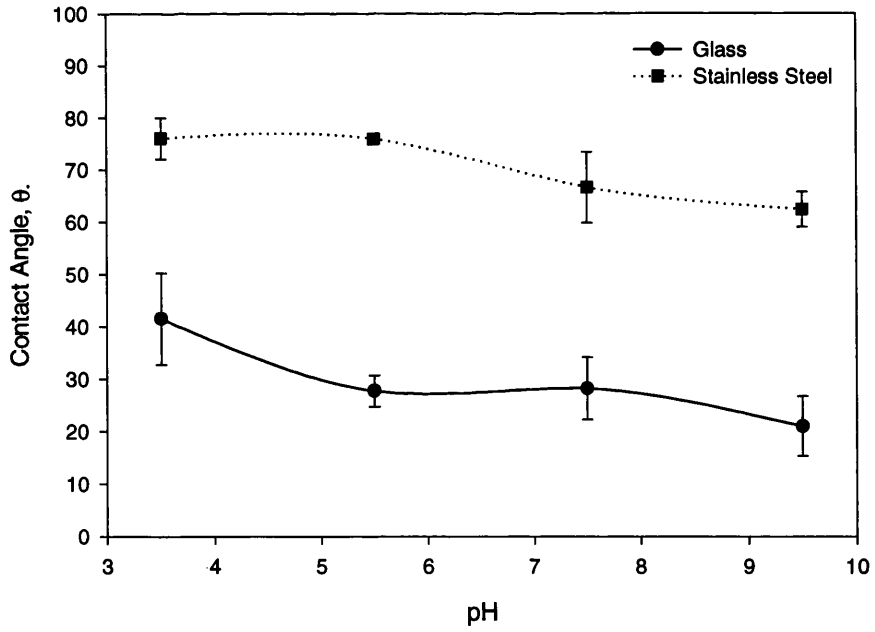

Figure 4.3: The contact angles of 25mM NaH_2PO_4 in distilled water on glass, and stainless steel, relative to pH. Measurements were taken 0.1 seconds after application. Standard deviation is shown where the error is larger than the symbols used. Experiments were conducted at 22 +/- 1°C. The pH was adjusted using HCl, or NaOH (1M) respectively. Surfaces were polished using 1μm diamond paste.

4.2.3.2 The Effect of pH on Contact Angle (t =1 and 10s)

The contact angle measurements performed using glass at 1 and 10 seconds were substantially lower than that observed with the stainless steel surface, as observed at 0.1 seconds. The data and graphical representation of contact angle measurements at both 1 and 10 seconds can be seen in Appendix B.

4.2.3.3 The Effect of Time on Contact Angle for both Glass and Steel

The contact angles of both glass and stainless steel changed insignificantly from the initial contact angle with respect to time as shown in Figures 4.4 and 4.5. Images were taken for both glass and stainless steel at t = 0.1, 1, 10 s at pH 9.5 which was used as an example pH. The decrease in angle was of no real consequence, as the dynamics of contact angle measurements were not being assessed. The contact angles presented in Table 4.1 were therefore used as the recorded contact angle measurements when considering the results obtained in Chapters 5, 6, and 7.

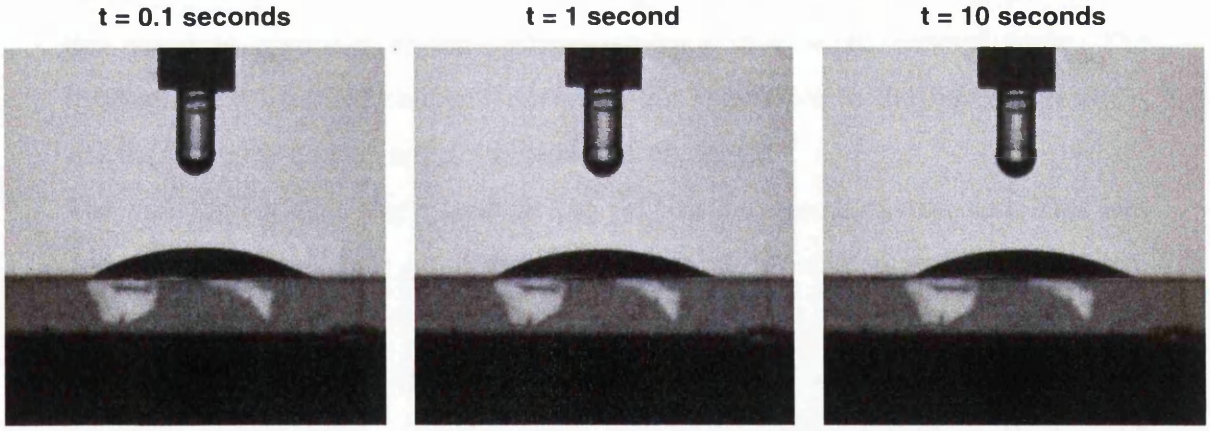

Figure 4.4: Captured images of 25mM NaH_2PO_4 in distilled water on glass, at pH 9.5. The volume of liquid applied to the surface was 4µℓ. The three images were taken at time intervals of 0.1, 1, and 10 seconds. Contact angles were 21.0+/- 5.7°, 21.0+/- 6.5°, and 23.9+/- 0.1° respectively.

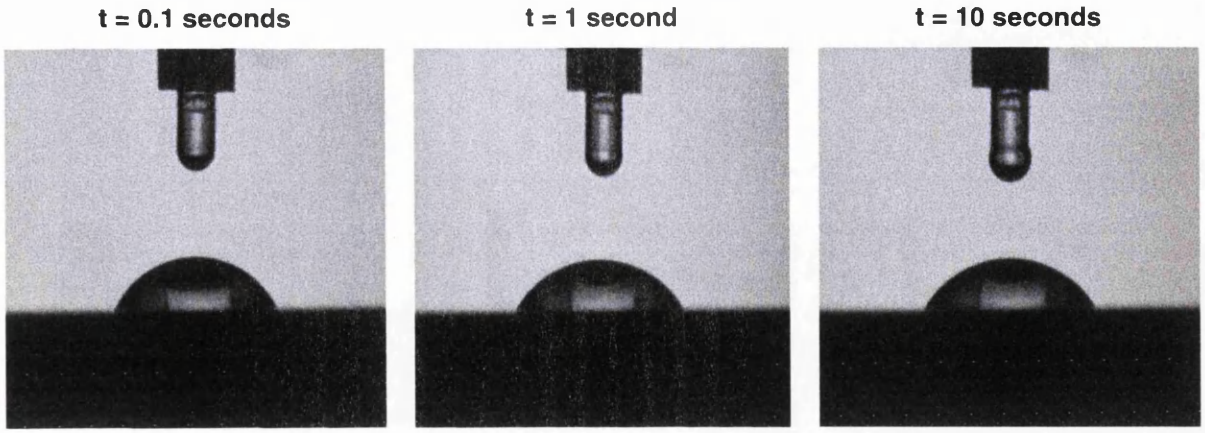

Figure 4.5: Captured images of 25mM NaH_2PO_4 in distilled water on stainless steel, at pH 9.5. The volume of liquid applied to the surface was 4µℓ. The three images were taken at time intervals of 0.1, 1, and 10 seconds. Contact angles were 62.4+/- 3.3°, 58.5+/- 4.5°, and 57.4+/- 4.6° respectively.

4.2.4 Summary of Contact Angle Measurements

The measured contact angles of glass and stainless steel differ substantially, which agrees with visual observations made using the Spinning Disc and Radial Flow Chamber (see proceeding Chapters). The high negative charge of the glass allowed the liquid to spread over the surface resulting in a small contact angle. The hydrophobic surface of stainless steel was not conducive to the liquid spreading, and therefore the contact angle was substantially larger.

The measured contact angle increased as pH was decreased, as expected. This was due to both glass and stainless steel becoming protonated as pH decreased, rendering the surface more hydrophobic.

The purpose of this investigation was to demonstrate that glass possessed noticeably different hydrophobic characteristics compared with stainless steel. The investigation was a qualitative, rather than quantitative exercise. The combination of these results with the equivalent data for the colloidal particles allowed the prediction of adhesion in relation to hydrophobicity, and also aided the explanation of the processes occurring within the interaction between the collector surface and the respective particle.

4.3 The Assessment of the Surface Topography of Glass and Stainless Steel

The surface roughness of both glass and stainless steel were assessed to ensure that the surfaces provided similar topologies. This enabled any conclusions to be made without taking into consideration the effect of the surface roughness of the collector on particle adhesion.

4.3.1 Theory

Surface topography has a noticeable effect on the adhesion of colloidal particles to a collector surface (Walz, 1998). Although both glass and stainless steel surfaces were polished using the same methods, it was necessary to ascertain that the surface roughness was similar in both cases, and that this roughness was small relative to the size of the adhering particles.

Vertical scanning interferometry (VSI) was employed as the method of surface analysis. VSI is a definite 'white light' procedure using short coherence light beams, which resulted in high fringe intensities, allowing accurate measurement of small dimensions. Interferometry is a non-contact and therefore non-destructive method of analysing the topography of the collector surface.

The instrument split white light, deflecting part of the light onto a reference sample (a mirror) and allowed the remainder of the beam to be projected onto the sample. The two beams return from their respective surfaces forming interference fringes. The beams returned either 'in phase', and formed bright fringes, or 'out of phase', and formed dark fringes. From this it was possible to build a profile of the sample surface using optical data. The basic principles of interferometry are shown in Figure 4.6.

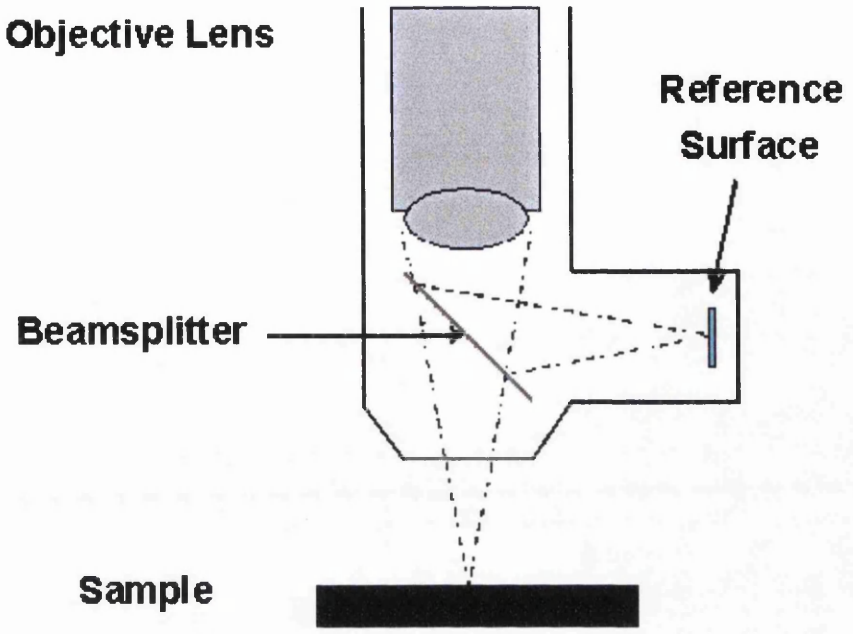

Figure 4.6: The Principles of Interferometry.

Fringes only appeared where the difference between sample and reference was small, due to the short coherence nature of white light, resulting in a maximal fringe contrast.

The sample was scanned vertically, and images were recorded at different heights over the surface as illustrated in Figure 4.7. The relative height of all the pixels in the image was calculated by finding their point of highest intensity modulation (fringe contrast).

The results obtained using interferometry can either be displayed in two or three dimension plots. However, the most significant results were statistical, and were the calculation of average roughness (R_a), the route mean square roughness (R_q), and the maximum profile height (R_t).

To ensure reliable results, the surface topography for both glass surfaces and stainless steel were measured at five randomly chosen areas of dimensions 736μm x 480μm. The values for roughness (R_a), the route mean square roughness (R_q), and the maximum profile height (R_t), were presented as an average of the five sample areas.

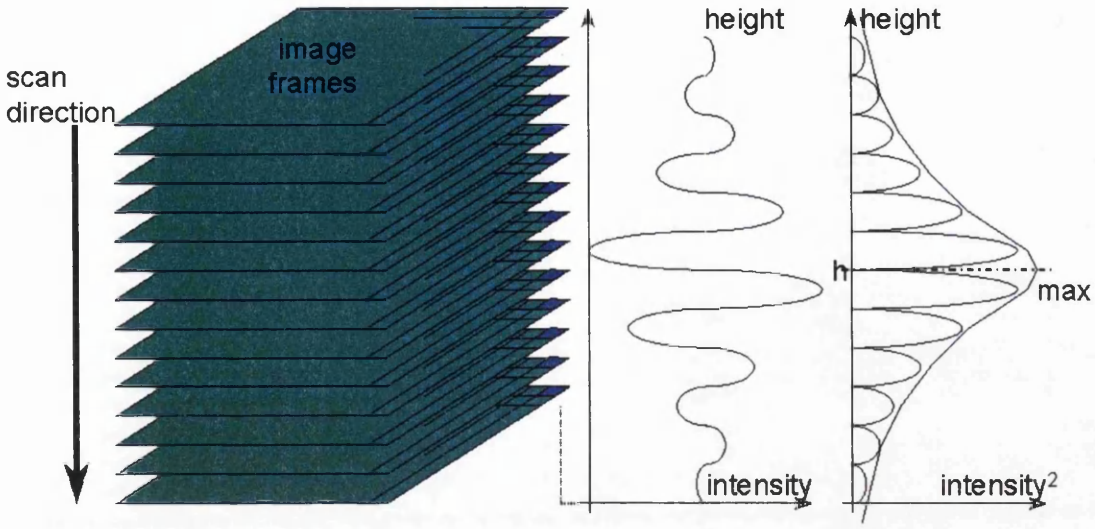

Figure 4.7: The Vertical Scanning Technique to assess Surface Topography.

4.3.2 The Assessment of Surface Topography: Materials

The interferometer was supplied by WYKO (now Veeco). The collector surface samples used were the Spinning Discs detailed in Chapter 6, as the dimensions of the discs were suitable in conjunction with the apparatus. The surfaces were polished and prepared as detailed in Section 2.3.3

4.3.3 Collector Surface Topography: Results

The following Section presents the surface topography of glass and steel incorporated within the project.

The collector surfaces are represented as 3-dimensional images, and the statistics gained from the surface assessment are stated in Table 4.2. The topography of the glass and stainless steel surfaces was assessed and showed that they were smooth relative to the size of particle used in experimentation as shown in Figures 4.8 and 4.9.

	Glass	Stainless Steel
Average Surface Roughness (*Ra*)	9.7 nm	8.8 nm
Root Mean Square Roughness (*Rq*)	12.8 nm	11.31nm
Max. Profile Height (*Rt*)	540.7 nm	396.1nm

Table 4.2: The statistical analysis of the surface topography of both glass and stainless steel. *Ra* represents the average surface roughness, the average of the values of the measured height deviations measured from the mean surface. *Rq* represents the root mean square of height deviations, and *Rt* represents the vertical distance between the highest and lowest points. Both glass and stainless steel were scanned five times over an area of approximately 0.35mm^2.

Both the Spinning Disc and Radial Flow Chamber used the same polishing technique to prepare the surface. The Packed Column, however, used a collector surface that could not be polished, and this may explain differences in attachment levels, as discussed in Chapter 9.

4.3.3.1 The Surface Topography of Glass

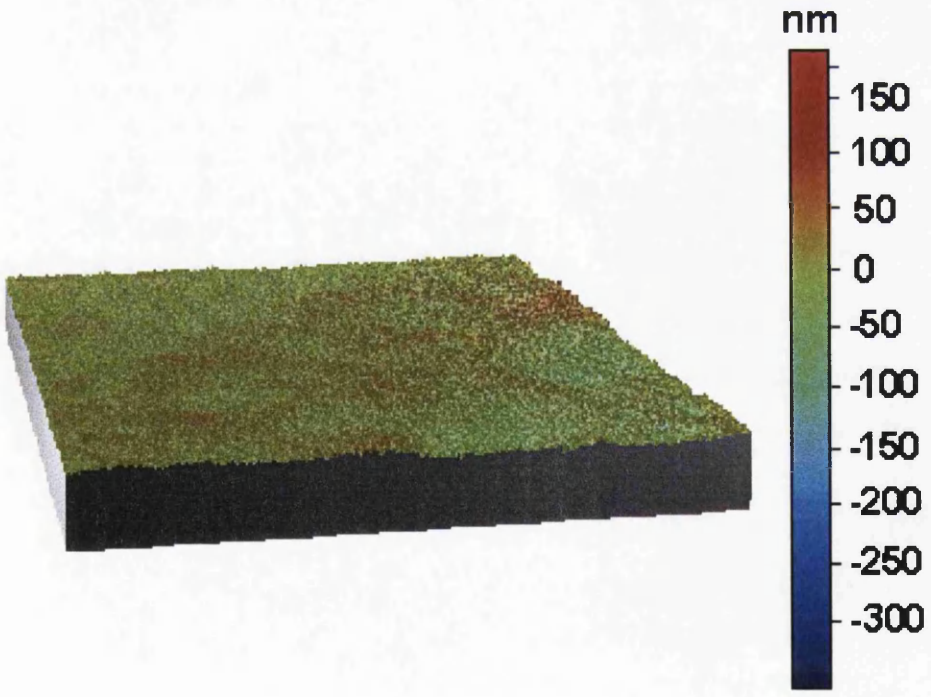

Figure 4.8: The surface topography of glass polished using 1µm diamond paste. The Figure represents an area of 736 x 480µm.

The average surface roughness and the root mean square of roughness, showed values that were small relative to the size of the latex beads and spores assumed to be approximately 2µm, as shown in Table 4.2. The distance between the highest and lowest points was approximately a quarter of the assumed diameter of the particles (540nm).

4.3.3.2 The Surface Topography of Stainless Steel

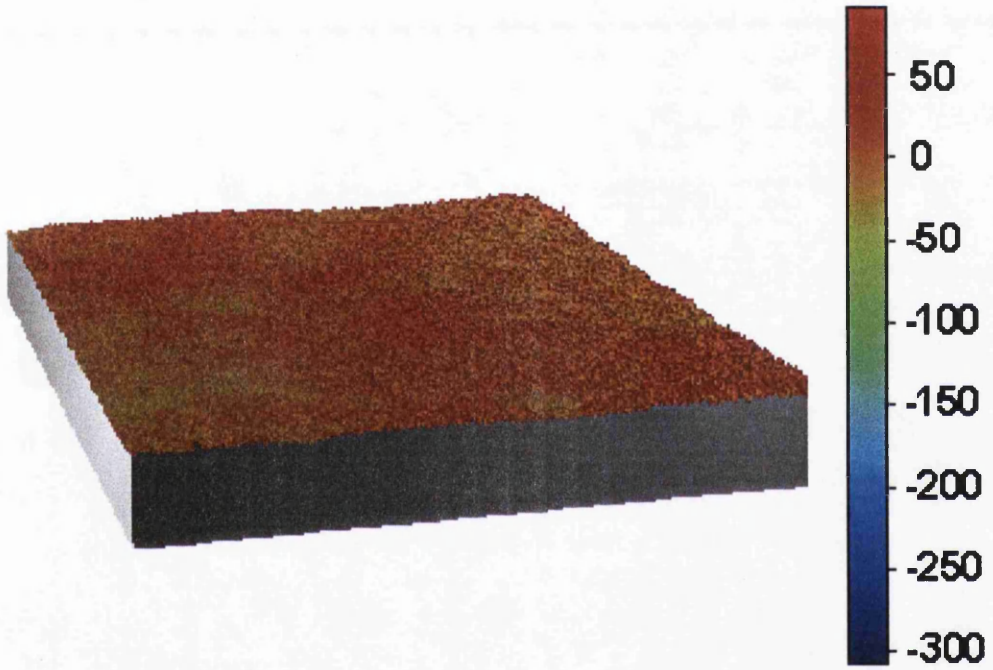

Figure 4.9: The surface topography of stainless steel polished using 1µm diamond paste. The Figure represents an area of 736 x 480µm.

The stainless steel surface was polished using the same protocol as the glass, and showed very similar statistics when assessing the surface roughness. The average surface roughness and root mean square showed values that were similar to glass, and small relative to the size of the latex beads and *Bacillus* spores (approx 2µm). The distance between the highest and lowest points was approximately a fifth of the assumed diameter of the particles.

4.3.4 Summary of Surface Roughness

The data and images obtained for both glass and stainless steel showed that the polishing method provided similar topographies in both cases. The average surface roughness (R_a) and root mean square (R_q) both had very similar values, and were the most important statistics. The distance between highest and lowest points, 541nm and 396nm for glass and steel respectively, showed a difference of 27%, but were insignificant relative to the size of the colloidal particles.

The investigation into the surface topography showed that the polishing method provided consistency between glass and stainless steel surfaces. This Section also showed that the average surface roughness was approximately 0.5% of the assumed size of the colloidal particles (2μm) used within this project.

4.4 Discussion of the Characterisation of Collector Surfaces

The two objectives of the work performed within this Chapter have been achieved. The first objective was to compare the hydrophobicity of glass and stainless steel, the results of which are conclusive: Stainless steel provides a more hydrophobic surface than glass. The contact angle measurements increased as pH was decreased, which was attributed to the protonation of both negatively charged surfaces.

The second was to ascertain that the surface roughness of both glass and stainless steel were i) comparable in size and variation, and ii) substantially smaller than the size of the particles used to perform adhesion assays within this project. The topographical statistics obtained for glass were very similar to those obtained using stainless steel, and comparatively small compared with the particles used within this project.

CHAPTER FIVE

The Development and Use of the Packed Column for Adhesion Studies

5.1 Introduction

This Chapter details the assessment of adhesion of aminated and carboxylated beads and the spores of *B.mycoides* and *B.subtilis* to glass and stainless steel using a Packed Column. As a novel method of measuring particle adhesion, the methods and techniques used in conjunction with this technique were initially developed and refined as experimental experience was gained. Once this had been completed, characterisation of the Column, and finally enumeration and quantification of the particles' adhesion to the respective surfaces was performed.

The following Section explains the relevance of the use of the Column, and theory involved in the development and characterisation of the Column.

5.1.1 Previous Uses and Relevance of the Packed Column

The Packed Column is a novel method of assessing microbial adhesion, and previous uses cannot be relevantly compared to its employment within this project. Previous work using a Column has involved the assessment of soils as the collector surface, combined with carboxylated latex beads used as a model system (Roy and Dzombak, 1996a; Grolimund *et al*, 1998).

Particle attachment was studied within this project, rather than kinetics of detachment, which are generally the subject of study of Bergendahl and Grasso (1999).

Many characteristics of packed bed flow and retention within the packed bed have been studied. The effect of microbial adhesion within the Packed Column has a great significance within the environment (Huysman and Verstraete, 1993).

For instance, groundwater flow through an aquifer is an example of a natural system of economic importance. Adhesion to granular collector surfaces is also of great significance that many engineering aspects incorporate porous media systems, such as heterogeneous catalysis and filtration.

5.1.2 Theory

The use of the Packed Column provided a system that allowed the determination of the effect of solution chemistry upon the adhesion of a colloidal particle to a collector surface. This method did not incorporate shear as a method of removing adhered colloids (Bergendahl and Grasso, 1999), as the flow rate through the Column did not provide sufficient shear to remove adhered particle, and that the movement of liquid is constant flow rather than variable as observed with other employed techniques e.g. Spinning Disc and Radial Flow Chamber. The Column allowed the calculation of irreversible binding, by analysing the percentage retention within the Column. The method also allowed an insight into reversible binding by assessing the shape of the particle break-through curve, by statistical analysis (Yan, 1996). The primary mechanisms controlling the transport of colloidal particles through the column were particle advection, dispersion, and deposition

(Grolimund *et al*, 1998). The deposition rates of the colloids within the packed bed can be calculated, although the discrepancy between theoretical and practical values cannot be explained (Litton and Olson, 1993). Adhesion kinetics within the Packed Column cannot be calculated purely from knowledge of DLVO theory (Elimelech and O'Melia, 1990).

5.1.2.1 Assumptions

Several assumptions were made when studying adhesion with the Packed Column, regarding the size, the packing, and flow through the Packed Column.

The first was the structure of the Column. The packing was assumed to consist of spheres of uniform size, with equal distribution of surface characteristics and that the packing within the Column was tetrahedral in arrangement (i.e. the best packed configuration).

The second assumption was that all particles have an equal opportunity to make contact with the collector surface. However, the particles may enter the Column as aggregates, and therefore adhere as aggregates. This was a mechanism that would naturally occur in the initial stages of colloidal adhesion, and therefore must be taken into consideration in this *in vitro* method of assessing adhesion (van de Ven, 1998).

The third assumption was that colloid deposition rates were independent of previously attached particles. This assumption can only be made when taking initial rates into consideration (Camesano *et al*, 1999). The fact that adhesion may occur between a colloid and a previously adhered colloid was a part of measuring adhesion, as the same process occurred *in vivo*. The assessment of adhesion was therefore not necessarily a colloid/collector interaction but adhesion of a population in general (van de Ven, 1998).

Due to the variety of the size and shape of the packing within the Column, the theory underestimates the surface area available for adhesion. Silica and stainless steel packing was used within the Column and ranged in size from 200-500μm in diameter. However, it was shown that flow through the Column was ideal, and therefore the assumptions were deemed acceptable.

5.1.2.2 Cake Formation and Straining of the Packed Bed

The effect of blocking upon the functioning of the Column and subsequent results has been covered extensively in previous work (Camesano *et al*, 1999; Madeani, 1998). Deposition within the Column may or may not affect colloidal adhesion, depending on the relative size of both the collector and colloid (Ruckenstein and Prieve, 1976). *Ripening* is generally seen with oppositely charged surfaces where the particles are attracted to the surface and remain attached, covering the collector surface. *Blocking* is observed when the opposite is true, and is a governed by DLVO theory, and steric interactions (Liu *et al*, 1995; Rijnaarts *et al*, 1996b). The Column apparatus should therefore be designed to provide a system that combines minimal blocking, but sufficiently reliable results that enabled analysis of adhesion.

5.1.2.3 Calculation of the Collector Surface Area

Knowing the dimensions of the glass column, and assuming that the voidage (e) was 0.4, (Bergendahl and Grasso, 1999), the volume of the collector ($V_{collector}$) within the column could be calculated. Consequently, knowing the volume of an individual collector sphere (V_{sphere}), assuming the packing is of uniform size (350μm diameter), and spherical, it is possible to determine the surface area of an individual sphere (A_{sphere}), and the available surface area of the collector within the column ($A_{collector}$). The calculations used to derive these figures are given in Appendix C.2.

$V_{collector} = 2.05 \times 10^{-5}\ m^3$

$V_{sphere} = 1.29 \times 10^{-12}\ m^3$

$A_{sphere,} = 5.73 \times 10^{-8}\ m^2$

$\mathbf{A_{collector} = 0.916\ m^2}$

Any adhesion to the glass Column itself was deemed negligible, and experiments were carried out to show that adhesion to the introduction apparatus was negligible as detailed in Section 5.4.3.

5.1.2.4 Packed Column Voidage

The theoretical voidage within the Column, assuming it was packed full of spheres in a tetrahedral arrangement is 0.4 (Bergendahl and Grasso, 1999). This was confirmed experimentally in Section 5.4.5 below.

5.1.2.5 Flow Rate and Reynold's Number

The flow rate within the Column should provide conditions where laminar flow was obtained rather than turbulent flow.
Having calculated an approximation for the surface area of the packing within the Column, the Reynold's Number was approximated using Equation 5.1.

$$Re = (u\,\rho) / s\,\mu\,(1-e) \qquad \textbf{5.1}$$

Where u represents the velocity over the surface of the collector (0.0095 m/s), ρ is density of water (1000 kg/m^3), s is the collector surface area / packed bed volume (44000 m^{-1}), μ represents fluid viscosity (1 x 10^{-3} kg/ms), and e is the column voidage (0.4).
The maximum Reynolds number for the system was approximated at 0.356. This low value agreed with the fact that shear force did not have a consequential effect within the Column (Bergendahl and Grasso, 1999).
Flow rate was measured experimentally in g/min, however, Equation 5.1 requires flow rate in m/s. The calculation for the flow rate over the collector surface area is given in Appendix C.3.

5.1.3 Methods of Interpreting Data

The analyses of break-through curves obtained from each run can be interpreted using two different methods. The first allowed the determination of irreversible binding by calculating the percentage recovery of the sample from the Packed Column. The concentration and volume of the starting sample were known, allowing the calculation of the total input of the sample into the Column. The break-through curve was integrated allowing the calculation of percentage recovery, by taking into consideration the volume eluted at each reading, and the concentration of the eluate at that point, using the trapezium rule. An example of a typical experiment with 5 break-through curves is given in Figure 5.1.

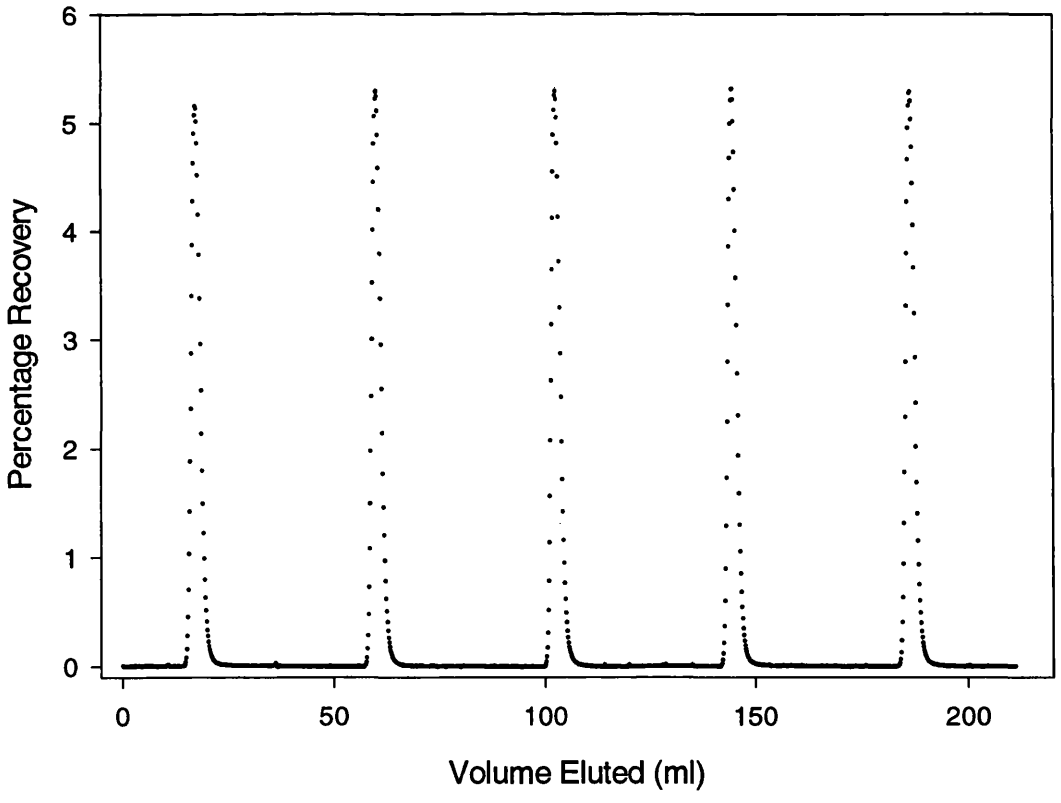

Figure 5.1: An example of an experiment investigating the adhesion of the spores of *B.subtilis* to silica (200-500μm). The spores were suspended in 25mM NaH_2PO_4, and adjusted to pH 9.5 using 1M NaOH. Five samples were introduced at regular intervals of 300 seconds.

Reversible binding can be characterised by taking the shape of the tail of the break-through curve into consideration (Roy and Dzombak, 1996b). Several factors, including variance can be investigated. In previous work, the log function of the break-through curve has been analysed (Yan, 1996), allowing analysis of the tail of the curve. In work with latex beads, the tail of the curve showed very small differences (Grolimund *et al*, 1998). The sensitivity of the spectrophotometer and supporting apparatus as detailed in Section 2.2.5 was not sufficient to obtain reliable data, and therefore the tail of the break-through curve was not analysed. Analysis of the tail of each individual break-through curve was also too time consuming for the amount of results that were generated by the experiments performed within this project.

Having noted the flow rate throughout the experiment, the volume eluted after each individual measurement was calculated in mℓ. This allowed the x-axis, (total volume eluted) to be determined.

The $OD_{(660nm)}$ was recorded using the PICO Analogue/Digital converter as detailed in Section 5.2.3 at set time intervals, and transferred onto a spreadsheet as Voltage as shown in Section 5.3.5. This was totalled, allowing the total percentage recovery to be calculated as detailed in Figure 5.6.

5.2 Materials for the Measurement of Adhesion using the Packed Column Technique

The following Section details apparatus, materials, and solutions used within the work performed using the Packed Column to assess adhesion.

5.2.1 The Column and Supporting Accessories

A borosilicate glass Column (diameter 10mm, length 50mm) was supplied by Omnifit (Cambridge, UK). Also supplied by Omnifit were the following accessories: an adjustable end piece, an on/off valve, a loop/inject valve, PTFE frits (pore size 25μm), and a septum injector. These were assembled and fitted to a board

together with a reservoir as pictured in Figure 5.2, and represented schematically in Figure 5.3. Pressure was applied to the reservoir of buffer by pressurised nitrogen as a head gas, which produced a smooth flow of liquid through the column, rather than in pulses that would be observed when using a pump.

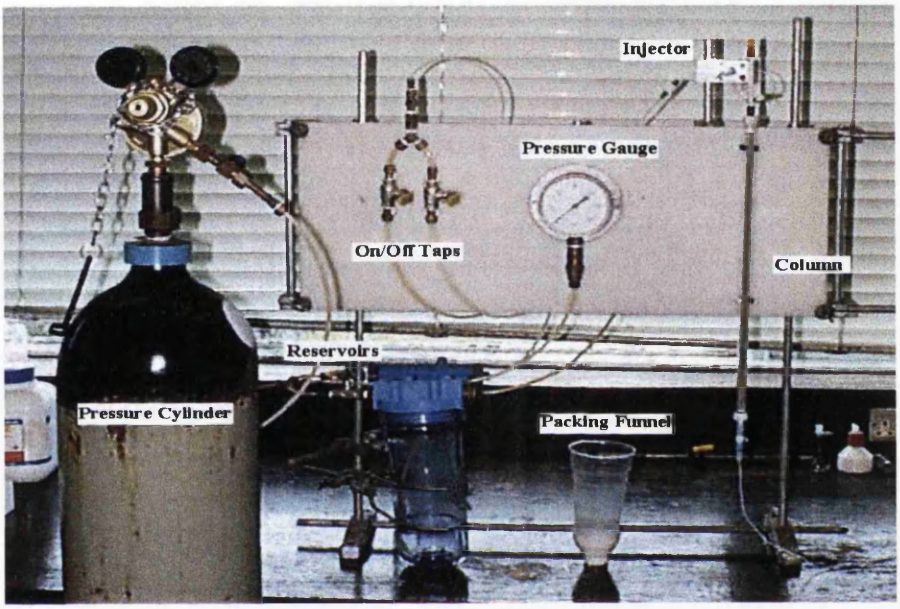

Figure 5.2: The Column apparatus and its arrangement. The image shows two buffer reservoirs, a pressure meter, an injection loop, a packing funnel, and the Column packed with stainless steel packing.

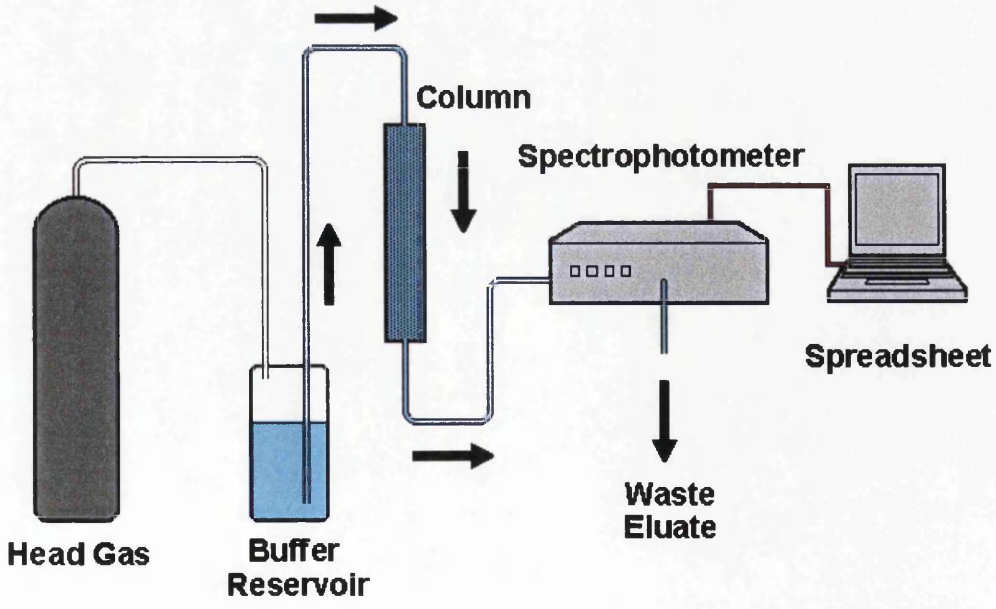

Figure 5.3: A diagrammatical representation of the Packed Column, and supporting apparatus.

5.2.2 Flow-through Cuvette

The eluate from the Column was assessed using a flow through cuvette (Hellma) with a path length of 10mm, over a period of five minutes. This was used in conjunction with a spectrophotometer (Pye Unicam), and OD was measured at 660nm in all cases.

5.2.3 PICO Technology Package

The output of the spectrophotometer was assessed using a package supplied by PICO Technology Ltd. The A/D converter computer interface was fitted to the parallel printer port of a Toshiba 75 MHz Pentium Laptop. This set-up enabled the voltage output to be measured each second over a given period of time, and recorded in a spreadsheet via the computer.

5.2.4 Silica Collector Surface

Matrex Silica 60 (Sigma), with a specification pore size of 60 Angstrom, for experiments conducted using the 70-200μm packing.
Silica 60 gel (Merck) was used for experiments conducted with 200-500μm packing.

5.2.5 Stainless Steel Collector Surface

Stainless steel powder was supplied by Osprey Metals Ltd (UK). Experiments were conducted using 75-180μm and 200-500μm packing. The stainless steel alloy used was 316L, and the composition of the steel particles is detailed in Appendix C.1.

5.2.6 The Preparation of Particulate Suspensions

The aminated and carboxylated beads, and the spores of *B.mycoides* and *B.subtilis*, were prepared as detailed in Section 2.3.

5.3 Methods for the Measurement of Adhesion Using the Packed Column Technique

The following Section details the initial protocol and techniques, developments and problem resolution, and the final protocol used when performing experiments with the Packed Column.

5.3.1 Initial Protocol

As the Packed Column was a novel method for assessing adhesion of colloids, techniques and methods required development and optimisation. The initial protocol was used in a general assessment of whether or not the method would be successful to assess adhesion. Many problems were encountered in the development from the initial to the final protocol, of which some are detailed in this Section.

5.3.1.1 Packing Protocol

The glass or stainless steel packing was suspended in distilled water for at least thirty minutes prior to packing, in order to remove any air that was resident on the pores of the collector surface. The ideal amount of packing for the Column was 17g and 40g for silica and stainless steel respectively, allowing sufficient room for the top end piece to be inserted into the Column. The suspension was poured into a water-filled Column as slurry with the bottom end-piece in place. The valve on the bottom end-piece was left open to allow liquid to flow through the Column whilst settling under gravity. At this point, the Column was rotated and tapped manually to

aid uniform settling within the Column. Having settled, the top end piece was inserted, taking care not to introduce air into the Column.

Distilled water was then passed through the Column for at least the equivalent of 5 Column voidages (approx. 75mℓ), under a pressure of 20psi. This was then repeated with the required buffer solution.

5.3.1.2 Sample Introduction: Injection Method

Initially the septum injector (Omnifit) was used to perform experiments with the Column. The sample (0.5mℓ) was introduced using a 1mℓ syringe, as shown in Figure 5.4.

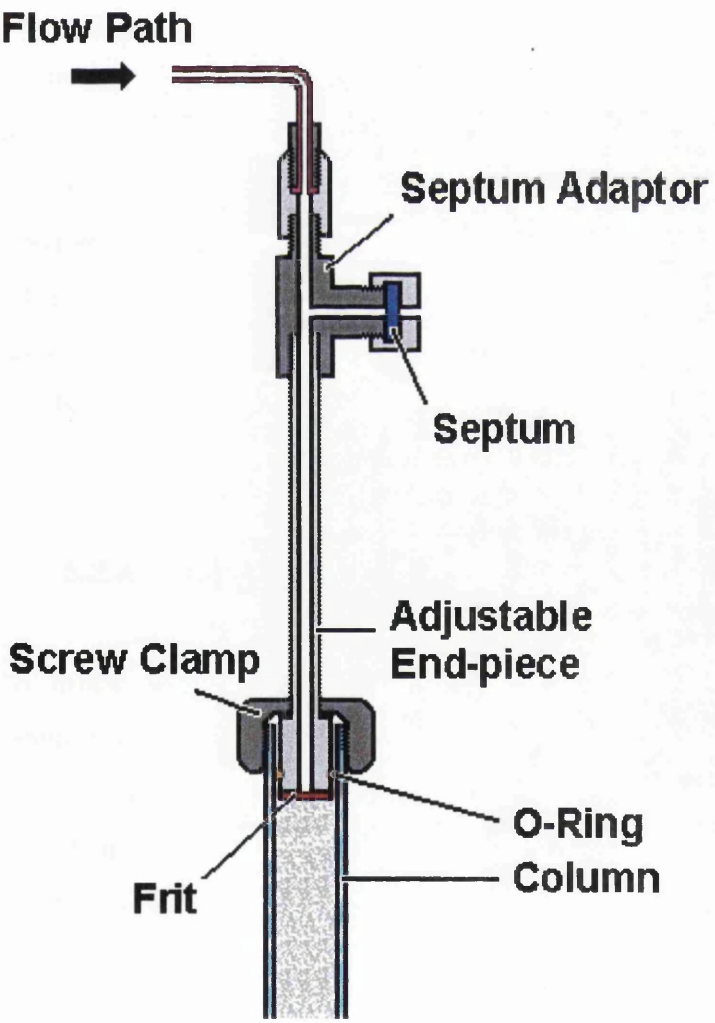

Figure 5.4: The septum injector and adjustable end-piece. This apparatus enabled samples to be introduced manually into the Column via a syringe.

5.3.1.3 Initial Eluate Assessment

Prior to obtaining a flow-through cuvette, the method of assessing the eluate from the Column, 1.5mℓ cuvettes were individually weighed, and 100 samples of approximately 0.5mℓ were continuously taken. The cuvettes were then weighed to assess the volume of each sample, and the $OD_{(660nm)}$ recorded.

The analysis of each experiment was exceptionally laborious, and susceptible to error due to the amount of cuvettes employed, and subsequently changed, as detailed in Section 5.3.4.

5.3.2 Development of Packing Protocol

The packing protocol gave reproducible results when using dextran blue as a sample injection, suggesting that the packing method was reliable for use. Air was occasionally trapped in the Column when packing, and therefore, the only alteration was to leave the packing suspended in distilled water for longer periods, with occasional manual agitation, to remove dissolved air. No washing of the silica was performed, as this introduced gas into the system, and also provided potential variation in surface preparation, which has been proven to alter latex adhesion to glass beads substantially (Litton and Olson, 1993).

5.3.3 Development of the Injection Method

The initial method of introducing the sample into the Column was performed manually through a septum, introducing the sample into the liquid flow from the buffer reservoir. This technique caused problems due to providing a non-uniform liquid front. The use of the septum injector was also identified as a potential cause for error, as the sample volume introduced into the Column may not be consistent, and was also prone to introducing air into the Column.

Subsequently the injection method was changed to using the loop method, which had two pathways from the reservoir of buffer to the Column. The first pathway

was directly from reservoir to Column. The second directed the flow pathway through a sample loop. The change of pathway was altered manually as shown in Figure 5.5. The loop method allowed a known volume of sample to be introduced into the Column as a uniform front as shown in Figure 5.6.

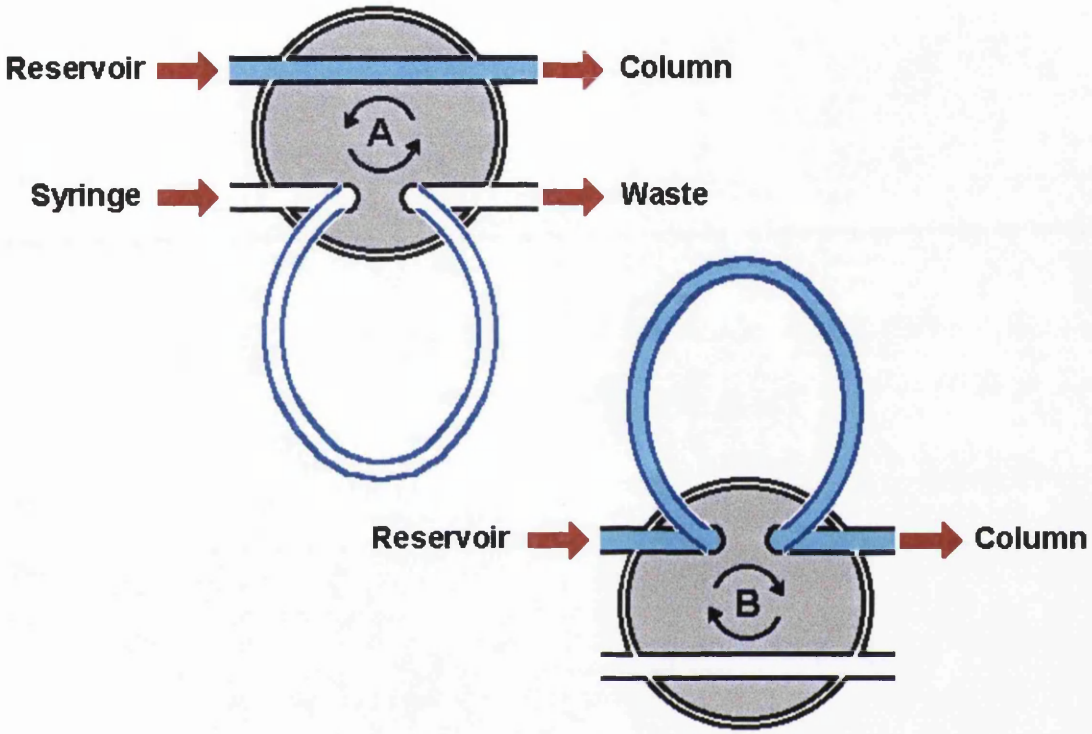

Figure 5.5: The Loop Injection Mechanism. Position A) directs the flow from the reservoir to the Column, allowing the loading of the loop with the sample. Position B) rotates the barrel and re-directs the flow through from the reservoir through the loop, introducing the sample to the Column.

5.3.4 Counting Technique Developments

The initial process of taking samples in individual 1.5mℓ cuvettes was too laborious, and was also prone to error, due to large sample volumes. A flow through cuvette (Hellma) was therefore obtained, providing continuous assessment of the eluate. This was used in combination with spectrophotometer (PYE Unicam), and a computer package (PICO technology), which allowed the analysis of the voltage output of the spectrophotometer over a period of 300 seconds (Δt = 1 sec).

5.3.5 Data Analysis Developments

The use of the flow through cuvette, and the PICO technology package allowed analysis of the break-through curves to be carried out using a spreadsheet as shown in Appendix C.4. An example a breakthrough curve is given in Figure 5.1.
The spectrophotometer provided a voltage output, corresponding to the OD measured through the flow through cuvette. Flow rate was recorded throughout each experiment, allowing the standard volume eluted per reading to be calculated, subsequently allowing the percentage recovery of the initial sample to be determined.

5.3.6 The Final Experimental Protocol

The following details describe the techniques used for sample injection and packing, and the experimental protocol used in Column characterisation experiments.

5.3.6.1 Packing Procedure

The collector surface was placed in distilled water for 30 minutes with regular manual agitation. The slurry was poured into a water filled Column, and allowed to settle whilst the Column was rotated and tapped manually. The top end-piece was inserted to the top of the Column, taking care to avoid the introduction of air into the system. Distilled water (100mℓ) was passed through the Column. This was repeated with the required buffer solution.

5.3.6.2 Injection Method

The introduction of the sample into the Column, as shown in Figure 5.6 was performed using the loop system, as shown in Figure 5.5, which allowed the introduction of a constant sample volume into the column. At each introduction of the sample, the loop was rinsed with distilled water, and re-loaded with a sample of known concentration.

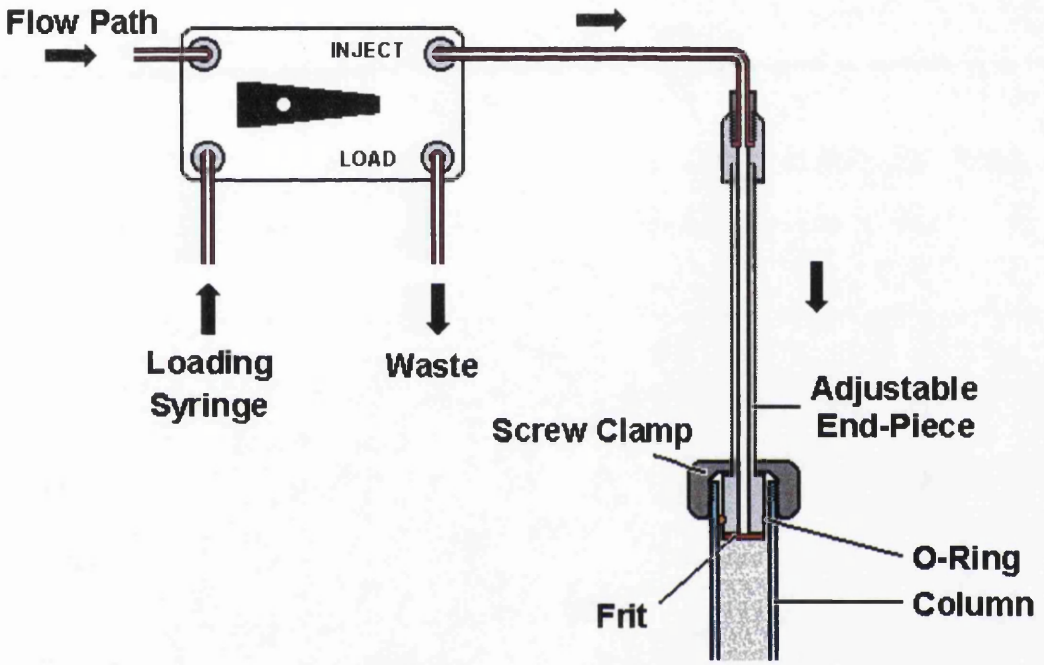

Figure 5.6: The accepted injection method used in all experiments. Rather than manual injection detailed in Figure 5.4, the sample loop was used, which allowed a constant sample volume to be introduced into the Column. The mechanism of the loop injector is shown in Figure 5.5.

5.3.6.3 Final Protocol for Characterisation Experiments

The following protocol was used for experiments to determine Column characteristics and the effects of various parameters within the Column, unless otherwise stated.

The sample was introduced into the Column manually through the loop introduction system. The recording package was started simultaneously, and allowed to run for 300 seconds. After 300 seconds, the loop was rinsed, reloaded, and the process

performed a total of five times. Buffer solution was passed through the Column whilst reloading, therefore keeping the flow constant, thus avoiding any disturbance by changing flow rates. The reloading process took approximately 5 seconds. Each experiment was carried out at 22 +/- 1°C.

5.4 Column Characterisation Experiments

Several experiments were necessary to assess the characteristics of the Column, to allow calculation and correct analysis of the results of the work performed with the Column. These included the determination of loop volume, the relationship between optical density between the cuvette and the flow through cell, and to assess if the injection apparatus was responsible for any colloidal retention.

5.4.1 The Determination of the Injection Loop Volume

In the analysis shown in Appendix C.4, it was of critical importance to assess the volume of the injection loop, and to ensure that this volume remained constant.
The volume of the sample injection loop was determined to allow calculation of the percentage recovery of the sample, by considering the volume and concentration of the initial sample.

Protocol:

The optical density of a solution of dextran blue dye was measured at 660nm, and was loaded into the sample loop, eluted from the loop, and collected from the top end piece without passing through the Packed Column. The collection volume was recorded, as was the optical density of the resulting eluate. The process was repeated seven times.

Results:

The data obtained, as shown in Table C.3 allowed the calculation of the loop volume (V_{Start}) to be 0.147mℓ with standard deviation of 0.006mℓ in conjunction with Equation 5.2. The standard deviation was 3.9% of the loop volume.

$$V_{Start} = (OD_{Eluate} \times V_{Eluate}) / OD_{Start} \qquad 5.2$$

where:

Starting sample solution $OD_{(660nm)}$, $\mathbf{OD_{Start} = 1.52 +/- 0.02}$

Average Eluate Volume, $\mathbf{V_{Eluate} = 2.66 +/- 0.112m\ell}$

Average Eluate $O.D_{(660nm)}$, $\mathbf{OD_{Eluate} = 0.084 +/- 0.006}$

5.4.2 The Relationship between $OD_{(cell)}$ and $OD_{(cuvette)}$

The flow through cuvette used to analyse the break-through curves generated from the Column gave appreciably different readings for optical density of the samples. The relationship between optical density measured in the flow through cell ($OD_{(cell)}$) and that observed in a standard 10mm path-length cuvette ($OD_{(cuvette)}$) was therefore determined.

Protocol:

Dextran blue solution was injected directly into the flow through cell, and optical density measured at 660nm. The optical density of the same solution was then measured in a standard 10mm path-length cuvette. This was performed fifteen times with the optical density of the solution ranging from 0 to 1 with respect to the standard cuvette.

Results:

Figure 5.7 shows that the flow through cell has a linear relationship with the standard 10mm path-length cuvette, and the relationship is defined in Equation 5.3. The cell has an intercept at 0.267, which was taken into consideration when analysing the results, shown in Appendix C.4. The gradient, however, shows that very little adjustment was required when converting the ($OD_{(cell)}$) into ($OD_{(cuvette)}$), once the intercept had been taken into consideration.

The relationship was defined as:

$$y = 1.01x + 0.27 \qquad 5.3$$

where y ($OD_{(cell)}$) was measured through the flow through cell, and x was the equivalent ($OD_{(cuvette)}$), as measured through the standard, 4mℓ, 10mm path-length cuvette.

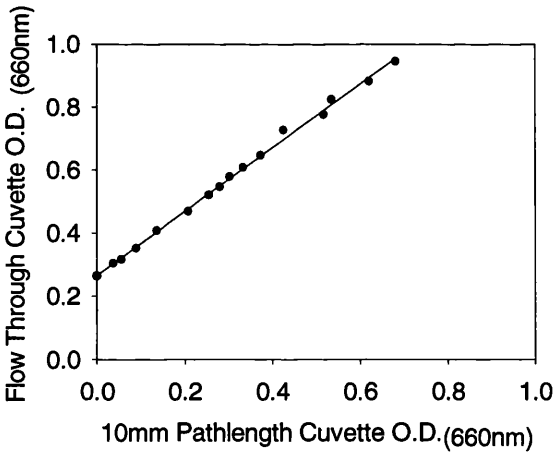

Figure 5.7: The relationship between (OD_{cell}) measured in the flow through cell, and $OD_{cuvette}$) measured in the standard 10mm cuvette. Dextran blue solutions of varying concentrations were used as the sample, and distilled water as the reference sample.

5.4.3 Determination of Recovery Rates from Injection Apparatus

Having determined the volume of the sample loop, the percentage recovery from the top end piece was calculated, to ensure that none of the sample was retained by the injection apparatus, and that any retention within the Column was therefore due

to retention by the collector surface as illustrated in Figure 5.6. This was especially important due to the presence of the Teflon frit with a pore size of 25μm. Both aminated and carboxylated beads and the spores of *B.mycoides* and *B.subtilis* were assessed.

Protocol:

A sample of known concentration was introduced into the injection loop and collected from either the end of the injection loop, or at the frit of the top end piece. The concentration of the collected eluate and its volume were recorded. This was repeated five times for each colloid type. Experiments were conducted at pH 3.5, and at 22 +/- 1°C.

Results:

The percentage recovery from both the loop and frit was calculated, and showed negligible retention and is shown in Appendix C.6. This demonstrated that any significant adhesion in subsequent experiments was due solely to adhesion to the collector surface in the Packed Column.

5.4.4 The Effect of Pressure on Flow within the Column

The effect of pressure on flow rate was assessed to ensure that no adverse effects due to small variations in pressure were observed within the Column apparatus.

Protocol:

The flow rate through the column was recorded, whilst pressure was increased from 5psi to 20psi. Silica (200-500μm) packing was used, with distilled water as the solution. No beads were introduced into the Column. Flow rates were measured in three Columns, over a period of five minutes at each pressure, at increments of 1psi.

Results:

The relationship between pressure and flow rate was linear as shown in Figure 5.8. The most important observation was that there was no significant deviation from the linear relationship, (r^2 =0.999). The relationship does not pass through the origin, as a pressure of 1.75 or more psi was required to force the eluent through the Packed Column.

The relationship between flow rate (*y*) and pressure (*x*) is represented by:

$$y = x - 1.75 \qquad 5.4$$

This allowed the measured flow rate to be relied upon, minimising the possibility of sharp increases or decreases in flow rate within the system.

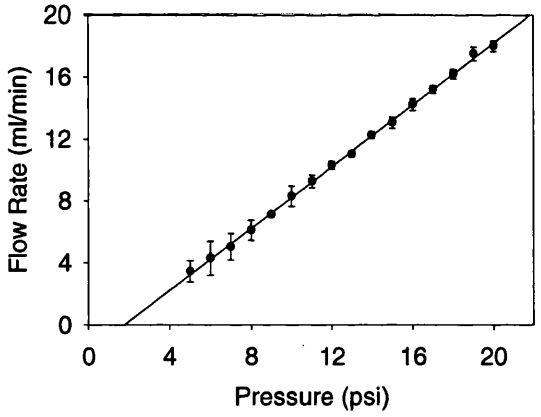

Figure 5.8: The effect of pressure on flow-rate through the column. Flow rate was increased by 1psi increments. Distilled water was used as the solution, in combination with silica (200-500μm) packing. Flow rate was measured over a period of 5 minutes at each pressure, and repeated three times in different columns. Experiments were conducted at 22 +/- 1°C.

5.4.5 Determination of Practical Voidage

The determination of the practical voidage of the Packed Column was required to compare with the theoretical voidage, as detailed in Section 5.1.2.3. The packing was not ideal as was mentioned above, so it was important to assess any radical difference from the theoretical voidage (*e*) of the Packed Column, which was 40% of the Column volume (Bergendahl and Grasso, 1999).

Protocol:

Three Columns were used in conjunction with dextran blue solution. The injection loop was loaded, eluted through a Column packed with silica (70-200 μm). The position of the peak of the resultant break-through curve was noted relative to eluted liquid. The concentration of the starting sample was not recorded, as it bore no relevance to the experiment. This was repeated with three Columns. Five peaks derived from each Column were recorded, and the mean value was determined.

Results:

The average difference between the theoretical and practical voidage was 1.16 +/- 0.82 %. The results obtained form this experiment demonstrated that although ideal packing did not occur, the voidage within the Column agreed with predicted values for a packed bed system and can be seen in Appendix C.7.

5.4.6 Discussion of Column Characterisation Experiments

The characterisation experiments performed above allowed the determination of the following:

1. The volume of the sample injection loop. This allowed the calculation of the amount of beads introduced to the Column, and subsequently the percentage recovery, when used in conjunction with concentration and volume of the eluted sample.
2. The relationship between OD measured in the flow-through cell, relative to the standard 4mℓ, 10mm path-length cuvette. This allowed comparison of start sample concentration, and eluate concentration.
3. There was negligible (approximately 0.5%) adhesion to the apparatus used for the introduction of the sample into the system, and therefore any adhesion that occurred within the Column was solely due to adhesion to the collector surface.

4. The effect of applied pressure on flow rate was a linear relationship. Any small changes in pressure would therefore have little effect on flow rate within the Column.

5. The comparison of practical with theoretical voidage. Voidage within the Column was predicted to be 40% of the total volume of the column. This assumed that there was ideal packing, and all the packing was spherical, and uniform shape. The Column did show very similar values for voidage (40.5% of the Column volume), compared with that predicted (40% of the Column volume).

5.5 Preliminary Experiments with the Packed Column

Experiments were undertaken to assess particle retention within the Column, with carboxylated latex beads of various sizes, using either silica or stainless steel as the collector surface. The following experiments were designed to assess the efficiency of the Column, and to determine the ideal parameters for data collection, rather than data collection itself, under defined conditions. The experiments also allowed the practice of skills associated with the use of the Column, and also to resolve problems that were encountered in the general use of the Column.

5.5.1 The Effect of Size Variation of both Collector and Colloid

The effect of size variation of both the collector and the colloid on adhesive characteristics was assessed to determine the final protocol to be used in the main data gathering experiment.

Protocol:

0.1, 0.5, 1, and 2μm carboxylated beads were introduced into the Column containing both 70-200μm silica 60, and 200-500μm matrex silica 60. Ten samples were introduced to each Column, and the experiment was repeated three times. The buffer solution was 25mM NaH_2PO_4 adjusted to pH 6.5 using NaOH (1M).

Results:

The relationship between adhesion and size was similar when either size of silica packing was used, as shown in Figure 5.9. As colloid size increased, it was expected that adhesion would increase. This was observed and was attributed to a combination of a larger surface area of the larger beads, and also filtering effects of the Column.

Results showed that a larger packing size would provide higher levels of recovery in all cases, due to larger paths of flow through the Packed Column. This net result was the likelihood of contact between the colloid and the collector being reduced. The larger packing also provided less collector surface area within the Packed Column.

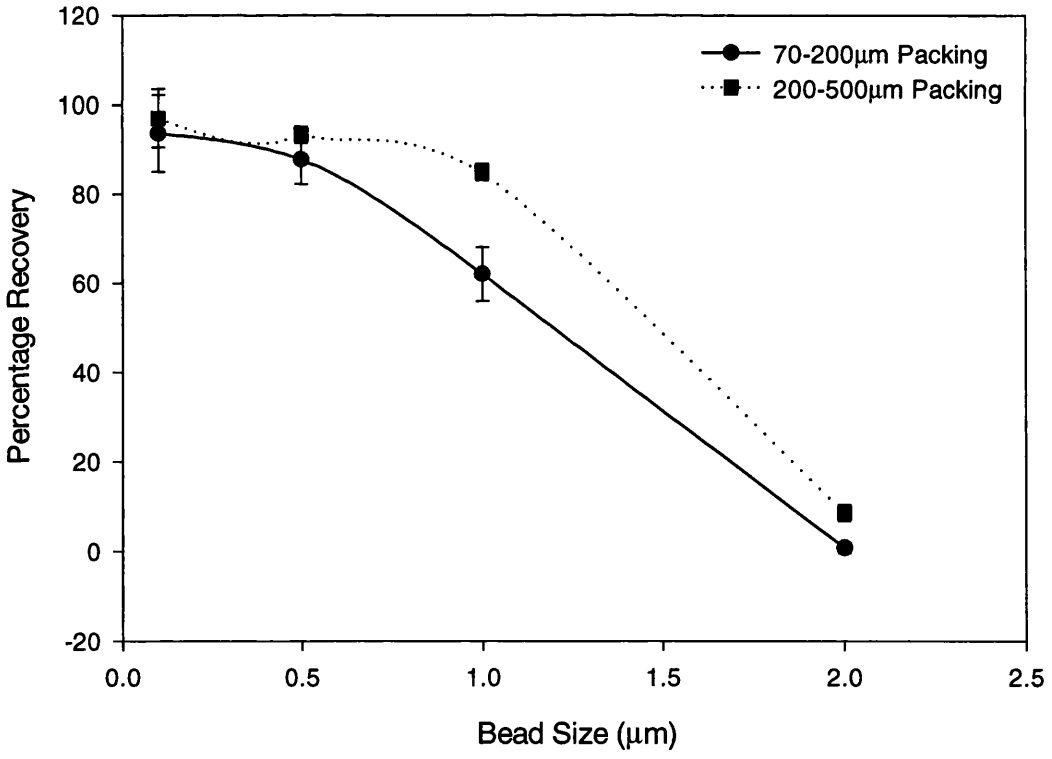

Figure 5.9: The effect of Colloid size on the Percentage Recovery from the Packed Column. Carboxylated latex beads (0.1, 0.5, 1, and 2µm) were introduced into the Column in was 25mM NaH_2PO_4, containing either 70-200µm or 200-500µm silica packing. Experiments were conducted at 22 +/- 1°C at pH 6.5.

5.5.2 The Effect of Flow Rate on Adhesion

The effect of flow rate on particle adhesion was assessed, to ascertain whether shear had any impact on adhesion within the Column. It has been predicted that the shear force generated within the Column was sufficiently low to be deemed insignificant, (Bergendahl and Grasso, 1999).
This subsequently rendered the Column method an assessment of the effect of solution chemistry upon adhesion, rather than a method of determining the effect of shear on adhesion.

Protocol:

The effect of flow rate was investigated using 0.5μm carboxylated latex beads in conjunction with 70-200μm silica 60 packing. Flow rate ranged from 4mℓ/min to 18mℓ/min, while pH was varied from 3.5 to 7.5.
The sample was introduced to the Packed Column using the standard method as outlined in Section 5.3.6, and percentage recovery was recorded and analysed as described in Sections 5.3.4 and 5.3.5.

Results:

5.5.2.1 Adhesion at pH 3.5 Relative to Flow Rate

The relationship between flow rate and adhesion was assessed, and represented in Figure 5.10. At pH 3.5, relatively high levels of adhesion were predicted, when taking into consideration the levels of hydrophobicity of the latex beads. Adhesion to silica was substantially lower relative to stainless steel, as expected, due to the difference in hydrophobic characteristics as defined by contact angle values as seen in Figure 4.3.

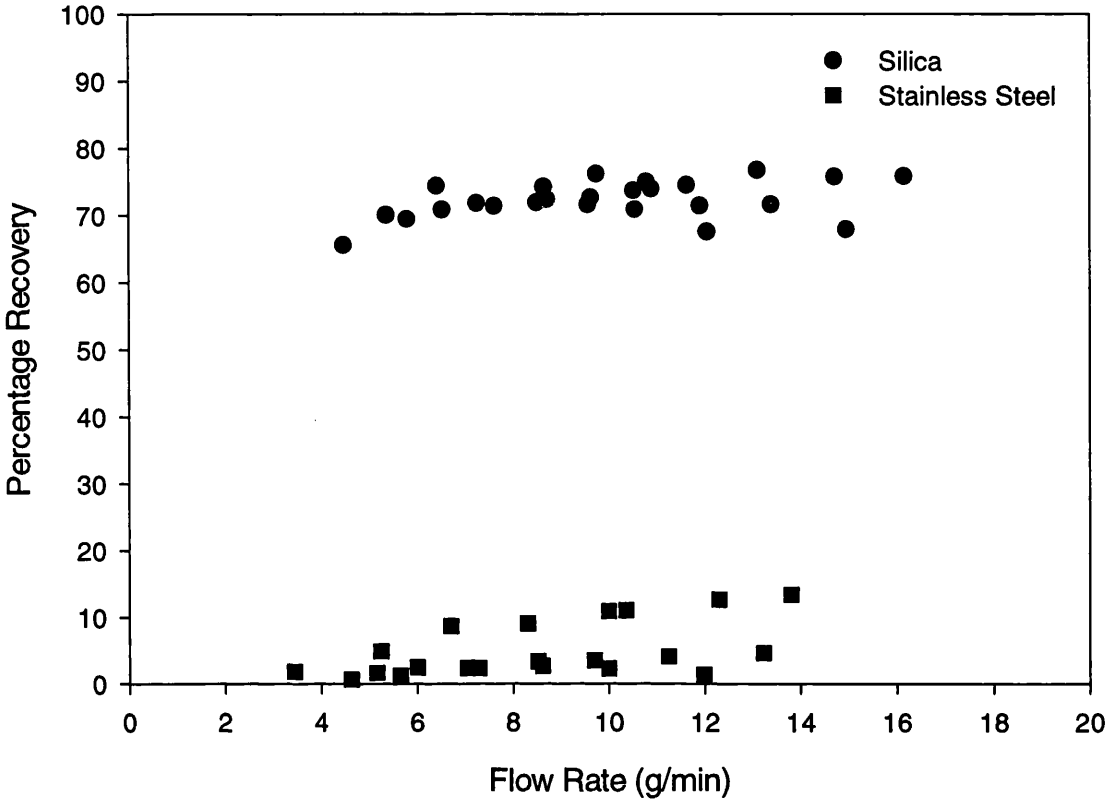

Figure 5.10: The effect of flow rate on adhesion. Silica and Stainless Steel packing (70-200μm) was used in conjunction with carboxylated latex beads (0.5μm) in three Columns, at pH 3.5 over a range of flow rates. Experiments were conducted at 22 +/- 1°C.

Flow rate had little effect on adhesion at this pH, although some increase in adhesion did occur at lower flow rates.

Adhesion to silica appeared to be independent of flow rates at high values. As flow rate increased, the percentage recovery increased from 65% to 78%. At very low values of flow rate, there seemed to be a deviation from the independent relationship. The reduction of flow rate to assess whether this trend continued was impossible (i.e. below 4g/min), due to the limitations of the apparatus. When fitting a linear regression, the relationships were:

Percentage Recovery (Silica) = 0.35 (Flow Rate) + 68.81

Percentage Recovery (Steel) = 0.75 (Flow Rate) – 1.37

There was a linear dependence on flow rate between percentage recovery and adhesion to stainless steel. This was not observed with silica as the collector surface, and could have been due to the increased sensitivity of the results, as a greater percentage of latex beads adhered to the stainless steel collector surface, due to the increased hydrophobicity of the collector surface.
Similar observations were made for the percentage recovery from steel at pH 4.5, and 5.5, as seen in Appendix C.8.

5.5.2.2 Adhesion at pH 4.5 and 5.5 Relative to Flow Rate

The effect of flow rate on adhesion of carboxylated latex beads to silica and stainless steel at pH 4.5 and 5.5 were similar to that observed at pH 3.5, and are shown in Appendix C.8. Adhesion to both surfaces was lower than the values observed at pH 3.5, as expected.

When applying a linear regression in both cases, the following relationships were determined for both silica and stainless steel at pH 4.5, and 5.5:

At pH 4.5:
Percentage Recovery (Silica) = -0.81 (Flow Rate) + 94.84
Percentage Recovery (Steel) = 1.36 (Flow Rate) - 2.13

At pH 5.5:
Percentage Recovery (Silica) = - 0.22 (Flow Rate) + 95.06
Percentage Recovery (Steel) = 1.374 (Flow Rate) + 6.65

The decrease in percentage recovery from silica at pH 4.5 as flow rate increases suggested that there might have been some ripening of the Column. When comparing these observations with the results from at pH 3.5 and 5.5, there was no agreement with these findings, and therefore attributed to experimental anomalies.

5.5.2.3 Adhesion at pH 6.5 and 7.5 Relative to Flow Rate

Adhesion was expected to decrease in both cases relative to the levels observed at pH 5.5. This was indeed the case as shown in Figure 5.11. Again, adhesion differed greatly between silica and stainless steel. Adhesion of the latex beads to the silica surface was linear, as was observed at lower pH, with approximately 90% of the beads recovered. Adhesion to stainless steel was also linear, although it did not follow the trend observed at lower pH. In this case the percentage recovered was approximately 45-50% for pH 6.5, and 60-70% for pH 7.5.

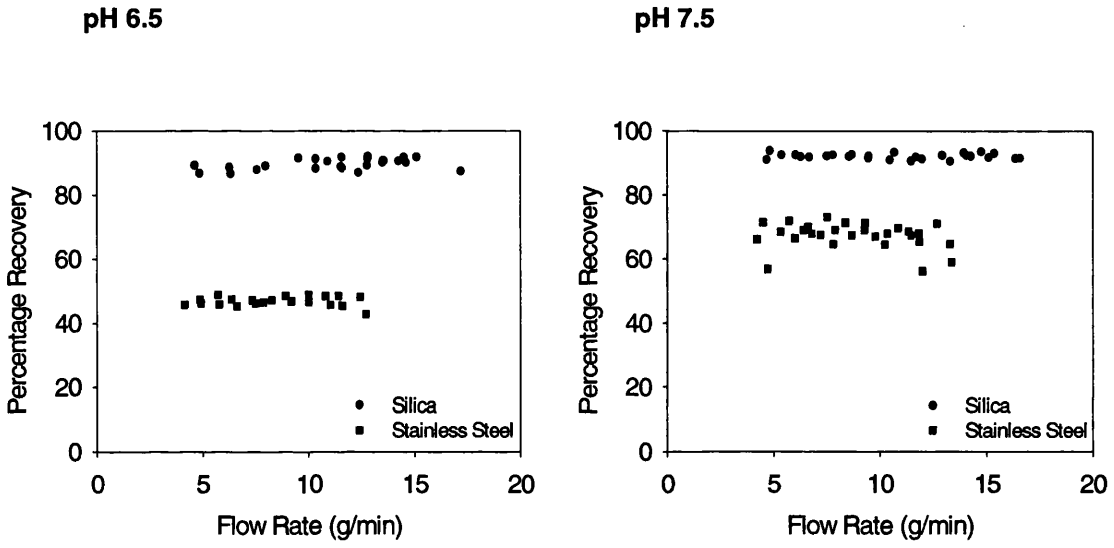

Figure 5.11: The effect of flow rate on adhesion at pH 6.5 and 7.5. Silica and Stainless Steel packing (70-200µm) was used in conjunction with carboxylated latex beads (0.5µm) in three Columns, at pH 6.5 over a range of flow rates. Experiments were conducted at 22 +/- 1°C.

The relationship between flow rate and percentage recovery were better defined at pH 6.5 and 7.5 compared with lower pH. There was also little dependence on flow rate, considering the very small change in gradient of both curves.

For pH 6.5:

Percentage Recovery (Silica) = - 0.23 (Flow Rate) + 86.99

Percentage Recovery (Steel) = -0.02 (Flow Rate) + 47.00

For pH 7.5:

Percentage Recovery (Silica) = - 0.02 (Flow Rate) + 92.28

Percentage Recovery (Steel) = -0.33 (Flow Rate) + 70.31

5.5.2.4 The Effect of Flow Rate on Adhesion: Summary

The effect of flow rate on adhesion was assessed using the Packed Column apparatus, in conjunction with 0.5μm carboxylated latex beads, using either silica or stainless steel as the collector surface within the Column.

Adhesion as increased pH was decreased, due to protonation of both collector surfaces as pH became more acidic. The surfaces' negative charge was therefore lessened, and subsequently the hydrophobic interaction, rather than DLVO forces governed the adhesion interaction.

There was also greater adhesion of the beads to stainless steel in relation to silica, due to differences in the hydrophobic characteristics of the surfaces, as demonstrated in Section 4.2.3.1. Stainless steel provided a more hydrophobic surface, and therefore provided more adhesion of the latex beads compared with the more negatively charged surface of silica.

When considering the effect of flow rate on adhesion, adhesion was assumed to be independent of flow rate due to the low values of shear force within the Column (Bergendahl and Grasso, 1999), and was generally observed. However, there did appear to be some dependence on flow rate in certain cases. With silica, adhesion increased slightly at low flow rates, at pH 3.5. The change in adhesion was not great, but was noticeable. At this pH, the silica was significantly more hydrophobic compared to the surface at higher pH values, as shown in Table 4.1.

The effect of flow rate on adhesion to stainless steel was noticeably affected at pH 3.5, 4.5, and 5.5. Adhesion to steel was governed predominantly by hydrophobic interactions, and at these pH values, the surface hydrophobicity increased, as pH decreased.

From this it can be concluded that flow did not affect the close range DLVO interactions, but does have a contribution to adhesion governed by hydrophobic interaction.

5.6 The Effect of pH on Attachment to the Packed Column

5.6.1 Introduction

The results obtained from Section 5.5 identified the potential capabilities, problems, and limitations of using the Packed Column to assess particle adhesion to granular collector surfaces.

The following experiments were performed to gather data on the adhesion of aminated and carboxylated latex beads, and the spores of *B.mycoides* and *B.subtilis* to both surfaces to be assessed as a function of pH. This allowed the effect of colloid type, the effect of collector type, and the effect of pH to be analysed individually and collectively.

5.6.2 Experimental Protocol

The Column was packed as detailed Section 5.3.6.1 and a sample of known OD introduced to the Column five times, at intervals of 300 seconds using the injection loop as detailed in Section 5.3.6.2. This was repeated using a total of three Columns for each set of conditions. The conditions are listed in Section 5.6.3. The flow rate used was monitored and kept at approximately 7mℓ/min. This flow rate did not affect the levels of adhesion, as shown in Section 5.5.2, and yet was sufficiently low to maximise the amount of data points encompassing the breakthrough curve, as described in Figure 5.1.

5.6.3 Materials and Solutions Utilised in the Main Experiment

The following Section lists the materials and solutions used in the main data gathering exercise.

5.6.3.1 Variation in Particle Type

The adhesion of aminated and carboxylated latex beads (2μm), as well as the spores of both *B.mycoides* and *B.subtilis* was assessed in the following experiments.

5.6.3.2 Variation in Collector Type

Silica 60 Gel (200-500μm) and Stainless Steel 316L (200-500μm) were used as the packing materials in the Column. These materials were chosen due to their availability, and their relevance within industrial processes. The larger size of packing was chosen as it provided sufficient adhesion, with less caking and filtering effects. The larger size of packing also settled more quickly when packing the Column, and was therefore more practical when preparing the apparatus.

5.6.3.3 Solution pH

The solutions in all cases are detailed in Section 2.2.3, at pH 3.5, 5.5, 7.5, and 9.5.

5.6.4 Particle Adhesion to Silica with respect to pH

The adhesion to silica of aminated and carboxylated latex beads, and the spores of *B.mycoides* and *B.subtilis*, over a range of pH, as determined using the Packed Column is illustrated in Figure 5.12. The spores of *B.mycoides* possessed the lowest recovery values from the Column, followed by the aminated beads, then the carboxylated beads, and finally the spores of *B.subtilis*.

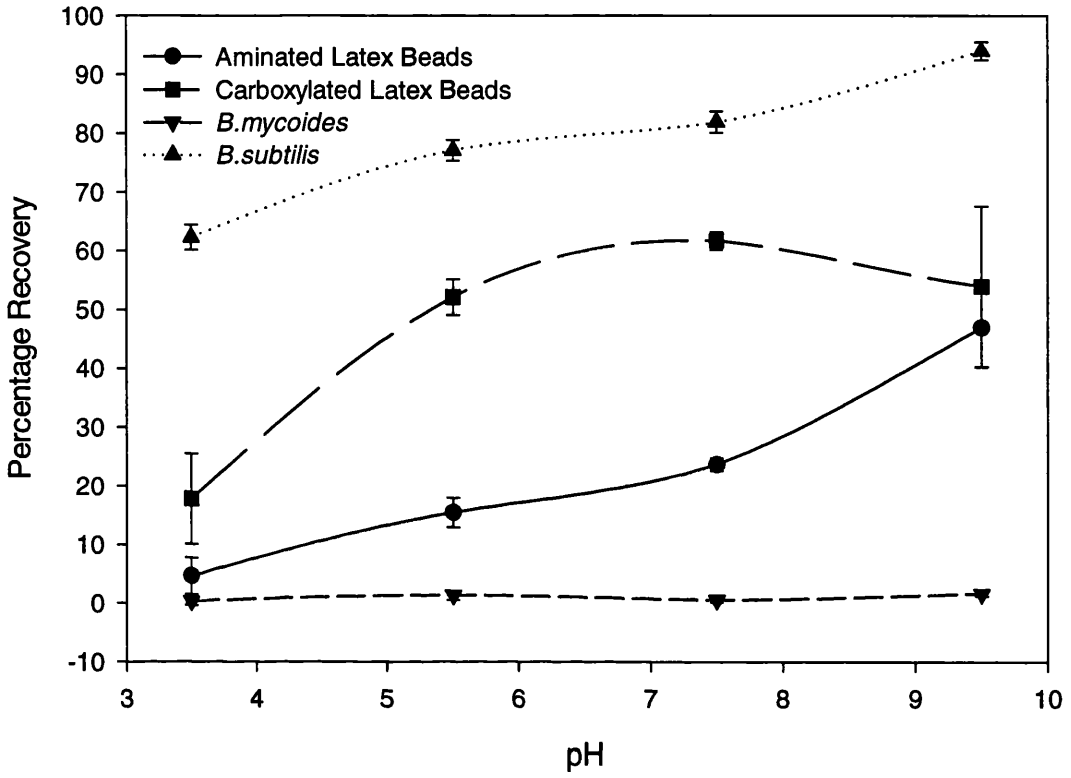

Figure 5.12: The adhesion of aminated and carboxylated latex beads (2μm), and the spores of *B.mycoides* and *B.subtilis* to silica (200-500μm) over a range of pH adjusted using HCl (1M) or NaOH (1M) in 25mM NaH_2PO_4, as measured by the percentage recovery from the column. Experiments were conducted at 22 +/- 1°C.

The percentage recovery of *B.mycoides* spores to the silica collector surface was between 0 and 4%, and was not affected significantly by the solution pH. Although the silica collector surface provided a relatively hydrophilic surface for attachment, the spores of *B.mycoides* were preferentially deposited on the surface rather than remain in suspension. The *B.mycoides* spore possessed a very low surface charge as shown in Table 3.1, and moderate hydrophobicity as seen in Table 3.3, which increased the preference of the spore to be deposited. The presence of appendages on the spores' surface also promoted adhesion to the silica collector surface (Husmark and Rönner, 1992). The spore was therefore preferentially deposited onto the collector surface.

The recovery of aminated latex beads from the Column packed with silica ranged between 5 and 45%. The most noticeable change in recovery levels was between pH 7.5 and 9.5. This was not reflected by the zeta potential measurements as shown in Table 3.1. These zeta potential results showed a change between pH 3.5 and 5.5, and then a maintained level at approximately -35mV. The recovery curve appeared to reflect the pKa of the amine group on the surface of the latex bead, even though the latex had the governing effect on surface charge.

The carboxylated beads showed more recovery than the aminated latex beads. The hydrophobicity of both the latex bead types was approximately the same, as shown in Table 3.3. The increased recovery was therefore due to the increased electrostatic repulsion between the carboxylated beads and the silica collector surface, as the carboxylated beads had increased values of zeta potential, as shown in Table 3.1. There was a large change in recovery from the Column as the solution pH changed between pH 3.5, and 5.5, which reflected the observations made when assessing the zeta potential, as shown in Table 3.1.

The recovery of the spores of *B.subtilis* was the highest of the four particles. The spore had a low hydrophobicity, and high zeta potential, and therefore was stable in suspension. There was a smaller recovery value of the spore at pH 3.5, and this can be explained by the increased hydrophobicity of the spore as shown in Table 3.3, and the silica collector surface, as shown in Table 4.1. There was also an increase in recovery between pH 7.5 and 9.5, where the contact angle of glass dropped from 28° to 21°, as shown in Table 4.1.

5.6.5 Particle Adhesion to Stainless Steel with respect to pH

The adhesion to stainless steel of aminated and carboxylated latex beads, and the spores of *B.mycoides* and *B.subtilis*, over a range of pH, as determined using the Packed Column is illustrated in Figure 5.13.

The spores of *B.mycoides* showed little or no recovery from the stainless steel Packed Column (approximately 0-5%), as was observed with silica, as shown in Figure 5.12.

The aminated and carboxylated latex beads showed more recovery compared with the *B.mycoides* spores, and finally, the spores of *B.subtilis* showed the most recovery of the four particles. This was qualitatively the same observation as observed with silica as the collector surface. The stainless steel collector produced lower recovery values compared to those observed with silica, which was due to the increased hydrophobicity of the stainless steel, as shown in Table 4.1.

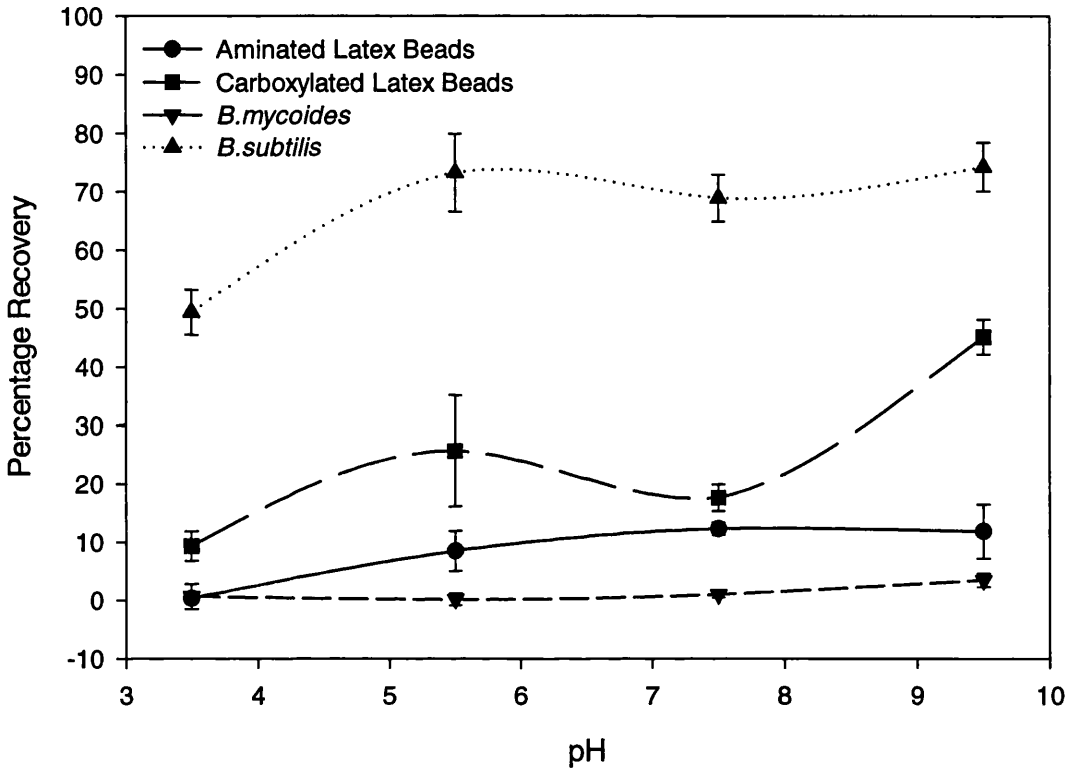

Figure 5.13: The adhesion of aminated and carboxylated latex beads (2μm), *B.mycoides*, and *B.subtilis* to stainless steel (200-500μm) over a range of pH adjusted using HCl (1M) or NaOH (1M) in 25mM NaH_2PO_4, as measured by the percentage recovery from the Packed Column. Experiments were conducted at 22 +/- 1°C.

The recovery of the spores of *B.mycoides* showed comparable levels with those observed with silica, and suggested that the deposition of the spores was therefore governed predominantly by the instability of the spore in solution, favouring deposition irrespective of the collector surface.

The recovery of the aminated and carboxylated latex beads from the Column both showed higher levels of retention of the beads on the Column, compared with those observed with silica. The lower values of recovery were due to the increase in the hydrophobic contribution between the stainless steel collector and the bead, and a decrease in the contribution of electrostatic repulsion between the two surfaces. The difference between the values of recovery of the aminated and carboxylated latex beads was smaller than that observed with silica, which emphasized the increase in the hydrophobic contribution to the attachment of the beads to the stainless steel collector.

The aminated and carboxylated latex beads had very similar values for hydrophobicity, as shown in Table 3.3, but different levels of zeta potential, as shown in Table 3.1, and the effect of hydrophobicity was reflected on the resulting recovery values.

The values of recovery obtained for the spores of *B.subtilis* were substantially higher than those obtained for the latex beads. The increase in hydrophobicity of the spore at pH 3.5, as shown in Table 3.3, was reflected in an increase of adhesion to stainless steel at pH 3.5, which was recorded at approximately 50%. The recovery of the spores then increased to between 70 and 75%, as pH was increased, as expected. These values were comparable with those obtained using silica as the collector surface, which provided values of approximately 75 to 80% recovery between pH 5.5 and 7.5. These results suggested that the lack of attachment of the spores of *B.subtilis* was due to the spores' stability in solution, although the spores did prefer a more hydrophobic surface when they were deposited.

Summarising, there were two considerations to make when assessing the attachment of particles to the Packed Column, as a function of pH. Firstly, the stability of the particle in suspension governed the preference of the particle to be deposited, irrespective of the characteristics of the collector surface. This was true in the case of the spores of *B.mycoides* and *B.subtilis*.

The second consideration was that, when dealing with marginally stable particle suspensions, the interaction between the collector and the particle was a sum of both the attractive, hydrophobic interaction, and the electrostatic repulsion. Therefore, a more hydrophobic surface will have a greater attractive hydrophobic interaction and less electrostatic repulsion than a more hydrophilic surface. Subsequently, a

hydrophobic collector will provide a more preferential surface for attachment than a hydrophilic surface, as was observed when considering the difference between silica and steel. Using the same theory, two particles with differing surface charge, but similar hydrophobicity, will provide different levels of attachment, with the less negatively charged particle providing more adhesion (due to reduced electrostatic repulsion). This was the case when comparing aminated and carboxylated beads.

5.6.6 A Direct Comparison of the Effect of pH on Attachment to the Packed Column, in Sequential Runs

The following Section directly compares attachment of aminated and carboxylated latex beads and the spores of *B.mycoides* and *B.subtilis* at the four different pH values investigated within this work in sequential additions. Each sub-section considers the attachment of a particle type to both silica and stainless steel at differing pH, with respect to run number. The data used to produce these analyses are a repeat of the data used in Sections 5.6.4 and 5.6.5, arranged to allow determination of the effect of previously deposited particles on the adhesion to the Packed Column, as well as a more direct analysis of the effect of pH on adhesion to the Packed Column. Details of experimental protocol are given in Section 5.6.2.

5.6.6.1 The Effect of pH on the Adhesion of Aminated Latex

The effect of pH on the adhesion of aminated latex beads to both silica and stainless steel in sequential runs is shown in Figure 5.14.

The percentage recovery of aminated beads increased with solution pH. This was more pronounced with the adhesion to silica, as the solution chemistry has more effect on the hydrophilic surface compared with the hydrophobic steel surface. The decrease in adhesion to silica of the aminated beads between pH 3.5 and 5.5, can be attributed to the decreased hydrophobicity of silica between pH 3.5 and 5.5, as shown in Table 4.1. The same statement can be made for the decreased adhesion of the beads between pH 7.5, and 9.5, which again reflects a drop in hydrophobicity.

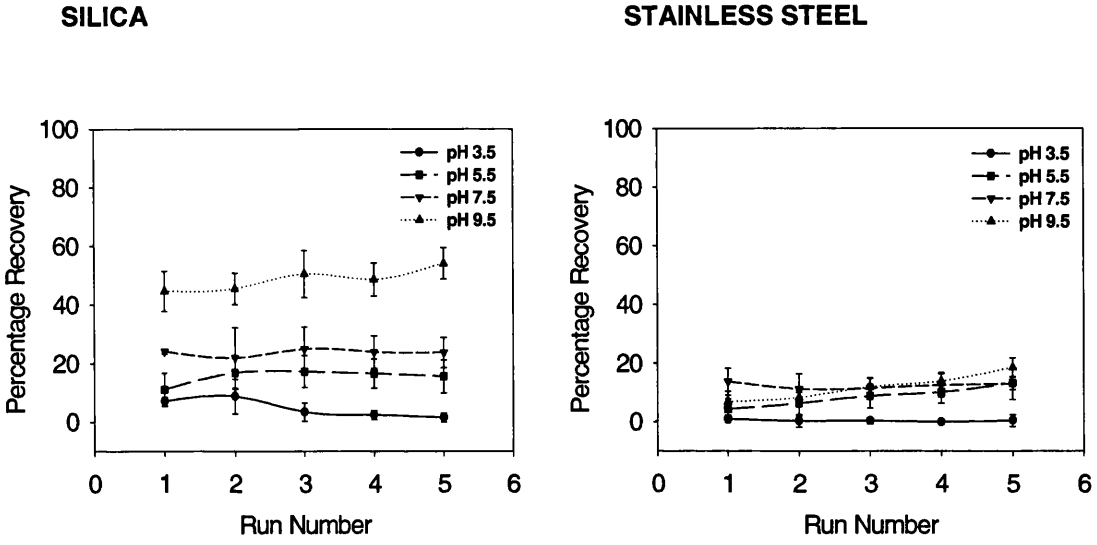

Figure 5.14: The adhesion of aminated latex beads (2μm) to silica and stainless steel (200-500μm) over a range of pH adjusted by 1M HCl or 1M NaOH in 25mM NaH_2PO_4, relative to run number, measured by percentage recovery from the Packed Column. Experiments were conducted at 22 +/- 1°C.

There was variation in the percentage recovery from the Column using both silica and stainless steel. With silica at pH 3.5, the presence of previously attached beads seemed to influence the further adhesion of beads. The beads at this pH possessed low zeta potential and high hydrophobicity as seen in Tables 3.1 and 3.3 respectively, and therefore were unstable in solution. The presence of other beads on the surface presented the beads in suspension with a hydrophobic surface, which was more suitable than the more hydrophilic silica. The dependence on run number was not observed with the attachment of the aminated beads to stainless steel at pH 3.5.

At pH 5.5, and 7.5 the adhesion of the aminated beads to silica did not vary with sequential additions, but there was a slight increase in recovery at pH 9.5. This may suggest that suitable binding sites on the collector were becoming saturated as more aminated beads were placed on the column. However, the variation in the results cast doubt on whether this conclusion could be made reliably.

There was a slight increase with the percentage recovery of the aminated beads from the stainless steel collector at all pH values, although, as observed with silica, the variation in results could not allow any reliable conclusion to be drawn from these values.

5.6.6.2 The Effect of pH on the Adhesion of Carboxylated Latex Beads

The effect of pH on the adhesion of carboxylated latex beads to both silica and stainless steel in sequential runs is shown in Figure 5.15.

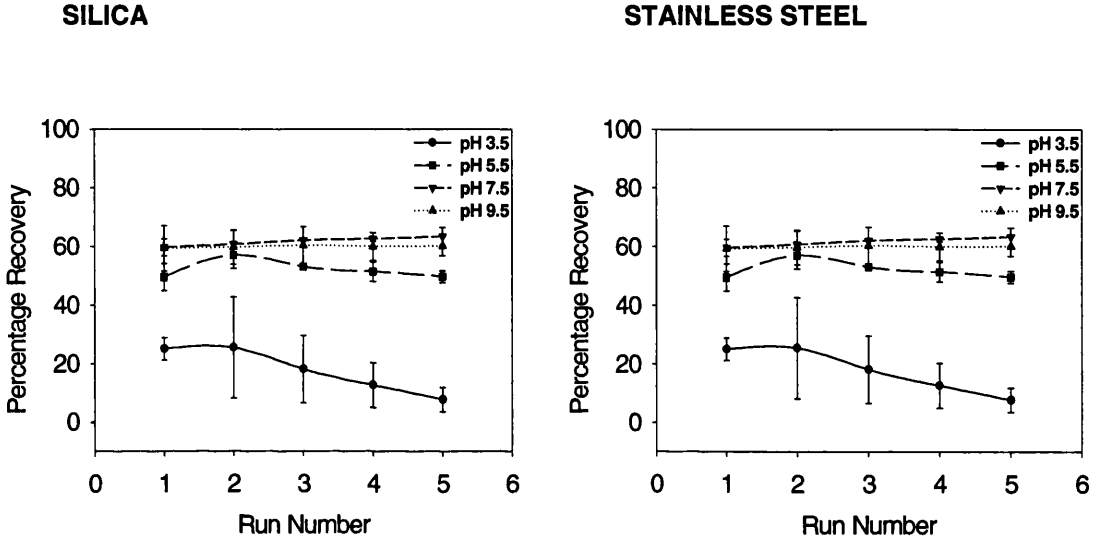

Figure 5.15: The adhesion of carboxylated latex beads (2μm) to silica and stainless steel (200-500μm) over a range of pH adjusted by 1M HCl or 1M NaOH in 25mM NaH_2PO_4, relative to run number, measured by the percentage recovery from the Packed Column. Experiments were conducted at 22 +/- 1°C.

As observed with aminated latex beads, the silica collector surface provided more recovery from the Column when compared with stainless steel. The attachment to silica at pH 3.5 was greater than that at increased values of pH. This was due to the substantial increase of the hydrophobicity of silica at pH 3.5, compared with pH 5.5 and above, as seen in Table 4.1. The values of attachment to silica at pH 3.5 confirmed that attachment to previously adhered beads did occur, as was suggested with the observations made with the attachment of aminated beads to silica. As stated in Section 5.6.6.1, the beads possessed high values of hydrophobicity, and low negative zeta potentials as seen in Tables 3.1 and 3.3, and therefore increasing the likelihood of deposition. The hydrophobic interaction between two beads provided a more suitable surface for attachment compared with the interaction of a bead with silica. This did not occur at pH 5.5 and above, as the beads were negatively charged, and therefore repulsive to each other.

The recovery of the carboxylated beads from stainless steel was less than the silica as was observed with aminated beads. There was an increase in the recovery with respect to run number at pH 5.5, although the values were expected to be nearer those values observed at pH 7.5, and should be treated with suspicion. The increase in recovery can be attributed to the decrease in available attachment sites as more carboxylated beads were introduced to the Packed Column.

5.6.6.3 The Effect of pH on the Adhesion of B.mycoides Spores

The effect of pH on the adhesion of the spores of *B.mycoides* to both silica and stainless steel in sequential runs is shown in Figure 5.16.

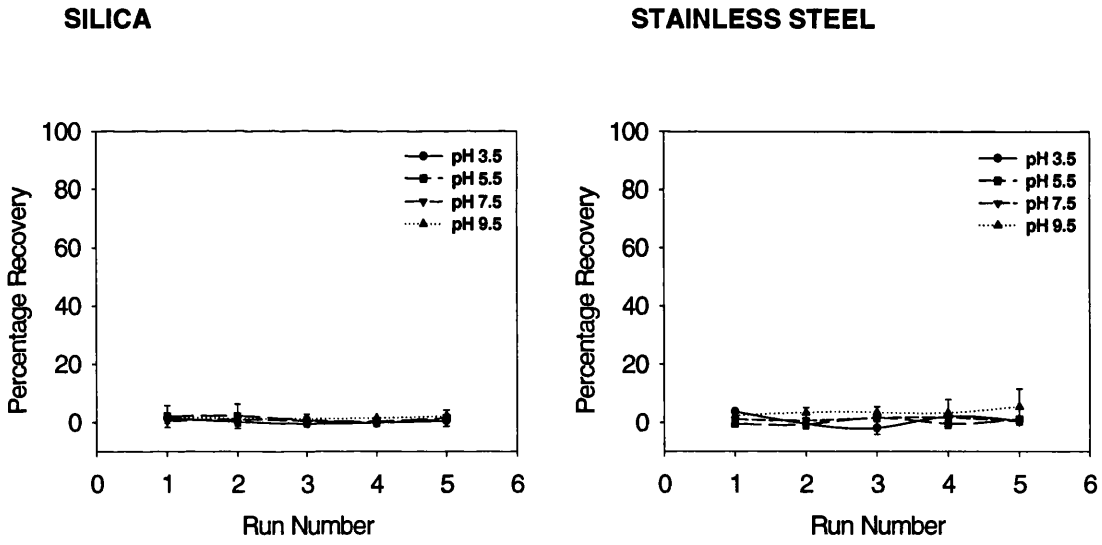

Figure 5.16: The adhesion of the spores of *B.mycoides* to silica and stainless steel (200-500μm) over a range of pH adjusted by 1M HCl or 1M NaOH in 25mM NaH_2PO_4, relative to run number, measured by the percentage recovery from the Packed Column. Experiments were conducted at 22 +/- 1°C.

The percentage recovery of the spores of *B.mycoides* showed values of approximately 0 to 5%, and there was no observed dependence on flow rate. The reasons for the low values of recovery are stated in Section 5.6.4 and 5.6.5. The fact that there was no increase in recovery observed in either the case of silica or stainless steel, suggested that saturation of binding sites as observed with aminated

and carboxylated beads was not observed. This observation may occur for two reasons; firstly the saturation observed with the aminated and carboxylated beads was due to experimental anomalies, or secondly, saturation of the available binding sites on the collector surface occurred, but did not affect percentage recovery of *B.mycoides* spores, which were binding to each other. This latter situation was more likely, as the low zeta potential and moderate hydrophobicity of the *B.mycoides* spores would promote aggregation on the surface of the collector, compared with the high charge of the latex beads.

5.6.6.4 The Effect of pH on the Adhesion of B.subtilis Spores

The effect of pH on the adhesion of the spores of *B.subtilis* to both silica and stainless steel in sequential runs is shown in Figure 5.17.

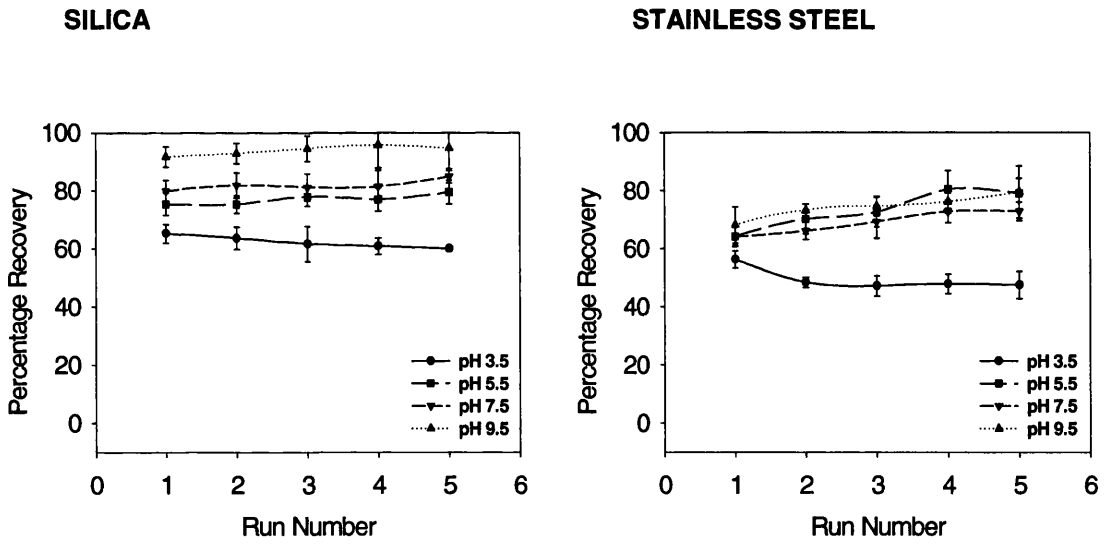

Figure 5.17: The adhesion of the spores of *B.subtilis* to silica and stainless steel (200-500μm) over a range of pH adjusted by 1M HCl or 1M NaOH in 25mM NaH_2PO_4, relative to run number, measured by the percentage recovery from the Packed Column. Experiments were conducted at 22 +/- 1°C.

The variation of attachment of the spores to *B.subtilis* to silica with pH reflected the variation in hydrophobicity of the collector surface, as shown in Table 4.1. The variation of the spores' recovery from stainless steel was reflected by the hydrophobicity of the spores, as shown in Table 3.3. The surface charge of the

spore had little effect on the adhesion to either silica or stainless steel. This confirms the theory that, although surface charge contributes to adhesion, the hydrophobicity of both the collector and the particle surface is the most important factor governing adhesion, and this is discussed later in Section 5.7.

5.6.7 Variation of Particle Adhesion using the Packed Column

The following Section represents the above data presented to allow direct comparison of the variation in attachment with respect to particle type.

5.6.7.1 Variation of Particle Adhesion to Silica using the Packed Column

The adhesion of aminated and carboxylated latex beads and the spores of *B.mycoides* and *B.subtilis* to silica with respect to run number are shown in direct contrast in Figure 5.18.

At pH 3.5, where the glass was most hydrophobic, the percentage recovery of the aminated and carboxylated latex beads were nearer the values obtained for the spores of *B.mycoides* than the spores of *B.subtilis*. This was attributed to the hydrophobicity of the silica at pH 3.5, and the low charge of the beads. This interaction was therefore predominantly hydrophobic attraction, and the values of recovery of the beads mimicked those of the spores of *B.mycoides*. As pH increased, the percentage recovery of the aminated and carboxylated beads became closer to the values observed with the recovery of the spores of *B.subtilis*. This was attributed to the decrease in the likelihood of deposition of the beads from solution, and therefore the interaction between particle and collector became similar to the *B.subtilis* spores.

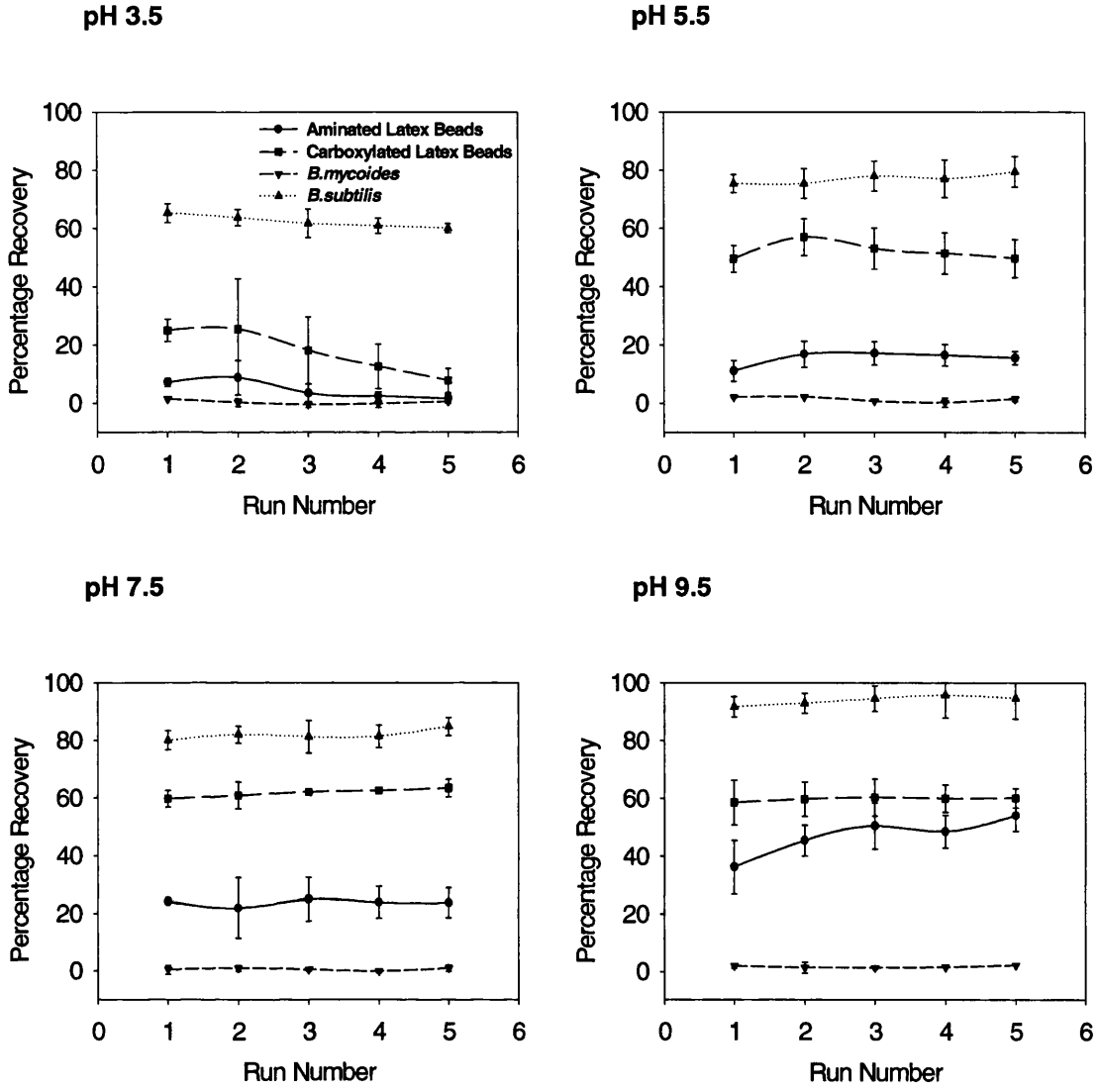

Figure 5.18: The adhesion of the aminated and carboxylated beads (2μm), and the spores of *B.mycoides* and *B.subtilis* to silica (200-500μm) at pH 3.5, 5.5, 7.5, and 9.5 in 25mM NaH_2PO_4 relative to run number. Adhesion is measured as a function of the percentage recovery from the Packed Column. Experiments were conducted at 22 +/- 1°C.

5.6.7.2 Variation of Particle Adhesion to Stainless Steel using the Packed Column

The adhesion of aminated and carboxylated latex beads and the spores of *B.mycoides* and *B.subtilis* to stainless steel with respect to run number are shown in direct contrast in Figure 5.19.

The recovery levels of the aminated and carboxylated latex beads were closer to the values obtained for the spores of *B.mycoides* compared with the spores of *B.subtilis*. The stainless steel collector surface was more hydrophobic compared with silica as shown in Table 4.1. The hydrophobic interaction was more dominant when considering the attraction to stainless steel, compared with the interaction with silica. The percentage recovery increased as run number increased, suggesting that the available binding sites became increasingly saturated, or that particles that had previously been attached, detached, and were released from the surface.

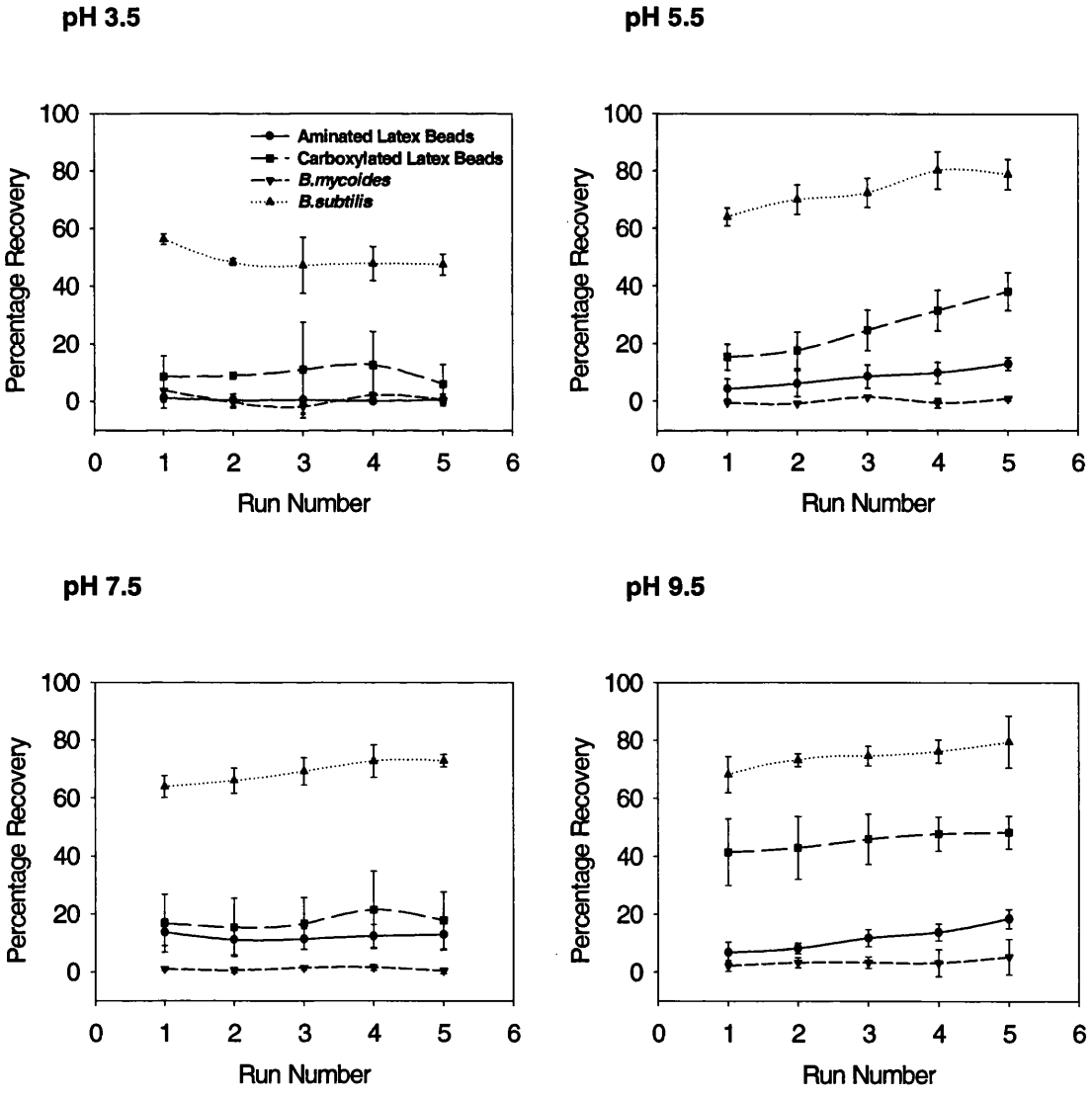

Figure 5.19: The adhesion of the aminated and carboxylated beads (2μm), and the spores of *B.mycoides* and *B.subtilis* to stainless steel (200-500μm) at pH 3.5, 5.5, 7.5, and 9.5 in 25mM NaH_2PO_4, relative to run number. Adhesion is measured as a function of the percentage recovery from the Packed Column. Experiments were conducted at 22 +/- 1°C.

5.7. Discussion

The results obtained from the Packed Column have provided an insight into the process of irreversible adhesion to a porous collector. Variation of the percentage recovery was large, but can be accounted for by the surface heterogeneity of both the collector and the colloid (Walz, 1998). Surface charge, surface roughness, and hydrophobicity all contribute differently towards adhesion of the colloid to the collector (Hermansson, 1999), and all are susceptible to variation within this system of assessing adhesion.

The development of the Packed Column Technique provided the biggest challenge when discussing its use as a method of reliably assessing microbial attachment.

With so much potential for variation in attachment levels, the limitation of experimental error was necessary.

5.7.1 Packing Developments

The method used to pack the Column (Litton and Olson, 1993), although primitive, provided a suitable Column structure to assess adhesion as detailed in Section 5.3.1.1. Dextran Blue dye was used initially to assess that packing would provide reproducible break-through curves, which was observed. Initially, when developing the Column, air was introduced, which was suspended in pores on the collector surface. The removal of air from the Column was essential, as introduction of gas into the system had a great effect on the break-through curve. Air would not only disturb the flow patterns of the Column, but was also trapped within the flow through cuvette, scattering the light path of the spectrophotometer, and subsequently rendering the experiment futile.

5.7.2 Sample Injection Developments

The initial injection method using a 1mℓ syringe to manually introduce the sample into the Column via the flow-path of the buffer was changed to the preferred loop method. This method allowed the introduction of a controlled volume of sample suspension into the system. The initial manual injection method was susceptible to human error when introducing the sample into the Column. The volume used (0.5mℓ) was also too large for the system, and did not provide a uniform flow front, distorting the break-through curve, whereas the use of the loop gave a much smaller sample volume. However, this smaller volume required a larger concentration of colloidal suspension to provide a large enough break-through curve to be produced for analysis. The benefits of the injection loop rather than using a manual method of introduction were therefore: 1) Maintenance of a constant sample volume, 2) Provided a uniform liquid front, due to its smaller volume, 3) A more user friendly system, with no requirement to change septa, and did not introduce air into the packed bed.

5.7.3 Spectrophotometer and Flow-Cuvette Developments

Initially, the assessment of the break-through curve was performed in 1.4 mℓ cuvettes. This method of assessment involved the weighing of each individual cuvette, and therefore calculating the volume of eluate deposited in each cuvette. Having done that, the Optical Density was measured for each of 80 cuvettes. Not only was this method very inaccurate, and prone to human error, the method was also very tedious. The introduction of the flow-through cuvette combined with the PICO package and laptop, allowed a more reliable method of assessing the break-through curve, and enabled the continual assessment of the eluate. The only disadvantage of using the flow-through cuvette was the increased likelihood of trapping air in the path of the spectrophotometer light source, requiring the repetition of the experiment.

5.7.4 Developing the Analysis of Results

The analysis of the results generated from the Packed Column assessed the irreversible attachment of the particles to the collector. The area under each break-through curves was assessed to calculate what percentage of the initial sample was recovered from the Column under the specified conditions. The results were left as percentage recovery to allow for differences in sample concentration to be considered.

The break-through curves in all cases demonstrated tailing off effects, and were not symmetrical. This observation was not as noticeable as previous work performed by Roy and Dzombak (1996b), where the tailing off of the break-through curves generated by latex beads detaching from a glass column was noticeable up to 6 pore volumes after the peak. Bergendahl and Grasso (1999) also demonstrated that the tail of the break-through curves extended up to 10 pore volumes after the peak. Both these pieces of work assessed the attachment of latex beads to glass Packed Columns. This did not agree with the findings of Grolimond *et al* (1998), and Rijnaarts *et al* (1996b), who demonstrated that the break-through curves from both carboxylated latex beads and soil particles, detaching from glass and sand respectively, did not extend past 2 pore volumes. This was in agreement with work performed in this project, where no recovery of particles was recorded after the elution of the equivalent of two pore volumes had occurred. The length of the Packed Column could be altered to assess whether this observation is due to reversible binding, or the back mixing of liquid within the column.

The area under the break-through curve allowed the assessment of irreversible binding (Grolimond *et al*, 1998), but did not consider the shape of the curve. The tail of the curve represents reversible binding within the system, and was assessed when considering the Log $_{10}$ Normalised Concentration of sulphated latex beads to glass beads (Yan, 1996). However, the accuracy of the Pye Spectrophotometer incorporated within this project did not allow the analysis of this effect.

Developments made using this technique allowed a simple method of analysing the break-through curves, and therefore irreversible adhesion. The final protocol was simple and relatively quick, with minimal scope for human error.

5.7.5 Discussion of Data

The following general observations can be made when considering the results generated using the Packed Column technique to assess particle attachment.

1) Particle adhesion was in the order of *B.mycoides* > Aminated Beads > Carboxylated Beads > *B.subtilis*, with *B.mycoides* being most adhesive. This was observed in all cases. Levels of attachment of latex beads were similar to those observed by Bergendahl and Grasso (1999). Recovery levels of *B.mycoides* spores were also similar to those obtained for the adhesion of *Bacillus* strain CB1 adhering to soil (Rijnaarts *et al*, 1996b).

2) Stainless Steel was a more adhesive surface relative to silica in all cases. The reasoning for this observation was the greater hydrophobicity of the stainless steel surface as detailed in Section 4.1. Colloidal particles either preferred to remain in suspension, or be deposited onto the collector surface, irrespective of the surface type. Silica was less hydrophobic than steel, and therefore showed less adhesion.

3) The contribution of surface charge was less than the equivalent hydrophobic contribution. This was expected, as the hydrophobic interaction occurs over a larger distance than interactions involving the surface charge of the particle.

4) Adhesion increased as pH decreased, as observed by Bergendahl and Grasso (1999), and Roy and Dzombak (1996b). This observation was due to the increased protonation of both surfaces, reducing the charge, allowing the attractive hydrophobic interaction to become more pronounced.

5) The presence or previously attached spheres did not significantly alter the amount of attachment on the Column. The surface area of the Column was approximately $1m^2$, assuming that packing was close tetrahedral, and that the collector was spherical and of 350μm diameter as shown in Section 5.1.2.3.

Using the attachment of *B.mycoides* spores as an example, the sample concentration was 5 OD, which provided 3.73×10^9 spores/mℓ, as shown in Figure 2.3. The loop volume was 0.147mℓ (Section 5.4.1), which resulted in the sample containing 5.48×10^8 spores.

If the spore diameter was 2μm, which is an overestimation, the area of the collector that the spore is in contact with is π x 10^{-12} m^2 (πr^2, where r = 1μm), as illustrated in Figure 5.20. The total occupied collector area is approximately 0.0017m^2 per sample introduction.

Although this is a gross over-simplification of the interaction, this example does show that, by considering the number of spores within the Column, and estimating the inaccessible area, only 1% of the available area of the Column was occupied, if all particles were bound in a colloid/collector interaction. This does not take into consideration that spore/spore interactions will decrease the percentage recovery of the spore.

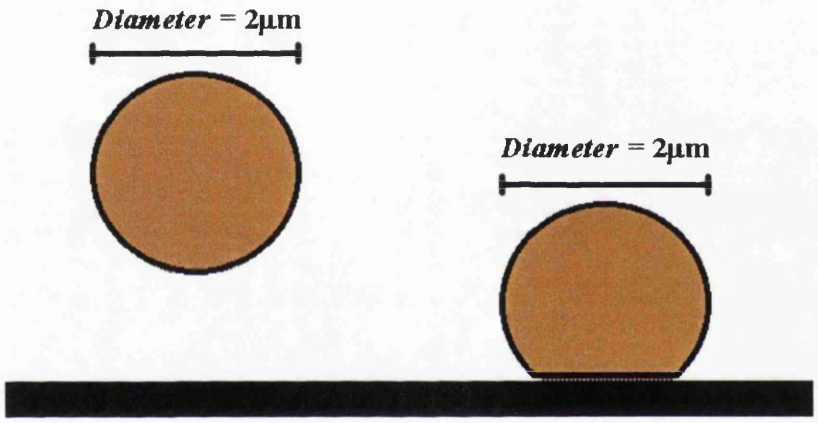

Figure 5.20: A simplification of the attachment of a deformable colloid to a collector surface. The diagram shows that although contact surface area can vary, the exclusion zone for further binding will remain approximately the same.

As stated, this is an over-simplification, but it does suggest that that saturation of the Column was an unlikely occurrence.

The results and observations made from the work performed in this Chapter, combined with the results from the characterisation of the particles and the collector surfaces will allow a more comprehensive explanation of the results obtained in work performed with the Spinning Disc and the Radial Flow Chamber, in Chapters 6 and 7 respectively.

CHAPTER SIX

The Development and Use of the Spinning Disc Technique for Adhesion Studies

6.1 Introduction

This Chapter describes the use of the Spinning Disc technique to assess the adhesion of aminated and carboxylated latex beads, and the spores of *B.mycoides* and *B.subtilis*, to glass and stainless steel.

The use of the Spinning Disc provides a method of applying a shear force gradient across the collector surface in question. Theoretically, the calculation of the shear force required to inhibit adhesion of a colloidal particle to a collector surface is possible, and therefore the adhesive strength of the interaction. The theory of the Disc's behaviour has been described extensively in previous work (Benton, 1966; Levich, 1962; Daily and Nece, 1960).

6.1.1 Previous Uses and Relevance of the Spinning Disc Technique

Although the Spinning Disc technique has been used in previous work, the uses have not been applied to the study of initial cellular adhesion. Work has been performed on non-biological colloids, and cells to a lesser extent. Experiments using the Spinning Disc have been performed on either mammalian cells, or bacteria on a time scale long enough to assess biofilm formation (Marshall and Kitchener, 1966) rather than adhesion itself. Previous work considered the adhesion and formation of biofilms using an enclosed Disc over periods of days (Weiss, 1961) rather than minutes. The enclosed system assessed the effect of the addition of collagen on the adhesion of rat fibroblasts. Different cells do vary in surface characteristics, and therefore their adhesive characteristics, and consequently the results obtained from the work performed in this project are not comparable with those obtained by Weiss, (1961). Weiss's work does, however, provide a simple definition of the relationship between radial distance and shear stress. The resulting observations from this work stated that deposition occurred with slightly unstable dispersions, and was greatest with zeta potential of opposite charges, as expected. Decreasing salt concentration decreased deposition, although DLVO theory could not explain all the results obtained for deposition rates. The work also identified a problem in visualisation of aggregates of both deposited, and dispersed particles, although work carried out using latex beads (Clint *et al*, 1973), showed a rate of deposition lower than that predicted by Levich (1962).

The shear generated by the Spinning Disc can be compared with the hydrodynamic shear encountered within the human blood stream (Shive *et al*, 1999; Wang *et al*, 1993a and 1993b). This similarity renders the application of the Spinning Disc a useful tool in the assessment of the adhesiveness of bacteria to biomedical polymers. The Spinning Disc technique allows the potential of different materials and/or surface coatings to be assessed with respect to bacterial adhesion.

The adhesion of *Staphylococcus epidermidis* is very important in infection of biopolymer implants (An and Friedman, 1997), and has been a subject of several in depth biomedical investigations (Wang *et al*, 1995; Vacheethasanee *et al*, 1998; Shive *et al*, 1999). The work performed by Wang *et al* showed that adhesion of the

bacteria to polyethylene modified with plasma proteins and platelets was reduced relative to the bare polymer surface (Wang *et al*, 1993a and 1993b), and demonstrates that the Spinning Disc technique can be developed to assess surface treatments as well as the bare surfaces when considering biomedical polymers.

The Spinning Disc technique also allows the determination of the effect that other proteins have on adhesion. Fibronectin, for example, can be adsorbed onto the collector surface and the adhesion of rat osteosarcoma cells assessed (Garcia *et al*, 1997).

Measurements of adhesion using adhesive cells provide less error compared with latex beads, due to the proteins on the surface designed specifically for adhesion, such as pili and fimbriae. The adhesion of latex beads, however, relies on the DLVO and the hydrophobic interactions between the bead and collector surface, as shown in Figures 9.5 and 9.6.

The shear stress along the collector surface varies linearly, and the resultant curve should therefore be a sigmoidal curve, due to the distribution of adhesive characteristics throughout the population of the adherent cells, as was found with work performed by Garcia *et al* (1997). This is not the case when considering the work performed by Wang *et al* (1995, 1993a and 1993b), who showed variation in curve shapes, from straight lines to exponential decay.

6.1.2 Theory

The use of the Spinning Disc relies on the fact that a shear force gradient is generated across the face of the Disc. The apparatus consisted of a Disc that was spun at a controlled, and constant angular velocity. Increasing the speed increased the shear force applied to the surface, but had no effect when plotting adhesion against shear force (Garcia *et al*, 1997).

Comprehensive characterisation of the liquid flow within this system has been performed (Benton, 1966; Daily and Nece, 1960). Fluid is drawn axially towards the surface of the Disc, gaining rotational velocity, and consequently exits from the Disc radially. The Disc surface is uniformly accessible, with a uniform diffusive

field over the surface. There is laminar flow across the surface, with the velocity and the boundary layer thickness constant, irrespective of radial distance.

The shear stress (τ, Nm^{-2}) varies linearly across the surface with radial distance. The shear stress can be defined as shown in Equation 6.1.

$$\tau = 0.800\, r\, (\rho\, \mu\, \omega^3)^{1/2} \qquad 6.1$$

r = Radial distance (m)

ρ = Fluid density (10^3 kg m^{-3})

μ = Fluid viscosity (8.94×10^{-4} kg $m^{-1}s^{-1}$)

ω = Angular velocity (10π radians s^{-1})

Shear stress can subsequently be converted into the force (F, N) upon the deposited particle using Equation 6.2, where R is the particle diameter, y is the perpendicular distance from the surface, and V is the liquid velocity across the collector surface, obtained from Equation 6.3, (O'Neill, 1967).

$$F = 1.7009 \left[6\, \mu\, \pi\, R\, V \Big|_{y=r} \right] \qquad 6.2$$

$$V = \left(\tau / \mu\right) y \qquad 6.3$$

An alternative approach to estimate the force values between a particle and a collector surface from the measured hydrodynamic shear data is to consider the surface contact area, macromolecular tether density, and the maximum separation distance between the particle and the surface. A model of the adhesion of a deformable sphere to a surface (Cozens-Roberts *et al*, 1990b) requires estimations

of the surface area, the macromolecular tether density (i.e. the density of macromolecular contacts between surface and sphere), and the mechanical properties of the adhered particle. This method was not considered due to complications in determining these parameters.

The relationship detailed in Equation 6.1, however, only applies to a Disc in an infinite medium, in which case there must be an insignificant edge effect. The thickness of the boundary layer in relation to angular velocity and kinematic viscosity is given by the Equation 6.4 (Wang *et al*, 1995):

$$\delta_0 = 3.6 \, (\nu / \omega)^{1/2} \qquad 6.4$$

where δ_0 is the thickness of the boundary layer, ν is the kinematic viscosity ($m^2 s^{-1}$), and ω is the angular velocity (radians s^{-1}).

The boundary layer thickness (δ_0) was substantially larger (1.92×10^{-4}m) than the approximate diameter of the particles investigated in the project (2×10^{-6}m), and therefore the presence of adhered particles did not affect the flow across the face of the collector surface.

6.2 Materials

The following Section details the apparatus, materials, and the solutions used specifically within the work performed using the Spinning Disc for the development and characterisation of the system, as well as the main assessment of adhesion.

6.2.1 Controller and Motor

The apparatus consists of a motor (model GPM9-395) and controller supplied by Printed Motors Ltd (UK). The Disc was connected to the shaft of the motor and was suspended in the buffer solution, as shown in Figure 6.1. The controller enabled the

speed of rotation to be maintained at 5hz (300rpm) with an accuracy of 2 decimal places. The dimensions of the apparatus are shown below in Figure 6.2. The dimensions of the system provided conditions where an infinite medium was observed (Daily and Nece, 1960). A supporting framework allowed the Disc to be lowered into the particle suspension. The Disc was separated from the motor unit by an adaptor piece, avoiding any contact between the suspension and the motor components.

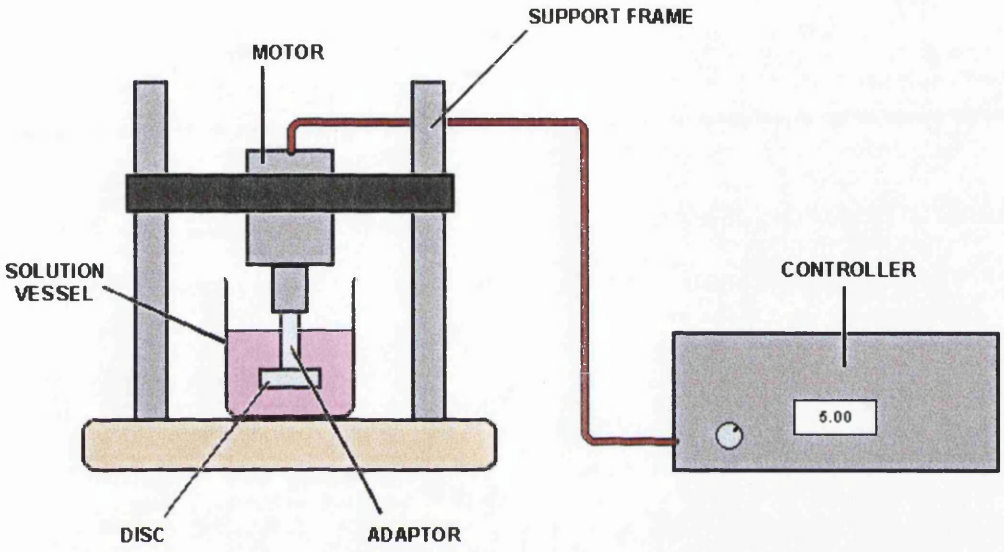

Figure 6.1: A diagrammatical representation of the Spinning Disc and supporting apparatus, showing the controller, support frame, motor, solution vessel, Disc, and the adaptor piece.

6.2.2 Glass and Stainless Steel Discs

Glass discs (30mm diameter, 1mm depth) were supplied by Jencons Ltd. (UK). The glass discs were then placed in 30mm diameter moulds, and resin poured on top of the glass discs, to an approximate depth of 10 mm. The discs were machined to 8mm in depth, and were then drilled and tapped to allow connection to the adaptor piece, ensuring that the thread was perpendicular to the Disc's face. The glass surfaces were polished to finish of 1μm as described in Section 2.3.3.

The resin (Metset FT) used for embedding the glass Discs below was supplied by Buehler.

Stainless steel (316L) Discs were cut from steel rods (30mm diameter, 8mm deep), machined and prepared as detailed with the glass Discs.

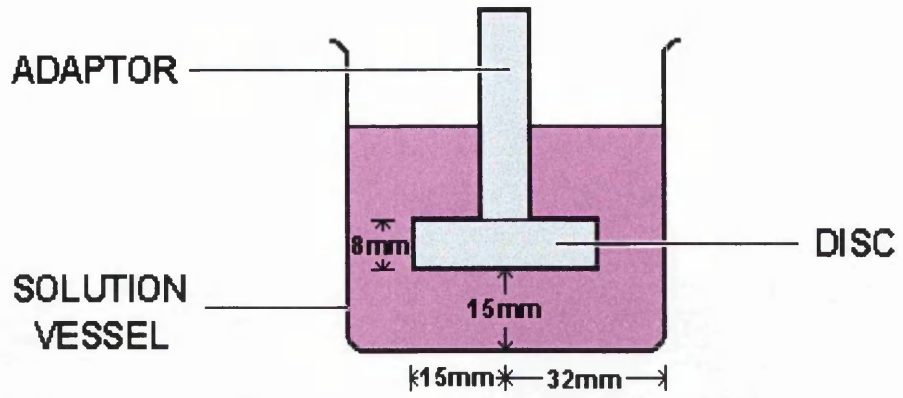

Figure 6.2: The dimensions of the Spinning Disc, and the suspension vessel.

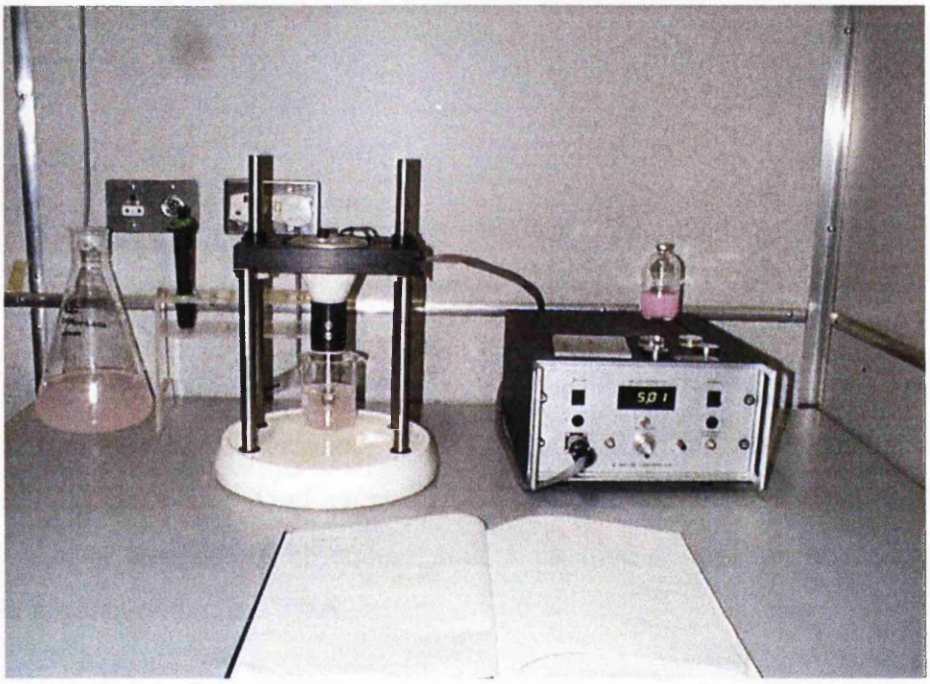

Figure 6.3: The Spinning Disc and supporting apparatus in a constant temperature room

6.2.3 The Micromanipulator and Supporting Software

Counting of adherent particles on the surface of the Spinning Disc was performed on a micromanipulator, supplied by Singer Instruments (UK) shown in Figure 6.4. The computer package used to take images in conjunction with the micromanipulator was VideoSnap^{TM}. The micromanipulator provided incident light, which allowed inspection of glass and stainless steel surfaces using reflective light, rather than transmitted.

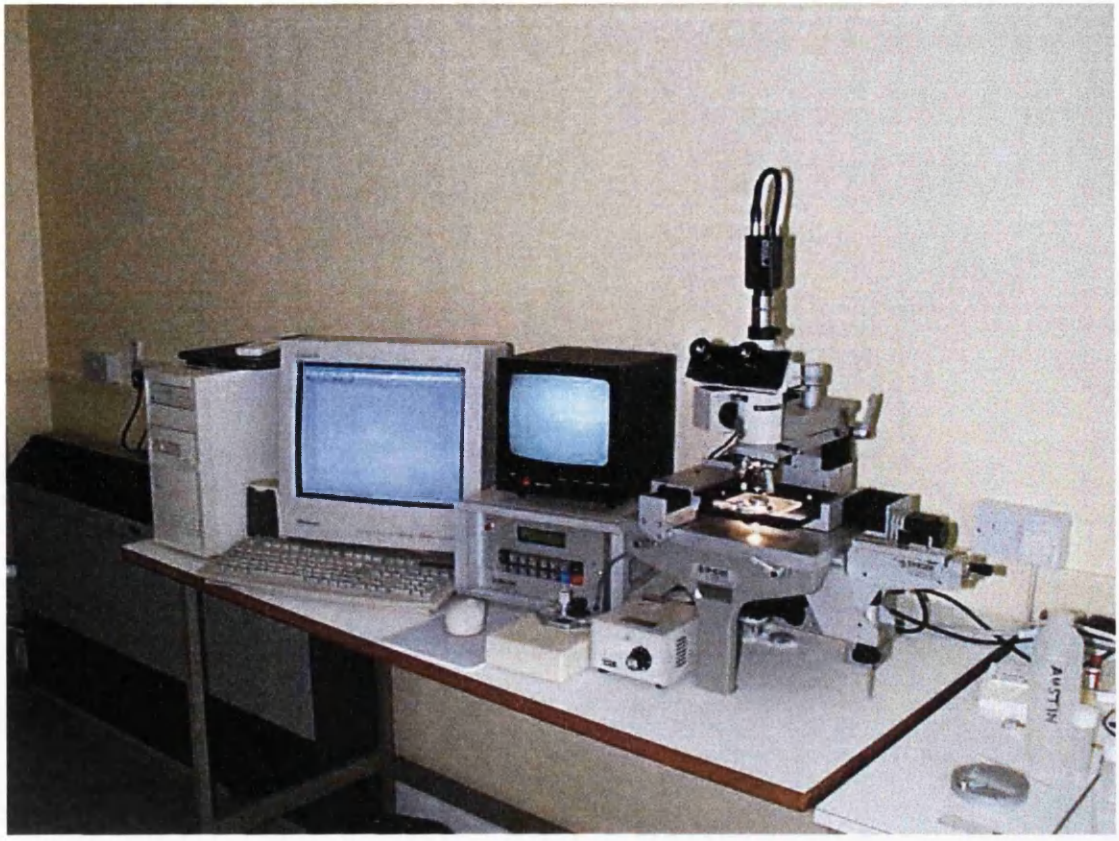

Figure 6.4: The Micromanipulator and Supporting Apparatus

The image on the monitor allowed the adhered particles to be observed and counted. The stage of the micromanipulator was fitted with a controlled stepper motor, and allowed the Disc to be moved incrementally, allowing a whole strip from the centre to the edge of the Disc to be enumerated. A detailed description of the counting method is given in Section 6.3.5.

6.2.4 Colloidal Particles

Aminated and carboxylated latex beads (2μm), and *B.mycoides* and *B.subtilis* spores were used in the experiments involving the Spinning Disc, as detailed in Section 2.2.1.

6.3 Methods

6.3.1 Collector Surface Preparation

The collector surface was prepared in all cases by washing in detergent, then soaking in ethanol (ten minutes), and finally rinsing in copious amounts of distilled water, and was finally dried at 80°C.

6.3.2 Preparation of Colloidal Suspensions

Particles were suspended in 25mM NaH_2PO_4. Prior to each experiment the beads were subjected to sonication to remove aggregates in the suspension. Sonication was not performed with the spores, which were grown as stated in Section 2.3.2.1, and frozen for storage. Particles were adjusted to their respective concentrations (2.7×10^7 /mℓ) by measuring $OD_{(660nm)}$, as stated in Section 2.4.3. pH was adjusted using HCl (1M) or NaOH (1M).

6.3.3 Experimental Protocol

The following Section details the experimental protocol used when performing adhesion experiments, unless otherwise stated.

The Disc was placed onto the adaptor piece, taking care not to touch the polished surface. Buffer solution (250mℓ) in a 500mℓ beaker was prepared and adjusted to the required pH. The Disc was spun in buffer solution for ten minutes to allow for equilibration with the solution, at 5 Hz (300 rpm). The Disc was then lifted from solution, which was replaced by the required colloidal suspension. The static Disc was lowered into the particle suspension, spun for 30 minutes, and removed slowly whilst rotating, allowing excess suspension to dissipate. The Disc was then removed from the apparatus without disturbing the surface, and counted as detailed below in Section 6.3.5.

6.3.4 Initial Visualisation Problems

The initial use of the Spinning Disc provided problems with visualisation techniques. The main problem was the presence of residual liquid on the surface of the Disc, which deposited particles upon drying. Several different methods were used to resolve this problem.

The first method was to inspect the Disc in buffer solution, by removing the Disc from the apparatus, and placing it under the microscope in a vessel containing solution. This method stopped residual solution drying on the Disc, but also removed adhered particles from the surface.

The second method was to remove the Disc from solution, and place a cover slip on the Disc and inspect the surface immediately. However, large variation was observed in adherent numbers, and there was little consistency with expected values. Adhered beads appeared to be displaced by the placing of the cover slip on the collector surface for inspection.

The third method was rinsing the Disc for five minutes in buffer solution. The process of changing solution and rinsing appeared to achieve nothing more than to remove the majority of latex beads from the surface, and was subsequently discarded as a reliable method.

The fourth option was to remove the Disc from solution whilst rotating. This allowed residual liquid to be removed by centrifugal force that would not surpass the force previously exerted on the surface. This was the accepted method incorporated in the final experimental protocol.

6.3.5 Counting Techniques and Statistics

The micromanipulator allowed the radial distance of the Disc to be measured accurately. The Disc was placed on a mounting that fixed into the tapped hole on the Disc, allowing a central location point.

The number of adhered particles was counted per screen, an area of $0.0378mm^2$. This was then standardised to a count/mm^2. Counting was performed over the Disc at increments of 1mm. Each Disc was counted six times, by simply rotating the Disc

by 60° on the plastic mounting. Experiments were repeated on six Discs, providing 36 readings per radial position.

Previous works using the Spinning Disc have presented their results as a measure of adhesive co-efficient (AC), rather than count/mm^2 (Shive *et al*, 1999; Vacheethasanee *et al*, 1998; Wang *et al*, 1995, 1993a and 1993b). The use of the adhesive co-efficient allowed variation of particle concentration to be disregarded, and therefore comparisons to be made between suspensions of different concentrations (Wang, 1993a and 1993b).

The adhesion coefficient represents the ratio of the number of adherent particles per mm^2 to the number of particles transported to the collector surface.

$$\mathbf{AC\ (\%) = [\ N / (\ j\ x\ t\ )\ ]\ x\ 100} \qquad \mathbf{6.6}$$

Where **N** is the number of adherent particles per mm^2, **j** is the particle flux (bacteria / s mm^2), and **t** represents the duration of the experiment in seconds.

However, to simplify results, suspension concentration was kept constant for all four particles. This allowed adhesion to be presented in count/mm^2, and the interpretation of results to be made without considering the effect of concentration on adhesion levels.

6.4 Experiments to Characterise Particulate Adhesion to the Spinning Disc

The following experiments were undertaken to assess the effect of time, concentration and surface treatment on attachment. Characterisation experiments were performed using stainless steel, which provided a more practical surface for assessing attachment, discussed in Section 6.6.1.

6.4.1 The Effect of Concentration on Adhesion of Carboxylated Beads

The effect of concentration on adhesion was determined by assessing adhesion at four radial distances using carboxylated latex beads. This was performed to determine the ideal suspension concentration for subsequent attachment experiments.

Protocol:

Experimental protocol is stated in Section 6.3.3. The solution pH was maintained at 3.5, which provided most adhesion, as determined in Chapter 5. The experiment was carried out at 22 +/- 1°C. The experiment was performed at six different solution concentrations ranging from 0 to 1 (OD_{660nm}). Adhesion Counts were taken where r = 1, 5, 9, and 13mm.

Results:

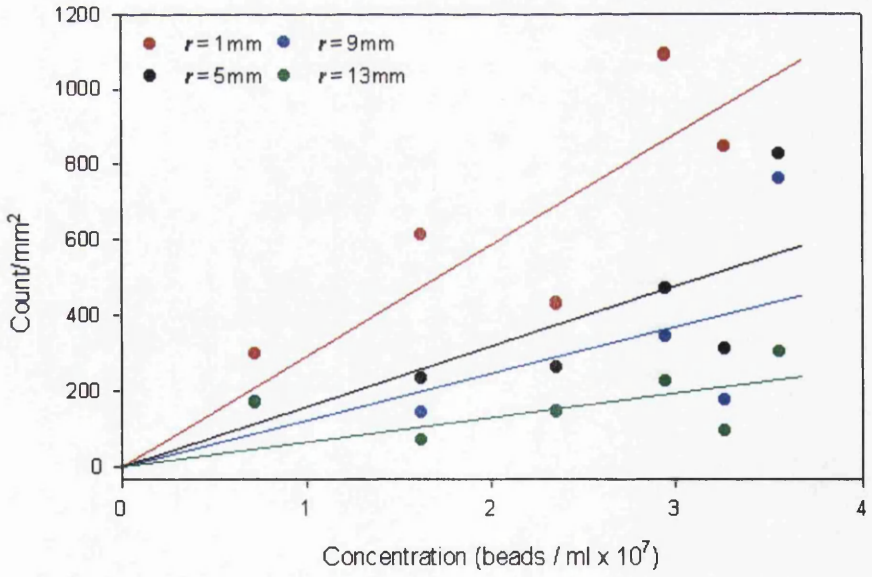

Figure 6.5: The effect of colloidal concentration on adhesion. Carboxylated latex beads (2μm) were used as the model colloid in the system. The solution was 25mM NaH_2PO_4, adjusted to pH 3.5 using HCl (1M). Temperature was kept constant at 22 +/- 1°C. The collector surface was stainless steel 316L. Adhesion was assessed at four different radial distances, 1, 5, 9, and 13mm. The experiments were conducted for 30 minutes.

The effect of concentration upon adhesion showed an increase in the amount of adhesion as particle concentration was increased as shown in Figure 6.5. Results showed a large amount of variation in adhesion.

The purpose of the experiment was to assess an ideal colloidal concentration that would provide sufficient numbers to count practically, i.e. not too high that adhesion was colloid/colloid aggregation, and not low that there was no adhesion at all. The larger radial distances provided more reliable data and it was decided that $2.7 \times 10^7/m\ell$ was a suitable concentration to perform adhesion experiments.

6.4.2 The Effect of Incubation Time on Adhesion of Carboxylated Beads

The effect of incubation time on adhesion was determined by assessing adhesion at four radial distances using carboxylated latex beads. This experiment was performed to determine the ideal duration for subsequent attachment experiments.

Protocol:

Concentration ($2.7 \times 10^7 m\ell$), pH (3.5), and temperature (22 +/- 1°C), were kept constant, and time varied from t = 0 to t = 30 minutes. The experimental procedure was as used in Section 6.4.1, except for the variation in time.

Results:

As expected, as radial distance was increased, adhesion decreases. There was little difference in adhesion relative to time, where attachment was independent to time after 5 minutes. Thirty minutes was the most practical time period for the experiment, as the counting of each Disc took approximately thirty minutes, and was therefore used in further experimentation.

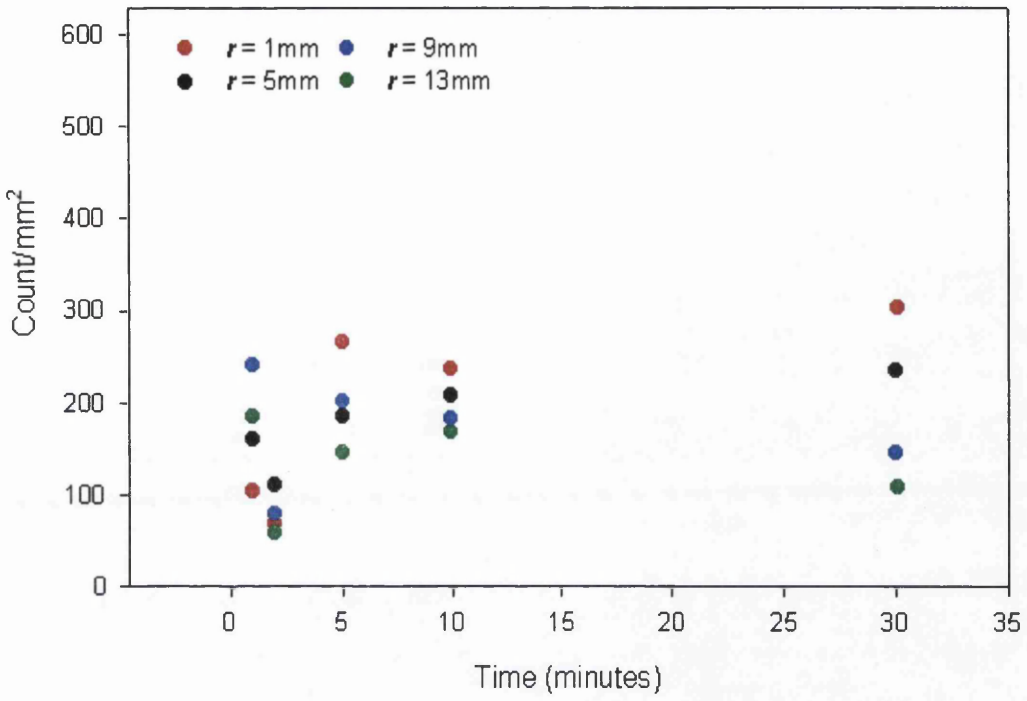

Figure 6.6: The effect of time on adhesion. Carboxylated latex beads (2μm) were used as the model colloid in the system. The solution was 25mM NaH_2PO_4, adjusted to pH 3.5 using HCl (1M). Temperature was kept constant at 22 +/- 1°C. The collector surface was stainless steel 316L. Adhesion was assessed at four different radial distances, 1, 5, 9, and 13mm. Concentration was kept constant at 2.7 x 10^7 beads/mℓ.

6.4.3 The Effect of Silanisation on Bacillus Spore Adhesion to Glass

6.4.3.1 Introduction

The effect of silanisation was investigated in conjunction with adhesion measurements performed with the Atomic Force Microscope (AFM), as detailed in Section 1.6.4.1. Silanisation resulted in a hydrophobic surface (Husmark and Rönner, 1992), changing the adhesive characteristics of the glass collector surface. This exercise served two purposes, firstly as an introduction to the use and potential problems of the Spinning Disc, and secondly to determine any correlation between the assessment of adhesion using the AFM and the Spinning Disc.

The experiment was performed using a different solution to those stated in Section 2.2.3, as was determined in previous work performed with the AFM (Bowen *et al*, 2000). Experiments were performed on the spores of *B.mycoides* and *B.subtilis* spores, rather than latex beads.

6.4.3.2 Silanisation of Glass

Glass surfaces were heated at 500°C for three hours, to remove any organic contaminants and rinsed repeatedly in deionised water. The surface was then immersed for 10 min in 5% dichloromethylsilane in toluene, and then washed sequentially in toluene, methanol, and deionised water. Silanised glass surfaces were then mounted as detailed in Section 6.2.2.

6.4.3.3 Experimental Procedure

Spores were taken from medium, harvested and washed three times in distilled water, and then a fourth time in 0.145M NaCl, and finally suspended in 0.145M NaCl solution giving a count of 2.7×10^7 spores/mℓ in approximately 250mℓ.

Protocol:

The experimental procedure was as detailed in Section 6.3.3.

Results:

6.4.3.4 The Adhesion of B.mycoides Spores to Untreated and Silanised Glass

The adhesion of *B.mycoides* spores to hydrophobic glass demonstrated the largest amount of adhesion as shown in Figure 6.7, as was expected. The spore has been shown to have low zeta potential, and a relative hydrophobicity value of

approximately 50% as shown in Chapter 3. These figures suggested that the preference of the spore was to be deposited from the solution. The silanised glass surface provided an ideal environment for this deposition to occur, resulting in high values of adhesion, peaking at approximately 7000mm^{-2}, and the lowest reading was approximately 2000mm^{-2}.

The shape of the graph showed that adhesion of *B.mycoides* was shear-dependent. The curve appeared to consist of two phases, a first phase, where radial distance was between 0 and 4mm, and a second phase after this point. From observations made when counting the spores on the surfaces, the first phase represented areas where spores were in contact with each other. The second phase showed minimal spore/spore interaction.

In the case of the untreated glass surface the adhesion of the *B.mycoides* spores to the collector surface was relatively low (peak at 4000mm^{-2}, and minimum of less than 100mm^{-2}). The highly negatively charged surface of the untreated glass was more repulsive to the spore than the silanised surface, and consequently inhibited the spores' deposition from suspension. There was, however a decrease in adhesion at radial distance between 0 and 4 mm. The curve, again, showed two distinct areas, where adhesion increased as radial distance decreased, and past 4mm where negligible adhesion occurred. As with adhesion to the silanised glass, at distances less than 4mm, spores were observed in multiple aggregates, although still forming a monolayer, whereas at radial distances greater than 4mm, adhesion was predominantly in singlets.

6.4.3.5 The Adhesion of B.subtilis Spores to Untreated and Silanised Glass

The adhesion of *B.subtilis* spores to both treated and untreated glass, was higher than expected. The spore was demonstrated to have relatively large zeta potential values and low hydrophobicity relative to *B.mycoides*, as seen in Tables 3.1 and 3.3 respectively. It must be noted that these zeta potentials were measured in 25mM NaH_2PO_4, whereas this experiment was conducted at 0.145M NaCl. The effect of

salt in this case would be to mask the DLVO interactions, and negate the contribution of electrostatic repulsion.

Levels of adhesion of *B.subtilis* to untreated glass were greater than the interaction between *B.mycoides* and untreated glass, but smaller than values obtained for the adhesion of *B.mycoides* to silanised glass. The adhesion of *B.subtilis* was greater to the silanised glass surface rather than untreated glass collector surface. This can be explained by the masking effect of 0.145M NaCl on the charge of the *B.subtilis*, rendering the hydrophobic interaction more prominent, and therefore increasing the spores' likelihood to be deposited on the hydrophobic surface. Having stated this, however, the salt does not mask charge completely, and for this reason higher attachment levels than expected were observed with the spores' adhesion to untreated glass. The glass surface charge was also masked relative to that observed at 25mM NaH_2PO_4. The presence of salt reduced the repulsive DLVO interactions by reducing the electrical double layer, therefore increasing adhesion.

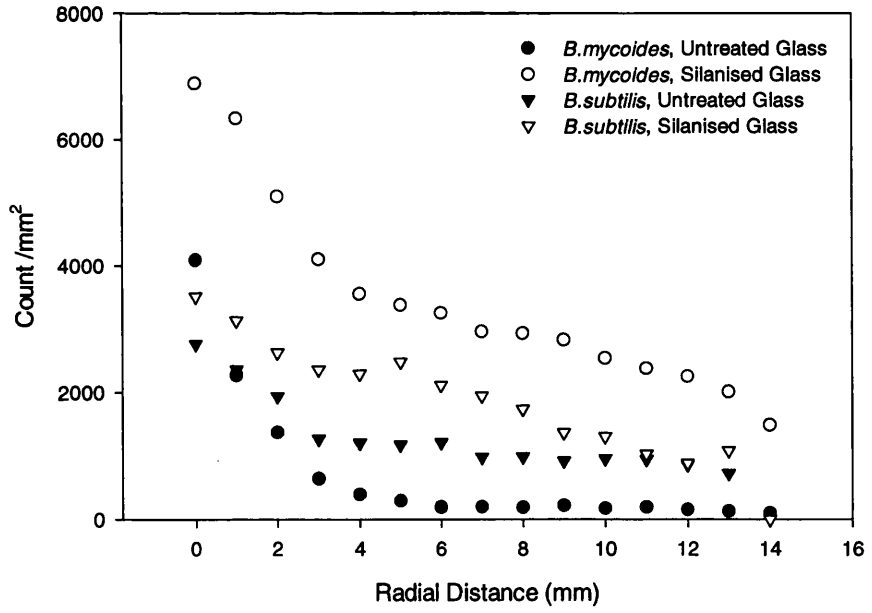

Figure 6.7: The Effect of Silanisation of glass on the Adhesion of *B.mycoides* and *B.subtilis* Spores. Experiments were performed using the Spinning Disc technique, with both untreated and silanised glass in 0.145M NaCl. Concentration of spores was maintained at 2.7 x 10^7 and temperature at 22 +/- 1°C. Error bars are omitted for reasons of clarity. The average standard deviations were 40.6, 11.9, 32.4, and 40.7 for Silanised glass with *B.mycoides*, Untreated glass with *B.mycoides*, Silanised glass with *B.subtilis*, and Untreated glass with *B.subtilis* respectively.

The shape of the curves obtained with *B.subtilis* spores were not as distinct as those observed with *B.mycoides* spores. Adhesion decreased as radial distance increased, showing a dependence on shear, but there were not two distinct phases as was observed with *B.mycoides*. Visual observations when counting the adhesion to the surface showed that there were significantly fewer spore clusters on the surface compared to *B.mycoides*, and this was the reason for the more linear shape of the curves.

6.4.3.6 Summary

The results did show correlation with observations made using the AFM (Bowen *et al*, 2000), as well as the results gathered using surface and collector characterisation techniques in Chapters 3 and 4. The function of the experiment was to prove that the qualitative observations made using the Spinning Disc could be relied upon, which was indeed demonstrated. A good deal of confidence can be placed on this technique and as such, could be studied further to assess the adhesion of aminated and carboxylated beads, as well as the spores of *B.mycoides* and *B.subtilis*.

6.5 Analysis of Particle Adhesion to Glass and Stainless Steel

The following Section describes the effect of pH on the adhesion of the aminated and carboxylated latex beads, and the spores of *B.mycoides* and *B.subtilis* using the Spinning Disc technique.

The attachment of each particle species to either glass or stainless steel is considered individually, allowing the effect of pH to be analysed. Results are given with respect to radial distance rather than shear force, which is analysed and considered in conjunction with the results generated from the Radial Flow Chamber in Chapter 8. The results can also been seen collectively in Appendix D.

Preparation of surfaces, colloids, and solutions and experimental protocol is detailed in Section 6.3.

6.5.1 The Effect of pH on the Adhesion of Aminated Beads

The attachment levels of aminated beads to glass and stainless steel using the Spinning Disc technique to assess adhesion at pH 3.5, 5.5, 7.5, and 9.5 are shown in Figure 6.8.

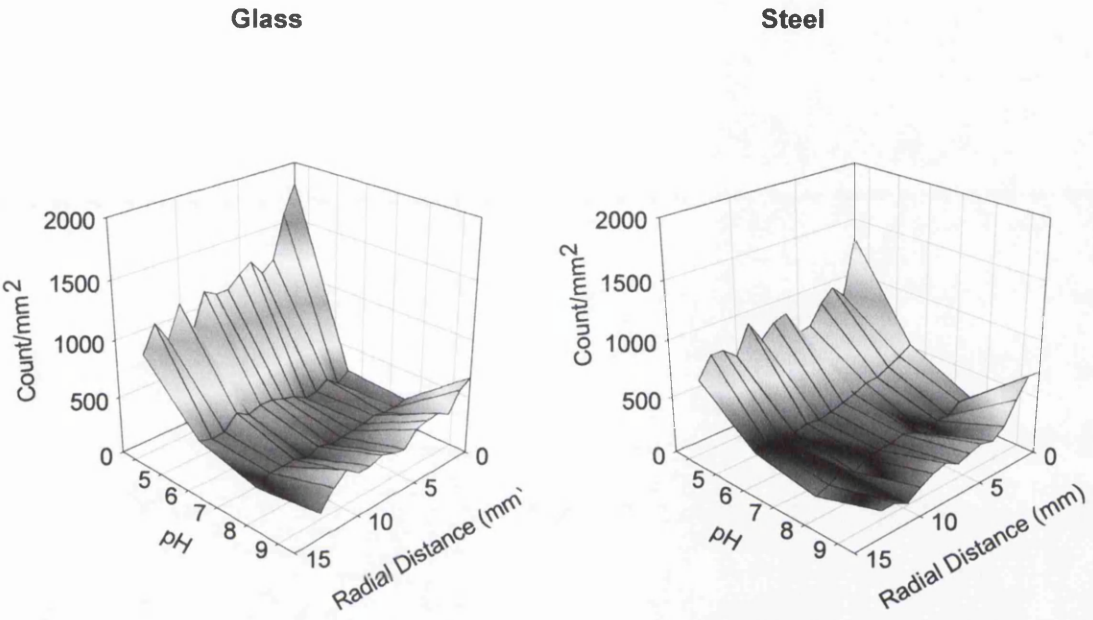

Figure 6.8: The adhesion of aminated latex beads to glass and stainless steel in relation to radial distance and pH. Aminated beads were suspended in 25mM NaH_2PO_4, and the solution pH was adjusted with HCl (1M) or NaOH (1M) accordingly. The experiment was conducted at 300rpm for 30 minutes, and temperature kept constant at 22 +/- 1°C. Error bars were omitted for reasons of clarity. The average standard deviation for each pH was 260, 894, 169, and 350 for pH 3.5, 5.5, 7.5, and 9.5 respectively.

The adhesion levels of aminated beads to stainless steel and glass were highest at pH 3.5, due to the interaction between the bead and the collector surface being predominantly hydrophobic. The hydrophobicity of both the collector surfaces was highest at pH 3.5 as measured by contact angle measurements, shown in Table 4.1. The surface charge of the aminated beads at pH 3.5 was low compared with the surface charge observed at higher pH as shown in Table 3.1. The resultant interaction between the aminated beads and the glass and stainless steel collector surface at pH 3.5 was due to the highly hydrophobic bead interacting with the collector surface, with little electrostatic repulsion. This was not the case at pH 5.5

and above, as the charge of the bead became highly negative as shown in Table 3.1, subsequently increasing the electrostatic repulsion between the two surfaces, and decreasing the hydrophobic contribution to the interaction between the bead and the glass or stainless steel surface.

The adhesion of the aminated beads was therefore lowest at pH 5.5 and 7.5, but increased at pH 9.5. The increase in adhesion levels at pH 9.5 did not, however, approach the levels reached at pH 3.5. The increase in the adhesion levels at pH 9.5 was attributed to the increased level of hydrophobicity of the aminated beads, as shown in Table 3.3. The increase in adhesion at pH 9.5 was not confirmed when considering the adhesion of the aminated beads to silica and stainless steel using the Packed Column method, as shown in Figure 5.14. The Packed Column method did, however, show that the adhesion values generated when considering stainless steel were relatively close, compared with those generated when assessing the attachment to silica. This observation was reflected using the Spinning Disc technique, shown in Figure 6.8.

There was minimal difference in the values of adhesion to glass and the values of adhesion to stainless steel when considering the adhesion of aminated beads. The results from the Packed Column also showed similar values of adhesion between glass and stainless steel.

The similarity in the attachment levels between glass and stainless steel was attributed to the presence of localised positive amine groups on the surface of the bead, resulting in electrostatic attraction between localised positive charge on the bead, and the negative charge of the collector surfaces. The electrostatic attraction reduced the contribution of the differing hydrophobic characteristics of both the glass and the stainless steel, and therefore the difference in surface characteristics.

The adhesion of the aminated beads to both collector surfaces was dependent on radial distance. Adhesion decreased as radial distance increased in all cases, although there was more dependence on radial distance when considering the adhesion of the aminated beads at pH 3.5, where the hydrophobic interaction was dominant. This agreed with the hypothesis that although hydrophobic interactions operate over a longer range than van der Waals forces, the van der Waals forces are stronger over the range they operate, than the hydrophobic forces, as concluded in Section 5.5.2.4.

6.5.2 The Effect of pH on the Adhesion of Carboxylated Beads

The attachment levels of carboxylated beads to glass and stainless steel using the Spinning Disc technique to assess adhesion at pH 3.5, 5.5, 7.5, and 9.5 are shown in Figure 6.9.

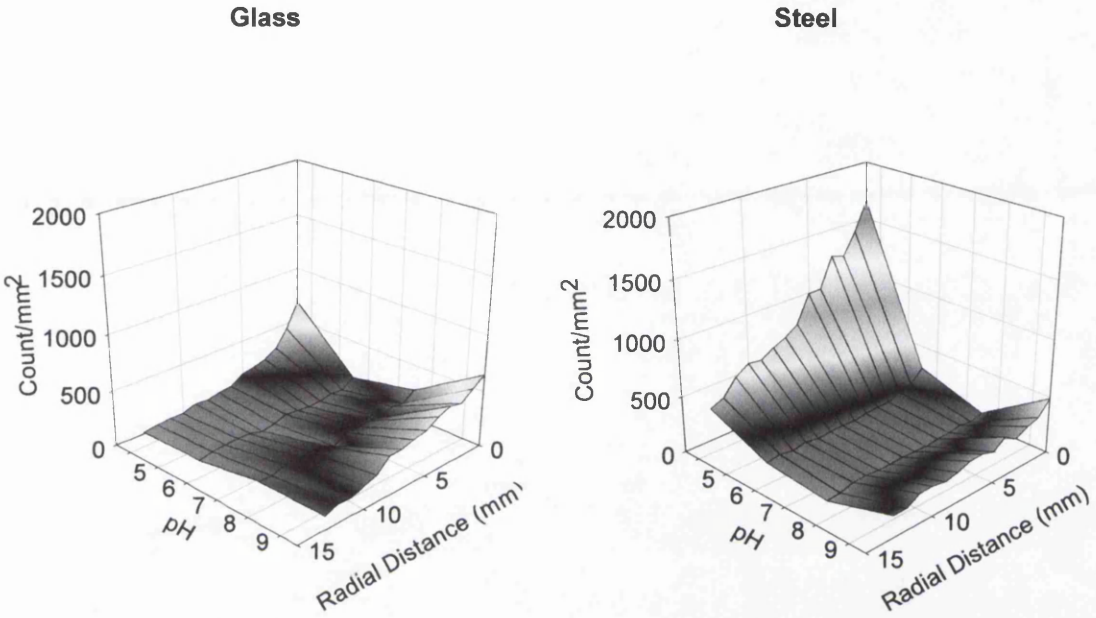

Figure 6.9: The adhesion of carboxylated latex beads to glass and stainless steel in relation to radial distance and pH. Carboxylated beads were suspended in 25mM NaH_2PO_4, and the solution pH was adjusted with HCl (1M) or NaOH (1M) accordingly. The experiment was conducted at 300rpm for 30 minutes, and temperature kept constant at 22 +/- 1°C. Error bars were omitted for reasons of clarity. The average standard deviation for each pH was 111, 40, 79, and 247 for pH 3.5, 5.5, 7.5, and 9.5 respectively.

The adhesion of carboxylated beads to glass and stainless steel showed similar trends to those observed when considering the adhesion of aminated beads to both collector surfaces. The adhesion at pH 3.5 was noticeably dependent on shear in both the cases of glass and stainless steel, as was observed with aminated beads.

The adhesion of carboxylated beads to both glass and stainless steel increased at pH 9.5, compared with the values obtained at pH 5.5 and 7.5, as was observed with aminated beads, due to the increased hydrophobicity of the bead at pH 9.5, as shown in Table 3.3.

Attachment to glass and stainless steel was comparable when considering aminated beads, but this was not the case when considering the attachment of carboxylated beads to glass and stainless steel. This was attributed to the presence of carboxyl groups on the beads' surface rather than amine groups. Consequently, there were no localised areas of positive charge on the carboxylated bead, and the carboxylated beads were subject to greater electrostatic repulsion from the glass collector surface, and this was reflected in the surface charge of the carboxylated beads as shown in Table 3.1. This observation was confirmed by the similarity of the adhesion levels of the aminated and carboxylated beads when interacting with stainless steel, which was dominated by the attractive hydrophobic interaction between the stainless steel an the beads. The hydrophobicity of both aminated beads and carboxylated beads were similar, and can be seen in Table 3.3.

Confirmation of these results was obtained when considering the results obtained from the use of the Packed Column for assessing the adhesion of aminated and carboxylated beads to silica and stainless steel. The difference in the adhesion levels between aminated beads and carboxylated beads to silica was relatively large, compared with the equivalent difference obtained for the adhesion to stainless steel, as shown in Figures 5.12 and 5.13 respectively.

6.5.3 The Effect of pH on the Adhesion of B.mycoides Spores

The attachment levels of *B.mycoides* spores to glass and stainless steel using the Spinning Disc technique to assess adhesion at pH 3.5, 5.5, 7.5, and 9.5 are shown in Figure 6.10.

The adhesion of the spores of *B.mycoides* to both glass and stainless steel showed very similar trends to each other. This comparison was due to the low charge and the moderate hydrophobicity of the spore, resulting in the spores' instability in suspension. The deposition of the spores was therefore deemed to be irrespective of the surface characteristics, and was confirmed by the low percentage recovery from the Packed Column, as shown in Figures 5.12 and 5.13, for both silica and stainless steel respectively.

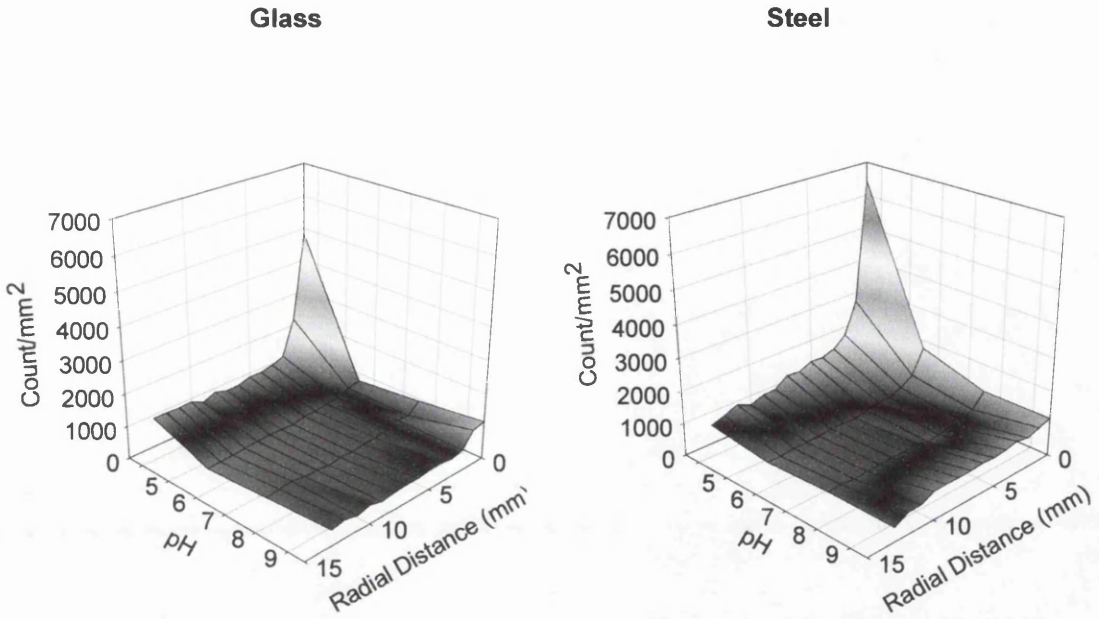

Figure 6.10: The adhesion of *B.mycoides* spores to glass and stainless steel in relation to radial distance and pH. *B.mycoides* spores were suspended in 25mM NaH_2PO_4, and the solution pH was adjusted with HCl (1M) or NaOH (1M) accordingly. The experiment was conducted at 300rpm for 30 minutes, and temperature kept constant at 22 +/- 1°C. Error bars were omitted for reasons of clarity. The average standard deviation for each pH was 708, 220, 396, and 453, for pH 3.5, 5.5, 7.5, and 9.5 respectively.

As observed with the adhesion of both aminated beads and carboxylated beads, the largest amount of adhesion occurred at pH 3.5 where the radial distance was small. The increase in adhesion at pH 9.5 observed with both latex beads did not occur with the *B.mycoides* spores, due to the independent relationship between hydrophobicity of the spore and pH, as shown in Table 3.3.

The attachment levels of the *B.mycoides* spores at the centre of the Disc were approximately 5000 for pH 3.5 and 1000 for pH 5.5, 7.5, and 9.5. Apart from the values obtained at pH 3.5 at radial distances less than 2mm, attachment of the spores of *B.mycoides* did not vary significantly with respect to radial distance. These observations suggested that the attachment of the spores were significantly affected by the presence of surface appendages and the spores' exosporium (Husmark and Rönner, 1992), rather than the combination of the DLVO and hydrophobic interaction forces experienced by the aminated and carboxylated beads. Consideration of this effect is given in Section 9.5.

6.5.4 The Effect of pH on the Adhesion of B.subtilis Spores

The attachment levels of *B.subtilis* spores to glass and stainless steel using the Spinning Disc technique to assess adhesion at pH 3.5, 5.5, 7.5, and 9.5 are shown in Figure 6.11.

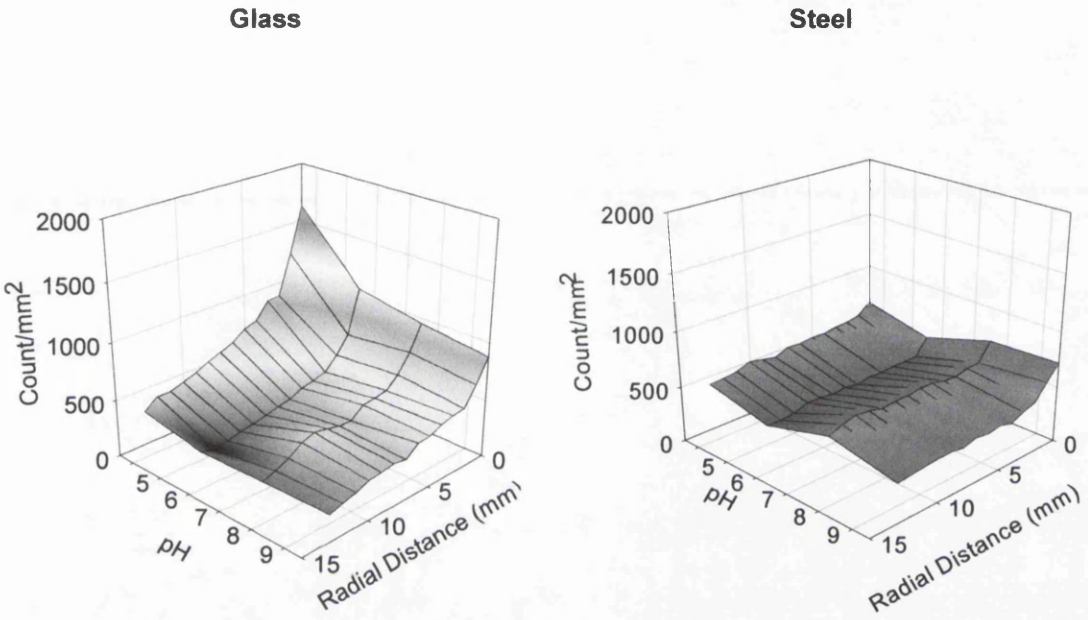

Figure 6.11: The adhesion of *B.subtilis* spores to glass and stainless steel in relation to radial distance and pH. *B.subtilis* spores were suspended in 25mM NaH_2PO_4, and the solution pH was adjusted with HCl (1M) or NaOH (1M) accordingly. The experiment was conducted at 300rpm for 30 minutes, and temperature kept constant at 22 +/- 1°C. Error bars were omitted for reasons of clarity. The average standard deviation for each pH was 251, 236, 203, and 157, for pH 3.5, 5.5, 7.5, and 9.5 respectively.

The adhesion values of the spores of *B.subtilis* to glass were noticeably different to the values obtained for the adhesion of the spores to stainless steel. The spore possessed a large negative charge, and very low hydrophobicity, as shown in Tables 3.1, and 3.3 respectively, except at pH 3.5, where the hydrophobicity of the spore was approximately 50%.

The adhesion of the *B.subtilis* spores to glass using the Spinning Disc decreased as pH increased, as was observed when assessing adhesion of the spores to silica using the Packed Column technique to assess adhesion, as shown in Figure 5.12. The adhesion of the spores to stainless steel using the Spinning Disc did not vary

significantly, which was also reflected by the equivalent experiments using the Packed Column, as shown in Figure 5.13.

Due to the biological nature of the spore, the spore surface is composed of many differing molecules, and subsequently possessed areas of differing charge on the surface of the spore, containing both positive and negative values. This heterogeneity in charge is comparable with the surface of aminated beads, which had a negative surface charge, but positive amine groups present on the beads' surface. The presence of these areas of local positive charge on the surfaces of aminated latex beads and the spores of *B.subtilis* increase the adhesion values of both particles to the negative, hydrophilic glass surface, compared with the expected values of adhesion if overall surface charge was considered. The adhesion values obtained for aminated beads and *B.subtilis* spores were higher than the equivalent values obtained for stainless steel, which reflects the heterogeneity on the surface of both these particle types, and can be seen when directly comparing Figure 6.8 with Figure 6.11.

6.6 Discussion

The following Section discusses the developments made using the Spinning Disc technique, the results from the silanisation experiments, and the results from the main assessment of adhesion

6.6.1 Visualisation and Counting Developments

The extraction of data from the use of the Spinning Disc to assess adhesion was inhibited by the inability to visualise particles adhered to the surface, as discussed in Section 6.3.4. The Spinning Disc required removal from the particulate suspension, and subsequent inspection to obtain experimental results. Visualisation of glass was hampered by the transparency of the collector surface, which hindered the process of focusing on the surface. This was not the case with stainless steel, due to the surfaces reflective properties. The hydrophilicity of the glass collector also provided

problems, due to the retention of suspension on the collector surface. Extraction of the Disc from solution whilst still spinning, and therefore allowing residual liquid to exit under centrifugal force, resolved this problem.

6.6.2 The Effect of Silanisation on Adhesion

The experiments using silanised and untreated glass were performed firstly to assess the ability of the Spinning Disc to assess adhesion, secondly to gain experience with the technique, and finally to obtain experimental data to compare with the data provided by the use of the AFM to assess adhesion. These objectives were achieved.

The results, presented in Figure 6.7, showed that *B.mycoides* spores attached in greater numbers to the hydrophobic, silanised surface compared with the data obtained for the hydrophilic untreated glass surface, which was reflected in Section 6.5.3, where greater adhesion was obtained for stainless steel than glass. The attachment values of the *B.mycoides* spores to stainless steel were comparable to the silanised glass surface (approximately 7000mm^{-2}), even though the ionic strength of the solution in the case of the experiments conducted with silanised glass was 145mM NaCl, compared with 25mM NaH_2PO_4 used with stainless steel. The interaction was predominantly hydrophobic, and was therefore not noticeably affected the suspensions' ionic strength. This was not the case when considering the attachment of *B.subtilis* spores, which presented higher values of attachment to silanised glass than to stainless steel. The increased ionic strength of the suspension used in conjunction with the silanised glass reduced the electrostatic repulsion between the *B.subtilis* spore and the silanised glass, increasing the contribution of the hydrophobic interaction, resulting in higher values of attachment.

This was confirmed by the attachment of the *B.subtilis* spores to untreated glass at 145mM NaCl (1000+ mm^{-2}) compared with 25mM NaH_2PO_4 (approximately 500mm^{-2}), as shown in Figures 6.7 and Section D.5. In this case, the ionic strength of the 145mM NaCl solution reduced the electrostatic repulsion between the *B.subtilis* spore and the untreated glass surface, increasing adhesion, compared with the 25mM NaH_2PO_4 solution.

6.6.3 Data Presentation

The presentation of data in 3-dimensional plots allowed a general impression and qualitative analysis of adhesion of the particles to the collector surfaces. The same data was also presented in 2-dimensional plots, and can be seen in Appendix D. This Chapter detailed the use of the Spinning Disc, and comparatively analyses the attachment of particles to the surfaces as a function of radial distance. The presentation of data in 3-dimensional plots allowed a more comprehensive appreciation of the adhesion of the latex beads, and the *Bacillus* spores, compared with the 2-dimensional plots.

The results generated using the Spinning Disc are presented in Chapter 8, as a function of shear force, and are directly compared with the equivalent results obtained with the Radial Flow Chamber. The comparisons made in Chapter 8 are a more quantitative analysis than the comparisons made in this Chapter, and results are presented in 2-dimensional plots.

6.6.4 Discussion of Data

The adhesion of aminated and carboxylated beads and the spores of *B.mycoides* and *B.subtilis* to glass and stainless steel was assessed using the Spinning Disc Technique, and are shown in Figures 6.8, 6.9, 6.10, and 6.11.

There were several observations that were consistent throughout the adhesion results. Firstly, adhesion was greatest at low pH, attributed to the decrease in surface charge of both glass and stainless steel collector surfaces.

Secondly, the presence of localised positive charge increased the adhesion of particles, as exemplified when considering the adhesion of aminated latex beads, and the spores of *B.subtilis*. In these cases, the difference between the adhesion to glass and stainless steel collector surfaces was smaller compared with the equivalent observations for carboxylated beads and the spores of *B.mycoides*.

Thirdly, attachment levels decreased as radial distance increased, and the decrease in attachment levels was largest at pH 3.5.

Fourthly, the results obtained using the Spinning Disc were consistent with the observations made when assessing adhesion using the Packed Column. The prediction of attachment was as expected, when taking into consideration colloid and collector properties, and the results obtained from the Packed Column, although the attachment levels of the spores of *B.subtilis* were slightly higher than predicted using the Packed Column, attributed to the complexity and resultant heterogeneity of the spore surface.

Finally, the main observation made from the results was that variation in adhesion was large and as shear stress was increased, adhesion decreased, as was expected, and can be attributed to heterogeneity of both the collector and the particle with respect to charge, surface roughness, and hydrophobicity, as detailed in Section 1.5. The shape of the curve was predicted as being sigmoidal, for a normally distributed population (Garcia *et al*, 1997). However, the attachment curves obtained in this project were either straight lines, or exponential decay, which agreed with curves obtained from previous work (Wang *et al*, 1995).

The results of adhesion were presented in Sections 6.5.1, 6.5.2, 6.5.3, and 6.5.4 in 3-dimensional plots, which allowed visual comparison, and qualitative analysis. The equivalent 2-dimensional plots, can be seen in Appendix D, allowing the comparison of the variation in adhesion of the four particles for glass and stainless steel respectively.

CHAPTER SEVEN

The Development and Use of the Radial Flow Chamber for Adhesion Studies

7.1 Introduction

As with the Spinning Disc technique detailed in Chapter 6, the Radial Flow Chamber (RFC) provides a method of assessing adhesion by generating a shear force gradient across the collector surface in question. Theoretically, the shear force required to inhibit adhesion can therefore be calculated relative to flow rate through the system, and used to predict the shear force required to inhibit particle adhesion of a percentage of a colloidal population.

The particle suspension enters the RFC through a central inlet, and flows over the collector surface (in this case glass and stainless steel). The suspension exits through three equally spaced outlets. Although both the RFC and the Spinning Disc use shear force to inhibit adhesion, there is an important difference between the two methods. The collector surface of the RFC remains static allowing inspection while the shear force is being applied to the collector surface. The movement used to generate shear using the Spinning Disc technique renders inspection of the surface

impossible whilst the shear is being applied, and therefore requires removal from the particle suspension as detailed in Section 6.3.4. This method therefore allows adhesion to both glass and stainless steel be assessed *in situ* simultaneously.

7.1.1 Theory

The geometry of radial flow provides a well-defined laminar flow field. The RFC consists of two parallel discs with a narrow space (1mm in this case). The gap between the discs should be kept at a minimum to ensure high flow pressure (Becker, 1998).

The shear gradient within the RFC decreases as radial distance increases. The applied shear force can be calculated when taking into consideration the simplest approximation for the wall shear stress for creeping flow of an incompressible Newtonian fluid, as seen in Equation 7.1 (Dickinson and Cooper, 1995; Cozens-Roberts *et al*, 1990a and 1990b; Groves and Riley, 1987; Moller, 1963).

$$\tau = 3(\mu Q) / \pi h^2 r \qquad 7.1$$

where μ is the fluid viscosity (8.94 x 10^{-4} kg/ms), h is the height of the gap between parallel surfaces (0.001 m), r is the radial position relative to the inlet pipe (m), Q is the volumetric flow rate (2.333 x 10^{-5} m^3/s, the equivalent of 1.4 ℓ/min). In this case, the values of shear stress where attachment was enumerated vary from 0.42 to 1.99 N/m^2.

Equation 7.1 assumes laminar flow is obtained within the system. Calculation of the flow pressure for turbulent flow requires an alternative formulation. Fowler and McKay (1980) found that turbulent flow was not reached at 20 ℓ/min, well above the flow rate used in these experiments.

7.1.2 Previous Uses

The use of the RFC allows the study of adhesion with respect to shear stress, under a variety of conditions. The RFC has been used to study both cellular adhesion and biofilm formation. The apparatus has few limitations, and can be used to study a range of surfaces, surface treatments, particles, and solution chemistry, as highlighted in Section 1.6.3.

The uses of Flow Chambers to study adhesion are wide, and are covered by Busscher and Van der Mei (1995a).

7.1.2.1 The Study of Biofilm Formation

Initial microbial adhesion is the first, and most important step involved in biofilm formation (Busscher and Van der Mei, 1995b). As would be expected, biofilm formation is substantially easier to study, due to the ability to inspect formation with the naked eye. For this reason, the RFC was initially used as a method of assessment of biofilm formation (Pyne *et al*, 1984; Fowler and McKay 1980; Fletcher and Loeb, 1979). These studies vary with respect to their subject cells, but are all in agreement when they conclude that bacteria, diatoms, and fungi increase their attachment strength substantially over periods of days, rather than hours.

Parallel plate flow Chambers can also be used to study adhesion, as exemplified by the study of the formation of biofilms with oral bacteria (Bos *et al*, 1994), although this method does not allow a shear gradient to be generated within the system.

7.1.2.2 The Study of Particle Adhesion

The study of the process of initial adhesion process using colloidal particles of no more than 2μm poses two major problems compared with the study of biofilm formation. Firstly, the particles must be counted individually with respect to distance, rather than the minimum radial distance that the biofilm covers. Secondly, the adhesion of colloidal particles to the surface will be a much quicker process and

the residency time of the particles on the surface must be considered. Consequently, the counting technique used for enumeration of adhered particles must be accurate. This involves the elimination of flowing bacteria from *in situ* enumeration (Meinders *et al*, 1992).

The RFC technique has been used for a variety of particle types including eukaryotic and prokaryotic cells, as well as non-biological particles. Work on eukaryotic cells has been limited to the adhesion of cells in conjunction with blood components, as the RFC allows shear to be generated that simulates hemodynamic shear. The investigation of the adherence of the cells of the immune system allows the development of biomedical polymers with respect to rejection. The system also allows the effect of blood components on adhesion to be assessed, for example human neutrophil adhesion in the presence of fibrinogen and kininogen (Yung *et al,* 1996). The work performed by Yung *et al* (1996) did not assess the effect of shear, but the effect of time on adhesion at one particular shear rate. The presence of pre-adsorbed fibrinogen provided similar adhesion levels as untreated glass whereas kininogen inhibited adhesion of neutrophils with typical values of cellular adhesion were in the range of 1000 counts/mm^2.

The adhesion of bacteria to biomedical materials has also been investigated and has been responsible for many hospital infections, thus is of great relevance in medicine as detailed in Section 1.2.2.1. *Staph.aureus* and *Staph.epidermis* are largely responsible for these infections (Verheyen *et al*, 1993), and consequently are well-studied bacteria. Albumin, Fibrinogen and Kininogen all affect the adhesion of *Staph.aureus* (Nagel *et al*, 1996). However, the work performed by Nagel *et al* (1996) did not analyse the dependency on shear rate, although the work did use a system that is "well characterised" and defined the shear rate across the surface of the collector. The work performed by Nagel *et al* (1996) was continued and developed (Baumgartner and Cooper, 1998) but again the effect of shear was not assessed, as was observed with the work of (Yung *et al*, 1996). The work performed by Nagel *et al* (1996) did show that attachment of bacteria increased linearly with time up to 10 minutes. The adhesion and the detachment kinetics of fibroblasts to glass was covered in work by Goldstein and DiMilla (1997), which applied models predicting fluid mechanics, adhesion strength probability distributions, and detachment kinetics, which showed a Gaussian distribution.

Problems encountered with the inspection method were overcome when studying the adhesion of silica particles (Bowen and Epstein, 1979), using radioactive tracers. Results showed that adhesion of a negatively charged colloid to a positive surface was as predicted, but the adhesion of a negatively charged colloid to a negatively charged collector was noticeably higher than expected. The use of radioactive tracers, however, is not practical within this project, and is therefore not used.

The use of latex beads in conjunction with the Radial Flow Chamber is an example of study with an inert colloid (Meinders *et al*, 1995) and showed that both bacterial and particle adhesion are reversible, and can be explained in terms of overall physicochemical surface properties, mediated by reversible, secondary minimum DLVO interaction. The results showed that adhesion does not increase linearly with time and values of $10{,}000mm^{-2}$ were obtained for latex beads. The paper summarizes that the deposition and reversibility of bacterial adhesion can be treated in the same way as for latex beads, and this is discussed in Section 9.5.

7.2 Materials

The following Section details the materials used specifically in conjunction with the assessment of adhesion performed using the RFC.

7.2.1 The Radial Flow Chamber

The Chamber used initially in this project was originally used to assess biofilm formation (Fowler and Mackay, 1980). The Chamber consisted of a central inlet pipe of an internal diameter of 5mm. The manifold outside radius of the Chamber was 85mm, and inside radius of the collector disc was 50mm. The collector disc itself was 60mm radius. Three spacers separated the parallel plates by 1mm at 120° intervals. The outlet pipes were also equally spaced around the circumference of the Chamber. Each outlet pipe had an external diameter of 10mm. The initial design is shown below in Figure 7.1.

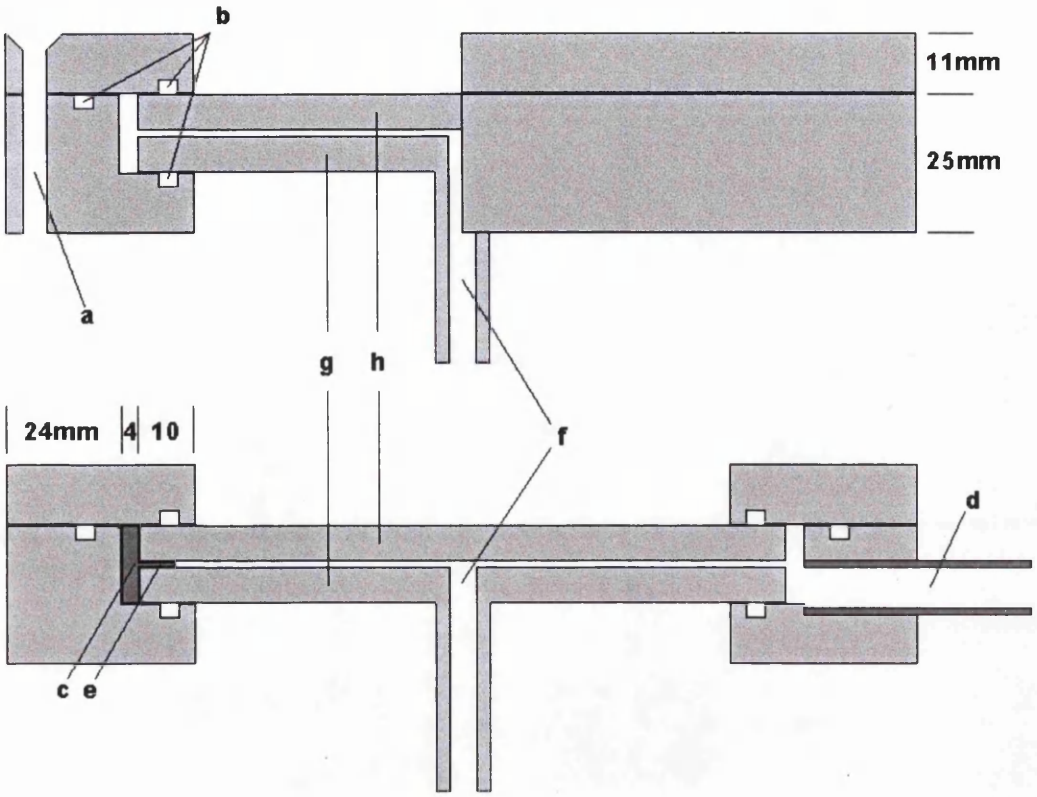

Figure 7.1: The original design of the Radial Flow Chamber used to conduct experiments on biofilm formation (Fowler and Mackay, 1980). a) hole for ¼ inch clamp bolt, b) grooves for O-rings, c) disc centring pin, d) outlet pipe (10mm o.d.), e) disc spacer (1mm), f) inlet pipe (5mm i.d.), g) back disc (60mm radius), h) front disc (60mm radius).

7.2.2 Pump

The pump used in conjunction with the RFC was supplied by Eheim (Model 1048). The maximum flow rate generated by the pump was 10 ℓ/min. The flow rate was adjusted to 1.4 ℓ/min by using a clamp to restrict the flow, and was kept constant throughout experiments. The pump was linked to the Chamber by silicone tubing, as shown in Figure 7.2. The suspension was pumped through the Chamber, and returned to the pump through three outlet pipes via a reservoir. The reservoir consisted of a 250mℓ Pyrex flask with a side arm at its base. The reservoir performed two functions. Firstly it enabled easy handling of the suspension within the apparatus. The second function was that the volume of the suspension ensured that concentration would not vary should large level of adhesion occur.

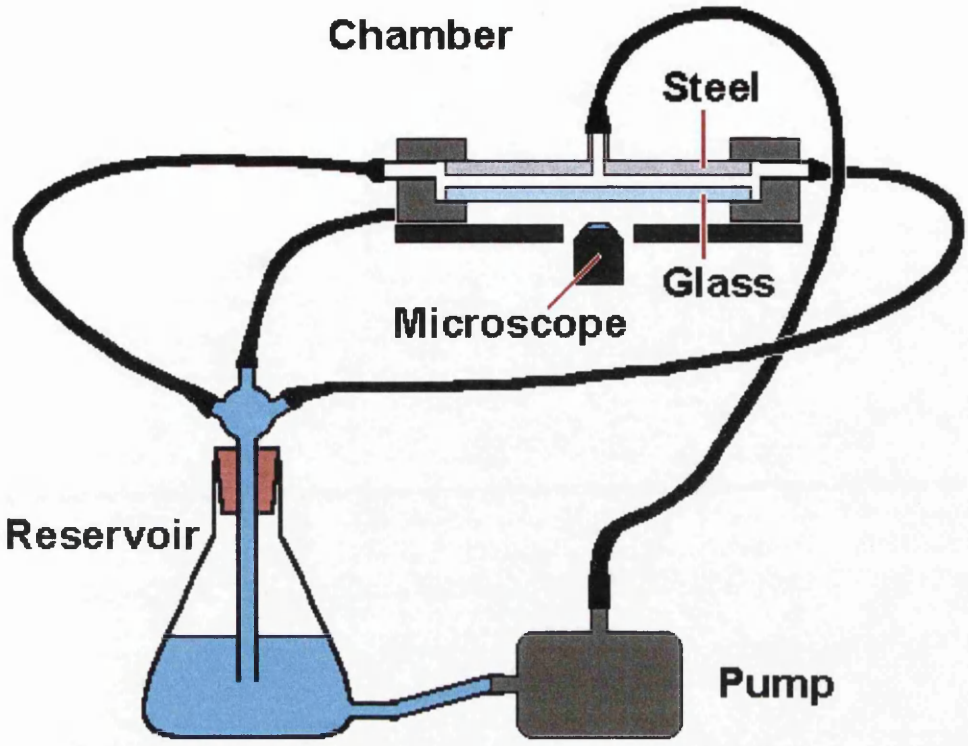

Figure 7.2: A diagrammatical representation of the Radial Flow Chamber and supporting apparatus. The figure shows the Chamber, reservoir, and the pump used to circulate the suspension.

7.2.3 Inverted Microscope

The use of the RFC allowed inspection of the surface area whilst shear was constantly applied. To allow the inspection, an inverted microscope was required with epi-illuminescence, as shown in Figure 7.2. The apparatus was unable to be placed on a standard microscope, due to obstruction of the inlet pipe. Unfortunately, the inverted microscope was not attached to an image analysis package as used with the Spinning Disc, resulting in extremely laborious manual counting. Image analysis has been shown to provide accurate results when enumerating bacterial adhesion in a flow Chamber, eliminating in focus flowing bacteria from the analysis (Meinders *et al*, 1992).

7.2.4 Collector Surfaces

Both glass and stainless steel were used in conjunction with the RFC. This allowed the comparison of results generated from the Spinning Disc and Column. The benefit of the RFC was that it enabled the adhesion of glass and steel to be assessed simultaneously.

7.2.4.1 Glass

The glass discs used in the original design were 8mm thick. This proved to be far too thick for microscopic inspection of both surfaces, due to the limited focal length of the microscopes' objectives. The apparatus therefore required adjustment to minimise the thickness of glass. The result was that glass with a thickness of 2mm was used (Tofts Glass, Swansea). The glass was supplied annealed, and was prepared to ensure that the surface roughness was equivalent to that obtained with the stainless steel. The annealed glass was polished using only the 6-micron, and 1-micron pastes. Initially the glass was subjected to the rougher abrasives, but this proved to irreparably damage the surface, due to the softness of the glass.

7.2.4.2 Stainless Steel

The stainless steel surface was as provided by Swansea Precision Engineering. No alterations were required, except polishing with abrasives, as described in Section 2.3.3.

7.2.5 Colloidal Suspensions

Suspensions for all experiments were constant with respect to concentration (2.7 x 10^7/mℓ). Particles were prepared as detailed in Section 2.3.1 and 2.3.2. The solutions were prepared as detailed in Section 2.2.3.

7.3 Development of Methods

The development of the RFC encountered fewer problems in comparison with the Spinning Disc. The Flow rate though the RFC, was calculated using Equation 7.1 to provide the same shear gradient when using the Spinning Disc. The experiment duration was also kept constant at thirty minutes. This allowed the duration of preliminary experiments to be kept to a minimum, but more importantly, allowed direct comparison between the Spinning Disc and the RFC, without complicated analysis of data. There were some parameters that were not maintained between the techniques, for example, the volume of sample used in the RFC was substantially larger than the volume incorporated in the Spinning Disc, due to the dimensions of the apparatus.

7.3.1 Visualisation Problems and Developments

The distance between the steel collector surface and the objective had to be minimised, which required adaptation of the RFC design shown in Figure 7.1, as the glass was too thick to focus on either the glass or the steel, and therefore was reduced from 8mm to 2mm. This also required the lower manifold of the RFC to be reduced, to house the thinner glass. A rubber spacer (1mm) was also placed between the glass and the upper manifold of the RFC, to ensure no leakage occurred.

The reduction of the thickness of the glass was not sufficient to allow visualisation of the surfaces, and it was decided to reduce the upper manifold of the RFC, from 11mm to 2mm. This had no effect on the thickness of the glass, but allowed the distance between the objective and the stainless steel to be minimised.

The two alterations reduced the distance between the objective and the stainless steel collector surface by 14mm. This allowed visualisation of both the glass and steel collector surfaces. The final design of the RFC is shown in Figure 7.3.

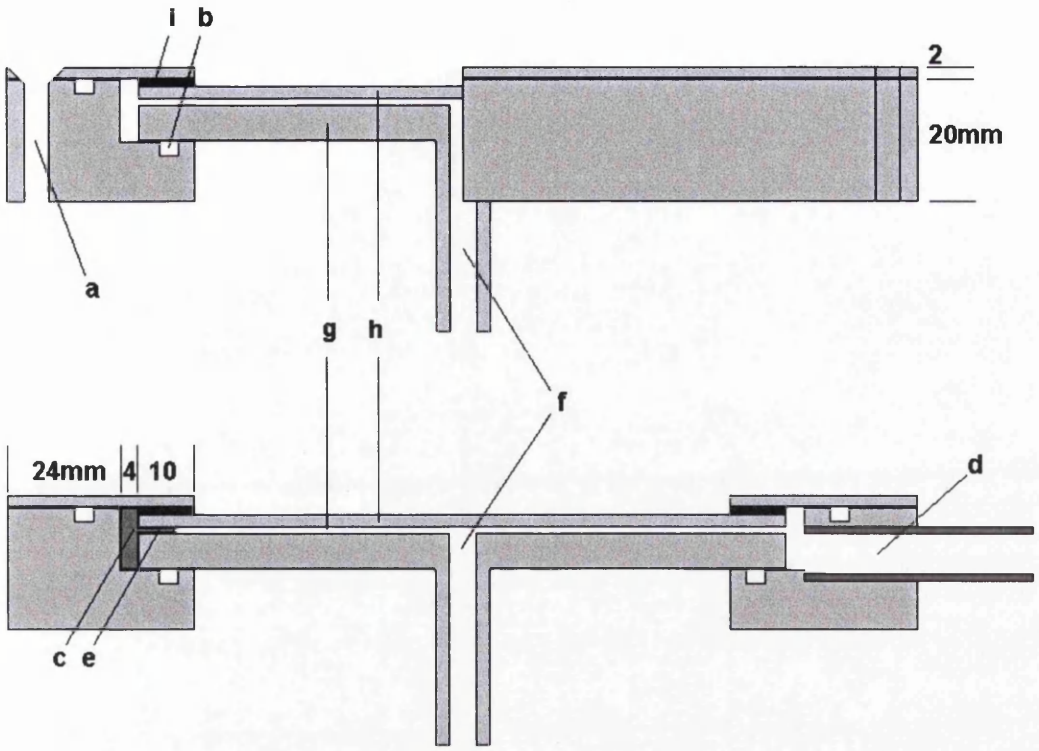

Figure 7.3: The adapted design of the Radial Flow Chamber. a) hole for ¼ inch clamp bolt, b) grooves for O-rings, c) disc centring pin, d) outlet pipe (10mm o.d.), e) disc spacer (1mm), .f) inlet pipe (5mm i.d.), g) back (steel) disc (60mm radius), h) front (glass) disc (60mm radius), i) silicone spacer (1mm).

7.3.2 Rinsing Developments

There was no problem with the residual liquid on the collector surface as observed with the Spinning Disc, as the surface did not require removal from the particle suspension. Rinsing with buffer solution was not performed, as changing the particle suspension to buffer solution, would require stopping and starting the pump, and potentially disturbing the collector surface and any adhered particles. Enumeration was performed whilst the experiment was in progress. The enumeration technique stipulated that no changes in adhesion should occur after 30 minutes of the experiment, which was investigated in Section 7.4.3.

7.3.3 Counting Method

The count was taken over an area of 570 x 430 microns, an area of 0.245mm^2. Counts were taken at 1, 1.5, 2, 2.5, 3, 3.2, 3.4, 3.6, 3.8, 4, 4.2, 4.4, and 4.6 cm from the centre of the disc. Control experiments were carried out using buffer solution to ensure that no artefacts due to the surface preparation could be mistakenly counted as deposited particles. This was important, as the magnification provided by the inverted microscope to focus on both the glass and the stainless steel collector surfaces was lower compared with the magnification provided using the micromanipulator in conjunction with the Spinning Disc, as detailed in Section 6.3.5.

7.3.4 A Summary of the Developments made using the RFC

The visualisation of the surfaces and the subsequent adaptation of the apparatus was the largest problem using the RFC. The arrangement of the apparatus *in situ* is shown below in Figure 7.4. Characterisation of the system was required before the main data gathering exercise, and is detailed in Section 7.4.

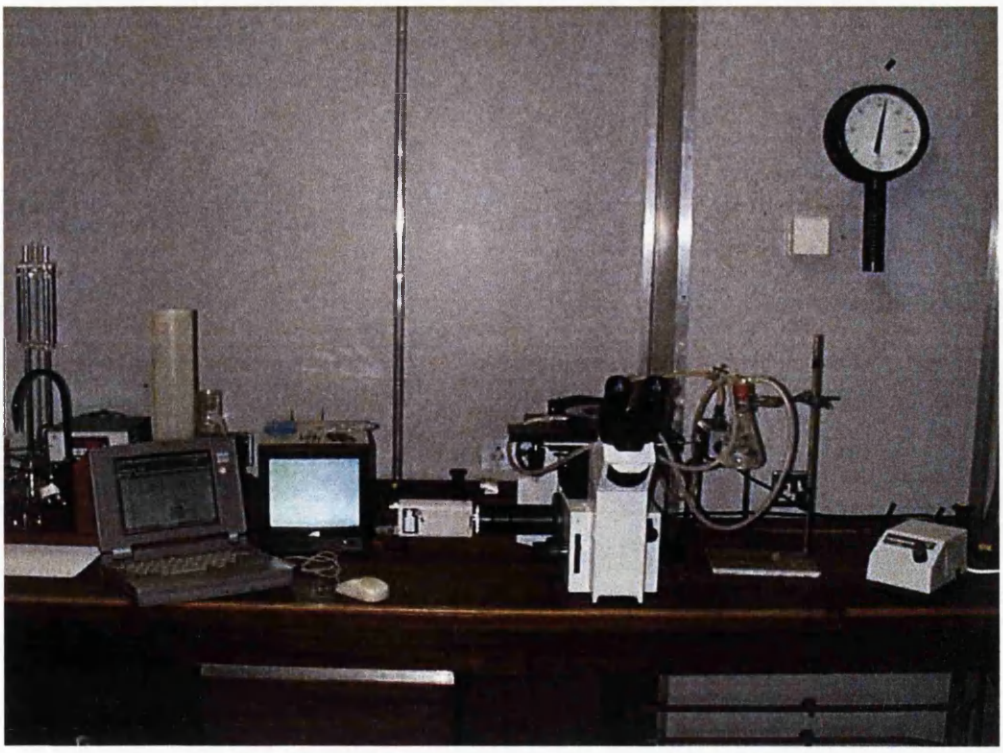

Figure 7.4: The RFC mounted on the Inverted Microscope

7.3.5 The Final Experimental Protocol

The duration of each experiment was 30 minutes, and the temperature was maintained at 22 +/- 1°C in a constant temperature room. Six counts were performed per disc separated by 60°. Glass and stainless steel collector surfaces were counted in the same experiment, as described in Section 7.3.3. Collector surfaces, and colloidal suspensions were prepared as stated in Sections 7.2.4 and 7.2.5 respectively. Each experiment was repeated six times, providing 36 values at each radial distance for each set of experimental conditions.

7.4 System Characterisation

As discussed in Section 7.1.2, there have been several uses of this method to apply shear force to a surface. However, the system has several parameters that can be altered, which due to time limitations were not investigated using the RFC.

7.4.1 The Effect of Concentration on Adhesion

Experiments assessing the effect of suspension concentration were not conducted. The suspension concentration was kept consistent with the Spinning Disc method, allowing direct comparison. This was determined in Section 6.4.1, and the concentration used in all experiments was 2.7×10^7 particles/mℓ.

7.4.2 The Effect of Flow Rate on Adhesion

The flow rate was adjusted to provide the maximum same shear force gradient generated using the Spinning Disc technique ($2Nm^{-2}$) using Equation 7.1. The resultant flow rate was 1.4 ℓ/min. The flow rate was kept constant throughout all experiments, and regularly monitored. Consequently, experiments were not performed to assess the effect of flow rate.

7.4.3 The Effect of Time on Adhesion

The incubation time of the experiment was initially planned to be 30 minutes, to maintain consistency with the Spinning Disc technique. However, as the collector surface was inspected whilst still in progress, experiments were performed to ascertain that adhesion levels of aminated and carboxylated beads, and the spores of *B.mycoides* and *B.subtilis* were constant after 30 minutes, the incubation time used in conjunction with the Spinning Disc technique.

Protocol:

Experiments were conducted with the particles suspended in 25mM Na_2PO_4, adjusted to pH 5.5 using NaOH (1M). The adhesion of aminated and carboxylated beads, and the spores of *B.mycoides* and *B.subtilis* to glass and stainless steel were assessed with respect to time. Each experiment lasted 2 hours, with counts taken at time intervals of 1, 2, 5, 10, 15, 30, 60, and 120 minutes. The counts were taken at 2 different radial positions on the collector, 20 and 40 mm from the centre of the disc. Each disc was counted once, due to time restrictions in each experiment. The experiment was repeated 9 times for both glass and stainless steel.

Results:

The following are the results obtained from the investigation of the effect of time on adhesion.

7.4.3.1 Particle Adhesion to Glass with Respect to Time

The effect of time on adhesion of aminated and carboxylated latex beads, and the spores of *B.mycoides* and *B.subtilis* to glass was recorded at 20mm and 40mm from the centre of the disc. The results are presented in Figure 7.5, and Appendix E.1 respectively.

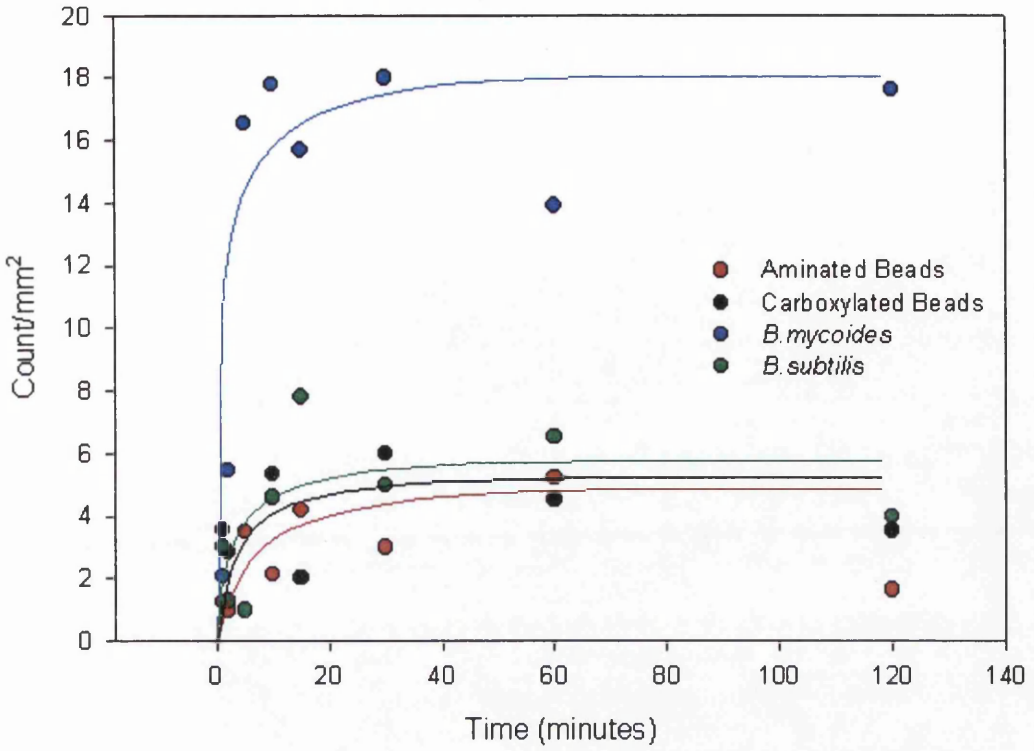

Figure 7.5: The effect of time on adhesion to glass of aminated and carboxylated beads, and *B.mycoides* and *B.subtilis* spores at a radial distance of 20mm (1 Nm^{-2}). Experiments were carried out at pH 5.5 over a time period ranging from t = 0 to t = 120 minutes. Temperature was maintained at 22 +/- 1°C. Error bars are omitted for the sake of clarity.

Adhesion to glass at a radial position of 20mm is represented in Figure 7.5, and showed that although there was much variation initially, no great change in adhesion occurred after 10 minutes. Levels of adhesion were similar ($4mm^{-2}$) in the case of both latex beads, and *B.subtilis* spores. *B.mycoides* spores showed much higher ($17mm^{-2}$) adhesion. However, levels of adhesion were very low compared to those observed with steel, as seen in Figure 7.6.

The adhesion to glass at 40mm follows the same trends as those observed at 20mm, although there was less variation from a linear relationship, shown in Appendix E.1. The effect of time on adhesion of the particles to glass did not alter with decreased shear stress.

7.4.3.2 Particle Adhesion to Stainless Steel with Respect to Time

The effect of time on adhesion of aminated and carboxylated latex beads, and *B.mycoides* and *B.subtilis* spores to stainless steel was recorded at 20mm and 40mm and are presented in Figure 7.6, and Appendix E.1 respectively.

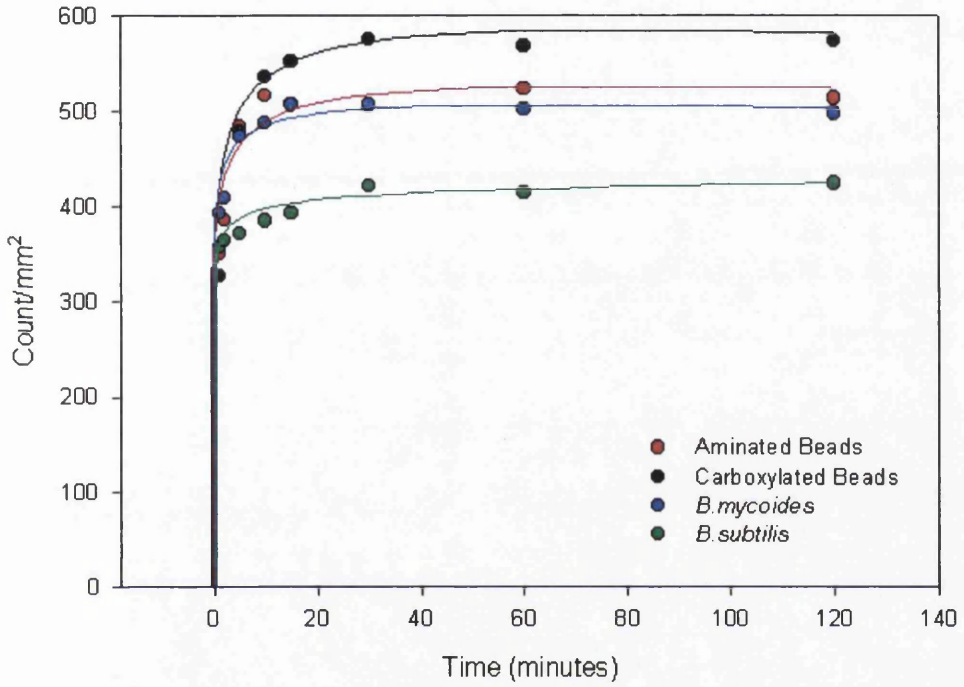

Figure 7.6: The effect of time on adhesion to stainless steel of aminated and carboxylated beads, and *B.mycoides* and *B.subtilis* spores at a radial distance of 20mm (1 Nm^{-2}). Experiments were carried out at pH 5.5 over a time period ranging from t = 0 to t = 120 minutes. Temperature was maintained at 22 +/- 1°C. Error bars are omitted for the sake of clarity.

Particle adhesion to stainless steel showed similar trends compared with glass, irrespective of particle type, and adhesion changed insignificantly after 10 minutes. There was a noticeable difference from the adhesion to glass, which was decreased by a factor of 100 compared with stainless steel. The carboxylated latex beads showed the most adhesion (575mm^{-2}) followed by aminated beads and *B.mycoides* (approximately 500mm^{-2}), and finally *B.subtilis* (420mm^{-2}). The particle adhesion to stainless steel at 40mm was higher than that observed at 20mm, but the same trends were observed at both 20 and 40mm, and the results for the values at 40mm are shown in Appendix E.1.

7.4.3.3 Particle Adhesion to with Respect to Time: Summary

The results obtained using glass as the collector surface were very low relative to those obtained with stainless steel. There was very little difference in the dependence on time between the two different radial positions.

The increase in adhesion to stainless steel between 20mm and 40mm was great, as was expected as the applied shear force was less. The experiment accomplished its task, to demonstrate that thirty minutes was sufficient time for adhesive interactions to occur and reach equilibrium.

7.5 The Effect of pH on Adhesion

The following Section describes the effect of pH on the adhesion of the aminated and carboxylated latex beads, and the spores of *B.mycoides* and *B.subtilis* with respect to pH and radial distance. The results in this Chapter are given in 3-dimensional plots as seen Chapter 6, and the adhesion is analysed for each particle to both glass and stainless steel. The collective results for all four particles are given in 3-dimensional form in Appendix E, as are the results presented in 2-dimensional plots.

The results from the use of the RFC are given with respect to radial distance rather than shear force. Adhesion with respect to applied shear force is considered in Chapter 8, where the results generated from the adhesion assays using the RFC are compared with the results obtained using the Spinning Disc to assess adhesion.

The preparation of the collector surfaces, colloids, and solutions, and details of the experimental protocol are given in Section 7.3.5.

7.5.1 The Effect of pH on the Adhesion of Aminated Beads

The adhesion of aminated latex beads to both glass and stainless steel is shown in Figure 7.7. The results are also presented in equivalent 2-dimensional plots in Appendix E.3.

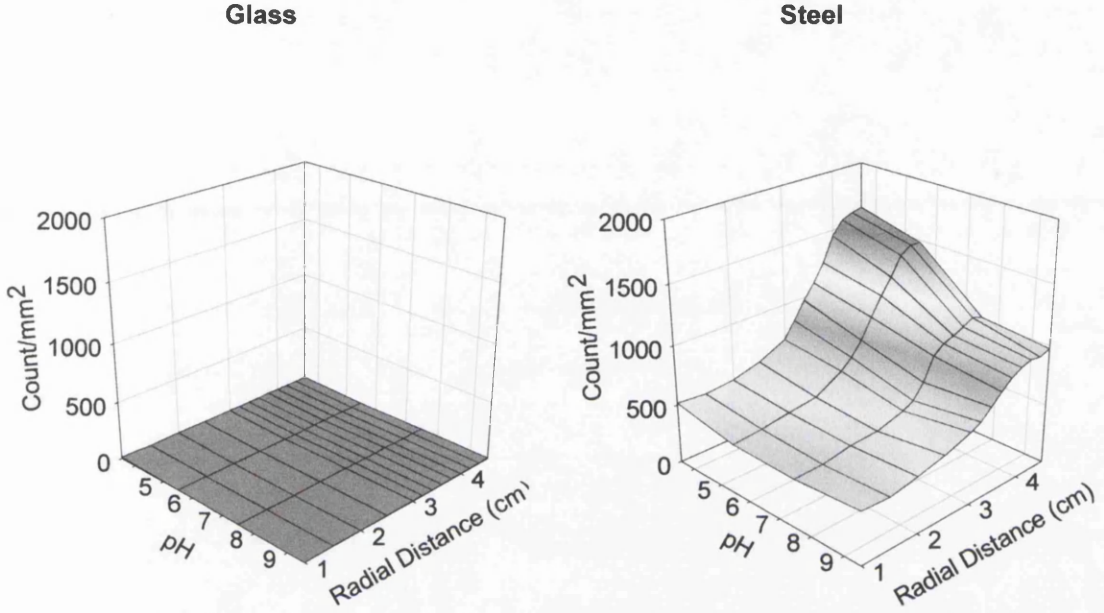

Figure 7.7: The adhesion of aminated latex beads to glass and stainless steel with respect to radial distance over a range of pH. Temperature was maintained at 22 +/- 1°C. Error bars were omitted for the sake of clarity. Values for error can be seen in Appendix E.3.

The results for the attachment of aminated beads to glass are significantly lower than the values obtained for the attachment of the beads to the stainless steel collector surface, and do not vary with radial distance. The values of attachment reached no more than $10mm^{-2}$ for glass, whereas the values for stainless steel varied from 400 to $1700mm^{-2}$, and increased as radial distance increased. The low values of attachment to glass were observed with all four particles using the RFC, and this effect is discussed in Chapter 8.

The attachment of the beads to stainless steel showed a similar pattern to the results obtained using the Spinning Disc as shown in Figure 6.8. The greatest value of adhesion was observed at pH 3.5, where the collector surface was most hydrophobic, as shown in Table 4.1. Adhesion values decreased as pH increased, which reflected the properties of both the bead and the collector surface. At pH 3.5,

the bead was highly hydrophobic, as shown in Table 3.3, and possessed relatively small surface charge, as shown in Table 3.1. This resulted in an interaction that was predominantly hydrophobic between the steel collector surface and the aminated beads. The largest dependency of adhesion on radial distance was at pH 3.5, as was observed with the Spinning Disc technique, supporting the theory that the hydrophobic interaction was highly susceptible to hydrodynamic shear. As pH increased, the dependency on radial distance became smaller. The adhesion of the beads to the steel collector surface at pH 5.5 was similar to that observed with pH 3.5, which was in contrast to the results obtained using the Spinning Disc and the Packed Column, as shown in Figures 6.8 and 5.13. This observation reflected the subtle change in contact angle of the stainless steel, as shown in Figure 4.3, and may suggest that the properties of the collector surface govern the interaction between the collector and the aminated beads, rather than the properties of the aminated beads.

The minimum level of adhesion remained constant between 400 and 500mm^{-2}, at which point adhesion appeared to be independent of both pH and radial distance. This may well be a function of the flow through the Chamber, and is discussed in Chapter 9.

The increase in adhesion at pH 9.5 observed using the Spinning Disc technique (attributed to the increase in the beads' hydrophobicity) was not observed using the RFC to assess adhesion. As suggested, the use of the RFC to assess adhesion appeared to be governed by the collector's characteristics, rather than the characteristics of the aminated bead, and therefore an increase in adhesion at pH 9.5 was not expected. The change in adhesion relative to the slight change in collector surface hydrophobicity can explain the minimal adhesion to glass, which possesses a much smaller contact angle compared with stainless steel, as shown in Table 4.1.

The change in adhesion where r = 4.4cm between pH 5.5 and 7.5 was 1500 to 1000mm^{-2}, and corresponded with a change in contact angle of from 76 to 67°, a reduction of 9°. The stainless steel contact angle at pH 5.5 is 76°, whereas the contact angle of glass at pH 5.5 is 28°. If the drop in contact angle of stainless steel of 9° was responsible for the drop of 500mm^{-2} in adhesion, then the decrease from 76° to 28°, from stainless steel to glass, would result in negligible adhesion, as was observed in Figure 7.7.

The RFC appeared to be sensitive to the change in collector hydrophobicity, whereas the Spinning Disc technique was more sensitive to the subject particles' characteristics. This theory will be considered when discussing the results of the adhesion of carboxylated beads, and the spores of *B.mycoides* and *B.subtilis* in Sections 7.5.2, 7.5.3, and 7.5.4 below.

7.5.2 The Effect of pH on the Adhesion of Carboxylated Beads

The adhesion of carboxylated latex beads to both glass and stainless steel is shown in Figure 7.8. The results are also presented in equivalent 2-dimensional plots in Appendix E.3.

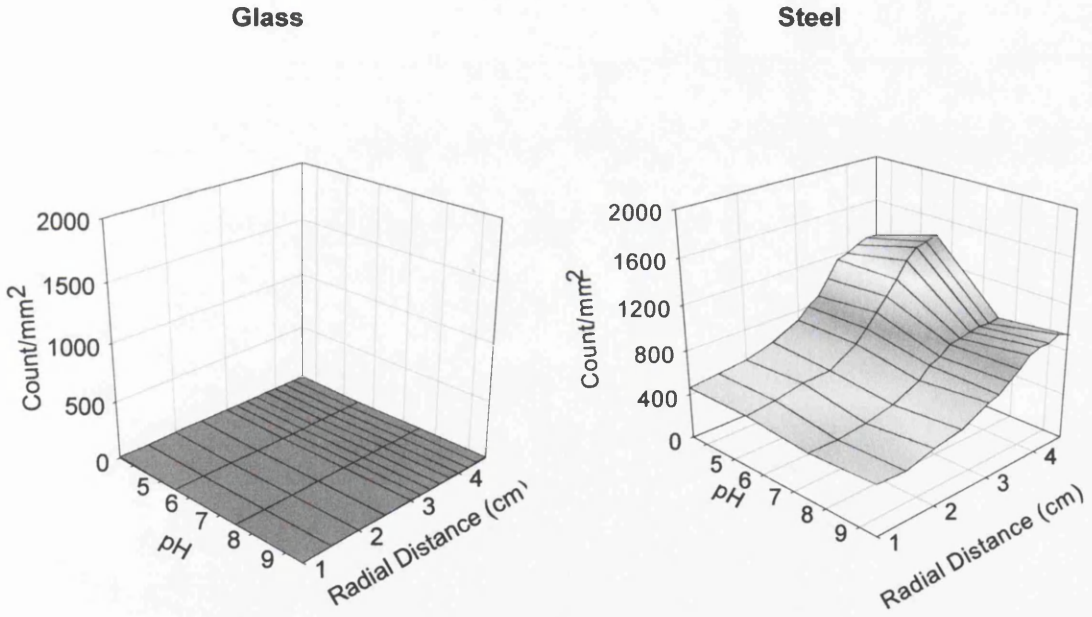

Figure 7.8: The adhesion of carboxylated latex beads to glass and stainless steel with respect to radial distance over a range of pH. Temperature was maintained at 22 +/- 1°C. Error bars were omitted for the sake of clarity. Values for error can be seen in Appendix E.3.

The adhesion of carboxylated beads to glass showed negligible adhesion when compared with the adhesion of the carboxylated beads to stainless steel. This was observed with the aminated beads, attributed to the difference in hydrophobicity of the glass and stainless steel collector surfaces. The attachment values of the carboxylated beads to glass varied between 0 and $10mm^{-2}$, and showed no

dependency on radial distance. The adhesion pattern of the carboxylated beads to stainless steel was very similar to those observed with aminated beads to stainless steel, with attachment levels ranging from 400 to 1700mm^{-2}, and increased as radial distance increased. This was reflected by the similar levels of percentage recovery of the aminated and carboxylated beads from stainless steel using the Packed Column, and also reflects the similarity in hydrophobicity of both beads, as seen in Table 3.3. The attachment levels were dependent on pH, and reflected by the contact angle of steel rather than the characteristics of the carboxylated beads. This substantiates the theory that the RFC technique was more sensitive to the collector surface properties, as suggested in Section 7.5.1. The difference in surface charge and hydrophobicity of the aminated and carboxylated latex beads, as shown in Tables 3.1 and 3.3 had little or no effect on the adhesion of the aminated and carboxylated beads.

7.5.3 The Effect of pH on the Adhesion of B.mycoides Spores

The adhesion of the spores of *B.mycoides* to both glass and stainless steel is shown in Figure 7.9. The results are also presented in equivalent 2-dimensional plots in Appendix E.3.

As observed with the adhesion of both aminated and carboxylated beads, there was minimal adhesion of the *B.mycoides* spores to glass compared with the spores' adhesion to stainless steel. The attachment levels of the spores to the glass collector surface were higher (up to 40mm^{-2}) than the aminated and carboxylated beads, as can be seen in Appendix E.3. The attachment levels to glass were unaffected by radial distance, and were greatest at pH 3.5, and decreased as pH increased. The attachment levels at pH 3.5 were distinctively separated from the attachment levels observed for the aminated and carboxylated beads, and the spores of *B.subtilis.* This observation reflected the increase in contact angle of glass at pH 3.5, to approximately 42°, compared with angles of 28 and 27° for pH 5.5 and 7.5. The levels of adhesion of the spore were similar at pH 5.5 and 7.5, and dropped at pH 9.5, reflecting the sensitivity to contact angle of the collector surface. These levels were, however, still very low compared with the values observed with steel.

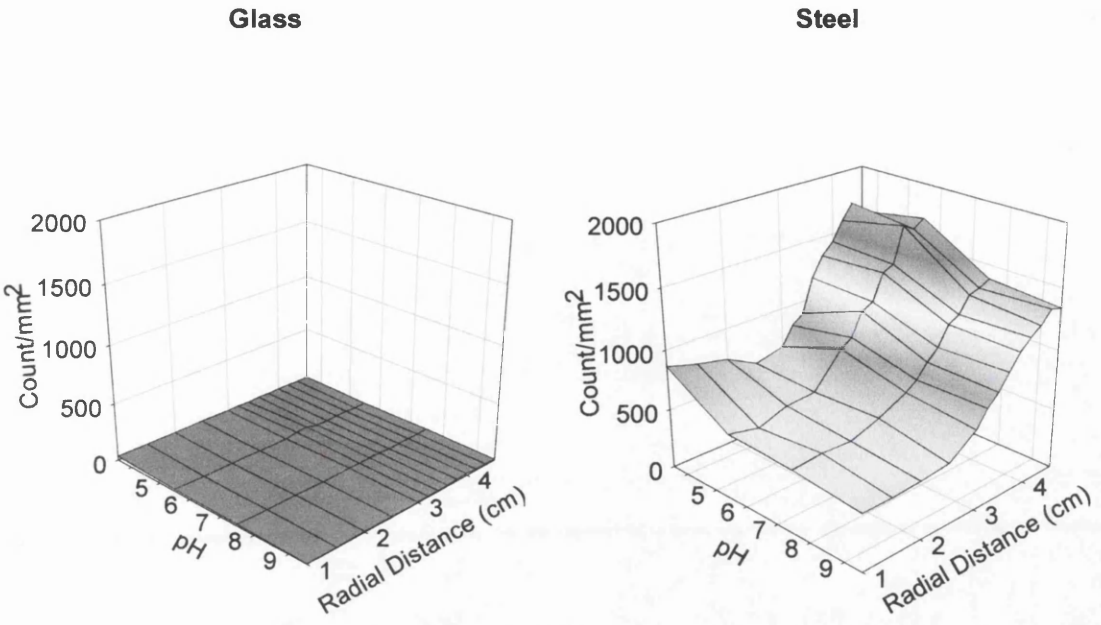

Figure 7.9: The adhesion of *B.mycoides* spores to glass and stainless steel with respect to radial distance over a range of pH. Temperature was maintained at 22 +/- 1°C. Error bars were omitted for the sake of clarity. Values for error can be seen in Appendix E.3.

The adhesion of the spores to stainless steel showed a similar trend to both the aminated and the carboxylated beads, although values were higher, ranging from 500 up to 1800mm^{-2}. Adhesion increased as radial distance increased, corresponding to the decrease in shear. This was not true in the case of the results at pH 3.5, which showed a decrease initially close to the inlet pipe, and then increase significantly. Visual observations at this point suggested that the areas enumerated showed very patchy adhesion, with increased contact between spores, suggesting that co-aggregation occurred, and also an effect from the heterogeneity of the collector surface.

The adhesion of the spores to stainless steel showed dependence on the hydrophobicity of the collector surface as was observed using the latex beads. Once again, there was similarity of adhesion levels between pH 3.5 and 5.5, and pH 7.5 and 9.5, reflecting the contact angle measurements of the stainless steel as shown in Table 4.1.

7.5.4 The Effect of pH on the Adhesion of B.subtilis Spores

The adhesion of the spores of *B.subtilis* to both glass and stainless steel is shown in Figure 7.10. The results are also presented in equivalent 2-dimensional plots in Appendix E.3.

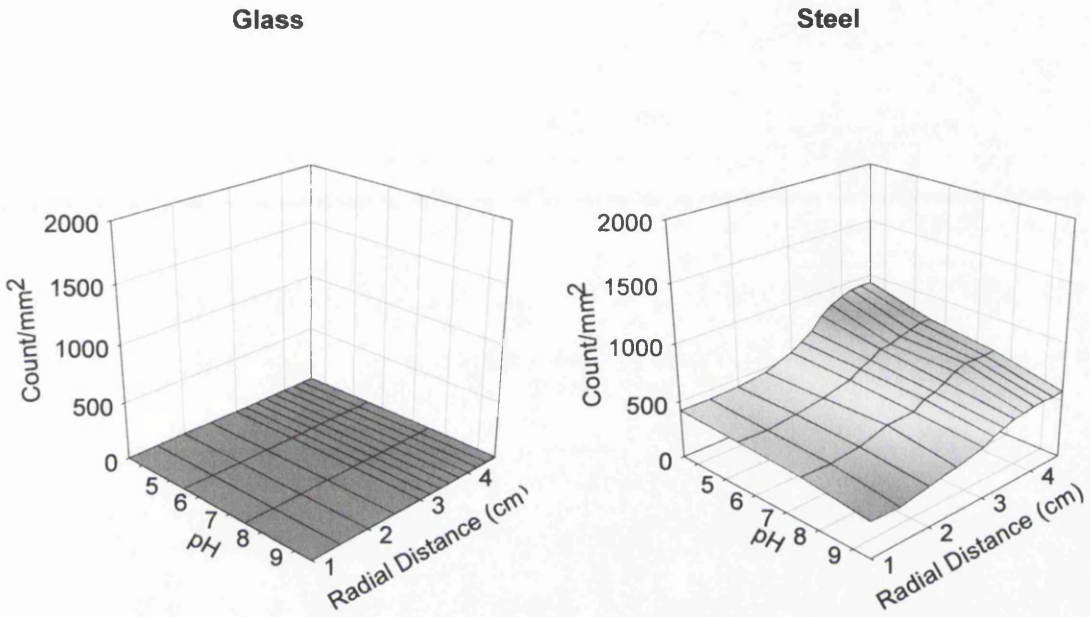

Figure 7.10: The adhesion of *B.subtilis* spores to glass and stainless steel with respect to radial distance over a range of pH. Temperature was maintained at 22 +/- 1°C. Error bars were omitted for the sake of clarity. Values for error can be seen in Appendix E.3.

The adhesion of *B.subtilis* spores to glass was again negligible compared with those obtained using stainless steel as the collector surface, and showed levels between 0 and 10mm^{-2}. These values were noticeably lower than the levels observed when assessing the adhesion of *B.mycoides* to glass, and were approximately the same as those levels observed for the latex beads.

The adhesion of the *B.subtilis* spores to stainless steel exhibited the lowest levels of adhesion of the four particles assessed, ranging from 300 to 900mm^{-2}, as can be seen in Appendix E.3. This correlates with the results obtained using the Packed Column, shown in Figure 5.13.

The attachment of the spores to stainless steel was again governed by the hydrophobicity of the stainless steel surface, rather than the characteristics of the *B.subtilis* spore. In the previous experiments with aminated and carboxylated latex

beads and the spores of *B.mycoides*, there was little change in hydrophobicity of the particle with respect to pH. The surface charge of the particles did change significantly between pH 3.5 and 5.5 in all three cases. This change in surface charge was not reflected in the adhesion of the particles to the stainless steel collector. *B.subtilis* was the only particle used, that changed its relative hydrophobicity significantly with pH, as shown in Figure 3.3. The adhesion of the *B.subtilis* spore to stainless steel showed no resulting effect of the change in hydrophobicity of the spore.

This provided conclusive proof that assessment of adhesion using the RFC was governed by the hydrophobic characteristics of the collector surface, rather than particle charge, as shown in the case of the latex beads and *B.mycoides* or particle hydrophobicity, as shown in the case of *B.subtilis*.

7.6 Summary

The following Section discusses the developments made using the RFC, the results from the silanisation experiments, and the results from the main assessment of adhesion.

7.6.1 Visualisation and Counting Developments

The visualisation and enumeration of adhered particles to the collector surface using the RFC was decidedly easier than the use of the Spinning Disc to assess adhesion. There was no requirement to remove the collector surface of the RFC from the particle suspension, and consequently there was no problem dealing with residual suspension as with the use of the Spinning Disc. The enumeration of the surface in question took place whilst the experiment was still in progress, and was theoretically subject to variation with respect to time. Experiments were enumerated after 30 minutes, at which point variation in adhesion levels with respect to time was assumed to be insignificant, as detailed in Section 7.4.3.

The area encompassed by the objective of the microscope, as detailed in Section 7.3.3, was larger than that of the Spinning Disc as detailed in Section 6.3.5, which resulted in larger numbers of particles per screen. This resulted in enumeration becoming a more tedious process, and susceptible to human error due to the larger numbers, but less susceptible to statistical variation due to the larger areas that were enumerated, compared with the Spinning Disc.

The development of the RFC from a method of assessing biofilm formation to a method for assessing initial particulate adhesion was successful, although adaptation of the apparatus was required, as detailed in Section 7.3.1. The apparatus has much potential as a method for assessing particulate adhesion as discussed in Chapter 9.

7.6.2 Data Presentation

As with the presentation of the data in Chapter 6, the results obtained using the RFC was presented in 3-dimensional graphs, which allowed a more comprehensive view of adhesion with respect to pH and radial distance. The data was also represented in 2-dimensional plots in Appendix E, which allowed a quantitative appreciation of the levels of adhesion.

The results generated using the Radial Flow Chamber are presented as a function of shear force in Chapter 8, and are directly compared with the equivalent results obtained with the Spinning Disc technique used to assess particulate adhesion. The comparisons made in Chapter 8 are a more quantitative analysis than the comparisons made in this Chapter, and results are presented in 2-dimensional plots.

7.6.3 Discussion of Data

The main observation to be made using the RFC was the difference in attachment to glass compared to stainless steel, which was not observed using the Spinning Disc. The results generated using the RFC to assess the adhesion of the aminated and carboxylated latex beads and the spores of *B.mycoides* and *B.subtilis* reflected the

characteristics of the collector surface more than the characteristics of the particle. Consequently, the low hydrophobicity of the glass collector surface resulted in negligible values of adhesion compared with the values obtained for the stainless steel collector surface. Levels of adhesion to glass were sufficiently high to notice the effect of pH only in the case of *B.mycoides* spores, which were distinctively higher than the latex beads and *B.subtilis* spores at pH 3.5, at which point the *B.mycoides* spore was positively charged, as shown in Table 3.1.

The adhesion to stainless steel was dependent on radial distance, and attachment increased as radial distance increased, which was as expected when considering the decrease in applied shear force to the collector surface. The adhesion to stainless steel did not show the same magnitude in adhesion values as the Spinning Disc, and this was attributed to the fact that enumeration of adhesion using the RFC was not performed at a point where theoretically no shear force was applied to the surface (i.e. at the centre of the Spinning Disc).

The spores of *B.mycoides* demonstrated the highest levels of adhesion, followed by the aminated and carboxylated latex beads, which were very similar in values, and finally, the spores of *B.subtilis* possessed the lowest values of adhesion. The difference in the adhesion between the four particles was not as great with the RFC when comparing with the results of the Spinning Disc. This was attributed to the smaller contribution that particle characteristics had on the adhesive interaction compared with the collector surfaces' contribution when considering the RFC. Adhesion was affected by the solution pH as was observed with the Spinning Disc, where the lowest pH provided the highest attachment levels, a reflection of the increased hydrophobicity of the stainless steel collector surface.

As stated, the RFC provided a different method of assessing adhesion compared with the Spinning Disc, and consequently differing results. Chapter 8 combines the results of both methods with respect to shear force where possible, and attempts to analyse the difference in the methods, even though both methods theoretically determine adhesion by applying shear force to the adhered particles on the collector surface in question. Chapter 9 considers the reasons for differences in adhesion between the two systems.

CHAPTER EIGHT

Discussion and Analysis of Comparative Data

8.1 Introduction

This Chapter compares and analyses the combined results obtained using the Spinning Disc and Radial Flow Chamber methods to assess adhesion of aminated and carboxylated latex beads, and the spores of *B.mycoides* and *B.subtilis* to both glass and stainless steel. Results in Chapters 6 and 7 are presented as a function of radial distance against particle count. Using Equations 6.1 and 7.1 applied to the Spinning Disc and the RFC respectively, this Chapter will present the adhesion profiles as a function of shear force (τ, Nm^{-2}), and allow direct comparison of the profiles with respect to shear force.

The low levels of adhesion obtained from the attachment of the particles to glass using the RFC, did not allow comparison with the results obtained from the Spinning Disc, and are consequently not considered in this Chapter. The reasons for this are discussed later in Chapter 9.

8.2 Analysis of Results

The Sections below detail the conversion of radial distance into the shear force applied to the collector surface, discuss the considerations that are made concerning the shapes of the adhesion profiles generated by the Spinning Disc and the RFC, and finally present the data obtained from the Spinning Disc and the RFC directly in 2-dimensional plots.

8.2.1 The Relationship between Radial Distance and Shear Force

The radial distance of both the Spinning Disc and RFC can be related to the shear stress applied to the collector surface.

The shear force generated by the Spinning Disc is defined by Equation 8.1, and represented graphically in Figure 8.1.

$$\tau = 0.800\, r\, (\rho \mu \omega^3)^{1/2} \qquad 8.1$$

where τ is shear stress (Nm^{-2}), r is radial distance (m), ρ is fluid density ($10^3 kg\ m^{-3}$), μ is fluid viscosity ($8.94 \times 10^{-4}\ kgm^{-1}s^{-1}$), and ω is angular velocity (10π radians s^{-1}, the equivalent of 300rpm)

The angular velocity of the Disc was maintained throughout all experiments, thus enabling a linear relationship to be defined between radial distance and applied shear stress from Equation 8.1, where:

$$\tau = 133.2\, r \qquad 8.2$$

The shear stress generated by the Spinning Disc ranged from 0 Nm^{-2} to approximately 2 Nm^{-2}. To enable the comparison of the two systems, the same range of force was applied to both the Spinning Disc and the RFC. The relationship between radial distance and shear stress using the RFC is given by Equation 8.3, and is graphically represented in Figure 8.1.

$$\tau = 3(\mu Q) / \pi h^2 r \qquad 8.3$$

where τ is shear stress (Nm^{-2}), r is radial distance (m), μ is fluid viscosity (8.94 x 10^{-4} $kgm^{-1}s^{-1}$), h is the height of the gap between parallel surfaces (0.001 m), r is the radial position relative to the inlet pipe (m), and Q is the volumetric flow rate (2.3 x 10^{-5} m^3s^{-1}, the equivalent of 1.4 ℓ/min).

The flow rate was constant throughout all experiments, allowing a constant relationship to be defined from Equation 8.3, where:

$$\tau = 0.02 / r \qquad 8.4$$

The inversely proportional relationship between shear stress and radial distance resulted in a steep gradient when converting radial distance into shear, and examples can be seen in Section 8.2.4.

Both assessment methods applied a similar shear force gradient over the collector, when maintaining the angular velocity at 300rpm and the flow rate at 1.4ℓ/min for the Spinning Disc and Radial Flow Chamber respectively, depicted in Figure 8.1. These figures are derived from Equations 8.2 and 8.4 for the Spinning Disc and the RFC respectively.

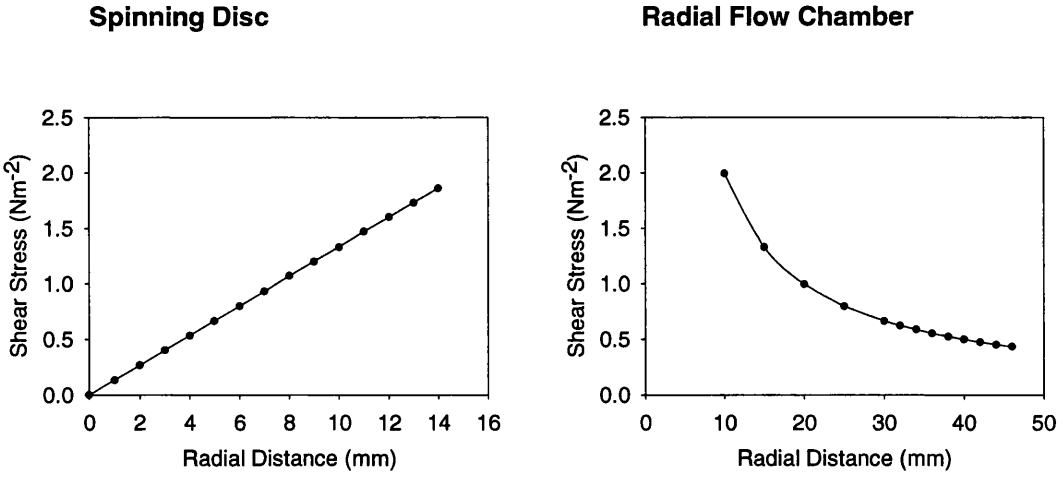

Figure 8.1: The relationship between radial distance and shear stress for the Spinning Disc technique (left) and the Radial Flow Chamber (right). The angular velocity and flow rate were maintained at 300rpm and 1.4ℓ/min, for the Spinning Disc and Radial Flow Chamber respectively.

8.2.2 Methods of Analysing The Attachment Profiles

The attachment curves obtained in Chapters 6 and 7 possessed a variety of shapes, and as a result of this, could not be consistently fitted to simple model equations. This was attributed to the limited range of shear provided using both methods, not allowing the whole relationship between applied shear force and attachment to be observed.

Ideally, a population of particles will attach to the collector surface in a sigmoidal distribution, with respect to shear. This would allow a logistic equation to be fitted to the attachment profile, and consequently a shear value where 50% of the adhered population were contained, as detailed and used by Garcia *et al* (1997).

The attachment profiles generated within this project showed a more comprehensive picture than that depicted by Garcia *et al* (1997). The Spinning Disc and RFC demonstrated differing sensitivities to the particle collector surface characteristics, and consequently, the results differed between the systems. Consequently, fitting a standard logistic equation to the attachment profiles was difficult, as was the determination of statistics referring to any percentage of the adhered population.

There were three reasons for this. Firstly, the results obtained when assessing adhesion to glass using the Radial Flow Chamber were so low (between 0 and

$20mm^{-2}$), that data were not statistically viable, and no obvious trend could be determined for either the latex beads or the spores. Consequently, no comparison could be made between the Spinning Disc and Radial Flow Chamber when considering glass as the collector surface. The reasons for this are discussed in Chapter 9.

Secondly, not all of the attachment profiles that showed sufficient levels of adhesion, provided a sigmoidal fit. There were six different types of adhesion profiles obtained when using the Spinning Disc and Radial Flow Chamber, illustrated in Figure 8.2.

The analysis of results as a function of percentage of adhered particles, can only be performed if the adhesion profile reaches negligible particles/mm^2, or can be extrapolated to produce this figure. These problems of analysing data have been encountered in previous work, but not resolved (Shive *et al*, 1999; Vacheethasanee *et al*, 1998; Goldstein and DiMilla, 1997; and Wang *et al*, 1995, 1993a and 1993b), as these papers generated adhesion profiles of different shapes but did not provide a distinct sigmoidal distribution.

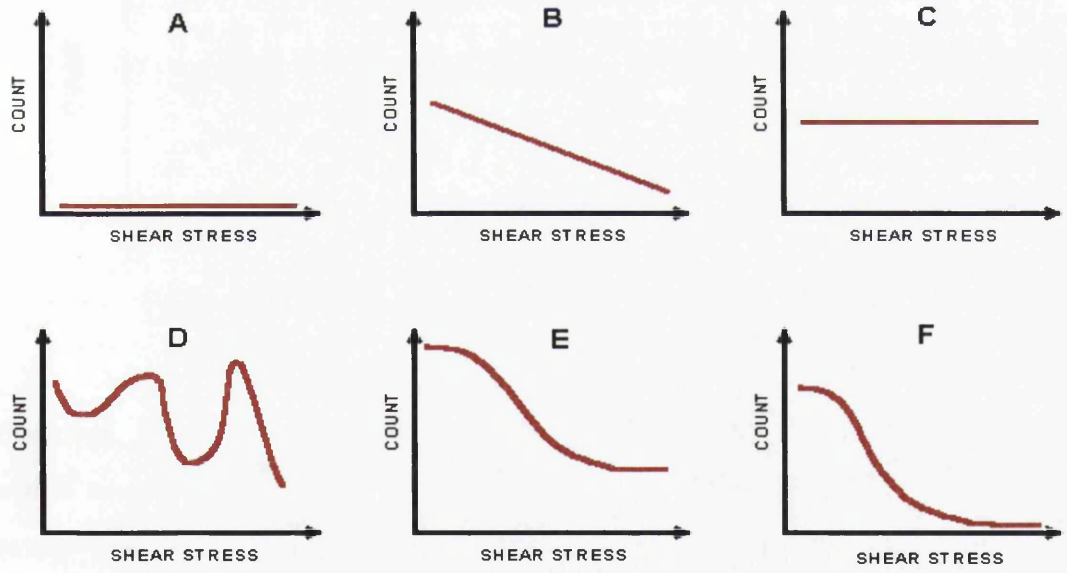

Figure 8.2: The differing types of adhesion profiles obtained using both the Spinning Disc and Radial Flow Chamber. Type A represents little or no adhesion. Type B represents a linear decrease as shear stress increases. Type C represents constant adhesion that is independent of shear stress. Type D represents adhesion that is both variable and independent of shear stress. Type E represents a sigmoidal attachment profile dependent on shear stress but does approach the x-axis, where little or no adhesion occurs. Type F shows a sigmoidal attachment profile, producing both a maximum, and approaches a point where little or no attachment occurs.

The adhesion profile represented by type E, was likely to result from the combination of processes represented by type C and F. The process of the particle rolling across the surface at a rate slow enough to allow enumeration, dynamic attachment, may explain the apparent independence of adhesion to applied shear force. The use of image analysis would benefit the use of these systems to detect if this was the case, and subsequently enable determination of the rate of movement across the surface.

The adhesion profiles represented by types B and F allowed the determination of the point of intersection of the x-axis, where no attachment occurred, and therefore allowed the integration of the profile. Integrating the adhesion profile allowed the determination of the total number of attached particles, and therefore the shear force at which 50% of the adhered population were attached, as shown in Figure 8.3.

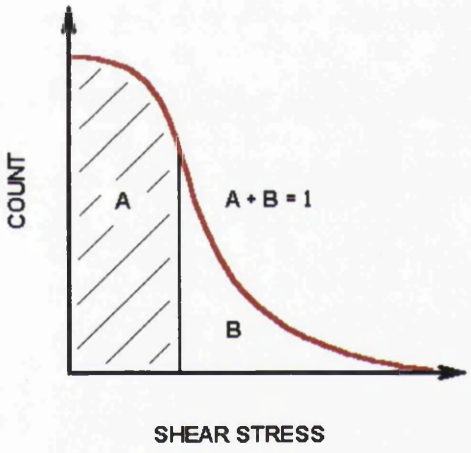

Figure 8.3: An example of a sigmoidal adhesion profile, allowing the point at which 50% of the spores are attached to be determined, with respect to shear force.

However, as stated, there were several different types of adhesion profiles, four of which would not permit the simple analysis as described in Figure 8.3, as the extrapolated adhesion profiles did not intersect the x-axis. Most adhesion profiles fitted the description of type E or C, where a point that minimal attachment occurred was not approached. In the case of type C, it was impossible to determine a force using any approach, as there was no dependence on applied shear force whatsoever.

In the case of type E, there were four variables within the graph, as described in Figure 8.4. Points A and B represent the maximum and minimum values of the adhesion profile, where attachment was deemed independent of radial distance.

Points C and D take into consideration the tangent of the adhesion profile, and extrapolates it to where it intercepts the highest and lowest values of attachment. This allows a relation to shear stress to be recorded at the point of intercept with the x-axis.

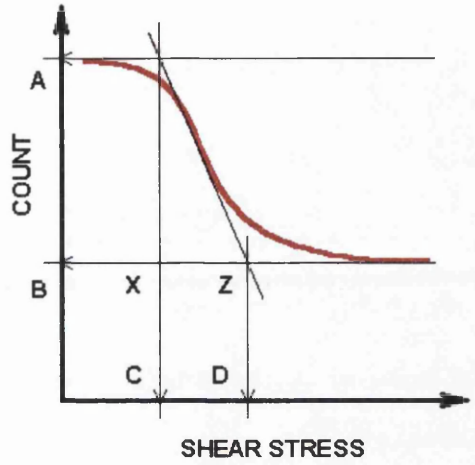

Figure 8.4: The method employed to analyse adhesion profiles. Points A and B give the maximum and minimum values of attachment. Points C and D are determined by the intersection of the tangent with the minimum and maximum values of adhesion respectively.

This method of analysis allowed comparison of both the maximum and minimum values obtained for the adhesion profiles generated using the Spinning Disc and Radial Flow Chamber to assess adhesion. The method also allowed a figure for shear stress to be determined, and is a very simple technique of assessing the characteristics of the adhesion profile, and is consequently prone to statistical error. The method does, however, allow the direct comparison of the adhesion profiles obtained from the experimental work performed within this project, without having to consider complicated mathematical modelling or further statistical analysis, and can be applied to adhesion profiles B, E, and F, to provide a figure for shear stress. This method of analysis would have to be substantiated by further experimentation, as discussed in Chapter 9.

8.2.3 Results with Respect to Applied Shear Force

This Section is designed to present results to allow the comparison of the Spinning Disc and Radial Flow Chamber, and in some cases, where allowed, determine a shear force. The analyses for each particle/pH combination for both glass and stainless steel are given in Appendix F, Tables F.1 and F.2 respectively.

However, the Tables represent a summary of the curves, but few conclusions can be drawn from these figures. The figures generated for the applied shear force did not show consistency with the maximum and minimum values of adhesion. The value of shear force generated by the analysis method assesses the change in adhesion with respect to shear force, rather than the adhesive properties of the given particle. The most important values obtained from the adhesion profiles were the maximum and minimum values, which provided a qualitative method of assessing adhesion. The gradient only assesses the amount of heterogeneity within the system. An adhesion profile with a steep gradient compared with an adhesion profile possessing a flatter gradient, represents a system with low heterogeneity of both particle and collector, compared with a system with large heterogeneity possessed by its components, as depicted in Figure 8.5.

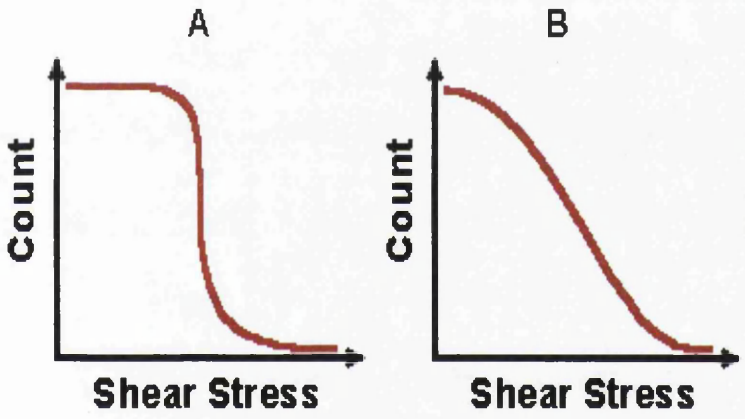

Figure 8.5: Two adhesion profiles showing the difference in A, a system possessing little heterogeneity, and B, a system showing a large amount of heterogeneity.

8.2.4 Comparison of Data from the Spinning Disc and RFC

This Section considers the adhesion profiles generated by experiments performed using both the Spinning Disc and RFC, and directly compares the results of adhesion assays to glass and stainless steel obtained using the latex beads and *Bacillus* spores. Ideally, both the Spinning Disc and RFC should provide results that are similar to each other, but this is not true in all cases.

The comparison of the Spinning Disc technique with the Radial Flow Chamber to assess adhesion to glass was not considered in this Chapter, and the results can be seen in Appendix F.1. This was due to the negligible adhesion observed when

assessing the adhesion profiles of both the latex beads and the *Bacillus* spores to glass. An example of this is given in Figure 8.6, representing the adhesion profiles of carboxylated beads to glass using both methods of assessing adhesion.

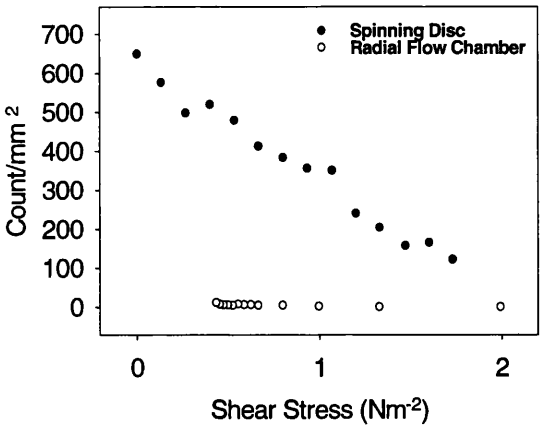

Figure 8.6: The adhesion profiles of the attachment of carboxylated latex beads to glass at pH 9.5 assessed using the Spinning Disc technique, and Radial Flow Chamber.

Using Figure 8.6 as an example, the attachment of carboxylated latex beads to glass using the Spinning Disc provided a linear relationship between attachment and shear stress, which decreased as shear increased. The results obtained using the Radial Flow Chamber, however, provided little or no adhesion, compared with the levels obtained using the Spinning Disc. The difference in results can be attributed to the sensitivity of the apparatus to either the particles' characteristics, or the collector surface characteristics as suggested in Section 7.6.3, and the difference in flow patterns across the collector surface as discussed in Section 9.2.4.

Having discounted the use of the glass collector surface when comparing the Spinning Disc and Radial Flow Chamber, adhesion to stainless steel was considered for all four particles at pH 3.5, 5.5, 7.5, and 9.5 with respect to radial distance.

8.2.4.1 The Adhesion Profiles of Aminated Beads to Stainless Steel

The adhesion profiles of aminated beads to stainless steel at pH 3.5 showed a smooth profile for results obtained using the RFC, whereas the corresponding results using the Spinning Disc showed great variety, as shown in Figure 8.7. The values did, however, show similar magnitude, ranging from 400 to 1400mm^{-2}. The

adhesion profiles at pH 3.5 were predominantly governed by the hydrophobic characteristics of the particle and the collector surface, as the aminated bead possessed a low negative zeta potential, and a high value of hydrophobicity. The stainless steel collector surface was most hydrophobic at pH 3.5.

The adhesion profiles of aminated beads to stainless steel at pH 5.5 and 7.5 did not show correlation between assessment methods. The attachment values obtained using the RFC were noticeably higher than those obtained when the Spinning Disc technique was employed to assess adhesion at pH 5.5 and 7.5. The aminated beads surface charge was approximately –33mV, as shown in Table 3.1, resulting in an increase in the electrostatic repulsion between the beads and the collector surface. The results generated from the use of the Spinning Disc appeared more susceptible to change in particle characteristics, and the RFC was more sensitive to the change in collector surface hydrophobicity. The difference between the values obtained using the Spinning Disc and the RFC therefore highlighted the comparative sensitivities of the two systems to the change in charge of the particle, and the change in hydrophobicity of the collector respectively, as suggested in Section 7.6.3.

The results generated at pH 9.5 were closer together for the Spinning Disc and the RFC, and reflects the increase in the values obtained using the Spinning Disc compared with those obtained at pH 7.5. This increase was attributed to the increase in hydrophobicity of the aminated bead, and was not observed using the RFC, due to the methods sensitivity to collector surface properties rather than the properties of the aminated bead.

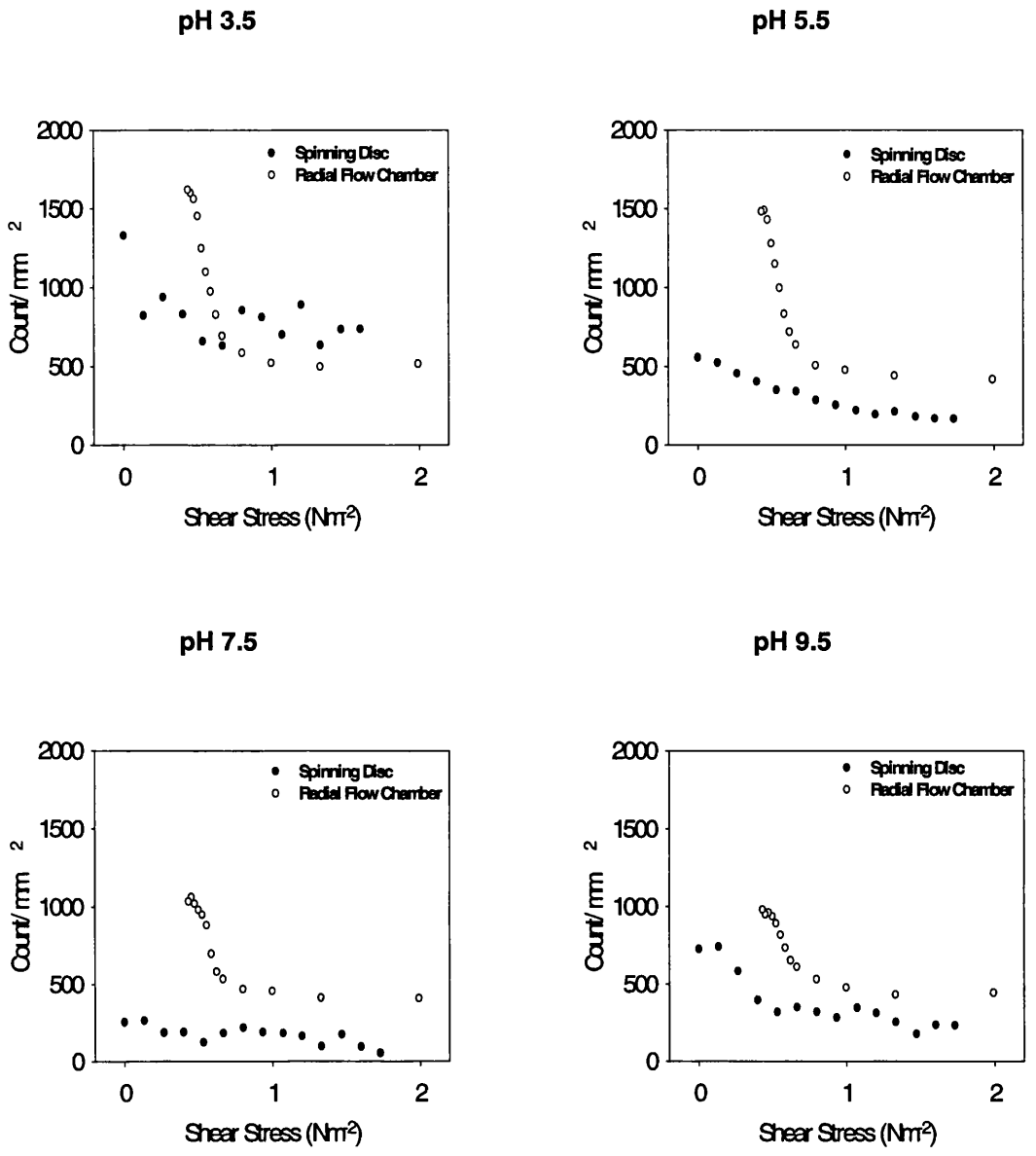

Figure 8.7: The adhesion profiles of aminated latex beads to stainless steel, obtained using both the Spinning Disc technique and Radial Flow Chamber over a range of pH. Details of experimental procedure are given in Chapters 6 and 7.

Although the difference in values obtained from the Spinning Disc and the RFC varied at different pH, the values generated from the Spinning Disc were generally less than those obtained with the RFC, suggesting that the shear force applied to the surface of the Spinning Disc was more complicated than stated Equation 8.1. The discrepancy in results will be discussed in more detail in Section 9.2.4.

The difference in adhesion was most noticeable at values of applied shear stress of $1Nm^{-2}$ and more, where attachment became independent of shear. The

independence of adhesion with respect to adhesion could be a function of dynamic attachment, as suggested in Section 8.2.2. If this was the case, then the properties of the dynamic attachment of the Spinning Disc would differ greatly to the properties of the dynamic attachment generated by the RFC, as the flow patterns across the collector surface differed. In the case of the Spinning Disc, the particles in suspension would accelerate across the surface, and the solution would also apply tangential shear to the collector surface. The flow generated by the RFC decelerates as the radial distance increases, which would allow greater levels of dynamic attachment compared with the values obtained with the Spinning Disc technique.

The difference in the flow generated by both methods was emphasized by the dramatic decrease in the levels of attachment as shear increased using the RFC. This was the case in all examples using the RFC to assess adhesion.

The suggestions made using aminated bead as the subject particle, will be considered when comparing the adhesion profiles of carboxylated latex beads, and the spores of *B.mycoides* and *B.subtilis*.

8.2.4.2 The Adhesion Profiles of Carboxylated Beads to Stainless Steel

As observed with the adhesion profiles of aminated beads to stainless steel, there was noticeable disparity between the values obtained using the Spinning Disc technique and the RFC, as shown in Figure 8.8. This was attributed to the difference in the quality of shear force exerted on the attached particles by the two methods, as discussed in Chapter 9. The values obtained using the Radial Flow Chamber at pH 5.5 and above were between 2 to 14 times higher than those obtained using the Spinning Disc technique. The adhesion profiles for the RFC also showed a greater dependence on the applied shear force compared with the Spinning Disc, which was largely unaffected by shear force. As a comparison, maximum values obtained using the Spinning Disc did not approach the minimum values resulting from assessment with the RFC at pH values higher than pH 5.5.

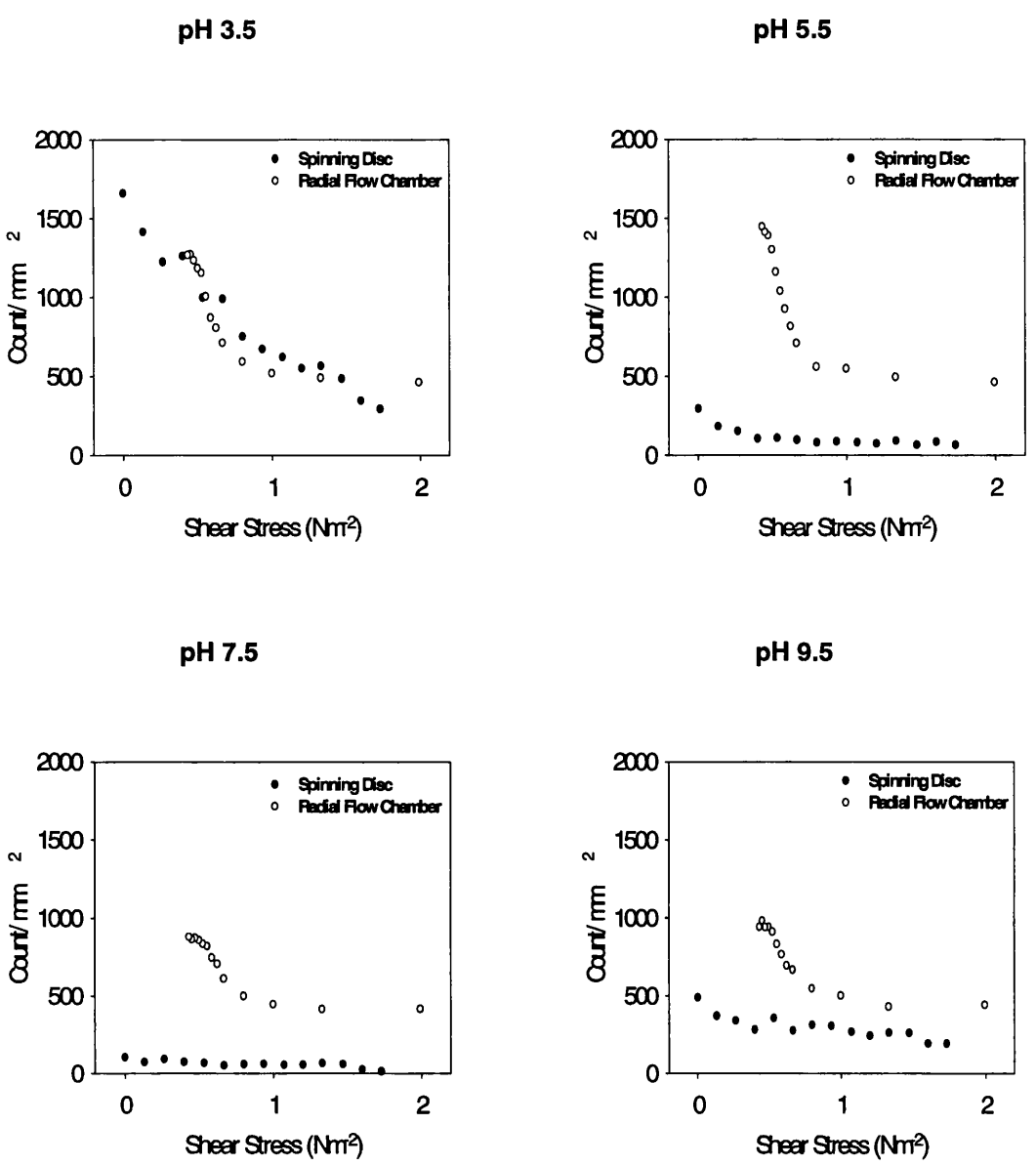

Figure 8.8: The adhesion profiles of carboxylated latex beads to stainless steel, obtained using both the Spinning Disc technique and Radial Flow Chamber over a range of pH. Details of experimental procedure are given in Chapters 6 and 7.

The adhesion profile obtained at pH 3.5, however, showed good agreement between the two methods of assessment. The adhesion profile obtained using the Radial Flow Chamber showed the same pattern as observed at higher pH, becoming independent of shear force at approximately 450 beads/mm^2. The maximum value of adhesion obtained with the RFC did vary as pH varied, but the same steep gradient was observed in all cases.

When considering the results obtained using the Spinning Disc at pH 5.5, 7.5, and 9.5, attachment was minimally affected by shear. At pH 3.5, however, adhesion decreased linearly as shear force increased.

The adhesion profiles of the carboxylated beads at pH 3.5 and 9.5 had comparable values obtained from both methods, as was observed with the adhesion of aminated beads, and was attributed to the sensitivity of the two methods to differing characteristics, of the collector surface and the particle. The adhesion profiles obtained at pH 9.5 were closer than the adhesion profiles obtained at pH 5.5 and 7.5, but not as close as the adhesion profiles obtained when considering the aminated beads at pH 9.5. The difference in adhesion profiles between aminated beads and carboxylated beads was attributed to the presence of local positive charge on the surface of the aminated beads, which were not present on the surface of carboxylated beads.

The comparison of the results of the carboxylated beads' adhesion to steel corroborates the theory that the RFC was more sensitive to the collector surface characteristics, whereas the Spinning Disc was more sensitive to the particles charge and hydrophobicity.

8.2.4.3 The Adhesion Profiles of B.mycoides Spores to Stainless Steel

The adhesion profiles of *B.mycoides* spores interacting with stainless steel for both the Spinning Disc and Radial Flow Chamber provided results that were comparable in magnitude in all cases, which was not the case when assessing both aminated and carboxylated beads, as depicted in Figure 8.9.

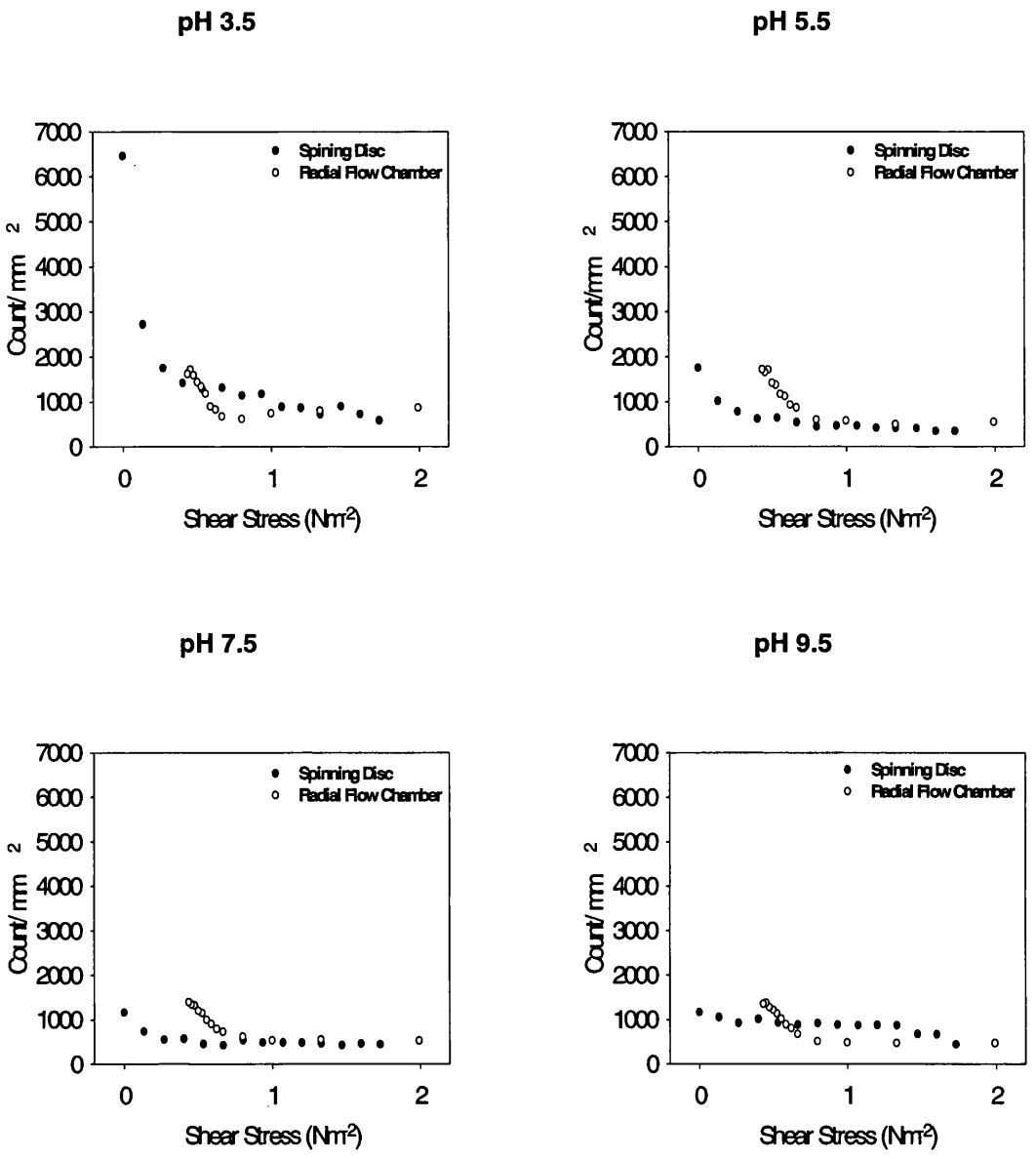

Figure 8.9: The adhesion profiles of *B.mycoides* spores to stainless steel, obtained using both the Spinning Disc technique and Radial Flow Chamber over a range of pH. Details of experimental procedure are given in Chapters 6 and 7.

At pH 3.5, the values obtained using the Spinning Disc technique showed a similar pattern to those obtained when assessing adhesion with the Radial Flow Chamber. The Spinning Disc technique allowed the assessment of attachment at a point where there is theoretically no shear stress applied to the collector surface (at the centre of the disc), where there was a great deal of attachment, approaching 7000 mm^{-2}. Assessment using the Radial Flow Chamber did not provide a point where the applied shear force was zero, due to the nature of the Chamber's design.

Consequently the high value of attachment obtained using the Spinning Disc could not be confirmed using the RFC. At higher pH, the adhesion profiles obtained using both the Spinning Disc and RFC were very similar, allowing direct comparison of values. At pH 5.5 and 7.5, adhesion profiles generated by the Spinning Disc technique showed lower values compared with the RFC where attachment was dependent on applied shear force. The point at which attachment became independent of shear provided levels of adhesion that were similar in both methods of assessment, and was observed for both the Spinning Disc and RFC at both pH 5.5 and 7.5. This suggests that the shear applied by the Spinning Disc technique was greater, as there appeared to be a shift to the left in the adhesion profile of the Spinning Disc compared with the RFC, rather than a shift down. This was consistent with the adhesion profiles of aminated and carboxylated beads at pH 9.5, and could not be discounted in the cases observed at lower pH for both aminated and carboxylated beads.

8.2.4.4 The Adhesion Profiles of B.subtilis Spores to Stainless Steel

The attachment of *B.subtilis* was lower than that observed when considering *B.mycoides*, but provided some interesting observations when comparing the Spinning Disc with the RFC. The adhesion profiles generated using *B.mycoides* spores for both methods showed good agreement irrespective of pH. This was the case when considering the adhesion of *B.subtilis*, as shown in Figure 8.10.

The theory that the shear force applied by the Spinning Disc differed to that of the RFC was supported by the results obtained using *B.subtilis*. At each pH, as shear increased, and attachment became less dependent on shear, and eventually remained constant for both methods at approximately the same values. The same observation was made with *B.mycoides* confirming the suggestion that there was a shift to the left of the adhesion profile generated using the Spinning Disc compared with the RFC. Consequently, the flow and applied shear force generated by both systems, as described in Equations 8.1 and 8.3 require revision, and differentiation of the forces applied to the collector surfaces in both cases.

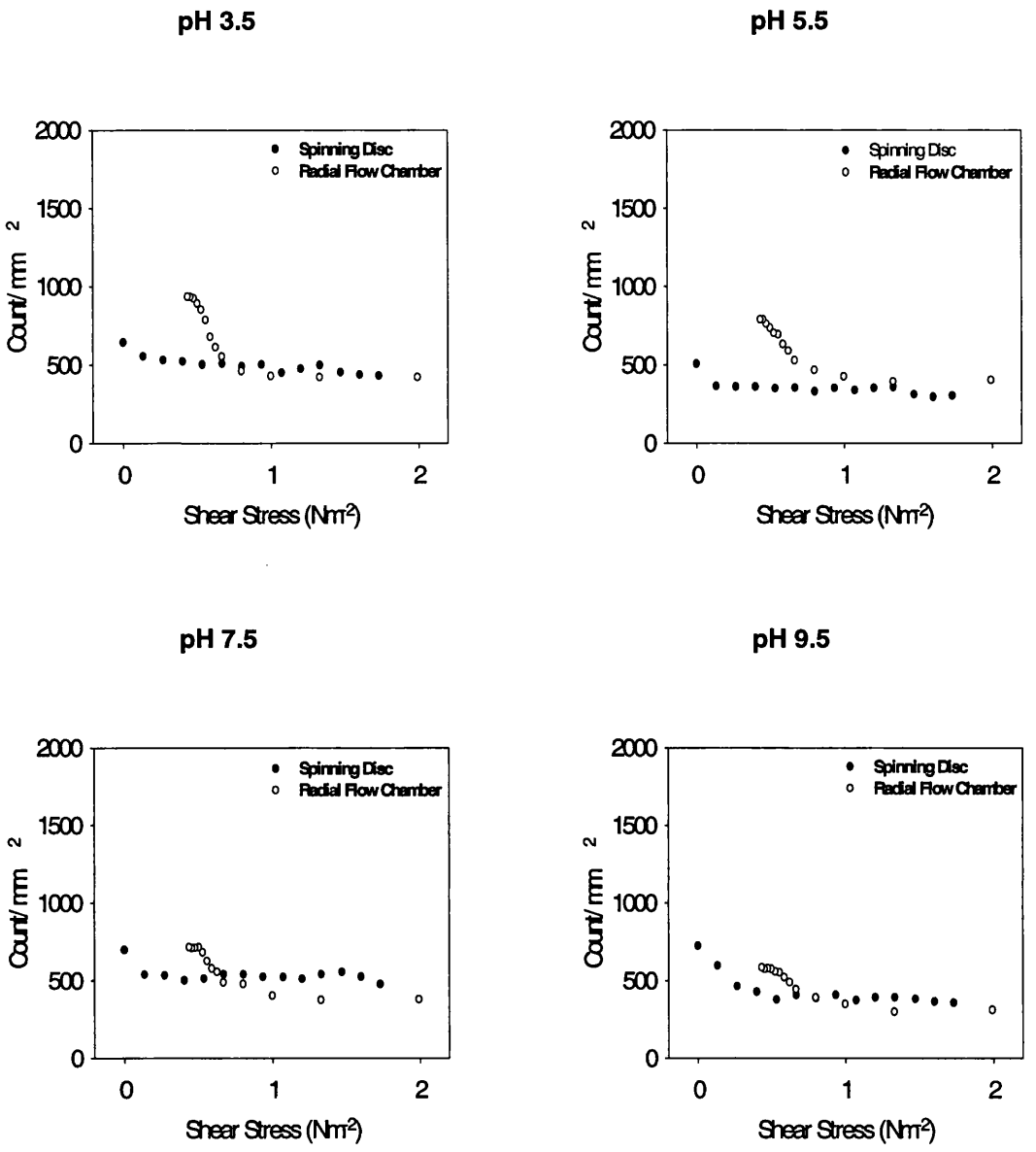

Figure 8.10: The adhesion profiles of *B.subtilis* spores to stainless steel, obtained using both the Spinning Disc technique and Radial Flow Chamber over a range of pH. Details of experimental procedure are given in Chapters 6 and 7.

The shift to the left of the adhesion profiles generated by the Spinning Disc technique was common for all four particles. However, the attachment values where adhesion was independent of shear showed good agreement between methods for the spores' attachment, but not for the attachment of latex beads. This could be a function of rolling of the latex beads across the collector surface, compared with the spores that were attached firmly to the collector surface. Rolling of the latex beads would be affected by the flow pattern of the system, which differed between the Spinning Disc and RFC, and is discussed in Section 9.2.4.

8.2.5 Summary of the Comparison Between the Spinning Disc and RFC

Simple mathematical analysis of the adhesion profiles proved impossible due to the variation in the shape of the adhesion profiles as discussed in Section 8.2.3, and consequently no values for the shear force required to inhibit adhesion could be reliable extracted from the data. The most productive method of assessing the adhesive qualities of the particle of study was to consider the maximum and minimum value of adhesion. However, the use of the Spinning Disc and RFC did provide comparable results in most cases, when considering the adhesion of the particles to stainless steel, especially in the case of the spores of *B.mycoides* and *B.subtilis*. The requirement for detailed mathematical analysis of the results obtained from the two methods is now necessary, and is discussed in Chapter 9.

Results from the Radial Flow Chamber provided a steeper gradient than observed with the Disc. This was attributed to the flow patterns across the surface of the Disc, which has the potential for more variation of the tangential forces applied using the Spinning Disc compared with the RFC, as discussed in Section 9.2.4.

The approach of the particles to the collector surface must also be considered in both cases when interpreting the data. In the case of the Spinning Disc, the suspended particles were initially exposed to an area where no shear force was applied (i.e. the centre of the disc), and subsequently accelerate with the flow. In the case of the RFC, the particles would be exposed to the maximum applied shear force within the system, and decelerate. Particles adhered to stainless steel in the case of the Spinning Disc were therefore more likely to adhere at the centre, and roll outwards, whereas particles in the RFC would not adhere until the shear force was sufficiently low, and were more likely to remain static at this point. This may account for the steep gradient of the adhesion profiles in the RFC, and the more random adhesion profiles generated by the Spinning Disc. The results presented in this Chapter show that the Spinning Disc and the RFC are systems that can be used to provide reliable results when considering and comparing particulate adhesion, providing more detailed analysis can be performed. This is discussed in Chapter 9, as well as further improvements to the system, and further work that should be performed to realise the full potential of these two systems.

CHAPTER NINE

Discussion and Summary

9.1 Introduction

The work performed within this project has developed and investigated the use of three techniques to assess microbial adhesion. This Chapter is designed to summarise the most important accomplishments achieved within this project, identify means of developing the methods incorporated within the project, and propose further work that that could be performed to improve the understanding and the ability to study microbial adhesion using these methods.

Having performed a literature survey, the need for reliable and uncomplicated methods to assess microbial adhesion was obvious. There have been many different methods used to analyse the processes involved in microbial adhesion, but none compare results of different methods, and none attempt to produce a figure representing a force of between the cell and the collector surface. In most cases, the interpretation of adhesion simply provides a 'yes' or a 'no' referring to the ability of a microbe to attach to a surface.

Three methods were identified to possess the ability to provide quantitative results and analyses when studying adhesion. These methods were the Packed Column, the Spinning Disc, and the Radial Flow Chamber, and all had relevance and

applications in natural processes. These methods have been previously used in similar experiments, but have not been applied directly to the study of the initial stage of microbial attachment. The methods therefore required development to provide systems that could be reliably used to assess adhesion.

9.2 Critical Assessment of the Methods

9.2.1 The Assessment of Adhesion using the Packed Column

The use of the Packed Column as a technique to assess adhesion allowed the study of processes occurring in the adhesion of bacteria to soils as well as some aspects of filtration. The development and characterisation of the Packed Column, detailed in Chapter 5, proved to be arduous, as previous uses of Columns to assess adhesion did not characterise the effect of different variables, such as particle size and flow rate. The method proved a good tool to assess microbial adhesion, and showed large differences in the adhesion of the latex beads and *Bacillus* spores, as well as the effect of pH and collector surface upon adhesion, as shown in Sections 5.6.4 and 5.6.5. A summary of the advantages and disadvantages of the use of the Packed Column to assess adhesion is given in Table 9.1.

Advantages	Disadvantages
Allows the calculation of irreversible binding.	Reversible binding required complex apparatus to analyse accurately.
Practical and simple methodology once the apparatus was prepared and characterised.	Problems preparing the apparatus. Prone to air in both the flow through cuvette and the column.
The method employed a simple, automated counting technique.	The collector surface was not reusable, and required re-packing regularly.
Allows the study of natural systems, and aspects of filtration.	Did not allow the contribution of shear force to be assessed due to limitations of applied pressure to the system.
Can analyse sequential additions to the column, and processes such as ripening.	High sample concentration may mean aggregation in solution, and subsequent binding in aggregates.

Table 9.1: The advantages and disadvantages of the use of the Packed Column to assess adhesion.

The preparation of the system was arduous when comparing the use of the Packed Column with the use of the Spinning Disc and the Radial Flow Chamber. This was due to the requirement of renewing and repacking the Column with unused collector surface. When considering the Spinning Disc and RFC, the process of surface preparation was a relatively simple cleaning technique. Packing the Column was susceptible to inconsistency, due to the introduction of air into the Column. Occasionally, the flow through cuvette was also liable to the presence of air bubbles, which would require restarting the experiment, and the renewal of the collector surface.

The method of recording and assessing adhesion was relatively simple compared with the Spinning Disc technique and Radial Flow Chamber. There was no requirement to count individual particles adhered to a surface, and the use of the package provided by PICO Technology, allowed direct transfer of the results generated by the spectrophotometer to an MS Excel spreadsheet, and subsequent manipulation of data.

Having stated the advantages and disadvantages of the use of the Packed Column to assess adhesion, the method did provide reproducible and reliable results, as demonstrated by the relatively low variation observed when performing duplicate experiments, shown in Figures 5.12 and 5.13.

The results generated from the Column allowed an overall appreciation of the effect of pH on the particle and the collector surface with respect to adhesion. The determination of zeta potential and the results from BATH tests, performed in Chapter 3 allowed the determination of surface charge and surface hydrophobicity, which can only be related to the adhesive properties of the system with a large amount of speculation. The contact angle measurements performed in Chapter 4 allowed the surface hydrophobicity of the particles to be determined. The Packed Column did not determine the individual contributions to adhesion made by the surface charge and hydrophobicity of the particle and the collector surface, but did allow the combined effects of the properties of both the collector surface and the particle to be assessed with respect to pH.

The use of the Column allowed the determination of the combined effect of these properties on adhesion without speculation on the amount that the surface charge and hydrophobicity contribute to adhesion.

9.2.2 The Assessment of Adhesion using the Spinning Disc

The use of the Spinning Disc technique to assess adhesion allows the evaluation of the effect of shear upon adhesion, and therefore simulates the effect of hydro and hemo dynamic shear that is experienced *in vivo* (Wang *et al*, 1995). A summary of the advantages and disadvantages are given in Table 9.2.

Advantages	Disadvantages
Simple surface preparation method.	Disc inspected out of solution, which resulted in the retention of residual liquid on the collector surface.
Shear range can be adjusted with angular velocity.	Extremely laborious counting to generate the adhesion profiles.
Simple methodology to perform experiments.	Microscopic inspection was harder with glass than with steel, due to reflective properties of glass.
Allowed the study of hydro and hemodynamic environments.	The method does not allow inspection whilst the experiment is in progress.

Table 9.2: The advantages and disadvantages of the use of the Spinning Disc technique to assess adhesion.

As with the use of the Packed Column, the development and characterisation of the experimental procedure and methodology of the Spinning Disc was demanding and fraught with problems. The initial characterisation work was performed using glass as the collector surface, and *B.subtilis* spores as the particle. The minimal adhesion of the spores, combined with the transparency of glass hindered the progress of the development, due to the inability to visualise the collector surface. Having overcome the problems of visualisation, a further problem was encountered. When assessing glass as the collector surface, residual liquid remained on its surface, a result of the low contact angle measurements recorded in Chapter 4. Several methods were performed to counter this, and the most successful was to remove the Disc from solution whilst still rotating, allowing the residual liquid to dissipate. The assessment of adhesion to stainless steel was not affected by residual liquid, due to the high hydrophobicity of the collector surface, as determined in Chapter 4.

Once the method had been developed, the system provided variable results, and was sensitive to both the collector surface and particle properties. The variation in results was negated by the repetition of experiments, allowing sufficient data to be collected.

The results did show a dependence on shear, and agreement in adhesion profiles between the Spinning Disc and RFC in most cases, particularly with the *Bacillus* spores. Improvements in the system must be made regarding the inspection of the surface with reference to the removal of the Disc from the particle suspension, as the technique has great potential to be an important method of assessing microbial adhesion.

9.2.3 The Assessment of Adhesion using the Radial Flow Chamber

As with the Spinning Disc, the Radial Flow Chamber allowed the study of microbial adhesion under shear conditions that are experienced *in vivo*.

The development of the Radial Flow Chamber was a more simple process compared with that of the development of the Spinning Disc. The two methods were designed to be compared directly with each other, and consequently the effect of flow rate through the chamber, suspension concentration, and time were not investigated, as these parameters were kept constant for both methods. The problems encountered when inspecting the Spinning Disc surface were avoided with the RFC, as experience had been gained from performing the experiments on the Spinning Disc. Inspection of the collector surface was also substantially easier, as inspection was performed whilst the experiment was in progress, as detailed in Section 7.3.2.

However, having stated the advantages and disadvantages of the RFC as a method of assessing adhesion, summarised in Table 9.3, the method did provide results with good consistency. Adhesion to glass was minimal when comparing the results with those obtained using stainless steel and was attributed to the dominance of the contribution of collector surface hydrophobicity, as reported in Section 7.5. The use of the RFC provided a method of assessing adhesion, and a good method to compare with equivalent results generated using the Spinning Disc.

Advantages	Disadvantages
Simple surface preparation method.	The chamber is subject to variation of flow around the inlet and outlets pipes
Shear range can be adjusted with flow rate.	Extremely laborious counting to generate the adhesion profiles.
Simple methodology to perform experiments.	Microscopic inspection was harder with glass than with steel, due to reflective properties of stainless steel.
Ability to assess adhesion whilst the experiment is still in progress.	An inverted microscope was required to inspect the surface.
Allowed the study of hydro- and hemodynamic environments.	The method does not allow inspection whilst the experiment is in progress.

Table 9.3: The advantages and disadvantages of the use of the Radial Flow Chamber to assess adhesion.

9.2.4 The Comparison of the Methods used to Assess Adhesion

As stated in Chapter 8, when comparing the results obtained for the Spinning Disc with the RFC, there appeared to be a shift to the left in the adhesion profile of the Spinning Disc, suggesting a difference in applied shear force. The relationship between shear force and radial distance was defined in both cases in Equations 6.1 and 7.1, and allow the applied shear force to be calculated quantitatively. However, there are qualitative differences in the flow across the collector surfaces in both cases, as described in Figure 9.1 and 9.2, which must be resolved to allow the consideration of the effects of flow on the applied shear force of each system.

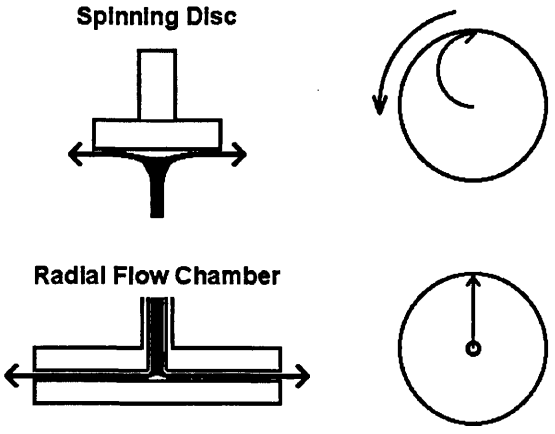

Figure 9.1: The difference in flow patterns across the surfaces of both the Spinning Disc and Radial Flow Chamber, resulting in tangential forces in the case of the Spinning Disc.

Although the respective equations allow applied shear to be calculated, they do not allow the direction of force to be considered, which was the most likely reason for the discrepancies in adhesion profiles.

When considering the Spinning Disc, the flow approached the collector surface axially, and exited radially. In this case, force will be applied to the surface in the z-axis, representing the suspension being drawn toward the surface, the y-axis, where fluid is exiting radially, and the x-axis, resulting from the rotation of the disc. Conversely, the flow patterns resulting from the RFC would affect the collector surface in the y-axis only, as shown in Figure 9.2.

The shear rate increases as radius increases in the case of the Spinning Disc, and as a result, particles will gather momentum. Therefore if an attached particle is dislodged, the particle is unlikely to reattach to the surface. The opposite is true when considering the RFC. The occurrence of dynamic attachment, as detailed in Section 8.2.2, would be affected by the applied force on the particle, and whether the particle was accelerating or decelerating over the collector surface.

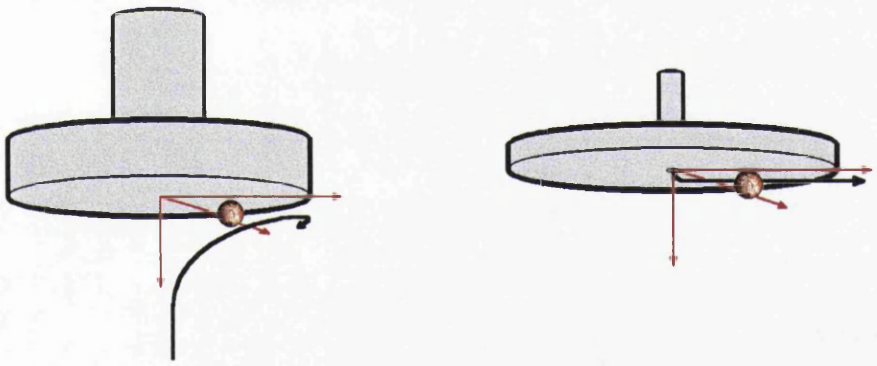

Figure 9.2: The hydrodynamic shear forces acting upon an adhered colloid. The Spinning Disc (left), has forces in three directions due to its pattern of flow, and the Radial Flow Chamber (right) has shear force in one direction.

The tangential forces applied to the Spinning Disc surface can be used to explain firstly the greater variation of results obtained using the spinning disc, and secondly the shift to the left of the adhesion profiles compared to those obtained using the RFC, as shown in Section 8.2.4.

The RFC was also susceptible to variation in shear force. The area around the inlet pipe was observed to have varying levels of adhesion, and was the reason that enumeration was not performed at radial distances less than 10mm.

Summarising, the Packed Column allowed the overall adhesion characteristics of a particle to be established, but did not allow the consideration of the contribution of applied shear force to the system. The Radial Flow Chamber and the Spinning Disc were similar in their ability to apply a shear force gradient, but differed in the respective systems sensitivity to particle or collector characteristics. Other factors that influence the choice of method to study adhesion are listed in Table 9.4.

	Packed Column	**Spinning Disc**	**Radial Flow Chamber**
Applications	Soils, and sand filters	Hemo- and hydrodynamic shear	Hemo- and hydrodynamic Shear
Shear gradient	No	Yes	Yes
Real time observation	No	No	Yes
Assessment method	Breakthrough curve	Adhesion profiles	Adhesion profiles
Susceptible to human counting error	No.	Yes	Yes
Ability to assess the effect of collector roughness	No	Yes	Yes
Collector coatings	No	Yes	Yes
Defined flow	No	Yes	Yes
Collector requirements	Granular	Flat	Flat
Specific apparatus requirements	Column and additional accessories, Spectrophotometer, gas cylinder, reservoirs, computer, flow through cuvette	Motor, controller and microscope	Pump, Radial Flow Chamber, inverted microscope
Abililty to assess attachment/detachment kinetics	Yes	No	Yes

Table 9.4: The benefits of the Packed Column, Spinning Disc, and Radial Flow Chamber, that should be considered when choosing a system to assess adhesion.

9.3 Overall Results and Findings

9.3.1 The Effect of pH on Adhesion

The observation made in most cases was that adhesion was greatest at pH 3.5, and decreased as pH increased. This was attributed to the fact that both the collector and particle surface were negatively charged, and as pH was lowered, protonation rendered the surface less negative, reducing the effect of electrostatic repulsion, and consequently increasing the contribution of the attractive forces involved in adhesion.

9.3.2 The Variation in Adhesion of Latex Beads and Bacillus Spores

The spores of *B.mycoides* were the most adhesive followed by the aminated and carboxylated latex beads, and finally, the spores of *B.subtilis*. The spores of *B.mycoides* provided the highest levels of adhesion, due to their complex structure, as detailed by Husmark and Rönner (1992). The presence of both a hydrophobic exosporium and surface appendages rendered the spores low in charge, and moderately hydrophobic.

The adhesion of both aminated and carboxylated latex beads showed lower values than the spores of *B.mycoides*. The surface charge and surface hydrophobicity of the latex beads recorded using zeta potential measurements and BATH tests respectively, were substantially higher than the values recorded for *B.mycoides* spores, reflecting the properties of latex compared with the bio-molecular components of the spores' surface. The decrease in adhesion of the latex beads could therefore be attributed to either the lack of exosporium and appendages, or the increased charge of the latex beads, increasing the electrostatic repulsion between the collector and the particle.

The adhesion of aminated beads was generally higher than that observed with the carboxylated beads. There was little or no difference in the hydrophobicity of the beads, but the zeta potential of the aminated beads was less negative, due to the

presence of the amine groups on the beads' surface, reducing the electrostatic repulsion between the aminated bead and collector surface. The effect of the positively charged groups on the aminated beads' surface was amplified by the uneven distribution of amine groups over the beads' surface, producing localised areas of positive charge.

Finally, the spores of *B.subtilis* were generally observed to produce the lowest values of adhesion. This was not true in all cases, especially when considering the use of the Spinning Disc to assess adhesion. When comparing the spores of *B.subtilis* with the spores of *B.mycoides*, the major structural difference is the lack of appendages and exosporium in the case of *B.subtilis*, which increased the zeta potential, and decreased the hydrophobicity of the *B.subtilis* spore. The difference in adhesion of the latex beads and the spores of *B.subtilis* can be attributed to the large decrease in hydrophobicity of the spores as shown in Table 9.5.

	Aminated Beads	**Carboxylated Beads**	***B.mycoides* Spores**	***B.subtilis* Spores**
Appendages/ Exosporium	No	No	Yes	No
Zeta Potential	High	High	Low	High
Hydrophobicity	High	High	Moderate	Low
Adhesion	Moderate	Moderate	High	Low

Table 9.5: The properties of aminated and carboxylated beads, and the spores of *B.mycoides* and *B.subtilis*.

As a result of the consideration of the properties and the adhesion profiles generated by the methods of assessment, the largest contributor to adhesion was the presence of appendages and/or exosporium. This is followed by the hydrophobic contribution of the interaction, and finally, the charge of the two interaction surfaces. This is concurrent with the distance that these forces are effective. The first initial interaction will be with molecules present on the surface of the particle, if present. The hydrophobic interaction, which is taken into consideration in the ex-DLVO theory, is effective at separation distances of approximately 50nm. The electrostatic repulsion contribution becomes effective at approximately 30nm, which is governed by surface charge.

9.3.3 The Effect of Collector Surface Hydrophobicity on Adhesion

The roughness of the collector surfaces used within this project was kept constant, which enabled adhesion to be assessed as a function of the hydrophobic properties of the respective collector surfaces. In all cases, stainless steel provided a more receptive surface for adhesion of colloidal particles. The difference in attachment levels between glass and stainless steel for *B.subtilis* spores, was noticeably smaller than those observed for both latex beads and the spores of *B.mycoides.* This was attributed to the low hydrophobicity of the *B.subtilis* spores, reducing the hydrophobic interaction between the spore and the stainless steel surface. This confirms the theory that surface hydrophobicity contributes more to adhesion than surface charge, as suggested in Section 9.3.2.

9.4 Studying Adhesion Systematically

When considering adhesion as a function of the respective surfaces characteristics, consideration of the surface charge, hydrophobicity, roughness, and morphological properties of the overall surface is not sufficient. The individual interactions that govern adhesion should be investigated on the molecular scale to provide a more accurate interpretation of adhesion. This requires the analysis of both surfaces, and the total of the individual interactions generated by these properties, requiring accurate characterisation enabling the accurate evaluation of the individual contributions to the forces involved in adhesion. For example, surfaces with specific indentations with the dimensions of the particle could be used to study the effect of heterogeneity on the system, as shown in Figure 9.3. The ability to characterise the interacting surfaces with great accuracy is a necessity, if a detailed interpretation and prediction of adhesion is to be obtained.

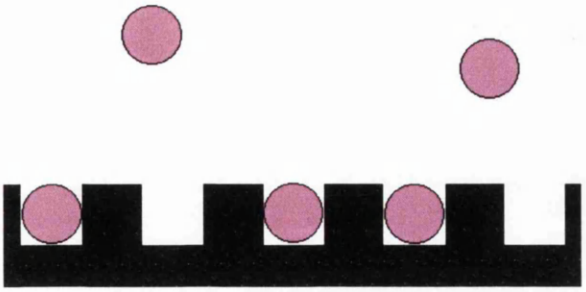

Figure 9.3: The adhesion of particles to a surface with specific heterogeneity with respect to roughness.

9.5 Forces involved in Adhesion and Approach of the Cell or Latex Bead to the Surface

The forces governing adhesion are based on the interaction of the cell and its structures with the collector surface. The long-range attractive forces are a total of vdW and hydrophobic interactions, and have a range of approximately 50nm. As the surfaces became closer, the interaction was dominated by electrostatic repulsion at approximately 30nm. If the particle had sufficient energy to pass this repulsion, vdW and hydration forces attracted the particle to the surface, at approximately 10nm separation distance. This is depicted in Figure 9.4, for three different particle types. Type A represents a particle that is stable in solution, type B represents a particle that is marginally stable, and type C represents a particle unstable in solution. Types A, B, and C could be applied to the adhesion of *B.subtilis* spores, latex beads, and *B.mycoides* spores respectively.

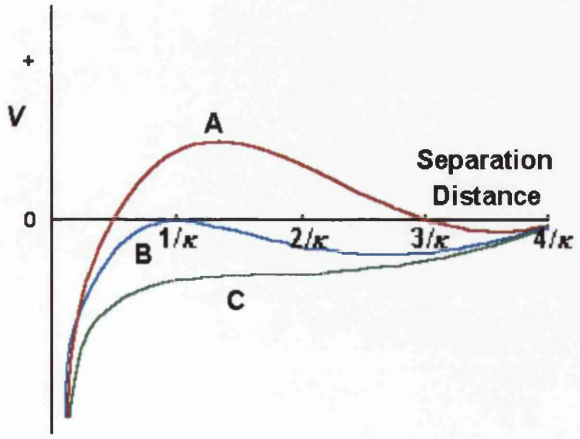

Figure 9.4: The total interaction energy profiles for (A) stable, (B), marginally stable, and (C) an unstable particles in solution.

The presence of cellular appendages, which can be up to 1μm in length, are also affected by the interactions depicted in Figure 9.4, and this fact explains the difference in adhesion of cells compared with non-biological colloids. This is depicted in Figures 9.5 and 9.6, which represent the approach of a cell and latex bead to a collector surface respectively.

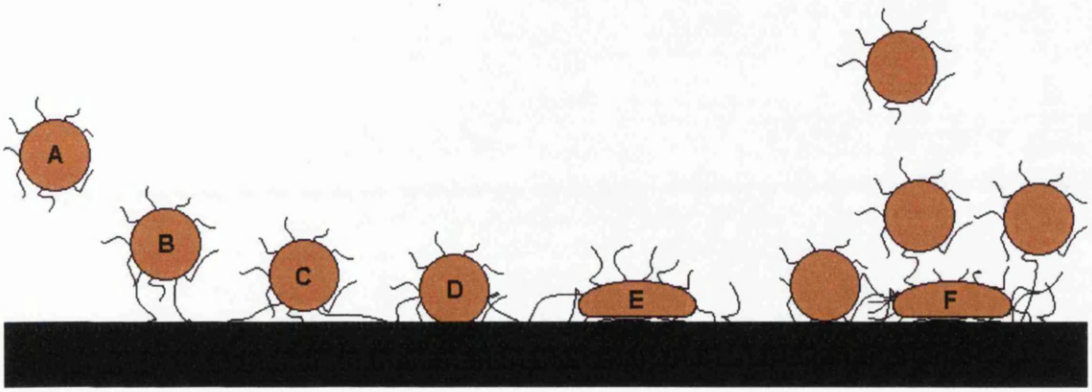

Figure 9.5: The approach of cells in solution to a collector surface

The first interaction of a cell in suspension (A), is the binding of cellular appendages (B), subject to hydrophobic, electrostatic and vdW forces, and subsequent binding promoted by the residency time in the proximity of the surface (C). The cell wall then adheres to the surface (D), which is followed elongation of the cell increasing the contact area between the cell and the surface (E). Finally, protein deposition occurs, promoting the adhesion of further cells to the activated surface (F). This is in contrast with the approach of latex beads to the collector, as represented in Figure 9.6 where the bead in solution (A) approaches the surface, and undergoes long-range hydrophobic and vdW forces (B), then experiences electrostatic repulsion (C), and if the bead has sufficient energy to overcome the electrostatic repulsion, adheres to the surface as a result of the short-range vdW and hydration forces (D). Adhesion of further spheres may be promoted by the presence of previously adhered beads (E).

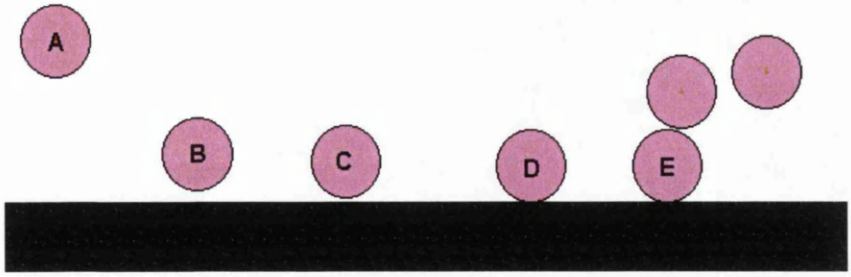

Figure 9.6: The approach of latex beads in solution to a collector surface

The approach of the particle to the collector surface, and subsequent adhesion is a sum total of the forces acting upon the particle, and is affected by the shear generated by the techniques used to study adhesion. These forces are summarised with respect to the particle in Figure 9.7 where $F(x_1)$ is the force generated by the fluid flow, $F(x_2)$ is the adhesive force, T is the torque generated by the fluid, and $F(y_1)$ and $F(y_2)$ are the forces required to counterbalance the torque generated by the system.

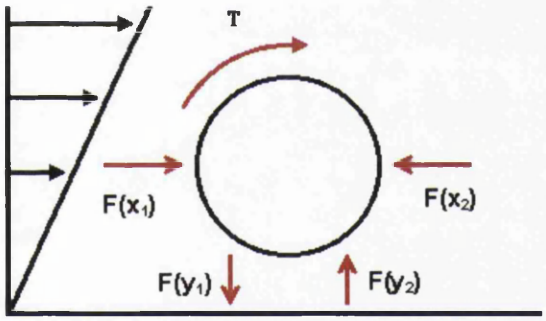

Figure 9.7: The total forces exerted on an adhered particle. $F(x_1)$ is the force generated by the fluid flow, $F(x_2)$ is the adhesive force, T is the torque generated by the fluid, and $F(y_1)$ and $F(y_2)$ are the forces required to counterbalance the torque generated by the system.

9.6 Further Work

9.6.1 Development of Adhesion Methods

Section 9.2 critically assesses the development and use of the Packed Column, Spinning Disc and Radial Flow Chamber. There were limitations within the project, and this Section describes developments that should be introduced to improve the methods used in this project to study adhesion.

9.6.1.1 The Use of the Packed Column

There are two simple developments that could be made to the use of the Packed Column. Firstly, the process of reversible adhesion can be assessed by analysing the tail of the curve, represented by the difference in the symmetrical reflection of the curve, compared with the actual curve, as depicted by Figure 9.8. In this case, the ability to monitor low particle concentrations would be required as detailed in Section 5.7.4.

Secondly, increased pressure would allow different shear rates to be applied to the Column, to assess adhesion as a function of shear. This would enable comparisons to be made with the Spinning Disc and the RFC.

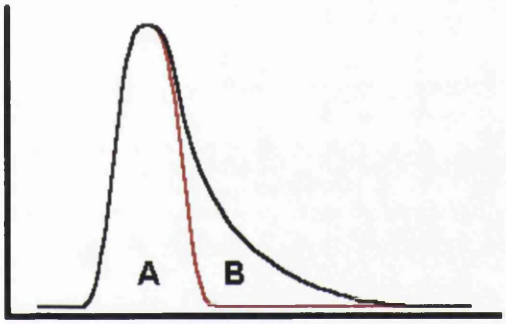

Figure 9.8: An example of a breakthrough curve generated from the column. The black line represents the actual curve. The red line represents the mirror image of the initial part of the curve up to the peak.

9.6.1.2 The Use of the Spinning Disc and the RFC

Problems were encountered when considering the use of the Spinning Disc and RFC, which were not resolved when performing developmental experiments. Improvements should be made to assess the flow patterns generated on the collector surfaces of both methods, and to assess that the relationship between applied shear force and radial distance is accurate in both cases. This could be achieved by comparing different adhesion profiles generated using different angular velocities of the Spinning Disc or the flow rate of the RFC respectively.

The introduction of image analysis would be the most important addition to the apparatus, however, as this would not only avoid the extremely laborious task of counting manually, but would also provide a more accurate counting method if

applied correctly. If applied further, image analysis could also be used to assess the kinetics of adhesion, and used to capture pictures of particles rolling, sliding, or elongating, for example, as detailed in Section 8.2.5. This would allow the kinetics and mechanisms of adsorption and retention to be investigated in further detail.

9.6.2 Potential Applications

Having applied these developments to the three assessment methods, the potential for further work has few limitations, and are highlighted in this Section.

9.6.2.1 Collector Surfaces

The systems used within the project stipulate that collector surfaces should be either granular or flat for the Packed Column and Spinning Disc/RFC respectively, enabling the investigation of polymers, metals and their alloys, and minerals with respect to adhesion. The effects of surface treatments, such as silanisation as used in Section 6.4.3, and surface roughness can also be investigated. Alternatively, the application of an electrical potential to a metal surface in conjunction with the Spinning Disc or RFC could provide a method of assessing the contribution of surface charge to adhesion.

9.6.2.2 The Study of Cells and Colloids

Adhesion of *Bacillus* spores are affected by the their morphology. This work could be extended to investigate the spores of *B.polymyxa* and *B.pumilis* that possess appendages, but no exosporium, to determine the effect of that presence of appendages and the exosporium have on adhesion (Husmark and Rönner, 1992).
The investigation of other cell types should also be performed to clarify the role that cellular diversity possesses in adhesion. Yeasts, fungi, and mammalian cells, as well as other bacterial cells should be investigated thoroughly for a more comprehensive

overview of adhesion. This should be combined with the assessment of various characteristics of the cells, as is investigated within this project.

The availability of genetically engineered bacteria also provides an interesting subject of study. The effect of cellular appendages could be investigated by genetically manipulating cells to inhibit or promote the expression of cellular structures thought to contribute to adhesion, for example. Latex beads modified with proteins may also be able to analyse this contribution. The introduction of fluorescent or radioactive markers would also benefit the enumeration of adhered cells to the collector surface.

With sufficient development, the methods incorporated in this project could be employed in the separation of bacteria with preferential adhesive characteristics, or to determine the processes involved in co-adhesion.

9.6.2.3 Investigation of Solution Contributions

As with the potential use of colloids, there is no limitation on the solution used in combination with the methods incorporated within this project. The project only investigated the effect of pH, but there are many parameters that can be investigated, such as the investigation of the effect of both mono- and poly-valent ions, or the presence of cleaning agents such as detergents or hydrocarbon based solvents.

9.7 Summary

The work performed within this project has developed three methods that can successfully analyse the binding of microbial cells to a chosen surface. These methods provide simple and effective assessments of microbial adhesion that have very few limitations, and could provide the basis of a greater understanding of microbial adhesion, which is applicable in many areas of science and technology.

Appendix A

Materials and Methods

A.1 The Particles Used in Adhesion Experiments

Sections A.1.1 and A.1.2 list the latex beads and cells detailed in Section 2.2.1

A.1.1 Latex Beads

Bead Type	Size	Cat. Number
Aminated Latex Beads	2μm	L 2653
Carboxylated Latex Beads	2μm	L 3030
Carboxylated Latex Beads	1μm	L 3155
Carboxylated Latex Beads	0.5μm	L 3280
Carboxylated Latex Beads	0.1μm	L 3405

Table A.1: The catalogue numbers of surface modified latex beads used in experiments. All beads were supplied by Sigma-Aldrich.

A.1.2 Cells

Cell Type	Strain Code
Bacillus mycoides	ATCC 6462; NCIMB 13305
Bacillus subtilis	ATCC 6051; NCIMB 3610
Escherichia coli	ATCC12435; NCIMB 9481
Sacchromyces cerevisiae	NCYC 1681

Table A.2: The strain codes of the cells used in experiments. All beads were supplied by the NCIMB (Aberdeen).

A.2 Media

This Section lists the components of the medium referred to in Section 2.3.2.1.

Component	Conc.
Lab Lemco	1 g/ℓ
Yeast Extract	2 g/ℓ
Bacteriological Peptone	5 g/ℓ
Trace Elements	20 mℓ/ℓ

Table A.3a: Components of standard medium used to produce both *B.mycoides,* and *B.subtilis* spores. 250mℓ cultures were allowed to sporulate over a period of 2 weeks. At this point, nutrients were depleted, and spore formation occurred. Trace Elements are shown in Table A.3b

Component	Conc. (g/l)
$MgCl_2.6H_2O$	5.00
$MnCl_2.4H_2O$	0.47
$FeCl_2.6H_2O$	0.35
$ZnCl_2$	0.20
$CaCl_2$	0.10
$CoCl_2.6H_2O$	0.02
$CuCl_2.2H_2O$	0.02
$NaMoO_4$	0.01
$Na_2B_4O_7$	0.01

Table A.3b: Components of the trace elements used in Table A.3a to grow *B.mycoides* and *B.subtilis*

Compounds	**Amount (g/l)**
Malt Extract	3
Yeast Extract	3
Glucose	10
Mycological Peptone	5

Table A.3c: Components of the MYGP broth used to grow S.cerevisiae in preliminary experiments, detailed in Section A.3.

A.3 Results for the Preliminary Investigation of Adhesion

A.3.1 Growth and Preparation of Cells

S.cerevisiae and *E.coli* were used in the following experiments, and their respective strains are given in Table A.2. *E.coli* were grown as a 24-hour culture, in nutrient broth at 37°C, adjusted to pH 5.5. *S.cerevisiae* was grown as a 24-hour culture in MYGP broth at pH 7.5, at 27°C.

The cells were then washed three times with either 25mM MOPS (3-[N-Morpholino] propane-sulphonic acid) or 25mM NaH_2PO_4, as stated. Finally the cells were harvested in the centrifuge and suspended in the respective buffer (2mℓ), with an OD of approximately 50 at 660nm. Cells were then used as required, without freezing and storing.

A.3.2 Introductory Work

The initial work in this project developed a general background for the investigation into cellular adhesion to glass. Although the experiments were simple compared to the proceeding methods of assessment, the experiments did allow for the determination of several important factors that contribute to the measurement of adhesion, such as the solution pH, the choice of suspension buffer, the ionic strength of the solution, methods of pre-treating of the glass surface, and the effect of the experimental incubation time on adhesion.

A.3.2.1 Apparatus for the Preliminary Assessment of Adhesion

The apparatus consisted of two rubber bungs attached to a stainless steel rod at each end as shown in Figure A.1. The two bungs were of different sizes. The top bung fitted into the neck of the conical flask. The smaller bung had a 10mm hole bored vertically into it, which was off-centre. Five slits were cut horizontally so as to enable the holding bung to suspend five circular cover slips in liquid at the bottom of the 1 litre conical flask.

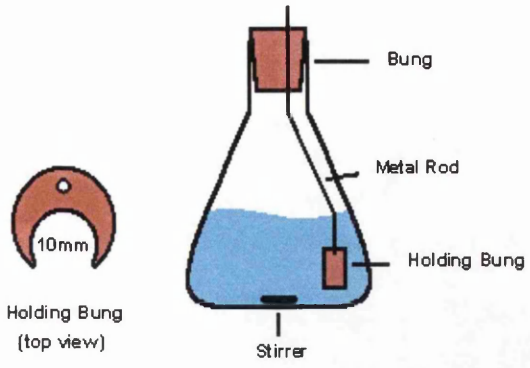

Figure A.1: The apparatus used for the preliminary experiments, consisting of a conical flask, on a magnetic stirrer, with a bung suspended below the level of the microbial suspension. The holding bung had a hole (10mm) cut vertically, to allow the circular cover slips to be held in the solution.

The glass slips (10mm diameter), were prepared by soaking in ethanol, and rinsed briefly prior to use with distilled water.

The cover slips were placed on a microscope slide and the underside of the slip inspected for adhered cells. Mobile cells in the liquid phase were not counted.

A.3.2.2 Assessing the Viability of the Apparatus

The first experiment was used to determine whether cells would adhere and grow on the glass slide. The experiment also allowed the identification of any potential problems that might be encountered with visual inspection techniques.

Protocol:

The apparatus was suspended in the appropriate media and sterilised at 121°C for 15 minutes. The apparatus was then inoculated with either *S.cerevisiae* or *E.coli*, and stirred over a period of 32 hours. The glass slips were taken aseptically from the cell culture at various intervals, and rinsed, by dipping the slip twice in three separate containers of distilled water to remove any residual cells and media. This was then inspected and the adherence assessed by simply either cross for no adhesion, a stroke for a small amount of adhesion, or two strokes for a large amount of adhesion. The method of assessing adhesion was initially to count adherent bacteria, but this proved impractical.

Results:

The visual inspection was not practical or reliable, as the cells could not be clearly identified (Table A.4), due to the deposition of media on the glass surface and biofilm formation. Further experiments were performed using buffer solution rather than media.

Time (hrs)	*E.coli*	*S.cerevisiae*
16	X	X
20	X	/
24	/	/
28	/	//
32	//	///

Table A.4: The qualitative assessment of adhesion of *S.cerevisiae* and *E.coli* to glass slips. X represents negligible adhesion, / represents limited adhesion, etc. Experiments were conducted in MYGP broth, at 22 +/- 1°C. Counting was judged impractical due to biofilm formation and deposition of media.

A.3.2.3 The Effect of Suspension Time

An investigation was performed to determine the effect of time on the adhesion of *S.cerevisiae* and *E.coli* to glass slips. This experiment gave an insight into the time required for adhesion to occur and was performed to allow further development of experimental procedure with respect to time.

Protocol:

S.cerevisiae and *E.coli* were grown in MYGP broth (250mℓ) for 24hrs as the previous experiments suggested that suitable adherence occurred at this point as described in Section A.3.2.2. After this time the cells were harvested, and washed three times, and finally suspended in distilled water (pH 7). Glass slips were then suspended in the cellular suspensions for 10min, 20min, 30min, 60min, and 240min.

Results:

Harvesting and washing the cells provided a substantially improved method for successful visual inspection, compared to media. There did seem to be higher levels of adhesion than in the previous experiment as listed in Table A.4. The improvement in inspection was attributed to the absence of media deposition on the glass surface.

This experiment determined that 30 minutes was sufficient time for cellular adherence from suspension to glass as shown in Table A.5.

Suspension Time (min)	*E.coli*	*S.cerevisiae*
10	/	/
20	//	//
30	//	//
60	//	//
240	///	///

Table A.5: The determination of the effect of suspension time on adhesion of *S.cerevisiae* and *E.coli* to glass slips. Glass slips were suspended in a suspension of cells in distilled water (pH 7). X represents negligible adhesion, / represents limited adhesion, etc. Experiments were conducted at 22 +/- 1°C.

The experiments detailed here and in Section A.3.2.2 have proved that the cells will readily adhere to the glass collector surface, using this simple apparatus. Further experiments were carried out to determine the optimal environment to encourage adhesion, and the practical parameters to conduct experiments.

A.3.2.4 The Effect of Growth Period

The effect of the growth period on the adhesion of both *S.cerevisiae* and *E.coli* to glass was assessed using the same apparatus. This experiment was performed to determine that 24-hour cultures were suitable for assessing adhesion, as this growth period was most practical for the performance of experiments.

Protocol:

Five cultures of both *S.cerevisiae* and *E.coli* were inoculated in respective media. At four-hour intervals from 16hrs to 32 hours inclusive, one of the cultures was harvested, washed three times, and finally suspended in 250mℓ of distilled water. Five slips were then suspended in the apparatus for thirty minutes, rinsed, and finally inspected, to determine the ideal growth period of the cells.

Results:

The adhesion of *S.cerevisiae* and *E.coli* was assessed qualitatively with respect to growth period, and displayed in Table A.6.

Growth time (h)	*E.coli*	*S.cerevisiae*
16	//	///
20	//	///
24	///	//
28	//	///
32	//	//

Table A.6: Glass slips were suspended for thirty minutes in microbial suspensions. The growth period of the suspensions varied from 16 to 32 hours, before cells were harvested and washed in distilled water. Cells were finally suspended in distilled water, and experiments were conducted at 22 +/- 1°C

The results showed that the effect of the growth period had little effect between 16 and 32 hours. The results did show that *S.cerevisiae* adhered more strongly to glass the *E.coli*. The experiment, however, did not take into consideration that as the cells grew, there would be a higher final concentration of cells in the suspension.
The adherence of *S.cerevisiae* and *E.coli* was assumed to be independent of growth period with respect to growth periods between 16 and 32 hours. Consequently, further experiments were performed using 24-hour cultures, as this was the most practical time scale to perform experiments.

A.3.2.5 The Effect of Solution Chemistry on Adhesion

This Section was designed to demonstrate the effect of buffer type and ionic strength had on the adhesion of *S.cerevisiae* and *E.coli* to glass.

Protocol:

Two buffer solutions with varying concentrations of NaCl were prepared. The two buffers were 3-[N-morpholino] propane-sulphonic acid and a NaH_2PO_4 buffer (both 25mM). The concentrations of NaCl used were 0, 10, 50, 100, and 500 mM.
24hr cultures of both *S.cerevisiae* and *E.coli* were grown, harvested, and washed in the respective buffer/NaCl solution three times, and finally suspended in the respective solution (250mℓ). Five slips were suspended for 30 minutes in each buffer/NaCl combination.
The glass slips were then rinsed and inspected by counting rather than using the previous qualitative analysis. Adhered bacteria were counted over a defined area ($0.0378mm^{-2}$). Three areas were counted per slip, and five slips were taken into consideration for each environment. The mean was taken for the fifteen counts, and results displayed as counts/mm^2.

Results

This experiment allowed the effect of NaCl concentration to be determined, as well as a direct comparison of the two different buffers used in the experiment. The adhesion of both *S.cerevisiae* and *E.coli* were shown in Tables A.7 and A.8 respectively.

[NaCl] (mM)	MOPS	NaH_2PO_4
0	1100	2000
10	5300	8000
50	6500	9000
100	8200	10000
500	8000	8000

Table A.7: The adherence of *S.cerevisiae* to glass cover slips. 24hr cultures were grown, harvested, and suspended in either MOPS (25mM), or NaH_2PO_4 (25mM). NaCl was used to adjust salt concentration to vary from 0mM [NaCl] to 500mM [NaCl]. Experiments were conducted at 22 +/- 1°C. This experiment was a duplicate of the results shown in Table A.4. Figures are given in Count/mm^2.

[NaCl] (mM)	MOPS	NaH_2PO_4
0	260	130
10	400	270
50	790	530
100	1100	800
500	800	660

Table A.8: The adherence of *E.coli* to glass cover slips. 24hr cultures were grown, harvested, and suspended in either MOPS (25mM), or NaH_2PO_4 (25mM). NaCl was used to adjust salt concentration to vary from 0mM [NaCl] to 500mM [NaCl]. Experiments were conducted at 22 +/- 1°C. This experiment was a duplicate of the results shown in Table A.5. Figures are given in Count/mm^2.

The results showed that *E.coli* adhered less to the glass compared with *S.cerevisiae*. *S.cerevisiae* showed higher levels of adhesion in phosphate buffer, whereas the bacteria seemed to show higher levels of adherence in MOPS solution. Reliable conclusions cannot be made from this experimental protocol when investigating the effect of ionic strength, due to the primitive nature of this method of assessment, especially the washing technique as illustrated in Figure 1.10. The method did however show that microbial cells adhere successfully to glass and can be successfully counted.

The effect of salt concentration does seem to affect the adhesion but this could not be reliably confirmed with the results obtained using this method. Adherence seemed to be at a maximum when the salt concentration was approximately 50mM.

A.3.2.6 Adhesion of S.cerevisiae and E.coli to Different Types of Glass

The aim of this experiment was to determine the effect of surface treatment of the glass on adhesion of the cells. Untreated, acid-washed and poly-l-lysine coated glass surfaces were assessed with respect to adhesion. Acid-washed glass should have a less negatively charged surface compared to the standard glass that was used. The lysine polymer used to coat glass was thought to promote bacterial adhesion (Jacobson and Branton, 1977).

Protocol:

Experiment A.3.2.5 was repeated using three types of glass. Acid-washed glass was prepared by soaking in ethanol (10 min), then soaked in 1M HCl (10 minutes), and rinsed in distilled water prior to use. Poly-l-lysine slides were obtained from Sigma, and also soaked in ethanol, and rinsed prior to use with distilled water. The standard glass was also used with previous buffers and salt solutions.

Results:

The results for the adhesion of *S.cerevisiae* in MOPS and phosphate buffer, and *E.coli* in MOPS and phosphate buffer to untreated, acid-washed, and poly-l-lysine coated glass are shown in Tables A.9, A.10, A.11, and A.12 respectively.

The results showed poly-l-lysine coated glass enhanced adhesion of *S.cerevisiae* and *E.coli* compared with the respective adhesion to the untreated glass surface. Acid-washed glass seemed to inhibit adhesion compared with the results obtained using untreated glass. The cell surface charge was assumed to be negative, and in relation to charge, would be attracted to a positive surface. However, glass was a negative surface, and acid washing negated this charge, making the surface more hydrophobic. Both *S.cerevisiae* and *E.coli* preferred remain in solution rather than be deposited on the more hydrophobic glass surface.

As a general rule, the cells prefer to adhere at salt concentrations between 50mM and 100mM as seen in Section A.3.2.5, but as previously acknowledged no reliable conclusions can be made from the experiments due to its primitive nature.

[NaCl]	Plain glass	Acid-Washed glass	Poly-l-lysine glass
0	3700	130	400
10	260	400	530
50	32	28	260
100	260	16	130

Table A.9: The adherence of *S.cerevisiae* to untreated, acid-washed, or poly-l-lysine coated glass. Experiments the suspension was in MOPS (25mM), and 0, 10, 50, and 100mM NaCl. Experiments were conducted at 22 +/- 1°C. Figures are given in Count/mm^2.

[NaCl]	Plain glass	Acid-washed glass	Poly-l-lysine glass
0	1200	130	270
10	3200	1300	10000+
50	400	1100	800
100	3600	800	300

Table A.10: The adherence of *S.cerevisiae* to untreated, acid-washed, or poly-l-lysine coated glass. Experiments the suspension was in NaH_2PO_4 (25mM), and 0, 10, 50, and 100mM NaCl. Experiments were conducted at 22 +/- 1°C. Figures are given in Count/mm^2.

[NaCl]	Plain glass	Acid-washed glass	Poly-l-lysine glass
0	400	260	10000+
10	1500	530	5700
50	8500	130	1100
100	32	37	3200

Table A.11: The adherence of *E.coli* to untreated, acid-washed, or poly-l-lysine coated glass. Experiments the suspension was in MOPS (25mM), and 0, 10, 50, and 100mM NaCl. Experiments were conducted at 22 +/- 1°C. Figures are given in Count/mm^2.

[NaCl]	Plain glass	Acid-washed glass	Poly-l-lysine glass
0	660	5300	10000+
10	4500	3600	10000+
50	3400	530	5300
100	24	130	10000+

Table A.12: The adherence of *E.coli* to untreated, acid-washed, or poly-l-lysine coated glass. Experiments the suspension was in NaH_2PO_4 (25mM), and 0, 10, 50, and 100mM NaCl. Experiments were conducted at 22 +/- 1°C. Figures are given in Count/mm^2.

A.3.2.7 The Use of a Different Rinsing Technique

The manual rinsing technique used in the previous experiments in this Chapter was identified as a potential source of error as detailed in Figure 1.10, as the surface of the cover slip was subjected to variation in the applied hydrodynamic force when rinsed. An alternative rinsing technique using a controlled stirrer over five minutes

was investigated. The new method would inevitably remove more attached cells, but would do so in a more controlled manner.

Protocol:

S.cerevisiae and *E.coli* and were grown in 24-hour cultures, harvested, and washed three times, in both MOPS or NaH_2PO_4 buffer with NaCl (50mM), and finally suspended in this buffer/salt solution. Five slips were suspended with the cells in the respective solutions, and removed after 5, 10, 20, 35, and 60mins. The resultant glass cover slips were rinsed for five minutes, by suspending in the apparatus with the buffer/salt solution only, and stirred at a constant rate. The experiment was also used to assess the effect of time on adhesion.

Results:

The adhesion of *S.cerevisiae* and *E.coli* incorporating new rinsing technique was are shown in Tables A.13 and A.14 respectively.

The results demonstrated that the washing technique was reliable, and the method provided more consistent results. The observed trends were that the adhesion of *S.cerevisiae* was higher in the phosphate buffer and *E.coli* adhered in greater levels with MOPS buffer, as previously observed, and the new washing process removed more residual cells from the surface see Tables A.9, A.10, A.11, and A.12.

With respect to the effect of time on adhesion, a maximum value of adhesion was achieved within 20 minutes with both *S.cerevisiae* and *E.coli.*

Any further experiments using this method were performed using the rinsing technique detailed in this Section.

Incubation Time (min)	MOPS	NaH_2PO_4
5	1500	2200
10	2000	3200
20	4200	7400
35	4000	8200
60	4600	7700

Table A.13: The adhesion of *S.cerevisiae* to glass slips. Time of incubation of the slips in suspension varied from 5 to 60 minutes. A new washing technique was also employed, in the hope of providing more consistent results. Suspensions were made in MOPS (25mM) or NaH_2PO_4 (25mM). Experiments were conducted at 22 +/- 1°C. Figures are given in Count/mm^2.

Incubation Time (min)	MOPS	NaH_2PO_4
5	1200	530
10	2100	800
20	2600	1060
35	2500	530
60	2400	400

Table A.14: The adhesion of *E.coli* to glass slips. Time of incubation of the slips in suspension varied from 5 to 60 minutes. A new washing technique was also employed, in the hope of providing more consistent results. Suspensions were made in MOPS (25mM) or NaH_2PO_4 (25mM). Experiments were conducted at 22 +/- 1°C. Figures are given in Count/mm^2.

A.3.2.8 The Relationship Between Optical Density (OD) and Adhesion of E.coli to Glass

Having developed a more reliable rinsing technique, the effect of cellular concentration on the adhesion of *E.coli* was to assessed.

Protocol:

E.coli was grown in 24hr broth, harvested, washed three times, and suspended in differing distilled water to provide differing cellular ODs between 0.1 and 1. Five slips were suspended with the cells at each OD, and removed after 20mins. The cover slips were rinsed for five minutes, as detailed in Section A.3.2.7.

Results:

As optical density increased, adherence increased linearly, as illustrated in Figure A.2. The results showed that the adhesion of *E.coli* increased linearly with the suspension concentration (OD) of the bacteria. However, these results showed variation that suggested that alternative methods should be used for assessing adhesion.

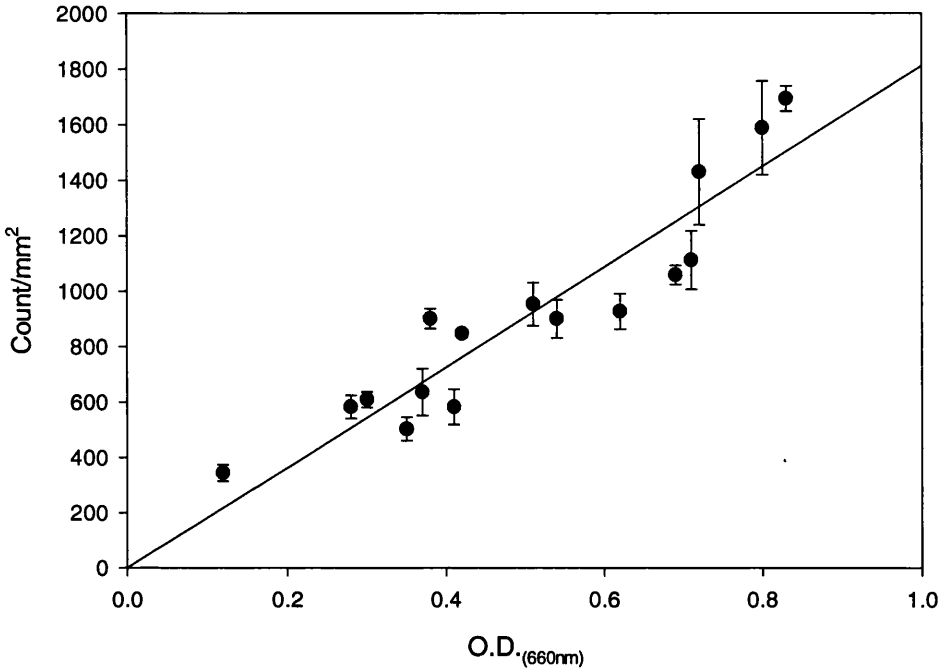

Figure A.2: The relationship between cellular concentration and adhesion to glass. Glass slips were incubated with varying concentrations of *E.coli* in distilled water. The slips were incubated in the bacterial suspension for 20 minutes, and conducted at 22 +/- 1°C.

A.3.2.9 Summary of Preliminary Experiments

Having considered the results of the preliminary experiments, the method of monitoring adhesion was deemed to have too much potential error. This method was a very simple assessment of adhesion, and allowed the comparison of certain parameters. This assessment method provided a limited understanding of cellular adhesion, which allowed a more experienced approach to the assessment of adhesion using other methods.

The use of magnetic stirrer to provide agitation in the cellular suspension, although an improvement on the manual rinsing technique, was still susceptible to variation, as the shear generated by the stirrer is unlikely to remain constant. The angle of contact between the glass slips and the suspension will also vary.

Although the method detailed in this Section did not provide reliable data, the work did, however, achieve its purpose, to determine the ease of assessing cellular adhesion, using visual methods of inspection.

There was little difference in the results obtained using both NaH_2PO_4 and MOPS as the solution buffer, and consequently, further adhesion experiments using other methods were performed with NaH_2PO_4 as the solution buffer, due to its availability.

Appendix B

Contact Angle Measurements of Glass and Stainless Steel

B.1 The Particles Used in Adhesion Experiments

The contact angles of buffered water were determined for glass and stainless steel as detailed in Section 4.2. Figures B.1 and B.2 represent the contact angle measurements taken at 1 and 10 seconds after application of the sample solution to the respective surface.

t = 1 second **t = 10 seconds**

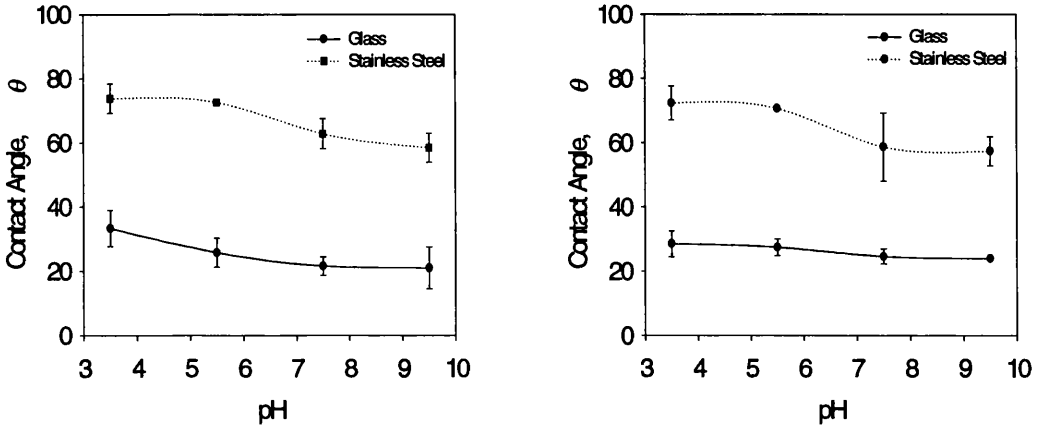

Figure B.1: The contact angles of 25mM NaH_2PO_4 in distilled water on glass, and stainless steel, relative to pH. Measurements were taken at 1 and 10 seconds respectively. Standard deviation is shown where the error is larger than the symbols used. Experiments were conducted at 22 +/- 1°C. The pH was adjusted using HCl, or NaOH (1M) respectively. Surfaces were polished using 1μm diamond paste.

Glass

pH	0.1 seconds	1 second	10 seconds
3.5	41.5 +/- 8.8	33.4 +/- 5.6	28.5 +/- 4.0
5.5	27.7 +/- 3.0	25.8 +/- 4.5	27.5 +/- 2.6
7.5	28.2 +/- 6.0	21.6 +/- 2.8	14.4 +/- 2.3
9.5	21.0 +/- 5.7	21.0 +/- 6.5	24.0 +/- 0.1

Stainless Steel

pH	0.1 seconds	1 second	10 seconds
3.5	76.1 +/- 4.0	73.8 +/- 4.6	72.3 +/- 5.2
5.5	76.0 +/- 0.1	72.6 +/- 0.2	70.6 +/- 0.1
7.5	66.6 +/- 6.8	62.7 +/- 4.7	58.6 +/- 10.6
9.5	62.4 +/- 3.3	58.5 +/- 4.5	57.4 +/- 4.6

Table B.1: The Contact Angles for Glass and Stainless Steel with respect to pH, at t=0.1, 1, and 10 seconds. 25mM NaH_2PO_4 was adjusted to the required pH using either HCl or NaOH (1M). Experiments were conducted at 22 +/- 1°C.

Appendix C

Materials and Results from the use of the Packed Column

C.1 The Composition of Stainless Steel 316L

The composition of the stainless steel used in conjunction with the Packed Column, referred to by Section 5.2.5.

Fe	Balance	**P**	0.023 %
Cr	16.2 %	**Si**	0.37 %
Ni	13.2 %	**C**	0.022 %
Mo	2.3 %	**S**	0.009 %
Mn	1.4 %		

Table C.1: The composition of Stainless Steel 316L powder, supplied by Osprey Metals, Ltd. (UK). Tel. No: (01639) 634121.

C.2 The Calculation of the Column Parameters

The calculation of the approximate volume and the surface area of the collector within the column referred to by Section 5.1.2.3 are given below in Sections C.2.1 and C.2.2.

C.2.1 The Calculation of The Total Volume of Collector Within the Packed Column

Column Radius (r_{column}) = 0.005 m
Average Column Length (h_{column}) = 0.435 m

Column Volume (V_{column}) = $\pi r^2 h = \pi (r_{column})^2 \times (h_{column})$

$$(V_{column}) = \mathbf{3.4165 \times 10^{-5} m^3}$$

The voidage e is 0.4 as shown in Section 5.4.5, and therefore:

Total Collector Volume in Column ($V_{collector}$) = $(1-e) \times (V_{column})$

$$(V_{collector}) = \mathbf{2.05 \times 10^{-5} m^3}$$

C.2.2 The Calculation of The Total Surface Area of Collector Within the Packed Column

Collector Sphere Radius (r_{sphere}) = 0.0000675 m

Volume of 1 sphere (V_{sphere}) = 4/3 π (r_{sphere})^3

Surface area of 1 sphere (A_{sphere}) = 4 π (r_{sphere})^2

$$(V_{sphere}) = \mathbf{1.288 \times 10^{-12}\ m^3}$$

$$(A_{sphere}) = \mathbf{5.726 \times 10^{-8}\ m^2}$$

The total number of spheres in the Packed Column (N_{sphere}) = ($V_{collector}$) / (V_{sphere})

$$(N_{sphere}) = \mathbf{1.6 \times 10^7}$$

Total Collector Surface Area ($A_{collector}$) = (N_{sphere}) x (A_{sphere})

$$(A_{collector}) = \mathbf{0.916\ m^2}$$

C.3 The Conversion of Flow Rate from g/min to m/s

The determination of the Reynolds Number for the flow across the collector surface in the column required the flow rate to be presented in m/s, shown in Section 5.1.2.5. The flow rate through the column was measured in g/min, and the conversion to m/s is shown below.

The maximum flow rate achieved within the Column was 18g/min, the equivalent to 3×10^{-7} m^3/sec.

The cross sectional area of the Column was 7.85×10^{-5} m^2.
The available area was therefore 7.85×10^{-5} m^2 x e, which equalled 3.14×10^{-5} m^2.

The velocity of the fluid over the collector surface (m/s) was therefore:

Flow Rate (m^3/sec) / Available area (m^2)

$(3 \times 10^{-7}) / (3.1415 \times 10^{-5})$

= 0.00955 m/s

C.4 The Analysis of Data generated by a Break-through Curve, using a Spreadsheet

Section 5.3.5 details the development of the analysis of data obtained from the break-through curves generated from the Packed Column. The data were transferred onto an Excel spreadsheet, and analysed as described below, allowing the total percentage recovery from the Column to be calculated.

Column 1	Column 2	Column 3	Column 4	Column 5	Column 6	Column 7	Column 8
Time (s)	Volume Eluted (mℓ)	Voltage (V)	Voltage-Baseline (V)	Cell OD	Actual OD	Area	%age sample area
128	13.65	0.846	0.002	0.001	0.001	0.00011	0.0090
129	13.76	0.846	0.002	0.001	0.001	0.00011	0.0090
130	13.87	0.848	0.004	0.002	0.002	0.00021	0.0181
131	13.97	0.853	0.009	0.005	0.004	0.00047	0.0406
132	14.08	0.858	0.014	0.007	0.007	0.00074	0.0632
133	14.19	0.868	0.024	0.012	0.012	0.00127	0.1084
134	14.29	0.877	0.033	0.017	0.016	0.00174	0.1490
135	14.4	0.893	0.049	0.025	0.024	0.00259	0.2212
136	14.51	0.91	0.066	0.033	0.033	0.00348	0.2980
137	14.61	0.931	0.087	0.044	0.043	0.00459	0.3928
138	14.72	0.956	0.112	0.056	0.055	0.00590	0.5057
139	14.83	0.986	0.142	0.071	0.070	0.00749	0.6411

Table C.2: An example of an analysis spreadsheet. Column 2 (x-axis) represents the volume eluted, with respect to the flow rate (5.48 mℓ/min) and time (Column 1). Column 3 represents the output from the spectrophotometer (V). This figure has the baseline removed, in this case 0.844 to produce Column 4. The OD of the flow-through cell (Column 5) is half of the real voltage. Column 6 takes into consideration the correction factor between the flow-through cuvette and 4mℓ cuvette. The eluate area (Column 7) is calculated by multiplying Column 6 ($OD_{cuvette}$) by the volume eluted each second (in this case 0.091mℓ). This figure is converted to percentage of start sample (Column 8), as the volume and OD of the start sample are known (in this case 0.362), and used as the y-axis. The percentage recovery for each reading is totalled for each run, and provides the total percentage recovery of the start sample.

C.5 The Determination of the Volume of the Sample Loop

The experiment detailed in Section 5.4.1 allowed the determination of the volume of the sample loop used to introduce the sample into the column, using Equation 5.2. The corresponding data is given below in Table C.3.

	Collected Volume (mℓ)	$OD_{(660nm)}$
1	2.78 +/- 0.005	0.083
2	2.58+/- 0.005	0.090
3	2.69+/- 0.005	0.080
4	2.75+/- 0.005	0.076
5	2.50+/- 0.005	0.092
6	2.76+/- 0.005	0.082
7	2.56+/- 0.005	0.086
Ave	**2.66 +/- 0.005**	**0.084**

Table C.3: $OD_{(660nm)}$ and volumes of samples collected when calculating the volume of the injection loop. Dextran blue was used as the sample solution. Sample OD was 1.52 +/- 0.02. The relationship between sample and eluate is given in Equation 5.2.

C.6 The Determination of the Percentage Recovery from the Injection Apparatus

Section 5.4.3 describes an experiment to determine that the retention by the injection apparatus was negligible. Table C.4 presents the corresponding data as percentage recovery from both the injection loop and the top end piece (frit), shown in Figure 5.6.

	Recovery from Loop (%)	**Recovery from Frit (%)**
Aminated Beads	99.89 +/- 0.34	99.54 +/- 0.51
Carboxylated Beads	99.75 +/- 0.62	99.56 +/- 0.12
***B.mycoides* Spores**	99.78 +/- 0.42	99.23 +/- 0.21
***B.subtilis* Spores**	99.33 +/- 0.82	99.27 +/- 0.13

Table C.4: The percentage recovery of aminated and carboxylated latex beads, and *B.mycoides* and *B.subtilis* spores, carried out at pH 3.5, and 22 +/- 1°C. Samples were taken directly from the injection loop, and from the frit.

C.7 The Determination of the Practical Voidage within the Column

Section 5.4.5 details the determination of the practical voidage in three columns, and compares the values to the theoretical voidage of 40%. Table C.5 presents the data generated from the experiment.

	Column 1	**Column 2**	**Column 3**
Column Length (cm)	43.9	45.3	46.4
Column Volume (cm^3)	34.48	35.58	36.44
Predicted Voidage (cm^3)	**13.79**	**14.23**	**14.58**
Practical Voidage (cm^3)	**13.96 +/- 0.09**	**14.51 +/- 0.21**	**14.62 +/- 0.05**
Percentage Difference	**1.23 +/- 0.65**	**1.97 +/- 1.48**	**0.27 +/- 0.34**
Practical Value for Voidage (*e*)	**0.405**	**0.408**	**0.401**

Table C.5: The comparison of practical and theoretical voidage within the Column. Three Columns of various lengths were analysed using dextran blue solution. The peak of the resultant breakthrough curve was interpreted as the voidage of the Column, relative to the volume of liquid eluted from the Column. Experiments were conducted at 22 +/- 1°C.

C.8 The Results from the Preliminary Experiments with the Packed Column

Section 5.5.2 determined the effect of flow rate on the adhesion of carboxylated latex beads (0.5μm). The results for pH 4.5, and 5.5, are shown in Figure C.1.

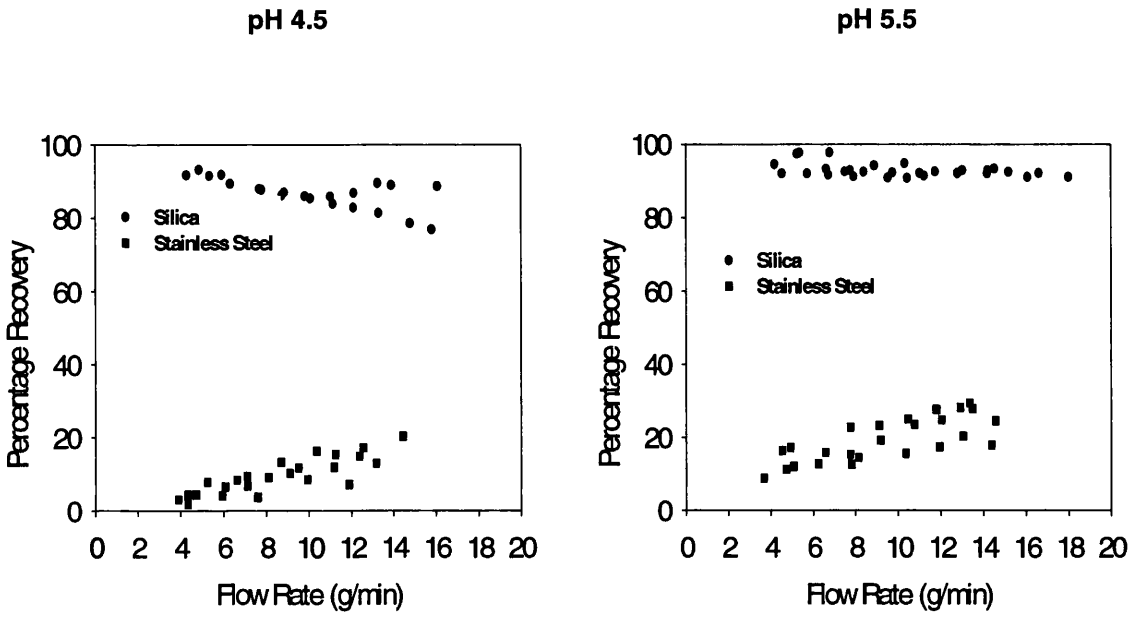

Figure C.1: The effect of flow rate on adhesion. Silica and Stainless Steel packing (70-200μm) was used in conjunction with carboxylated latex beads (0.5μm) in three Columns, at pH 4.5, and 5.5 over a range of flow rates. Experiments were conducted at 22 +/- 1°C.

Appendix D

Results from the Spinning Disc

D.1 The Results of the Spinning Disc presented in 3-Dimensional Plots

The following plots represent the results discussed in Section 6.5. The results presented here allow a direct qualitative comparison of the adhesion of aminated and carboxylated latex beads, and the spores of *B.mycoides* and *B.subtilis* to glass and stainless steel.

D.1.1 Aminated Beads

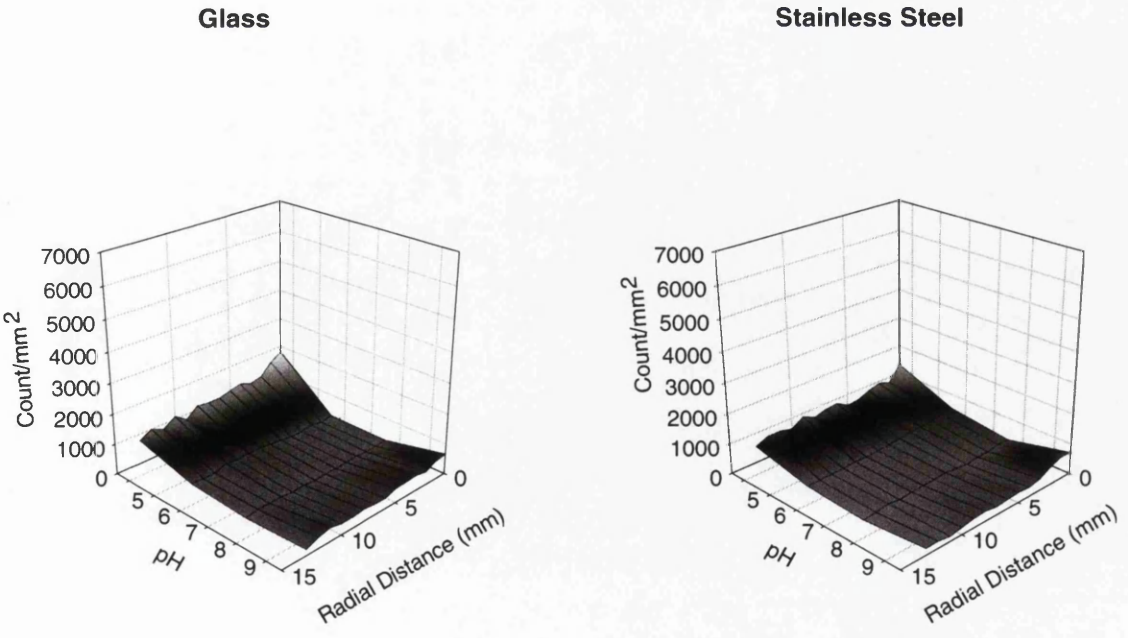

Figure D.1: The adhesion of aminated latex beads to silica and stainless steel as a function of radial distance and pH.

D.1.2 Carboxylated Beads

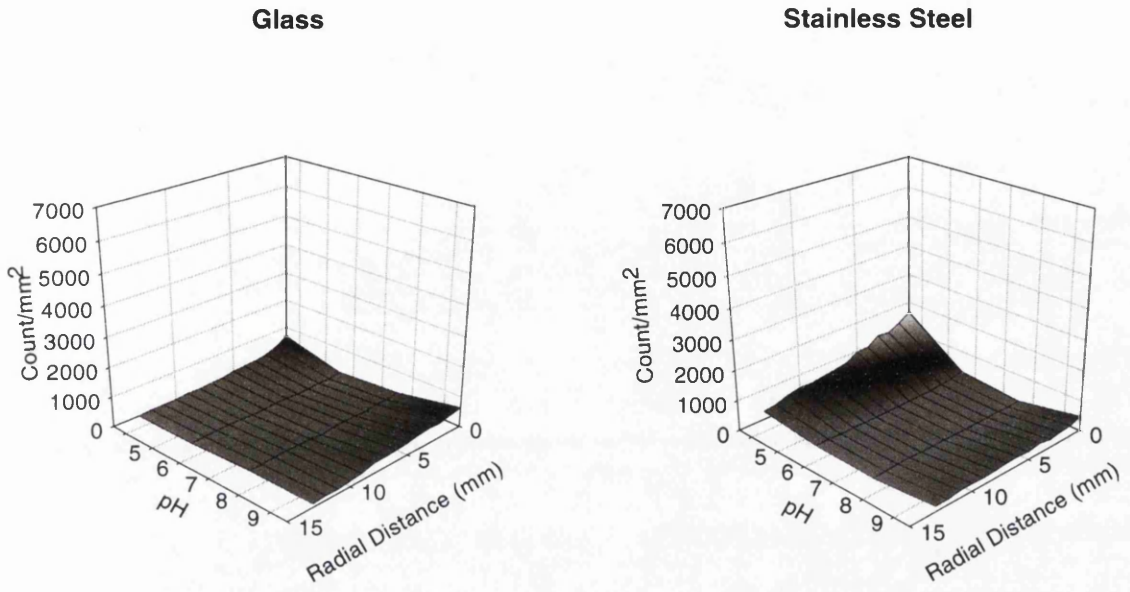

Figure D.2: The adhesion of carboxylated latex beads to silica and stainless steel as a function of radial distance and pH.

D.1.3 B.mycoides Spores

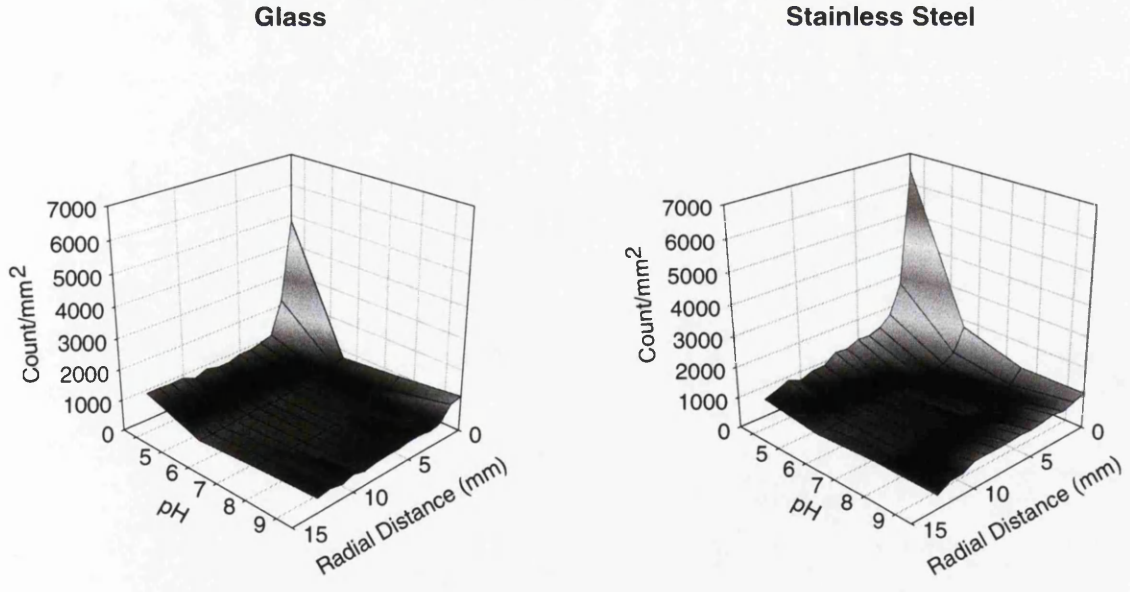

Figure D.3: The adhesion of *B.mycoides* spores to silica and stainless steel as a function of radial distance and pH.

D.1.4 B.subtilis Spores

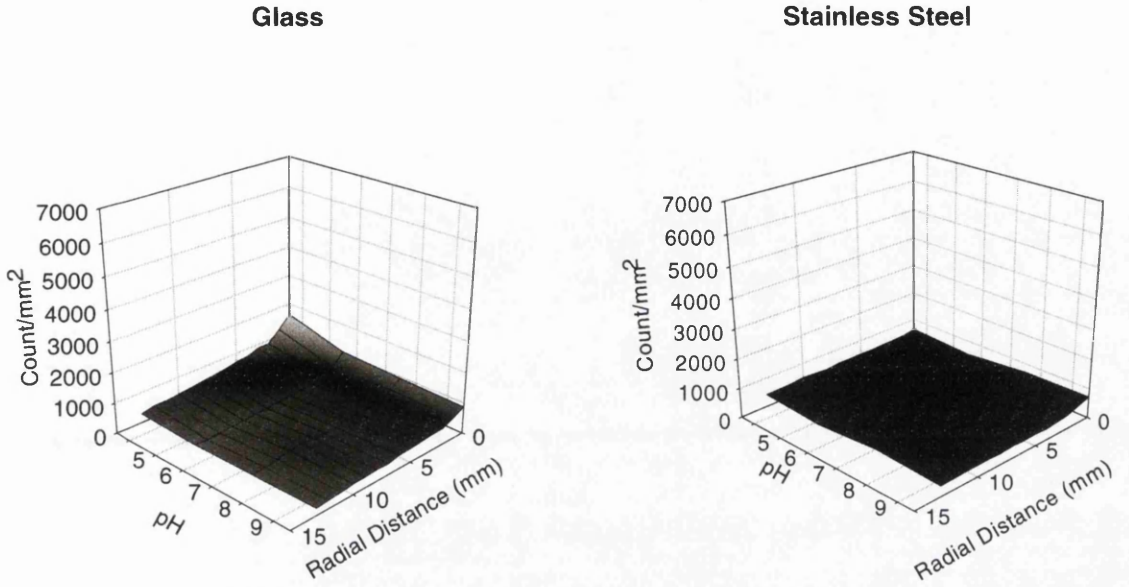

Figure D.4: The adhesion of *B.subtilis* spores to silica and stainless steel as a function of radial distance and pH.

D.2 The Results of the Spinning Disc presented in 2-Dimensional Plots

The following plots represent the results discussed in Section 6.5. The results presented here allow a quantitative comparison of the adhesion of aminated and carboxylated latex beads, and the spores of *B.mycoides* and *B.subtilis* to glass and stainless steel.

D.2.1 Adhesion to Glass

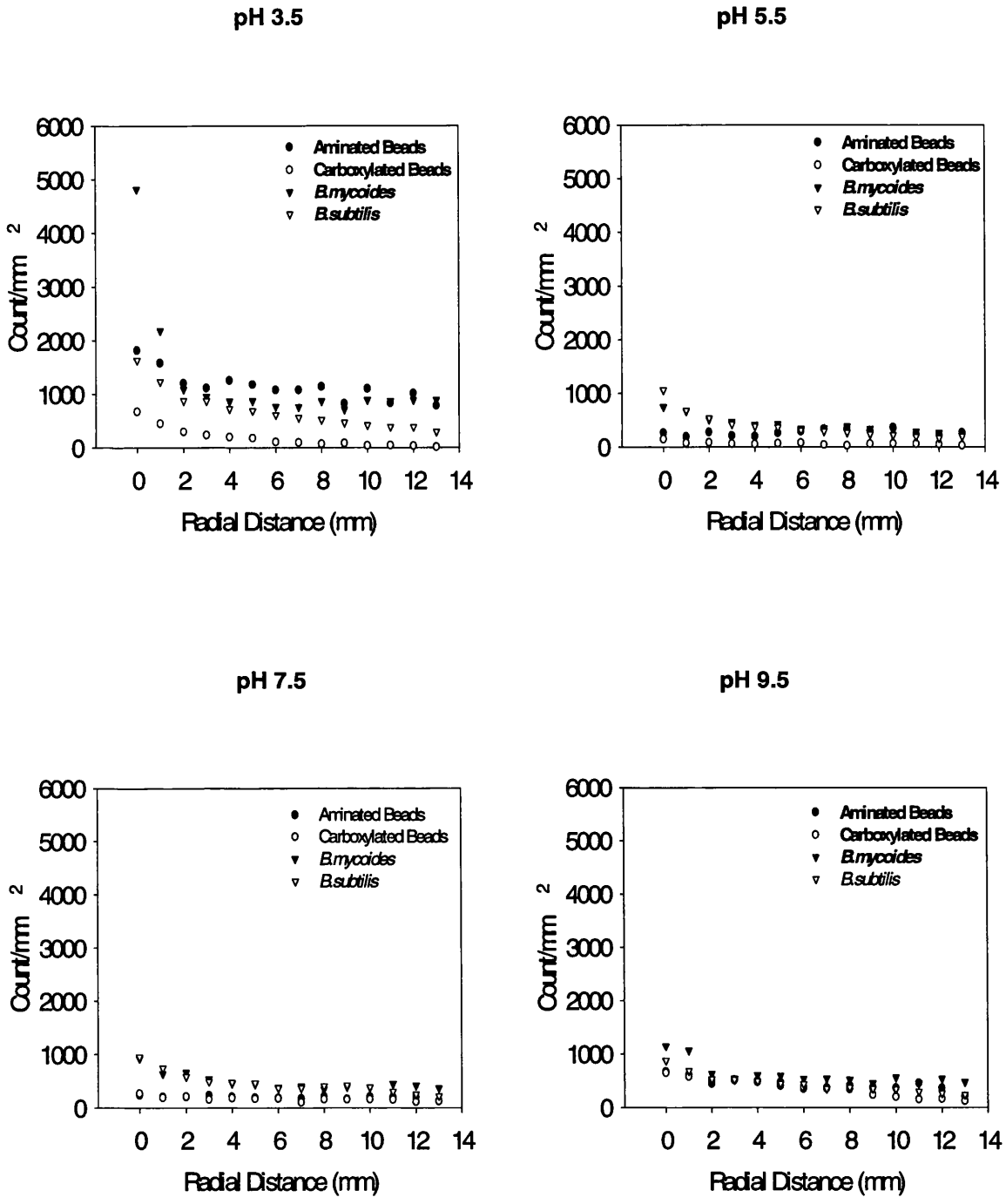

Figure D.5: The adhesion of four colloidal particles to glass in relation to radial distance. Particles were suspended in 25mM NaH_2PO_4, and pH adjusted with HCl (1M) or NaOH (1M). The experiment was conducted at 300rpm for 30 minutes, and temperature kept constant at 22 +/- 1°C. Error bars were omitted for reasons of clarity. The average standard deviation for each colloid was 260, 111, 708, and 251, for aminated and carboxylated latex beads, and the spores of *B.mycoides* and *B.subtilis* respectively.

D.2.2 Adhesion to Stainless Steel

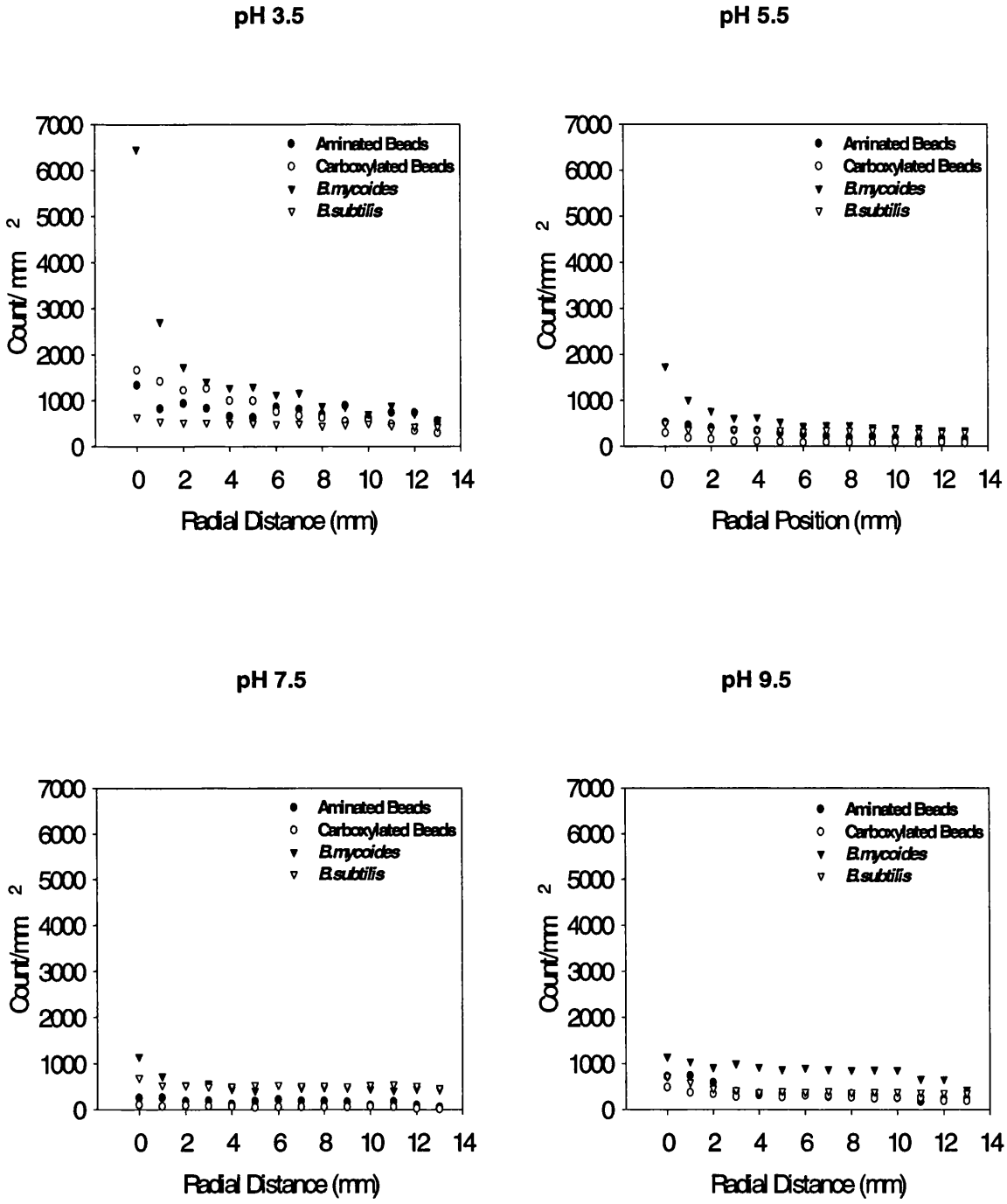

Figure D.6: The adhesion of four colloidal particles to stainless steel in relation to radial distance. Particles were suspended in 25mM NaH_2PO_4, and pH adjusted with HCl (1M) or NaOH (1M). The experiment was conducted at 300rpm for 30 minutes, and temperature kept constant at 22 +/- 1°C. Error bars were omitted for reasons of clarity. The average standard deviation for each colloid was 193, 321, 1220, and 167, for aminated and carboxylated latex beads, and *B.mycoides* and *B.subtilis* respectively.

Appendix E

Results from the Radial Flow Chamber

E.1 The Dependence of Adhesion on Time

The following data represents the dependence of adhesion with respect to time, at a radial distance of 40mm, as detailed in Section 7.4.3.

Glass

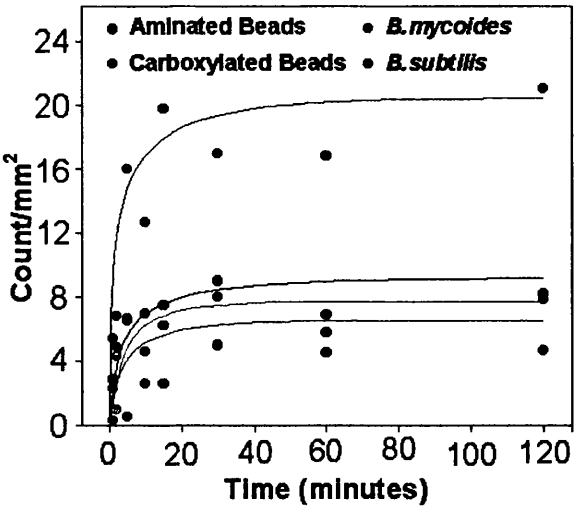

Figure E.1: The effect of time on adhesion of aminated and carboxylated beads, and *B.mycoides* and *B.subtilis* spores to glass at a radial distance of 40mm. Experiments were carried out at pH 5.5 over a time period ranging from t = 0 to t = 120 minutes. Temperature was maintained at 22 +/- 1°C. Error bars are omitted for the sake of clarity.

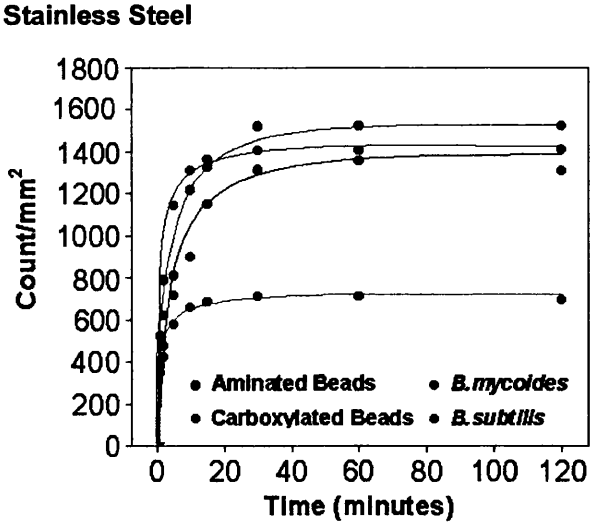

Figure E.2: The effect of time on adhesion of aminated and carboxylated beads, and *B.mycoides* and *B.subtilis* spores to stainless steel at a radial distance of 40mm. Experiments were carried out at pH 5.5 over a time period ranging from t = 0 to t = 120 minutes. Temperature was maintained at 22 +/- 1°C. Error bars are omitted for the sake of clarity.

E.2 The Results of the Radial Flow Chamber presented in 3-Dimensional Plots

The following plots represent the results discussed in Section 7.5, presented here allow a direct qualitative comparison of adhesion to glass and stainless steel.

E.2.1 Aminated Beads

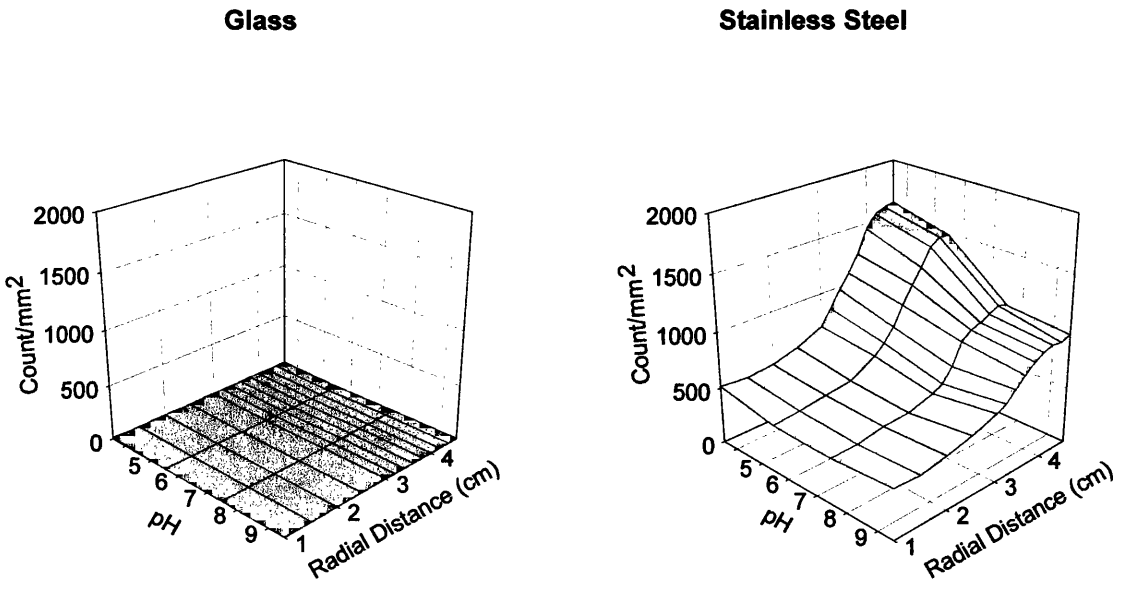

Figure E.3: The adhesion of aminated latex beads to silica and stainless steel as a function of radial distance and pH.

E.2.2 Carboxylated Beads

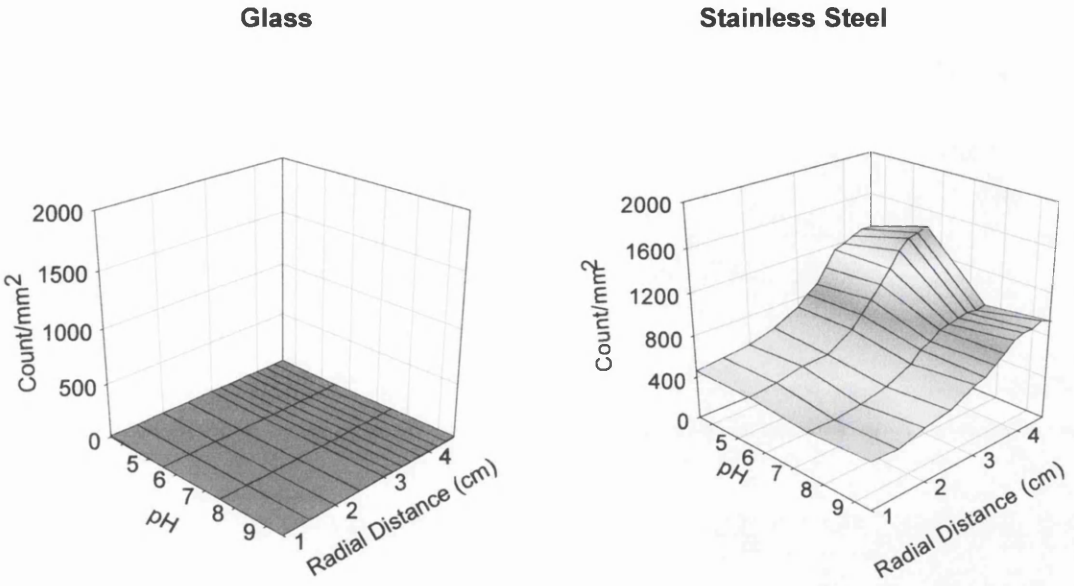

Figure E.4: The adhesion of carboxylated latex beads to silica and stainless steel as a function of radial distance and pH.

E.2.3 B.mycoides Spores

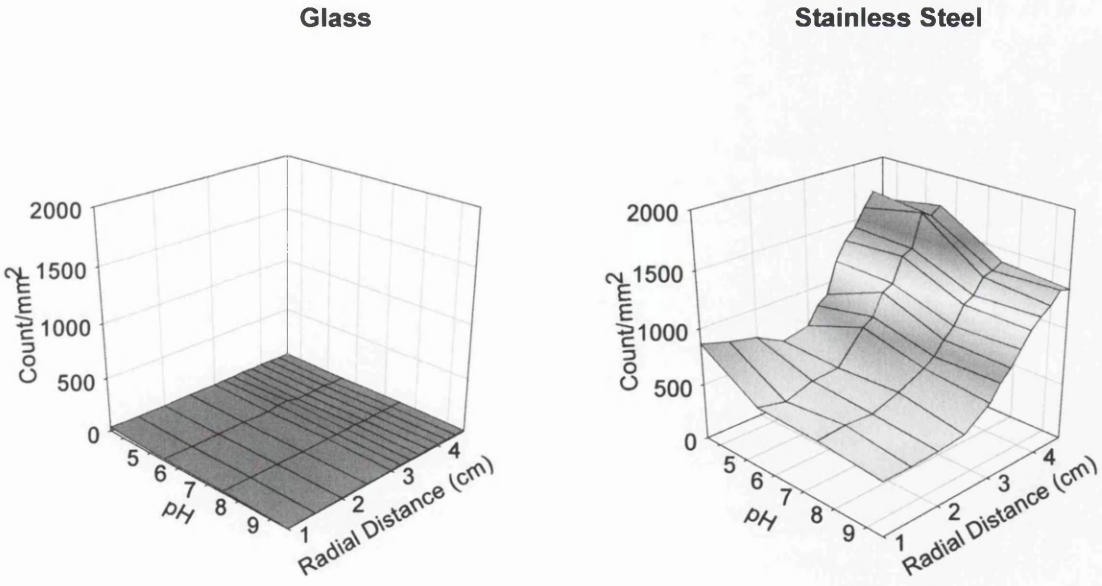

Figure E.5: The adhesion of *B.mycoides* spores to silica and stainless steel as a function of radial distance and pH.

E.2.4 B.subtilis Spores

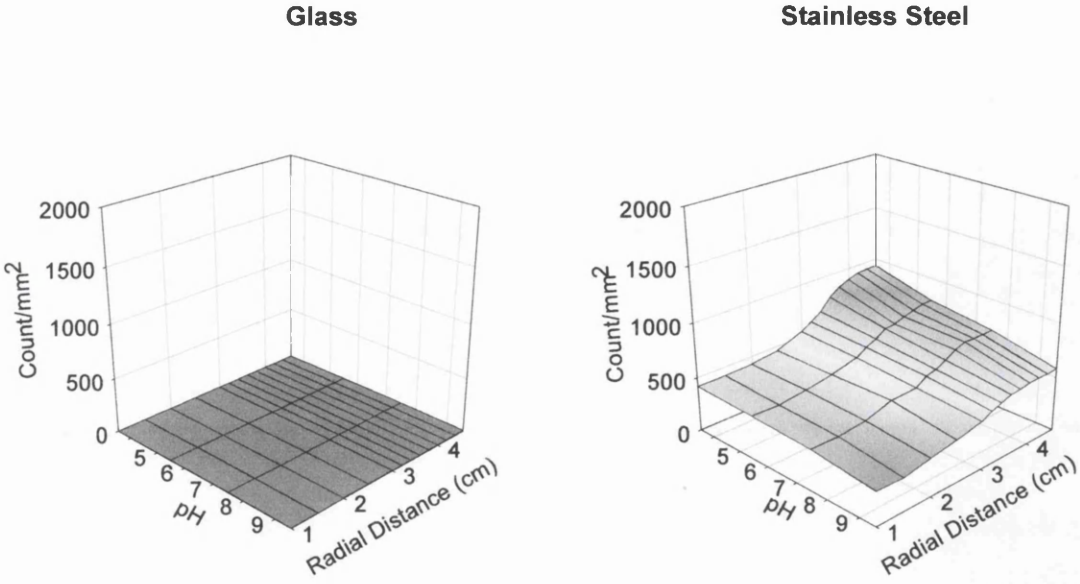

Figure E.6: The adhesion of *B.subtilis* spores to silica and stainless steel as a function of radial distance and pH.

E.3 The Results of the Radial Flow Chamber presented in 2-Dimensional Plots

The following plots represent the results discussed in Section 7.5. The results presented here allow a quantitative comparison of the adhesion of aminated and carboxylated latex beads, and the spores of *B.mycoides* and *B.subtilis* to glass and stainless steel.

E.3.1 Adhesion to Glass

pH 3.5

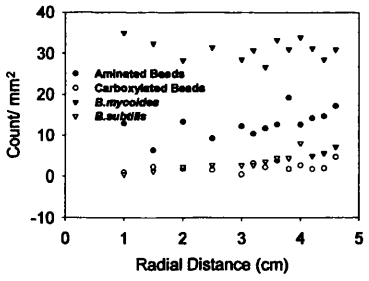

pH 5.5

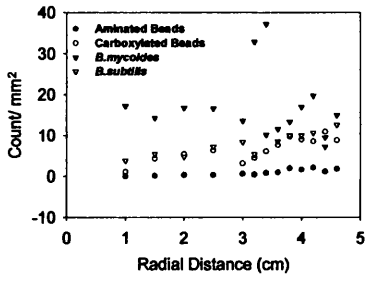

pH 7.5

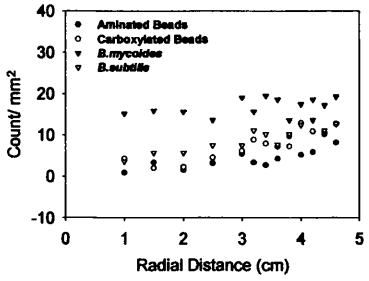

pH 9.5

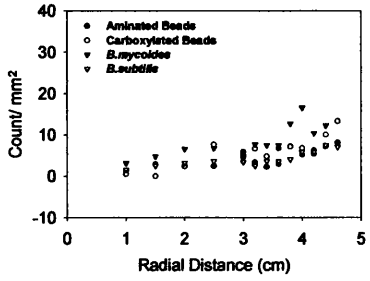

Figure E.7: The adhesion to glass in relation to radial distance. Particles were suspended in 25mM NaH_2PO_4, and pH adjusted with HCl (1M) or NaOH (1M). The experiment was conducted at 1.4ℓ/min for 30 minutes, and temperature kept constant at 22 +/- 1°C. Error bars were omitted for reasons of clarity. The average standard deviation for each colloid was 5, 22, 13, and 7mm^{-2}, for aminated and carboxylated latex beads, and the spores of *B.mycoides* and *B.subtilis* respectively.

E.3.2 Adhesion to Stainless Steel

pH 3.5

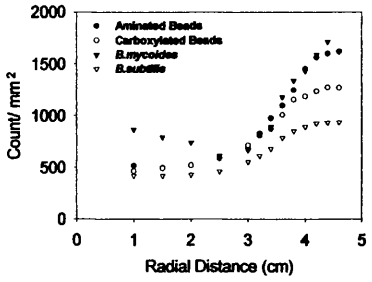

pH 5.5

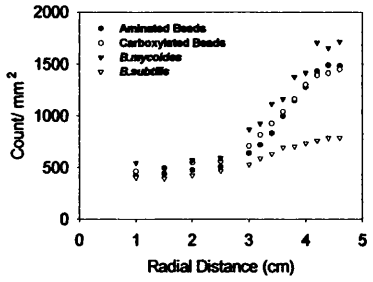

pH 7.5

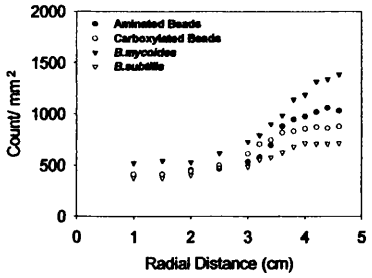

pH 9.5

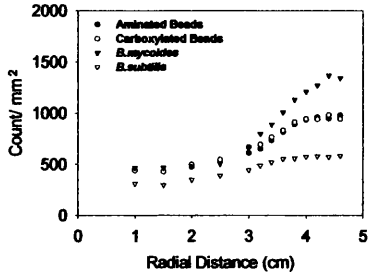

Figure E.8: The adhesion of four colloidal particles to stainless steel in relation to radial distance. Particles were suspended in 25mM NaH_2PO_4, and pH adjusted with HCl (1M) or NaOH (1M). The experiment was conducted at 1.4ℓ/min for 30 minutes, and temperature kept constant at 22 +/- 1°C. Error bars were omitted for reasons of clarity. The average standard deviation for each colloid was 94, 81, 156, and 55 mm^{-2}, for aminated and carboxylated latex beads, and *B.mycoides* and *B.subtilis* respectively.

Appendix F

Results from the Combination of the Spinning Disc and the RFC

F.1 The Comparative Data of the Adhesion to Glass Assessed Using the Spinning Disc and the RFC

The following data represents the results of the comparative analyses of the adhesion of aminated and carboxylated latex beads and the spores of *B.mycoides* and *B.subtilis* to glass, assessed using the Spinning Disc and the RFC, as detailed in Chapters 6 and 7 respectively. The adhesion of aminated and carboxylated latex beads and the spores of *B.mycoides* and *B.subtilis* to glass to steel is discussed and compared in Chapter 8.

F.1.1 The Adhesion of Aminated Beads to Glass

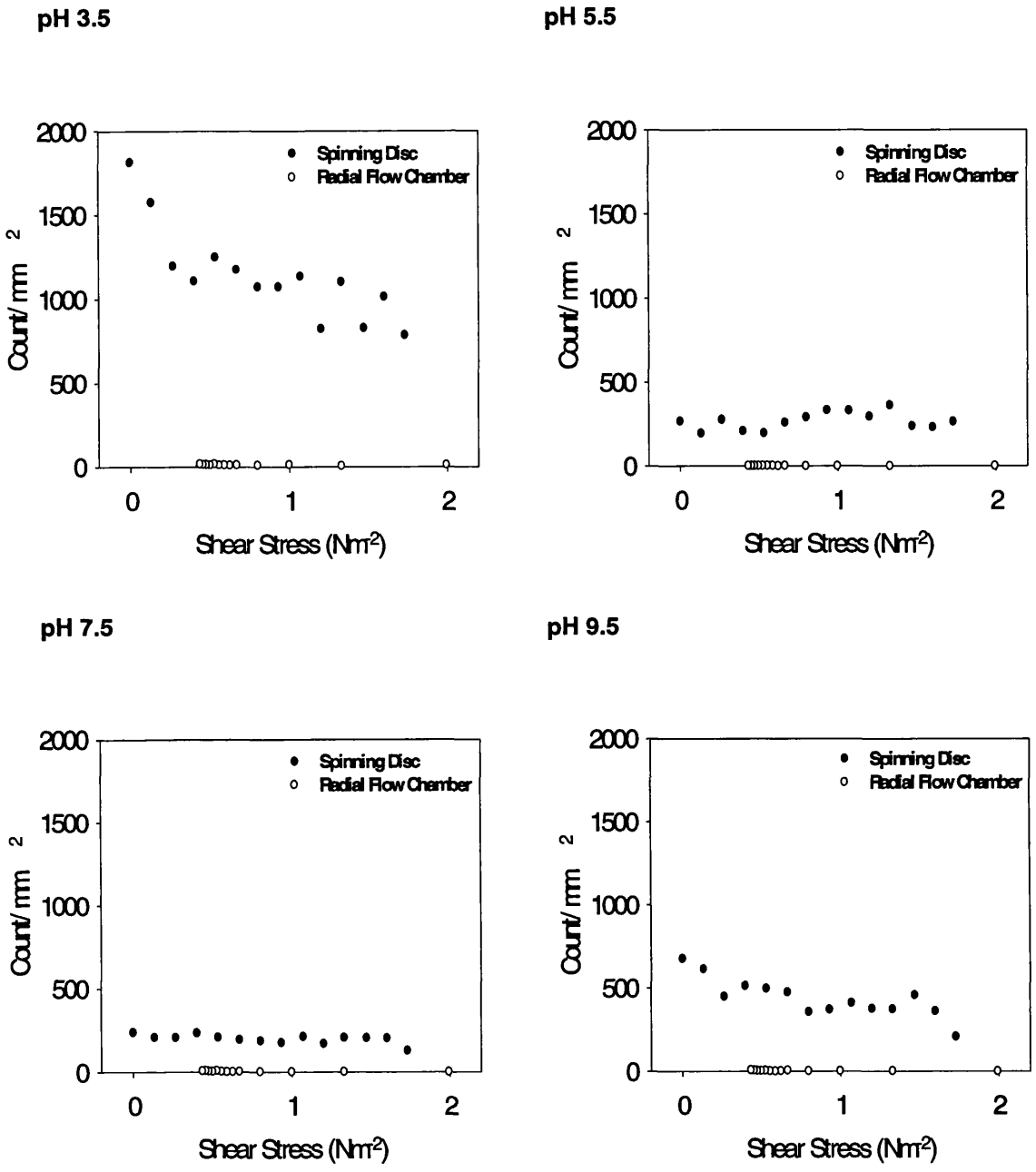

Figure F.1: The adhesion of aminated latex beads to glass using the Spinning Disc and the RFC at pH 3.5, 5.5, 7.5, and 9.5, with respect to shear stress. Experimental procedure is given in Chapters 6 and 7 for the Spinning Disc and the RFC respectively.

F.1.2 The Adhesion of Carboxylated Beads to Glass

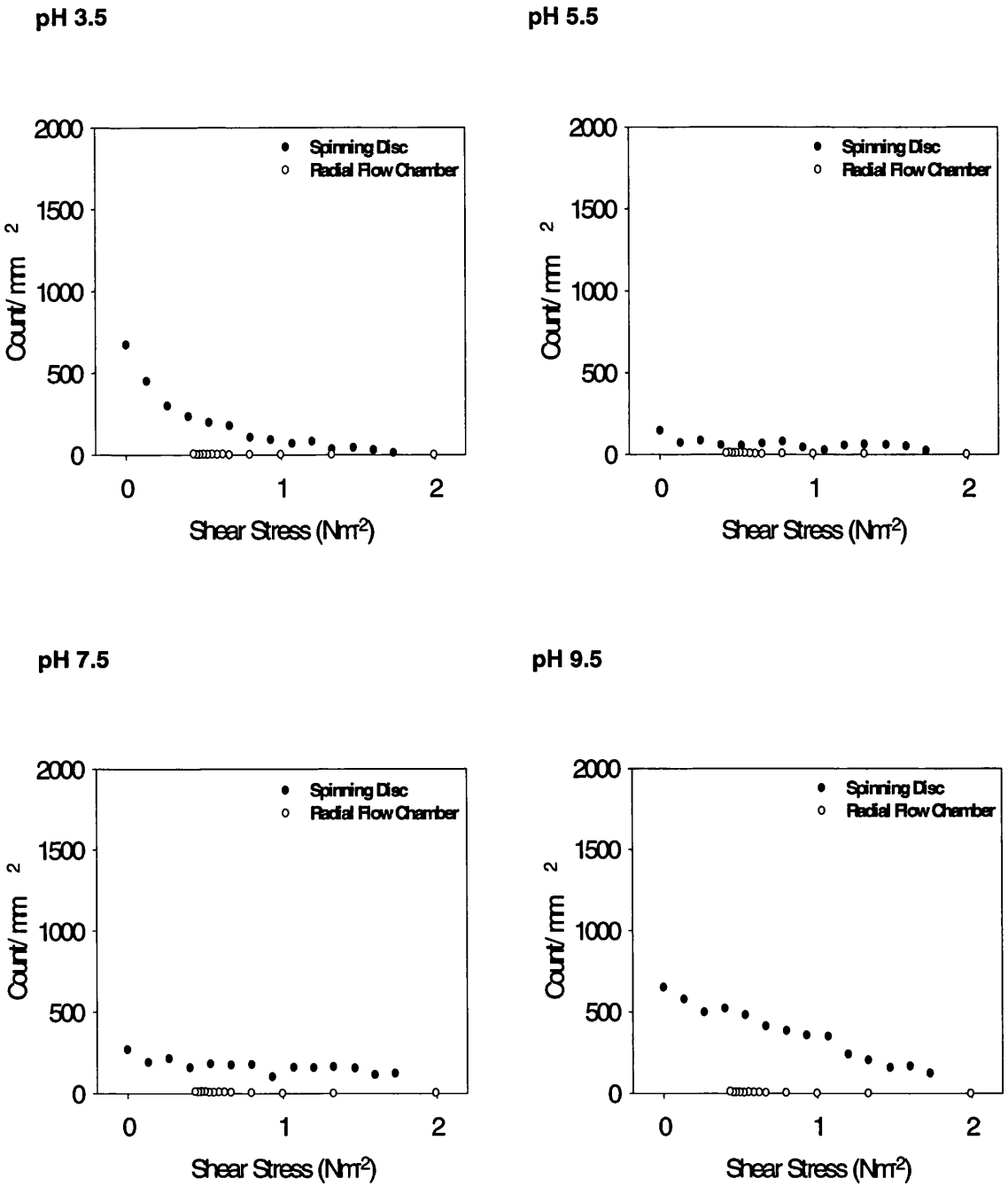

Figure F.2: The adhesion of carboxylated latex beads to glass using the Spinning Disc and the RFC at pH 3.5, 5.5, 7.5, and 9.5, with respect to shear stress. Experimental procedure is given in Chapters 6 and 7 for the Spinning Disc and the RFC respectively.

F.1.3 The Adhesion of the Spores of B.mycoides to Glass

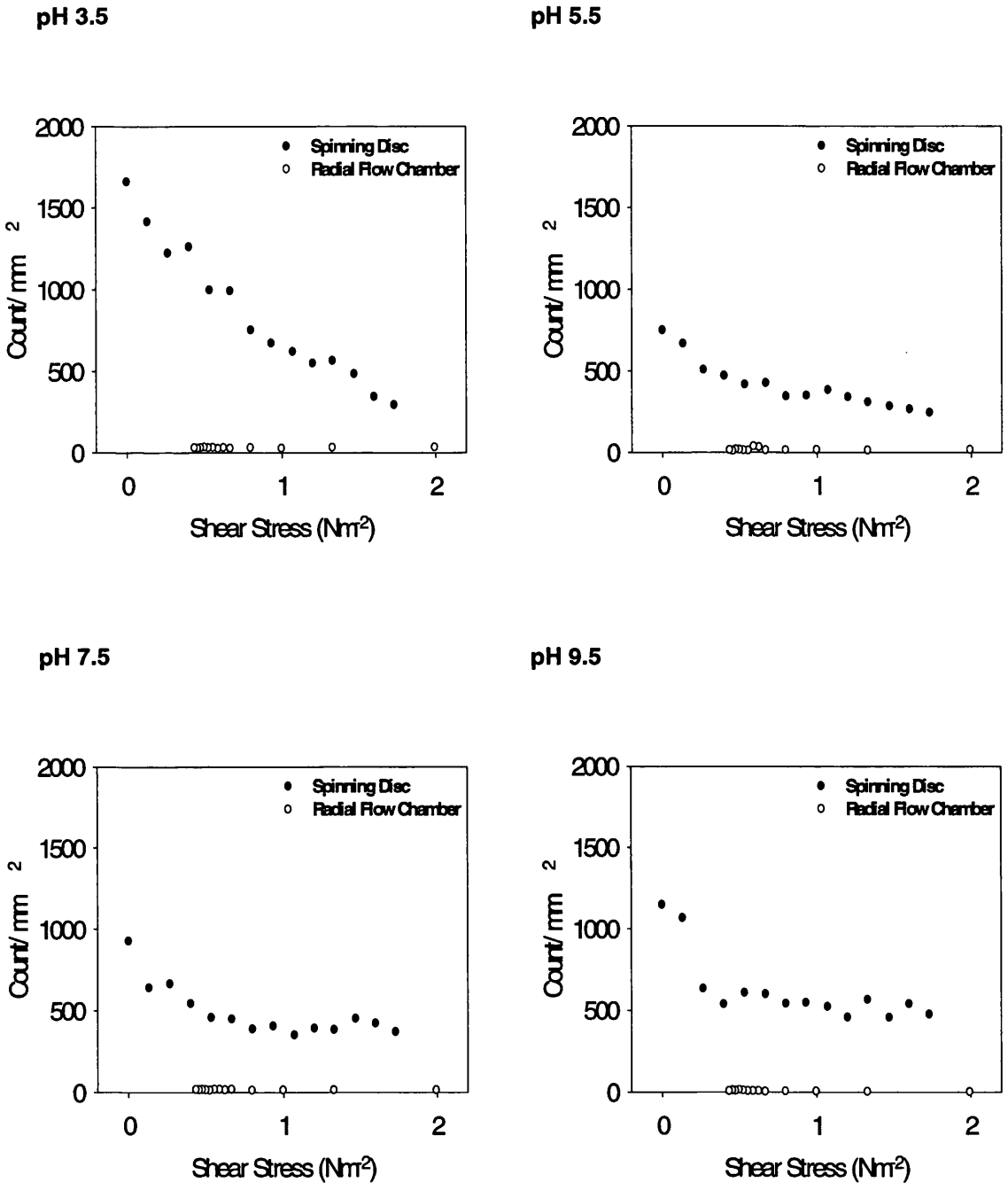

Figure F.3: The adhesion of the spores of *B.mycoides* to glass using the Spinning Disc and the RFC at pH 3.5, 5.5, 7.5, and 9.5, with respect to shear stress. Experimental procedure is given in Chapters 6 and 7 for the Spinning Disc and the RFC respectively.

F.1.4 The Adhesion of the Spores of B.subtilis to Glass

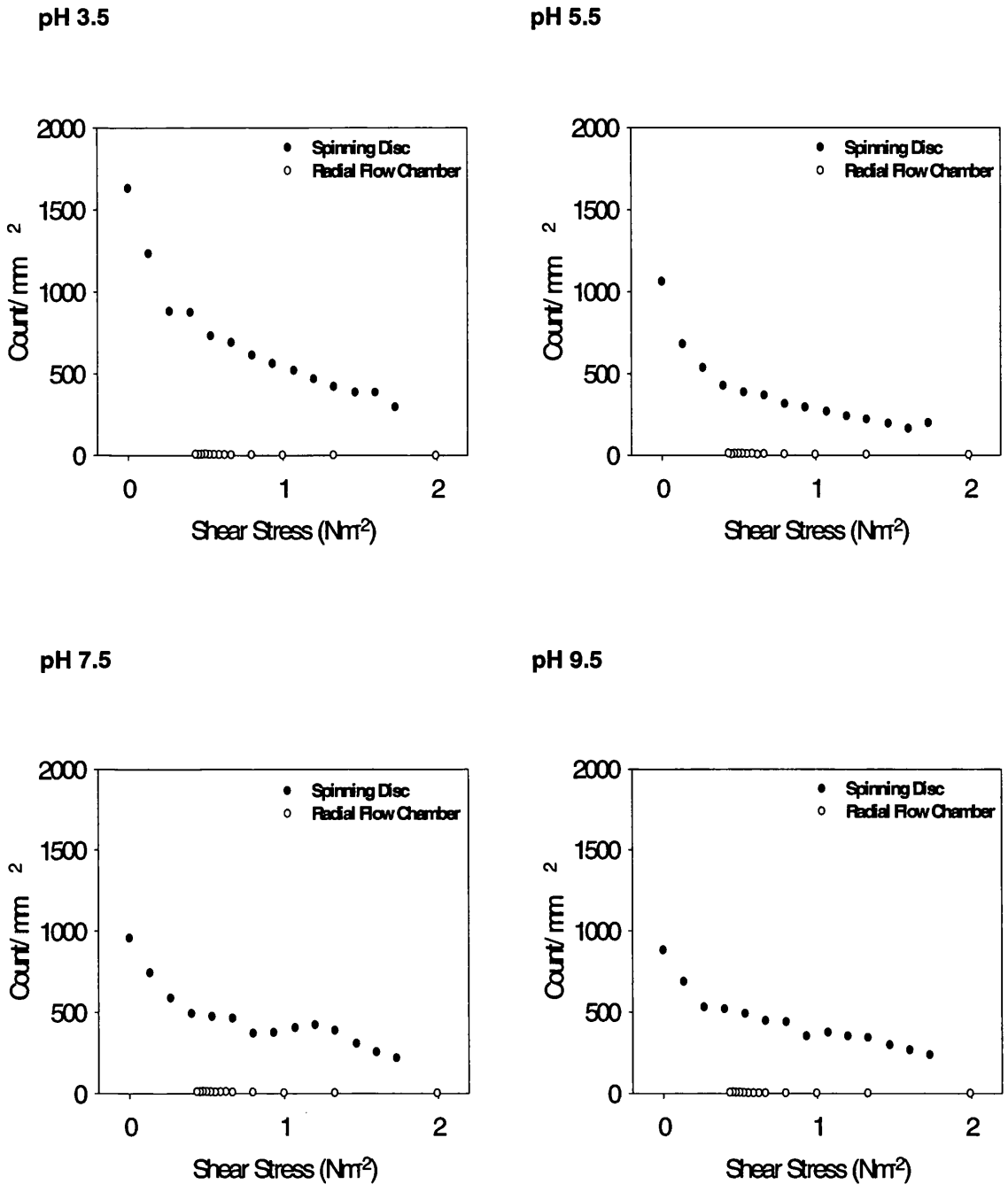

Figure F.4: The adhesion of the spores of *B.subtilis* to glass using the Spinning Disc and the RFC at pH 3.5, 5.5, 7.5, and 9.5, with respect to shear stress. Experimental procedure is given in Chapters 6 and 7 for the Spinning Disc and the RFC respectively.

F.2 The Statistical Comparison of the Adhesion Profiles Generated using the Spinning Disc and the RFC

The two tables shown below show the description of the adhesion profiles generated from the use of the Spinning Disc and the RFC, as described in Section 8.2.2.

F.2.1 Adhesion to Glass

Particle	pH	Recovery From Column (%)	Type 1 SD 2 RFC	Maximum Value, A	Minimum Value, B	Shear Stress Value, C
Aminated Beads	**3.5**	4.6	D A			
	5.5	15.4	E A	1800	800	0.5
	7.5	23.7	B A	250	0	4
	9.5	46.9	B A	700	0	3.2
Carboxylated Beads	**3.5**	17.8	F A	700	0	0.5
	5.5	52.1	D A			
	7.5	61.7	E A	275	125	0.5
	9.5	54.0	B A	650	0	2.5
***B.mycoides* Spores**	**3.5**	0.3	F A	1700	0	1.3
	5.5	1.3	E A	800	100	1.2
	7.5	0.6	E A	275	125	0.6
	9.5	1.6	E A	1200	400	0.5
***B.subtilis* Spores**	**3.5**	62.3	E A	1600	200	0.8
	5.5	77.1	E A	1100	200	0.6
	7.5	81.9	E A	1000	200	0.6
	9.5	93.9	E A	900	200	0.5

Table F.1: Comparison of the adhesion profiles generated for each particle/pH combination to glass. The table states the percentage recovery from the column in each case, the shape of the curve as designated in Figure 8.2, the maximum and minimum attachment values, and a value for shear stress as defined in Figure 8.4. Where these respective figures were unable to be generated, spaces have been left blank.

Particle	pH	Recovery From Column (%)	Type 1 SD 2 RFC	Maximum Value, A	Minimum Value, B	Shear Stress Value, C
Aminated Beads	**3.5**	0.4	E E	550 1700	200 550	0.6 0.7
	5.5	8.5	D E	 1500	 400	 0.7
	7.5	12.3	D E	 1100	 400	 0.7
	9.5	11.8	E E	800 1000	200 400	0.5 0.6
Carboxylated Beads	**3.5**	9.3	B E	1700 1300	0 500	1.9 0.6
	5.5	25.6	E E	350 1500	100 500	0.4 0.6
	7.5	17.6	C E	100 900	100 400	 0.8
	9.5	45.2	E E	500 1000	200 450	0.5 0.8
B.mycoides	**3.5**	0.7	E E	7000 2000	700 600	0.6 0.6
	5.5	0.2	E E	1800 1800	500 400	0.6 0.8
	7.5	1.0	E E	1200 1400	450 550	0.4 0.8
	9.5	3.5	D E	 1400	 450	 0.8
B.subtilis	**3.5**	49.4	E E	650 950	450 450	0.3 0.8
	5.5	73.2	E E	500 800	300 420	0.2 0.8
	7.5	68.9	E E	700 700	500 350	0.1 0.7
	9.5	74.3	E E	750 600	350 300	0.5 0.7

Table F.2: Comparison of the adhesion profiles generated for each particle/pH combination to stainless steel. The table states the percentage recovery from the column in each case, the shape of the curve as designated in Figure 8.2, the maximum and minimum attachment values, and a value for shear stress as defined in Figure 8.4. Where these respective figures were unable to be generated, spaces have been left blank.

REFERENCES

An Y. H. and Friedman R. J. (1997). *Journal of Microbiological Methods*, **30**, 141-152. Laboratory methods for studies of bacterial adhesion.

Andersson A., Rönner U., and Granum P. E. (1995). *International Journal of Food Microbiology*, **28**, 144-155. What problems does the food industry have with the spore-forming pathogens *Bacillus cereus* and *Clostridium perfringens*?

Aronson A. I. and Fitz-James P. (1976). *Bacteriology Reviews*, **40**, 360-402. Structure and morphogenesis of the bacterial spore coat.

Aronson A. I. and Pandey N. K. (1978). *In* G. Chambliss and J.C. Vary (ed.), 54-61. Comparative structural and functional aspects of spore coats.

Arvanitoyannis I. S. and Mavropoulos A. A. (2000). *Food Control*, **11**, 31-40. Implementation of the hazard analysis critical control point (HACCP) system to Kasseri/Kefalotiri and Anevato chees production lines.

Arciola R., Radin L., Alvergna P., Cenni E., and Pizzoferrato A. (1993). *Biomaterials*, **14**, 1161-1164. Heparin surface treatment of PMMA alters adhesion of a Staphylococcus aureus strain: utility of a bacterial fatty analysis.

Bal B. S. (1978). *MSc. Thesis, University of Wales*. Method of measurement of adhesion of microbial films to surfaces by a rotating disc under aseptic conditions.

Baumgartner J. N. and Cooper S. L. (1998). *Journal of Biomedical Materials Research*, **40**, 660-670. Influence of thrombus components in mediating *Staph. aureus* adhesion to polyurethane surfaces.

Becker K. (1998). *International Biodeterioration & Biodegradation*, **41**, 93-100. Detachment studies on microfouling in natural biofilms on substrata with different surface tensions.

Benton E. R. (1966). *Journal of Fluid Mechanics*, **24**, 781-800. On the flow due to a rotating disk.

Bergendahl J. and Grasso D. (1999). *AIChE Journal*, **45**, 475-484. Prediction of colloid detachment in a model porous media: Thermodynamics.

Binnig G., Quate C. F., and Berger C. (1986). *Physical Review Letters*, **56**, 930-933. Atomic force microscope.

Bos R., van der Mei H. C., Meinders, J. M., and Busscher H. J. (1994). *Journal of Microbiological Methods*, **20**, 289-305. A quantitative method to study co-adhesion of microorganisms in a parallel plate flow chamber: basic principles of the analysis.

Boulange-Petermann L. (1996). *Biofouling*, **10**, 275-300. Processes of bioadhesion on stainless steel surfaces and cleanabililty: A review with special reference to the food industry.

Bowen B. D. and Epstein N. (1979). *Journal of Colloid and Interface Science*, **72**, 81-97. Fine particle deposition in smooth parallel-plate channels.

Bowen W. R., Hilal N., Lovitt R. W., and Wright C. J. (1998a). *Colloids and Surfaces A: Physicochemical and Engineering Aspects*, **136**, 231-234. Direct measurement of the force of adhesion of a single biological cell using an atomic force microscope.

Bowen W. R., Hilal N., Lovitt R. W., and Wright C. J. (1998b). *Journal of Membrane Science*, **139**, 269-274. A new technique for membrane characterisation: direct measurement of force of adhesion of a single particle using an atomic force microscope.

Bowen W. R., Hilal N., Lovitt R. W., and Wright C. J. (1998c). *Journal of Colloid and Interface Science*, **197**, 348-352. Direct measurement of interactions between adsorbed protein layers using an atomic force microscope.

Bowen, W. R., Hilal N., Lovitt R. W., and Wright C. J. (1999). *Journal of Membrane Science*, **154**, 205-212. Characterisation of Membrane Surfaces: Direct Measurement of Biological Adhesion Using an Atomic Force Microscope.

Bowen W. R., Fenton A. S., Lovitt R. W., Wright C. J. (2000). Submitted for Publication. The measurement of *Bacillus mycoides* spore adhesion using atomic force microscopy, simple counting methods and a spinning disc technique.

Brown K. L. (2000). *British Medical Bulletin*, **56**, 158-171. Control of bacterial spores.

Bryers, J.D. (1984). *Colloids and Surfaces B: Biointerfaces*, **2**, 9-23. Biofilms and the Technological Implications of Microbial Cell Adhesion.

Bunt C. R., Jones D. S., and Tucker I.G. (1995). *International Journal of Pharmaceutics*, **113**, 257-261. The effects of pH, ionic strength and polyvalent ions on the cell surface hydrophobicity of *Escherichia coli* evaluated by the BATH and HIC methods.

Bunt C. R., Jones D. S., and Tucker I. G. (1993). *International Journal of Pharmaceutics*, **99**, 93-98. The effects of pH, ionic strength and organic phase on the bacterial adhesion to hydrocarbons (BATH) test.

Busscher H. J. and van der Mei H. C. (1995a). *Methods in Enzymology*, **253**, 455-476. Use of flow chamber devices and image analysis methods to study microbial adhesion.

Busscher H. J., Bos R., and van der Mei H. C. (1995b). *FEMS Microbiology Letters*, **128**, 229-234. Initial microbial adhesion is a determinant for the strength of biofilm adhesion.

Butkus M. A. and Grasso D. (1998). *Journal of Colloid and Interface Science*, **200**, 172-181. Impact of aqueous electrolytes on interfacial energy.

Camesano T. A., Unice K. M., and Logan B. E. (1999). *Colloids and Surfaces A: Physicochemical and Engineering Aspects*, **160**, 291-308. Blocking and Ripening of colloids in porous media and theor implications for bacterial transport.

Cantineaux B., Courtoy P., and Fondu P. (1993). *Pathobiology*, **61**, 95-97. Accurate flow cytometric measurement of bacteria concentrations.

Carratelli R., Nuzzo C., and Galdiero M. (1997). *Microbiologica*, **10**, 55-61. Surface poperties of *Escherichia coli* strains responsible for urinary infections.

Casey E., Glennon B., and Hamer G. (2000). *Biotech. Bioeng.*, **67**, 476-486. Biofilm development in a membrane-aerated biofilm reactor effect of flow velocity on performance.

Cassell E. A. (1965). *Applied Microbiology*, **13**, 293-296. Rapid graphical method for estimating the precision of direct microscopic counting data.

Clint G. E., Clint J. H., Corkill J. M., and Walker T. (1973). *Journal of Colloid and Interface Science*, **44**, 121-132. Deposition of latex particles on to a planar surface.

Colchero J., Bielefeldt H., Ruf A., Hipp M., Marti O., Mlynek J. (1992). Phys. Stat. Sol., **131**, 73-75. Scanning Force and Friction Microscopy.

Costerton J.W. and Stewart P.S. (2000). Biofilms and Device-Related Infections *In: J.P. Nataro, M.J. Blaser, and S. Cunningham-Rundle (eds.), Persistent Bacterial Infections*, 423-439. ASM Press, Washington, D.C.

Costerton J.W. Stewart P.S., and Greenberg E.P. (1999). *Science*, **284**, 1318-1322. Bacterial Biofilms: A Common Cause of Persistent Infections.

Costerton J.W. and Lewandowski Z. (1997). *Advances in Dental Research*, **11**, 192-195. The Biofilm Lifestyle.

Costerton J.W. and Lappin-Scott H.M. (1995). Introduction to Microbial Biofilms *In: H.M. Lappin-Scott and J.W. Costerton (eds.), Microbial Biofilms.* 1-11.

Cozens-Roberts C., Quinn J. A., and Lauffenberger D. A. (1990a). *Biophysical Journal*, **58**, 107-125. Receptor mediated adhesion phenomena – model studies with a radial-flow detachment assay.

Cozens-Roberts C., Quinn J. A., and Lauffenberger D. A. (1990b). *Biophysical Journal*, **58**, 857-872. Receptor mediated cell attachment and detachment kinetics II experimental model studies with the radial-flow detachment assay

Crielly E. M., Logan N. A., and Anderton A. (1994). *Journal of Applied Bacteriology*, **77**, 256-263. Studies on the *Bacillus* flora of milk and milk products.

Daily J. W. and Nece R. E. (1960). *Journal of Basic Engineering*, **82**, 217-232. Chamber dimensional effect on induced flow and frictional resistance of enclosed rotating disks.

Dammer U., Popescu O., Wagner P., Anselmetti D., Güntherodt H-J., and Misevic G., G. N. (1995). *Science*, **267**, 1173-1175. Binding strength between cell adhesion proteoglycans measured by atomic force microscopy.

Dart J. K.and Badenoch P. R. (1986). *CLAO*, **12**, 220-224. Bacterial adherence to contact lenses.

Dickinson R. B. and Cooper S.L. (1995). *AIChE Journal*, **41**, 2160-2173. Analysis of shear-dependent bacterial adhesion kinetics to biomaterial surfaces.

Driks A. (1999). *Microbiology and Molecular Biology Reviews*, **63**, 1-20. *Bacillus subtilis* spore coat.

Elimelech M. and O'Melia C. R. (1990). *Environmental Science and Technology*, **24**, 1528-1536. Kinetics of deposition of colloidal particles in porous media.

Elimelech M., Gregory J., Jia X., and Williams R. A., (1995). *Particle Deposition and Aggregation. Measurement, modelling and simulation*; Butterworth-Heinemann, Oxford:

Falk P., Borén T., Haslam D., and Caparon M. 1994. *Methods in Cell Biology*, **45**, 165-192. Bacterial adhesion and colonization assays.

Faille C., Fontaine F., and Bénézech T. (2001). *Journal of Applied Microbiology*, **90**, 892-900. Potential occurrence of adhering living ***Bacillus*** spores in milk product processing lines.

Fletcher M. and Loeb G. I. (1979). *Applied Environmental Microbiology*, **37**, 67-72. Influence of substratum characteristics on the attachment of a marine *Pseudomonas* to solid surfaces.

Florin E-L, Moy V. T., and Gaub H.E., (1994). *Science,* **264**, 415-417. Adhesion forces between individual ligand-receptor pairs

Fowler H. W. and McKay A. J. (1980). The measurement of microbial adhesion *In: R.C.W Berkeley, J. M. Lynch, J. Melling, P. R. Rutter, and B. Vincent (eds.), microbial adhesion to surfaces.* Ellis Horwood, Chichester, England.

García A. J., Ducheyne P., and Bottiger D. (1997). *Biomaterials*, **18**, 1091-1098. Quantification of cell adhesion using a spinning disc device and application to surface-reactive materials.

Gatenholm P., Fell C. J., and Fane A. G. (1988). *Desalination*, **70**, 363-378. Influence of the membrane structure on the composition of the deposit-layerduring processing of microbial suspensions.

Gerstner J. A., Bell J. A., and Cramer S. M. (1994). *Biophysical Chemistry*, **52**, 97-106. Gibbs free energy of adsorption for biomolecules in ion-exchange systems.

Goldstein A. S. and DiMilla P. A. (1997). *Biotechnology and Bioengineering*, **55**, 616-629. Application of fluid mechanic and kinetic models to characterise mammalian cell detachment in a radial flow chamber.

Goodwin A. E. and Pauli B. U. (1995). *Journal of Immunological Methods*, **187**, 213-219. A new adhesion assay using buoyancy to remove non-adherent cells.

Gould G. W. (1971). Methods in Microbiology, Volume **6A**, Chapter 6, 327-389 Published by Academic Press. Methods for studying bacterial spores.

Gould S. A. C., Drake B., Prater C. B., Weisonhron A. L., Manne S., Kelderman G. L., Butt H-J., Hansma H., and Hansma P.K. (1990). *Ultramicroscopy*, **33**, 93-98. The atomic force microscope: A tool for science and industry.

Grolimund D., Elimelech M., Borkovec M., Kretzschmar R., and Sticher H. (1998). *Environmental Science & Technology*, **32**, 3562-3569. Transport of *in situ* mobilized colloidal particles in packed soil columns.

Groves B. J. and Riley P. A. (1987) *Cytobios*, **52**, 49-62. A miniaturised parallel-plate shearing apparatus for the measurement of cell adhesion.

Hachisuka Y., Kozuka S., and Tsujikawa M. (1984). *Microbiol. Immunol.*, **28,** 619-624. Exosporia and appendages of spores of *Bacillus species*.

Hansma H. G. and Hoh J.H. (1994). *Annu. Rev. Biophys. Biomol. Struct.*, **23**, 115-139. Biomolecular imaging with the atomic force microscope.

Harkes G., Feijen J., and Dankert J. (1991). *Biomaterials*, **12**, 853-860. Adhesion of *Escherichia coli* on to a series of poly(methacrylates) differing in charge and hydrophobicity.

Helgason E., Caugant D. A., Lecadet M-M., Chen Y., Mahillon J., Lovgren A., Hegna I., Kvaløy K., Kolstø A-B. (1998). *Current Microbiology*, **37**, 80-87. Genetic diversity of *Bacillus cereus/B. thuringiensis* isolates from natural sources.

Hermansson M. (1999). *Colloids and Surfaces B: Biointerfaces*, **14**, 105-119. The DLVO theory in microbial adhesion.

Huang D. D., Nandy S., and Thorgerson E. J. (1997). In:*Technology for Waterborne Coatings*. Chapter 11, 196-211. Application of electrosterically stabilised latex in waterborne coatings.

Hull M. and Kitchener J. A. (1969). *Ibid*, **65**, 3093. Interaction of spherical colloidal particles with planar surfaces.

Husmark U. and Rönner U. (1992). *Biofouling*, **5**, 335-344. The influence of hydrophobic, electrostatic and morphologic properties on the adhesion of *bacillus* spores.

Huysman F. and Verstraete W. (1993). *Biology and Fertility of Soils*, **16**, 21-26. Effect of cell surface characteristics on the adhesion of bacteria soil particles.

Israelachvili J. and Wennerstrom H. (1996). *Nature* **379**, 219-225. Role of hydration and water structure in biological and colloidal interactions.

Jacobson B. S. and Branton D. (1977). *Science*, **195**, 302-304. Plasma membrane: Rapid isolation and exposure of the cytoplasmic surface by use of positively charged beads.

Jenkins B. G. M. (1976). *MSc Thesis, University of Wales.* A preliminary investigation in the use of a rotating disc for measuring the adhesion of microbial film to surfaces.

Jones D. S., Adair C. G., Mawhinney W. M., and Gorman S. P. (1996). *International Journal of Pharmaceutics*, **131**, 83-89. Standardisation and comparison of methods employed for microbial cell surface hydrophobicity and charge determination.

Jucker B. A., Harms H., Zehnder, A. J. B. (1998). *Colloids and Surfaces B: Biointerfaces*, **11**, 33-45. Polymer interactions between five gram-negative bacteria and glass investigated using LPS micelles and vesicles as model systems.

Kallay N., Biškup B., Tomić M., and Matijević E. (1986). *Journal of Colloid and Interface Science*, **114**, 357-362. Particle adhesion and removal in model systems.

Khilar K. C. and Fogler H. S. (1984). *Journal of Colloid and Interface Science*, **101**, 214-224. The existence of a critical salt concentration for particle release.

Kramer J. M. and Gilbert R. J. (1989).*Bacillus cereus* and other *Bacillus* species. *In M.P. Doyle (ed), Foodborne Bacterial Pathogens.* Marcel Dekker, New York.

Lee G.U., Kidwell D. A., and Colton R. J. (1994). *Langmuir*, **10**, 354. Sensing Discrete Streptavidin-Biotin Interactions with Atomic Force Microscopy

Lele S. S., Kulkarni A. G., and Kulkarni P. R. (1996). *Biotechnology Letters*, **18**, 515-520. Immobilisation of fungal spores on synthetic polymers.

Levich V. G. (1962). *Physicochemical Hydrodynamics*, Prentice-Hall, New Jersey.

Lei X-Y., Wan P., Zhou C-H., and Ming N-B. (1996). *Physical Review E*, **54**, 5298-5301. Kinetic crossover of rough surface growth in a colloidal system.

Litton G. M. and Olson T. M. (1993). *Environmental Science &. Technology*, **27**, 185-193. Colloid deposition rates on silica bed media and artefacts related to collector preparation methods.

Liu D., Johnson P.R., and Elimelech M. (1995) *Environmental Science & Technology*, 2963-2973. Colloid deposition dynamics in flow through porous media: Role of electrolyte concentration.

Luckham P. F. and Hartley P.G. (1994). *Advances in Colloid and Interface Science*, **49**, 341-386. Interactions between biosurfaces.

Madeani S. S. (1998). *Iranian Polymer Journal*, **7**, 177-184. On the specific resistance of cakes of latexes.

Marshall J. K. and Kitchener J. A. (1966). *Journal of Colloid and Interface Science*, **22**, 342-351. The deposition of colloidal particles on smooth solids.

McKay A. J. (1980) *PhD. Thesis, University of Wales*. The measurement of microbial adhesion.

Meinders J.M., van der Mei H. C., and Busscher H.J. (1995). *Journal of Colloid and Interface Science*, **176**, 329-341. Deposition efficiency and reversibility of bacterial adhesion under flow.

Meinders J.M., van der Mei H. C., and Busscher H.J. (1992). *Journal of Microbiological Methods*, **16**, 119-124. *In situ* enumeration of bacterial adhesion in a parallel plate flow chamber – elimination of in focus flowing bacteria from analysis.

Mittelman M. W. (1995). Biofilm development in purified water systems. *In: H.M. Lappin-Scott and J.W. Costerton (eds.), Microbial Biofilms.* Cambridge University Press, Cambridge, UK. 133-147.

Mohandas N., Hochmuth R. M., and Spaeth E. E. (1974). *Journal of Biomedical Material Research*, **8**, 119-136. Adhesion of red cells to foreign surfaces in the presence of flow.

Moller P.S. (1963). *Aero. Quart.,* **14**, 163-186. Radial flow without swirl between parallel discs.

Moruzzi G., Garthwright W. E., and Floros J. D. (2000). *Food Control*, **11**, 57-66. Aseptic packaging machine pre-sterilisation and package sterilisation: statistical aspects of microbiological validation.

Nagel J. A., Dickinson R. B., and Cooper S. L. (1996). *Journal of Biomaterial Science Polymer Edn.*, **7**, 769-780. Bacterial adhesion to polyurethane surfaces in the presence of pre-adsorbed high molecular weight kininogen.

Nagel-Baumgartner J. A. and Cooper S. L. (1998). *Journal of Biomedical Materials Research*, **40**, 660-670. Influence of Thrombus Components in Mediating *Staphylococcus aureus* adhesion to polyurethane surfaces.

Nakae H., Inup R., Hirata Y., and Saito H., (1998). *Acta Mater.*, **46**, 2313-2318. Effects of surface roughness on wettability.

Neu T.R., Verkerke G. J., Herrmann I. F., Schutte H. K., van der Mei H. C., and Busscher H. J. (1994). *Journal of Applied Bacteriology*, **76**, 521-528. Microflora on explanted silicone rubber voice protheses: Taxonomy, hydrophobicity and electrophoretic mobility.

O'Neill M.E. (1967). *Chemical Engineering Science*, **23**, 1293-1298. A sphere in contact with a plane wall in a slow linear shear flow.

Oga M., Arizono T., and Sugioka Y. (1993). *Acta Orthopaedica Scandinavica*, **64**, 273-276. Bacterial adherence to bioinert and bioactive materials studied *in vitro*.

Old D. C., (1985). *Medical Laboratory Sciences*, **43**, 78-85. Bacterial Adherence.

Parkar S. G., Flint S. H., Palmer J. S., and Brooks J. D. (2001). *Journal of Applied Microbiology*, **90**, 901-908. Factors influencing attachment of thermophilic *bacilli* to stainless steel.

Personal correspondence with Dr. Chris Wright, (2001). *University of Wales Swansea.*

Personal correspondence with Dr. Teodora Doneva (2001). *University of Wales Swansea.*

Pontefract R. D. (1991). *Canadian Institute of Food Science and Technology Journal*, **24**, 113-117. Bacterial adherence: Its consequence in food processing.

Pritchard C. and Walker E. (1998). *Food Control*, **9**, 61-64. Challenges for the enforcement of food safety in Britain.

Pyne S., Fletcher R. L., Jones E. G. B. (1984). In: *Proc 6th international congress on marine corrosion and fouling, Athens*, 99-112. Attachment studies on three common fouling diatoms.

Rijnaarts H. H. M., Norde W., Bouwer E. J., Lyklema J., and Zehnder A. J. B. (1996a). *Environmental Science and Technology*, **30**, 2877-2883. Bacterial Deposition in Porous Media: Effects of cell-coating, substratum hydrophobicity, and electrolyte concentration.

Rijnaarts H. H. M., Norde W., Bouwer E. J., Lyklema J., and Zehnder A. J. B. (1996b). *Environmental Science and Technology*, **30**, 2869-2876. Bacterial deposition in porous media related to the clean bed collision efficiency and to substratum blocking by attached cells.

Rijnaarts H. H. M., Norde W., Lyklema J., and Zehnder A. J. B. (1999). *Colloids and Surfaces B: Biointerfaces*, **14**, 179-195. DLVO and steric contribution to bacterial deposition in media of different ionic strengths.

Rimondi L., Farè S., Brambilla E., Felloni A., Consonni C., Brossa F., and Carrassi A. (1997). *Journal of Periodontology*, **68**, 556-562.

Romano Carratelli C., Nuzzo I., and Galdiero M. (1987). *Microbiologica*, **10**, 55-61. Surface properties of *Escherichia coli* strains responsible for urinary infections.

Rosenberg M., Gutnick D., and Rosenberg E. (1980). *FEMS Microbiology Letters*, **9**, 29-33. Adherence of bacteria to hydrocarbons: A simple method for measuring cell surface hydrophobicity.

Roy S. B. and Dzombak D. A. (1996a). *Colloids and Surfaces A: Physicochemical and Engineering Aspects*, **119**, 133-139. Na^+-Ca^+ exchange effects in the detachment of latex colloids deposited in glass bead porous media.

Roy S. B. and Dzombak D. A. (1996b). *Colloids and Surfaces A: Physicochemical and Engineering Aspects*, **107**, 245-262. Colloid release and transport processes in natural and model porous media.

Ruckenstein E. and Prieve D. C. (1976). *AIChE Journal*, **22**, 276-283. Adsorption and desorption of particles and their chromatographic separation.

Rukure G. and Bester B. H. (2001). *Food Control*, **12**, 31-36. Survival and growth of *Bacillus cereus* during Gouda cheese manufacturing.

Schilling K. M. and Doyle R. (1995). *Methods in Enzymology*, **253**, 536-542. Bacterial adhesion to hydroxylapatite.

Schultz C. L., Pezzutti M. R., Silor D., and White R. (1995). *Journal of Industrial Microbiology*, **15**, 243-247. Bacterial adhesion measurements on soft contact lenses using a modified vortex device and a modified Robbins device.

Shive M. S., Hasan S. M., and Anderson J. M. (1999). *Journal of Biomedical Materials Research*, **46**, 511-519. Shear stress effects on bacterial adhesion, leukocyte adhesion and leukocyte oxidative capacity on a polyetherurethane.

Singer S. J. and Nicolson G.L. (1972). *Science*, **175**, 720-731. The fluid mosaic model of the structure of cell membranes.

von Smoluchowski M. (1918). *Z. Phys. Chem*, **93**, 129-168. Versuch einer mathematischen theorie der koagulationskinetik kolloider Lösungen.

Sonak S. and Bhosle N. B. (1995). *Biofouling*, **9**, 31-38. A simple method to assess bacterial attachment to surfaces.

Sorongon M. L., Bloodgood R. A., and Burchard R. P., (1991). *Applied and Environmental Microbiology*, **57**, 3193-3199. Hydrophobicity, adhesion and surface-exposed proteins of gliding bacteria.

St John J. J., Schroen D. J., and Cheung H. T. (1994). *Journal of Immunological Methods*, **170**, 159-166. An adhesion assay using minimal shear force to remove nonadherent cells.

Stollenwerk M., Fallgren C., Lundberg F., and Tegenfeldt J. O. (1998). *Zentrablatt für Bakteriologie*, **287**, 7-18. Quantification of bacterial adhesion to polymer surfaces by bioluminescence.

Tripp B. C., Kaler E. W., Sandler S. I., and Kopatsis, A. (1996). *Colloids and Surfaces B: Biointerfaces*, **6**, 151-164. Effect of ionic strength and ionic species on partitioning behaviour of hydrophobic and hydrophilic polystyrene latex beads in aqueous two-phase polymer systems.

Ubeda J. F. and Briones A. I. (1999). *Food Control*, **10**, 41-45. Microbiological quality control of filtered and non-filtered wines.

Vacheethasanee K., Temenoff J. S., Higashi J. M., Gary A., Anderson J. M. Bayston R., Marchant R. E. (1998). *Journal of Biomedical Materials Research*, **42**, 425-432. Bacterial surface properties of clinically isolated *Staphylococcus epidermis* strains determine adhesion on polyethylene.

Vaidyanathan R. and Tien C. (1988). *Chemical Engineering Science*, **43**, 289-302. Hydrosol deposition in granular beds.

van de Ven T. G. M. (1998). *Colloids and Surfaces A: Physicochemical and Engineering Aspects*, **138**, 207-216. The capture of colloidal particles on surfaces and in porous material: basic principles.

van Loosdrecht M. C. M., Lyklema J., Norde W., Schraa G., and Zehnder A. J. B. (1987). *Applied and Environmental Microbiology*, **53**, 1898-1901. Electrophoretic mobility and hydrophobicity as a measure to predict the initial steps of bacterial adhesion.

van Oss, C.J (1995). *Colloids and Surfaces B: Biointerfaces*, **5**, 91-116. Hydrophobicity of biosurfaces:- Origin, quantitative determination and interaction energies.

Verheyen C. C. P. M., Dhert W. J. A., de Blieck-Hogervorst J. M. A., van der Reijden T. J. K., Petit P. L. C., and de Groot K. (1993). *Biomaterials*, **14**, 383-391. Adherence to a metal, polymer and composite by *Staphylococcus aureus* and *Staphylococcus epidermidis*.

Verran J. and Boyd R. D. (2001). *Biofouling*, **17**, 59-71. The relationship between substratum surface roughness and microbiological and organic soiling: A review.

Verran J., Taylor R. L., and Lees G. C. (1994). *Binary*, **6**, 55-57. The use of image analysis to quantify microorganisms adherent to surfaces.

Walz J. Y. (1998). *Advances in Colloid and Interface Science*, **74**, 119-168. The effect of surface heterogeneities on colloidal forces.

Wang I., Anderson J. M., and Marchant R. E. (1993a). *Journal of Biomedical Materials Research*, **27**, 1119-1128. Platelet-mediated adhesion of *Staphylococcus epidermis* to hydrophobic NHLBI reference polyethylene.

Wang I., Anderson J. M., and Marchant R. E. (1993b). *The Journal of Infectious Diseases*, **167**, 329-336. *Staphylococcus epidermis* adhesion to hydrophobic biomedical polymer is mediated by platelets.

Wang I., Anderson J. M., Jacobs M. R., and Marchant R. E. (1995). *Journal of Biomedical Materials Research*, **29**, 485-493. Adhesion of *Staphylococcus epidermis* to biomedical polymers: Contributions of surface thermodynamics and hemodynamic shear conditions.

Weiss L. (1961). *Experimental Cell Research*, Supplement, **8**, 141-153. The measurement of cell adhesion.

Weiss L. (1968). *Experimental Cell Research*, **53**, 603-614. Studies on cellular adhesion in tissue-culture.

Weyn B., Kalle W., Kumar-Singh S., van Marck E., Tanke H., and Jacob W. (1998). *Journal of Microscopy*, **189**, 172-180. Atomic force microscopy: influence of air drying and fixation on the morphology and viscoelasticity of cultured cells.

Wiencek K. M., Klapes N. A., and Foegeding P. M. (1990). *Environmental Microbiology*, **56**, 2600-2605. Hydrophobicity of ***Bacillus*** and *Clostridium* spores.

Yamamoto T., Periasmay R. P., and Donovan D. (1994). *Journal of Adhesion Science and Technology*, **8**, 543-552. Flow cell for real time observation of single particle adhesion and detachment.

Yan Y. D. (1996) *Langmuir*, **12**, 3383-3388. Pulse-injection chromatographic determination of the deposition and release rate constants of colloidal particles in porous media.

Yung L-Y. L., Lim F., Khan M. M. H., Kunapuli S. P., Rick L., Colman R.W., Cooper S. L. (1996). *Immunopharmacology*, **32**, 19-23. Neutrophil adhesion on surfaces preadsorbed with high molecular weight kininogen under well-defined flow conditions.